Green Energy and Technology

Maria Turco
Angelo Ausiello
Luca Micoli

Treatment of Biogas for Feeding High Temperature Fuel Cells

Removal of Harmful Compounds by Adsorption Processes

Springer

Green Energy and Technology

More information about this series at http://www.springer.com/series/8059

Maria Turco · Angelo Ausiello
Luca Micoli

Treatment of Biogas for Feeding High Temperature Fuel Cells

Removal of Harmful Compounds by Adsorption Processes

Springer

Maria Turco
Department of Chemical Engineering,
Materials and Industrial Production
University of Naples Federico II
Naples
Italy

Luca Micoli
Department of Chemical Engineering,
Materials and Industrial Production
University of Naples Federico II
Naples
Italy

Angelo Ausiello
Department of Chemical Engineering,
Materials and Industrial Production
University of Naples Federico II
Naples
Italy

ISSN 1865-3529 ISSN 1865-3537 (electronic)
Green Energy and Technology
ISBN 978-3-319-03214-6 ISBN 978-3-319-03215-3 (eBook)
DOI 10.1007/978-3-319-03215-3

Library of Congress Control Number: 2016931600

Printed on acid-free paper

This Springer imprint is published by SpringerNature
The registered company is Springer International Publishing AG Switzerland

To Prof. Umberto Costantino
and Prof. Giulio Alberti

Preface

Professor Maria Turco is Associated Professor at the Faculty of Engineering of University "Federico II" of Napoli, where she teaches courses in "Industrial Chemistry," "Traditional and Innovative Fuels and Fuel Cells," and "Catalysis". Professor Maria Turco carried out research activity, mainly in the field of the technologies for the production of energy with low environmental impact, such as catalytic processes for removal of gaseous pollutants and processes for hydrogen production. A large part of her recent activity is devoted to the study of fuel cells for mobile or stationary applications.

Dr. Luca Micoli is a Ph.D. Chemical Engineer and researcher at the Department of Chemical, Materials and Production Engineering of University "Federico II" of Naples. His research activities are focused on fuel cells for different applications, such as portable and stationary power generation, and on methodologies for the clean-up stage.

Dr. Angelo Ausiello is a Ph.D. student in Chemical Engineering at the University of Naples "Federico II". His research activities include the development of energy production systems based on fuel cells fueled by biogas produced from the anaerobic digestion of different kinds of biomass.

The interest in fuel cells (FCs) technology is growing continuously, since they have high potential of applications for many reasons such as emission-free energy supply, high efficiency, wide range of power generation from a few watts to some megawatts, and the possibility to be fed with different fuels including biogas. These and many other advantages have encouraged academic and industrial researchers worldwide to improve performances and the cost-effectiveness of fuel cells. Nowadays, the considerable level of technological readiness that has been reached finally allows to expect that fuel cells will penetrate into a large market.

The authors of this book are of the opinion that the FC technology has great potential and that it can play a key role in adapting the worldwide energy supply systems toward efficiencies and emission levels allowing a long-term stable and sustainable development for the world economy and environment.

Nevertheless, the authors consider that efforts on improving performances FCs are not enough to enter the market successfully, because the quality and the purity of the fuels, in particular biogas, need specific attention due to the presence of impurities or undesirable compounds in the fuels that can damage the components of a fuel cell (electrodes and electrolyte) and reduce the overall efficiency.

In the field of stationary power production high temperature fuel cells (MCFC and SOFC) are emerging as a promising alternative to combustion heat engines for the production of electrical power and cogeneration, and the possibility of feeding biogas as alternative fuel increases the interest for the evident environmental advantages. The use of biogas as fuel for FCs is an important task in the development of technologies for production of energy from renewable sources and is largely treated in the literature. At the same time gas purification processes based on adsorption on microporus materials are widely studied in the literature. This book reviews in a comprehensive way the main aspects regarding the purification procedures of biogas for fuelling MCFCs or SOFCs.

In Chap. 1 different processes of biogas production (fermentation, digestion, etc.) are described evidencing the dependence of the gas composition and content of noxious compounds on the specific process and on the source of biomass. Attention is focused on the different types of compounds that can be harmful for high temperature fuel cells and their reformer systems such as sulfur compounds inorganic and organic) and siloxanes.

Chapter 2 summarizes the operating principles of the fuel cells in order to provide an understanding of the basic operations.

Chapter 3 is an overview of the main challenges that such new technology meets shifting from a well-established niche market to the civilian one in a commercialization process.

In Chap. 4 the technologies proposed in the literature for removal of noxious substances are reviewed with particular attention to adsorption processes. The adsorbent materials that appear the most probable candidates for this application (based on zeolites and activated carbons) are described with emphasis on the methodologies aimed to improve the adsorption properties. The regeneration of the materials is also taken into account.

In Chaps. 5–7 the effects of sulfur compounds and siloxanes on performances of MCFC and SOFC are described. The mechanisms of interaction of these compounds with the components of FCs (electrodes and electrolyte) are also treated.

Contents

Chapter 1
Processes of Biogas Production: Anaerobic Digestion and Thermal Gasification

1.1 Introduction

The global energy demand is growing rapidly, and about 88 % of this demand is met at present time by fossil fuels [1]. Scenarios have shown that the energy demand will increase during this century by a factor of two or three (IEA 2006) [1]. At the same time, concentrations of greenhouse gases (GHGs) in the atmosphere are rising rapidly, with fossil fuel-derived CO_2 emissions being the most important contributor. In order to minimize related global warming and climate change impacts, GHG emissions must be reduced to less than half of global emission levels of 1990 (IPCC 2000). The Kyoto Protocol identifies several key points to curb greenhouse gas emissions (GHG), among which is production of renewable fuels from organic waste.

Another important global challenge is the certainty of energy supply, because most of the known conventional oil and gas reserves are concentrated in politically unstable regions.

There exists significant and increasing interest in the utilization of biogases for their energy value.

Biogas from organic materials consists mainly of CH_4 and CO_2. Trace components that are often present in biogas are water vapor, hydrogen sulfide, siloxanes, hydrocarbons, ammonia, oxygen, carbon monoxide, and nitrogen. Considering the biogas is a clean and renewable form of energy that could well substitute the conventional source of energy such as fossil fuels, the optimization of this type of energy becomes crucial [2].

The predictably high percentage of methane in biogases from both biomass sources with an energy content equivalent to approximatively one-half that of natural gas has provided significant opportunities for a large number of applications [2]. In particular for waste water treatment plants, the use of biogas for on-site generation of electricity has provided significant cost saving as the electricity can match on-site electricity needs [3].

M. Turco et al., *Treatment of Biogas for Feeding High Temperature Fuel Cells*,
Green Energy and Technology, DOI 10.1007/978-3-319-03215-3_1

Biogas is a versatile renewable energy source, which can be used for replacement of fossil fuels in power and heat production, and as gaseous vehicle fuel. Methane-rich biogas (biomethane) can also replace natural gas as a feedstock for producing chemicals and materials.

The production of biogas through anaerobic digestion (AD) offers significant advantages over other technologies of bioenergy production. It has been acknowledged as one of the most energy-efficient and environmentally beneficial technology for bioenergy production [4] for many reasons: (1) the produced biogas can drastically reduce GHG emissions compared to fossil fuels by utilization of locally available resources; (2) it reduces the release of methane to the environment, (by combusting the biogases to convert methane to CO_2, the global warming potential of the biogases is reduced to 8 % of its former impact as methane is considered 21 times (IPCC 1996) more impacting as a greenhouse gas in comparison with CO_2 (as calculated from $(1 + 1)/(21 + 1) \times 100 = 8$ %, assuming methane is 50 % of the biogas stream. Hence from combustion of the biogas that transforms methane to CO_2 carbon leads to some abatement of global warming impacts [3]; (3) it can be used as an alternative to fossil fuels [5]; the digestate can substitute mineral fertilizer and can be used as improved fertilizer.

1.2 Anaerobic Digestion

Anaerobic digestion (AD) has been developed mainly to process agricultural wastes in order to provide renewable sources of energy, but other benefits, such as environmental, agronomic, hygienic and social ones, can be obtained by the use of this technology [6].

The agricultural sector deserves great interest: in the European Union (EU), 1500 million tons of biomass could be digested anaerobically each year, and half of this potential is accounted for by energy crops [7].

Anaerobic digester effluents have other agronomic advantages because the pH in manure fed digesters increases from 7.0 to 8.0 during AD. Because of this higher pH, AD effluent is more appropriate to fertilize acid soils [8]. Anaerobic digestion also has the potential to reduce viability of weed seeds in livestock manure [9, 10] thereby reducing needs for herbicides and makes the manure suitable for organic farms.

According to the Food and Agriculture Organization of the United Nations (FAO) report entitled “Livestock’s Long Shadow” [11], livestock production is achieved at a substantial environmental cost. On a worldwide basis, it contributes 18 % of global greenhouse gas (GHG) emissions. GHG emissions from animal production include CH_4 directly emitted from domestic animals or livestock manures, and N_2O emitted from land applied manures and grazed lands [12].

Methane recovery from animal waste has been extensively investigated and is 0.2–0.4, 0.2–0.3, and 0.35–0.6 L CH_4/g volatile solids (VS) from swine, cow, and poultry slurries, respectively [10, 13–31].

Reported values for CH_4 recovery from grass, waste grease, and food wastes are 0.55, 1.00, and 0.60 L/g VS, respectively [31]. Farm bioreactor energy output can be substantially increased by improving the C:N ratio via co-digestion of animal manure having low C:N ratio with high C:N ratio feedstocks: municipal organic wastes [32, 33], industrial organic wastes [34] or crops such as grasses, grass silages, or crop residues [35–37]. For example, Comino et al. [36] reported a 109 % increase of CH_4 yield during co-digestion of cow manure and a crop compared to manure alone. Another important environmental benefit of co-digestion is that it reduces the volume of municipal solid and industrial organic waste going to landfills as these nutrients are recycled onto farmland.

AD can contribute to drastically reduce uncontrolled fugitive CH_4 emissions from stored manure, provided that some conditions occur: (1) bioreactor is properly designed (2) bioreactor retention time is enough to give the almost complete digestion of substrate; (3) the long-term storage tank receiving the biogas should have a gas tight cover to collect and recycle residual CH_4.

A limited number of studies addressing effects of AD treatment on N_2O emissions have been reported. Amon et al. [7] indicated that AD is an effective way to reduce GHG emissions from dairy manure slurries, as AD-treated dairy manure emitted 28 % less N_2O than raw manure after field application.

Studies dealing with effects of manure AD on NH_3 emissions from fields have been contradictory with some authors reporting lower NH_3 emissions with digested manure than with raw manure.

One of the main advantages of AD is that it conserves crop nutrients. In addition, the mineralized fraction of N and P is increased [38–42].

The N/P ratio was increased from 3.9 in raw manure to 5.2 in the bioreactor effluent and to 9.2 in the supernatant fraction of settled effluent. This separation of nutrients increased the agronomic value of manure as it more closely matched crop nutrient requirements. Another advantage of AD manure as fertilizer is reduction in odor, with a high mineralized N content and N:P ratio, increases the window in which it can be applied to land to meet nutrient requirements at various stages of crop growth.

1.2.1 Anaerobic Digestion Steps

Anaerobic digestion is a complex biological process that converts organic materials to methane through three major steps occurring with the help of enzymes acting as catalysts: hydrolysis, acetogenesis, and methanogenesis. Biogas contains mainly CH_4 40–75 % vol. and CO_2 15–60 % vol. Trace amounts of other components such as H_2O 5–10 % vol., H_2S 0.005–2 % vol., siloxanes 0–0.02 % vol., halogenated hydrocarbons (VOC) < 0.6 % vol., NH_3 < 1 % vol., O_2 0–1 % vol., CO < 0.6 % vol., and N_2 0–2 % vol. can be present and might be inconvenient when not removed [43, 44].

The theoretical or stoichiometric production of methane in anaerobic digestion can be calculated according to [45]:

$$C_\alpha H_\beta O_\delta N_\gamma S_\varepsilon + yH_2O \rightarrow xCH_4 + \gamma NH_3 + \varepsilon H_2S + (\alpha - x)CO_2 \quad (1.1)$$

In which

$$x = (4\alpha + \beta - 2\delta - 3\gamma - 2\varepsilon)/8 \quad (1.2)$$

and

$$y = (4\alpha - \beta - 2\delta + 3\gamma + 2\varepsilon)/4 \quad (1.3)$$

Taking into account the stoichiometry of the above equations, the levels of methane and CO_2 produced from the decomposition of different substrates can be estimated: 50–70 % for CH_4 and 30–50 % for CO_2 [46]. Levels of methane from the decomposition of fat were about 70 %, about 63 % from protein, and about 50 % from cellulose decomposition [2].

AD process can be divided up into four phases: hydrolysis, acidogenesis, acetogenesis/dehydrogenation, and methanation (Fig. 1.1).

The different phases are carried out by different consortia of microorganisms [1, 47].

A microbial community may contain up to 60 bacterial and Archaean species growing under anoxic conditions [48, 49]. Their coexistence is based on trophic interactions, growth factor exchange, and the action of physiologically active substances [50, 51].

A microbial community consumes a broad range of organic substrates: poly and monosaccharides, proteins, amino acids, organic acids, alcohols, aromatic compounds, etc. [49, 52, 53]. As reported by Davies [54], the following amounts of final products are produced from one glucose molecule:

$$1.0\,\text{g}\,C_6H_{12}O_6 \rightarrow 0.25\text{g}\,CH_4 + 0.69\text{g}\,CO_2 + 0.06\text{g of cells} + 632\,\text{kJ of energy} \quad (1.4)$$

In other words, 2.8 mol of CH_4 and 2.6 mol of CO_2 can be produced from 1 mol of glucose.

Methane-producing microorganisms (or methanogens) are obligate anaerobes, which represent a dominant group of Archaea. They are included in five orders of the Euryarchaeota phylum: Methanobacteriales, Methanococcales, Methanosarcinales, Methanomicrobiales, and Methanopyrales [55–58].

Methanogens are very diverse in morphology (from simple rods, cocci, or sarcinae to spirals and irregular coccoids), cell wall structure, metabolism, and physiology [59]. Many species can utilize single carbon compounds (methanol, formate, or methylated amines) as carbon sources. For example, methanol is an important methanogenesis substrate. It is formed during the hydrolysis of pectin, which is common in cellulose containing substrates [60, 61]. Recent studies have revealed numerous newly identified methanogen strains and taxa [58].

Methanogens are narrowly focused "specialists." They consume a limited range of substrates produced by other members of the community. The main

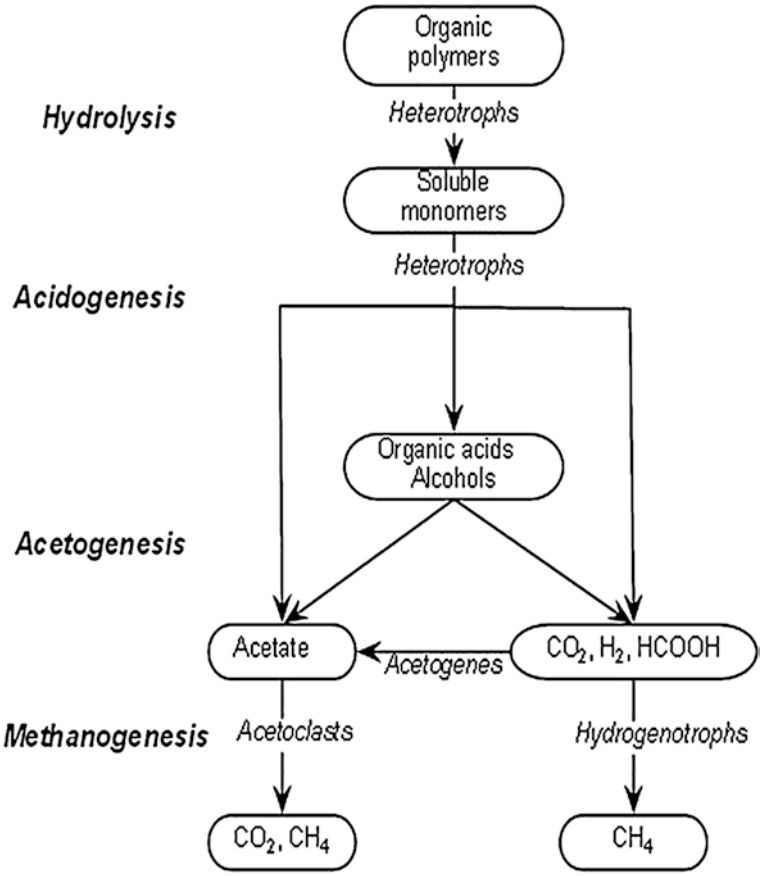

Fig. 1.1 Anaerobic digestion scheme

methanogenesis substrates are carbon dioxide and hydrogen (hydrogenotrophic methanogenesis), acetate (acetoclastic methanogenesis), formate, methanol, and methyl amines. The most energetically favorable process is the formation of methane and water [62, 63]:

$$4H_2 + CO_2 = CH_4 + 2H_2O\ \Delta G^\circ = +135.6\ \text{kJ/mol} \tag{1.5}$$

Hydrolyzing and fermenting microorganisms are responsible for the initial attack on polymers and monomers and produce mainly acetate and hydrogen and some amounts of volatile fatty acids (VFA) such as propionate and butyrate. Hydrolytic microorganisms lead to hydrolytic enzymes, e.g., cellulose, cellobiase, xylanase, amylase, lipase, and protease.

Most of the bacteria are anaerobes such as Bacteriocides, Clostridia, and Bifidobacteria, but some facultative anaerobes such as Streptococci and Enterobacteriaceae can take part. The higher VFA are converted into acetate

and hydrogen by obligate hydrogen-producing acetogenic bacteria, like as *Acetobacterium woodii* and *Clostridium aceticum*. The accumulation of hydrogen can inhibit the metabolism of the acetogenic bacteria. Therefore, an extremely low partial pressure of hydrogen is essential for the acetogenic and hydrohen-producing bacteria. Although many microbial details of metabolic networks in a methanogenic consortium are not clear, present knowledge suggests that hydrogen may be a limiting substrate for methanogens [64]. Since it is recognized that the addition of hydrogen-producing bacteria to the natural biogas-producing consortium increases the daily biogas production [1].

Acs et al. [65] had found the positive correlation between the enhancement of biogas production and the presence of an added hydrogen-producing new member into the natural consortia such as *Caldicellulosiruptor saccharolyticus* [66].

CO_2 is produced in large amounts from the acetogenesis and methanogenesis while the H_2 produced with very small quantities from acetogenesis process. Approximately 70 % CH_4 in biogas produced from acetate, and 30 % CH_4 produced from CO_2 and H_2 [67].

At the end of the degradation chain, two groups of methanogenic strict anaerobes bacteria produce methane from acetate or hydrogen and carbon dioxide. Only few species are able to degrade acetate into CH_4 and CO_2, e.g., *Methanosarcina barkeri*, *Metanonococcus mazei*, and *Methanotrix soehngenii*, whereas all methanogenic bacteria are able to use hydrogen to form methane. The first and second groups of microbes as well as the third and fourth groups are linked closely with each other [68]. Therefore, the process is completed in two stages that requires equal rates so that anaerobic digestion should be balanced. If the first degradation step is too fast, the acid concentration rises, and the pH drops below 7.0 which inhibits the methanogenic bacteria. On the contrary if the second phase is too fast, methane production is limited by the hydrolytic stage. Thus, the rate-limiting step depends on the nature of the substrate used for AD. For example compounds like cellulose, proteins, or fats are cracked slowly into monomers within several days, whereas the hydrolysis of soluble carbohydrates occurs within few hours.

It is difficult to describe the whole process by reliable kinetics since hydrolysis of complex insoluble substrate depends on many different parameters such as particle size, production of enzymes, pH, and temperature. A systematic description of the complex kinetics models is given in few works on organic waste digestion [47, 69]. For solid wastes, several kinetic models were developed for mesophilic and thermophilic digestion [70–72]. The kinetic of biogas production from energy crops and manure was studied recently in detail by Anhuradha et al. [73]. Results from quasi-continuous digestion experiments have shown that the degradation can be described by a simple first-order reaction. For the application of this simple model, only the maximum gas yield of the substrate and the specific reaction rate must be known from a continuously digestion test.

The digestion process takes place at psicofilic (5–20 °C), mesophilic (30–45 °C), or thermophilic (45–60 °C) temperature conditions. It is important to keep a constant temperature during the digestion process, as temperature changes or fluctuations will effect the biogas production negatively.

Thermophilic processes are more sensitive to temperature fluctuations and require longer time to adapt to a new temperature. Mesophilic bacteria tolerate temperature fluctuations of ±3 °C without significant reductions in methane production. The growth rate of methanogenic bacteria is higher at thermophilic temperatures making the process faster and more efficient. Therefore, thermophilic digester can operate at higher loadings or at a lower retention times than at mesophilic conditions. But the thermophilic process temperature results in higher instability and a higher risk for ammonia inhibition. Ammonia toxicity increases with increasing temperature, and washout of microbial population can occur [74, 75]. Ammonia is considered to be responsible for process inhibition at high concentrations [76].

For the growth and survival of the specific groups of microorganisms, several macro- and micronutrients are necessary. Macronutrients are carbon, phosphor, and sulfur. The need of nutrients is very low due to the fact that not much biomass is developed, so that a nutrient ratio of C:N: P:S = 600:15:5:1 is sufficient. Trace elements like iron, nickel, cobalt, selenium, molybdenum, and tungsten are important for the growth rate of microorganisms and must be added if, e.g., energy crops are used for biogas production as the only substrate [77, 78].

The necessary concentration for the micronutrients is very low and in the range between 0.05 und 0.06 mg/L. Only iron is necessary in higher concentration between 1 and 10 mg/L [79].

Variations in pH may be crucial for the operation of a methanogenic community. Neutral pH values are optimal for methanogen growth, and values below 5.0 suppress it. However, it has been reported by Kim et al. [80] that low pH (4.5) does not inhibit hydrogenotrophic methanogenesis in a methanogenic community grown in a semibatch fermenter process with glucose as a substrate and the hydraulic retention time equal to 9 days. Other authors [81] suppose that a fermenter has niches with neutral pH, where methanogenesis can be initiated. Methane formation takes place within a relatively narrow pH interval, from 6.5 to 8.5 with an optimum interval between 7.0 and 8.0. The process is severely inhibited if the pH decreases below 6.0 or rises above 8.5.

1.2.2 Substrates for Anaerobic Digestion

All types of biomass can be used as substrates for biogas production as long as they contain carbohydrates, proteins, fats, cellulose, and hemicelluloses as main components. The composition of biogas and the methane yield depends on the feedstock type, the digestion system, and the retention time [82]. The theoretical gas yield varies with the content of carbohydrates, proteins, and fats (Table 1.1).

The real methane content in practice is generally higher than the theoretical values shown in Table 1.1 because a part of CO_2 is solubilized in the digestate.

Carbohydrates and proteins show much faster conversion rates but lower gas yields. All substrates should be free of pathogens and other organisms; otherwise, pasteurization at 70 °C or sterilization at 130 °C is necessary prior fermentation.

Table 1.1 Maximal gas yields and theoretical methane contents [82]

Substrate	Biogas (Nm^3/t TS)	CH_4 (%)	CO_2 (%)
Carbohydrates[a]	790–800	50	50
Raw protein	700	70–71	29–30
Raw fat	1200–1250	67–68	32–33
Lignin	0	0	0

[a]Only polymers from hexoses, not inulins and single hexoses

Table 1.2 Amount of biogas for biomass used [174]

Biomass	m^3biogas/t TSV
Animal residues	200–500
Agricultural residues	350–400
Industrial residues	400–800
Organic waste from slaughter	550–1000
Sawage	250–350
Municipal solid waste	400–600
Energy crops	550–750

The contents of nutrients, respectively, the C/N ratio should be well balanced to avoid process failure by ammonia accumulation. The C/N ratio should be in the range 15–30 [83, 84]. The composition of the fermentation residue should be such that it can be used as fertilizer.

Forage crops have the advantage of being suitable for harvesting and storing with existing machinery and methods. The specific methane yield is affected by the chemical composition of the crop which changes as the plant matures [85]. Harvesting time and frequency of harvest thus affect the substrate quality and biogas yield. Amon et al. [7] have shown that maize crops were harvested after 97 days of vegetation at milk ripeness produced up to 37 % greater methane yields when compared with maize at full ripeness.

In Table 1.2, the biogas amounts from different substrates are reported [86, 87].

The main materials for biogas production in industrial enterprises are manure and the organic fraction of household and industrial waste in the form of sewage [86, 87]. Studies are being conducted on biogas production from hard to process materials, such as peat and coal [88, 89].

Numerous basic and biotechnological studies are dedicated to biogas formation from manure, sewage sludge, and various kinds of organic waste [90–93]. Animal manure has a surplus of alkalinity which stabilizes the pH value at VFA accumulation. VFA are a key intermediate in the process and can inhibit methanogenesis in high concentrations. Acetic acid is usually present in higher concentration than other fatty acids, but propionic and butyric acids have more inhibitory effective to methanogens [94, 95].

Anaerobic digestion produces biogas at average rates of 0.30, 0.25, and 0.48 L/g volatile solids from swine, bovine, and poultry slurries, respectively. The biogas produced is of high quality with a CH_4 concentration of 60–80 %.

It is much more profitable from both economic and environmental viewpoints to supplement pure waste with cosubstrates, for example, matter obtained from energetic plants. Such plants are purposely grown herbs (sugarcane, maize, millet, sunflower, silver grass, rapeseed, etc.) or underwood [96–98]. Plant waste obtained from wood processing, agriculture, and animal husbandry can also improve the biogas yield significantly. Additional benefit is that their growth, collection, and processing do not require additional costs [96]. Some authors [49, 99] reported that the yields of biogas with the use of grass, potato tops, maize stems, sunflower husk, and wheat straw were 630, 420, 420, 300, and 340 L CH_4/kg, respectively, whereas the fermentation of cattle manure alone yields 250 CH_4/kg. In other studies [97], the yields of biogas from cattle feces, pig feces, and farmyard manure were 25, 30, and 60 L CH_4/kg of wet biomass, respectively. The fermentation of beet leaves, fodder beet, Sudan grass (*Sorghum vulgare* var. *sudanense*), herb silage, maize silage, and grain residues yielded 60, 90, 130, 160, 230, and 550 L CH_4/kg of wet biomass, respectively. Maize and herb silages are most commonly used in Germany as cosubstrates in fermenters [97].

The most important parameter for choosing energy crops is their net energy yield per hectare. Many conventional forage crops produce large amounts of easily degradable biomass which is necessary for high biogas yields [82].

The methane-rich biogas from lignocellulosic materials comes mostly from hemicelluloses and cellulose [45]. The production of biogas from lignocellulosic materials was dependent on the performance, cost effectiveness, and product generation of pretreatment process. Hence, the methane yield per wastes volume can be further improved.

Few data are reported on cellulose as a substrate for biogas production, although cellulose is the abundant component of municipal solid waste (MSW) [100–102]. Nowadays, the conversion of paper materials to biogas attracts attention again. It is partially related to the separate collection of waste, used in many countries. In addition, paper and cardboard are the largest biodegradable MSW fraction [96, 102, 103] and the sewage formed in anaerobic degradation of cellulose containing materials is nontoxic [103].

The main feature of anaerobic degradation of cellulose is the complex structure of the microbial communities, which form a specific food chain [99]. Due to its complexity, the organic compounds in lignocellulosic material were not fully degraded during the process [111, 112]. Hydrolysis can be the rate-limiting step for anaerobic digestion process in cases that the substrate was in particulate form [113].

Microbial populations converting cellulose to biogas are taxonomically diverse. They are different under psychrophilic, mesophilic, or thermophilic conditions, but they generally act in similar way [104–106]. The composition and stability of a microbial community and, consequently, the efficiency of the whole process depends on the growth conditions (temperature and pH), organic substrate composition and structure, the rate of organic material load in the fermenter, the retention time of the solid matter, and other factors [92, 107–109].

In using the lignocellulosic materials, the biodegradability of the substrate was a key factor in determine the percentage of the theoretical yield [110].

1.3 Improvement of Biogas Production Techniques

To enhance biogas production, various techniques can be applied, such as pretreatments (chemical, thermal, enzymatic) and/or biotechnological such as co-digestion of the substrate (manure, sewage sludge) with other wastes that make the anaerobic digestion more profitable [114], the use of serial digester. Co-digestion with other wastes, whether industrial (glycerin), agricultural (fruit and vegetable wastes), or domestic (municipal solid waste) is a profitable option for improving biogas production [114–116]. Serial digester configuration which consists of main digester with long retention time and post-digester with short retention time could improve biogas production and achieve better effluent quality in terms of VFA concentration compared to a single reactor [117].

Maceration of biomass, like as manure, to produce particle sizes below 0.35 mm has increased biogas yield by 15–20 % [118]. Thermal treatment of sewage sludge has been shown to increase the biogas yield by 50 and 80 % after heating to 70 and 170 °C, respectively [119]. Alkaline treatment of sewage sludge had been observed to increase the speed of biogas production and to cause an initial rate increase of 150 % [120]. Pretreatment using *N*-methylmorpholine-*N*-oxide (NMMO or NMO) had been reported by Teghammar et al. [110]. This pretreatment improved the methane yield by 400–1,200 % compared to untreated materials. Ozone oxidation of sewage sludge resulted in an initial biogas yield increase of 200 % [121], while wet oxidation produced 35 % methane yield increase. Ultrasound and microwave treatments of sewage sludge had been shown to increase initial gas production by 20–50 % [122]. Extrusion as pretreatment was reported by Hjorth et al. [111] and it had shown 18–70 % increment of biogas yield after 28 days. Biological pretreatment could also be an effective method for optimizing biodegradability and enhancing the highly efficient biological conversion of lignocellulosic wastes into biogas. Zong et al. [123] used corn straw at ambient temperature (about 20 °C) treated by new complex microbial agents to improve anaerobic biogas production. These treatment resulted in an increase of total biogas yield of 33.07 %, of 75.57 % for methane yield, and 34.6 % shorter technical digestion time compared with the untreated sample.

1.3.1 Pretreatment of Biomass

Hydrolysis of organic matter is considered to be the rate-limiting step in biomass degradation. If biomass have low biodegradability, high sludge handling/disposal costs, and/or produce a low amount of biogas, pretreatments (PTs) can be incorporated as sustainable improvements [124]. Such PTs include mechanical, thermal, chemical, biological, and combinations of them [125]. PTs further hydrolyze the so-treated feed, thus improving the AD step, since organic matter is now more accessible to the anaerobic microorganism consortium [126]. Solubilization of

chemical oxygen demand (COD) and reductions of total and volatile solids (TS, VS) are achieved for greater solids reduction rates during mesophilic and thermophilic AD. This typically leads to added pathogen reduction, shorter hydraulic residence times, reduction of residual solids, and smaller reactor volumes.

Such treatments generally favor the access of methanogenic bacteria to the intracellular matter, thereby improving biogas production by 30–50 % [127]. It is also important the efficacy of PTs typically increases with the concentration of feed solids, so it could be relevant to evaluate cost and energy demands of concentrating the sludge prior to PT [126]. More research is needed to ascertain the level of benefit that would be gained by applying PTs under full-scale conditions [124, 128].

The PTs described in literature [129] were ultrasound (ULT), chemical (CM), conventional heating (CH), and microwave heating (MWH), based on energy intensiveness, commonality, feasibility, and novelty, respectively.

1.3.1.1 Ultrasound PT

ULT frequency and specific energy (E_s) are the main factors affecting chemical oxygen demand (COD) solubilization and biogas production. Low frequencies (<100 kHz) can promote mechanical and physical degradation while high frequencies promote sonochemical favoring the solubilization of the organic matter. Optimal working ranges (20–42 kHz, 70–300 W, 6,000–18,000 kJ/kg TS) for frequencies and E_s have been found and do not demonstrate much significant variance regardless of feed characteristics [124, 128].

1.3.1.2 Chemical PT

Acid and alkaline PTs can be used to degrade complex organic compounds regardless of low temperatures. Alkaline treatment is performed by increasing the sludge pH to 12 and sustaining it for an optimal duration. Complex organics such as polycyclic aromatic hydrocarbons, lipids, and proteins are hydrolyzed into smaller and more soluble compounds. Desired bacteria can be harmed, however, and chemical addition speeds up equipment corrosion and fouling. Additionally, some of the soluble compounds that are formed are not biodegradable [130, 131] Energy demands in these processes include also mixing and any heating energy. Typical working ranges are: 1–21 kg/m^3 NaOH, 0.25–24 h, pH = 10–12 [129].

1.3.1.3 Conventional heating PT

Temperatures required for conventional heating PT typically range from 60 to 180 °C. Heating is supplied by heat exchangers or steam injection. Though conventional heating requires a high increase in energy demand, it is balanced by higher sludge biodegradability and by the use of sludge residual heat to maintain

the temperature in the digester. Dewaterability and pathogen reduction are increased with thermal pretreatment and result in reduced sludge disposal costs and improved sludge stabilization. Heat transfer is limited by the wastewater's (WW) thermal conductivity, density, viscosity, and specific heat; moreover heating to the depth of the material is time-consuming [127]. Energy is also lost in the process. Demands in the proc conventional heating include heat and mixing energy. Working ranges are: 50–170 °C, 0.25–1 h.

1.3.1.4 Microwave Heating PT

Microwave irradiation has been studied as an alternative to conventional heating [129, 132, 133]. The irradiation corresponds to 1 mm–1 m wavelengths in the electromagnetic spectrum with equivalent frequencies of 300 GHz–300 MHz, respectively. For the heating or drying of thin substances, frequencies of 2,450 MHz with correspondingly short wavelengths (12.24 cm) are adequate. If deep penetration into materials is required, frequencies of 900 MHz with correspondingly long wavelengths (37.24 cm) and energy outputs of up to 100 kW are required. MWH is absorbed selectively by substances containing more moisture, sugars, or fats. The distribution of heat in microwave irradiated WW is thus not uniform because the fluid is two-phase (solid and liquid) and heterogeneous in both phases. Warming or cooling the unit as in conventional heating is not required and energy is conserved because microwaves can be instantly activated or deactivated. Microwave irradiation can be up to 50 % more efficient than conventional heating methods. Microwave units also experience less fouling because their surfaces are not brought to the same high temperatures as the surfaces of conventional heating units [126]. Energy demands in microwave irradiation processes include the necessary conversion efficiencies from "at-the-wall" power to applied heat and mixing energy. Working ranges are: 2,450 MHz, 400–1250 W, 0.03–025 h [129].

Bordelau and Droste [129] evaluated the costs of the different pretreatments processes using a model created with Microsoft excel and its Visual Basic Assistant. Net costs per influent flow for ultrasound, chemical, conventional heating, and microwave were 0.0166, 0.0217, 0.0124, 0.0119 $/m^3 and 0.0264, 0.0357, 0.0187, and 0.0162 $/m^3 for average and high conditions, respectively. The average cost increase from results excluding pretreatment use for all processes was 0.003 and 0.0055 $/m^3 for average and high conditions, respectively.

1.4 Co-digestion

An interesting option for optimizing biogas production yields was using co-digestion technique [134]. This technique can be defined as the combined anaerobic treatment of several substrates with complementary characteristics. The benefits of using co-digestion techniques including dilution of potential toxic compounds,

improved balance nutrients, synergistic effect of microorganism, increased load of biodegradable organic matter, and higher biogas yield [135].

According to Mata-Alvarez et al., digestion of more than one substrate in the same digester can establish positive synergism and the added nutrients can support microbial growth [136].

Various co-digestion techniques had been done by mixing the substrate for biogas production with compound such as glycerol, agricultural wastes, and food wastes.

The benefits of using mixing animal manure and glycerol were (1) the elevated content of water in manure acts as solvent for glycerol; (2) the high alkalinity of manure gives a buffering capacity for the temporary accumulation of volatile fatty acids; (3) the wide range of macro- and micronutrients present in the manure were essential for bacterial growth; and (4) glycerol supplies rapidly biodegradable matter [136]. Co-digestion with other wastes, whether industrial (glycerin), agricultural (fruit and vegetable wastes), or domestic (municipal solid waste) was also a suitable option for improving biogas production [115, 116].

1.5 Reactors

Anaerobic digestion for biogas production was commonly carried out in continuously stirred tank reactor (CSTR) [137, 138].

Jeihanipour et al. [139] investigated a two-phase CSTR, modified as stirred batch reactor (SBR) and up-flow anaerobic sludge blanket bed (UASB) process in producing biogas from pretreated and untreated textiles substrates. However, although should enhance digestion performance, the biogas yield by two-phase system was nearly the same as the single CSTR, probably because the two-phase system was sensitive to the substrate with high easily degradable organic load [140]. The main disadvantage of using two-phase system is the separation of acidogenic and methanogenic step can disrupt the synthrophic relationship between bacteria and methanogens, which can cause product inhibition in the acidogenic reactor [140, 141].

An alternative approach to overcome the problems with one-step CSTR and two-phase system is to operate two methanogenic reactors connected in series (serial digestion system) [137]. Some researches in biogas production using serial digestion have been done. Boe has demonstrated that serial digestion, with percent volume distributions of 90/10 or 80/20 between the two methanogenic reactors, improved biogas production by 11 % compared to a traditional one-step CSTR process [142]. Boe and Batstone [143] confirmed that the longer the retention time in the post-digester (second reactor of serial process), the higher the methane recovery of the overall serial digestion. Kaparaju et al. examined the possibility of optimizing biogas production from manure in a bench scale cascade of two methanogenic serial CSTR at mesophilic conditions operated at 55 °C with 15 days hydraulic retention time (HRT) [137]. Some works showed that serial digestion improved biogas production from manure, as compared to one-step process, and

that the best volume distribution was 70/30 and 50/50 %. Ge et al. [144] achieved 44 % volatile solid (VS) reduction in a bench scale system of working volume of 4.6 L, the dual mesophilic digestion of primary sludge with HRTs 2 and 14 days for first and second stage, respectively. Thus, serial digestion can be considered a method to improve conversion efficiency. However, the extra installation costs and process complexity in executing serial digestion concept should be evaluated with the economic gain achieved due to extra biogas produced.

1.6 Thermal Gasification

Gasification is one of the promising technologies to exploit energy from renewable biomass, which is derived from all living matters, and thus is located everywhere on the earth. Forest residues such as dead trees and wood chips, agricultural residues, municipal organic wastes, and animal wastes are common examples of biomass that can be gasified.

However, biomass is locally distributed across the regions. For example, forest residues are distributed throughout the forest and so are agricultural residues in the rural area. In addition, biomass is excessively moist (>50 %) at the source which makes it difficult to transport and it is not feasible to store it at the place of origin [145]; so the transportation of raw biomass is cost-intensive [146]. Moreover it is irregular in size, and thus difficult to feed into the conversion unit. Therefore, development of a biomass-based power generation facility needs several factors to be considered such as supply chain management [147–149], pretreatment of biomass [150–152], conversion of biomass to fuel gas [153, 154], and cleaning and utilization of fuel gas for power generation [155–158].

Biomass gasification gas can be used in different ways to produce energy. For instance, it can be used in combination with a steam turbine and boiler, where fuel gas can be burned in the boiler to generate high-temperature and high-pressure steam which is then passed through the steam turbine to generate electricity [159]. The challenge of this system is related to the net electrical efficiency, which is extremely low (10–20 %) that increases the capital cost.

In gasification, moisture content in biomass has a significant role. Under gasification temperature, steam generated from moisture works as a gasifying agent, reacting with volatiles and char to convert them to product gas as well as taking part in water–gas shift reaction in order to enhance the hydrogen content [160, 161]. However, the excessive moisture content in biomass (more than 40 wt%) reduces the thermal efficiency of the gasification system [162]. This is because the heat absorbed by the unreacted steam in three steps, including heating of moisture from room temperature to 100 °C latent heat of vaporization and heating of steam to gasification temperature is totally lost from the system, and thus increases the thermal cost [163]. On the other hand, the complete drying of biomass is cost-intensive as well as during gasification it needs further addition of water to balance

the hydrogen content in the product gas. Therefore, a limited amount of moisture in biomass usually around 40 wt% is beneficial for gasification [164, 165].

1.6.1 Operating Variables

1.6.1.1 Temperature

Two major problems limit high-temperature gasification above 1000 °C are: (1) the ash melting, especially when high ash containing biomass (ash content around 20 %) and (2) the requirement of stringent reactor specification. Therefore, numerous studies have been conducted to investigate the gas composition, tar concentration, and other requirements within the temperature range of 750–900 °C. For instance, an attempt has been made to produce biogas for feeding solid oxide fuel cells (SOFC) [157, 166–169] and MCFC [170, 171]. An increase in CO and H_2 content and a decrease in CO_2 and CH_4 were observed when temperature was increased from 650 to 800 °C in a bubbling fluidized bed gasifier. The raising of temperature from 750 to 850 °C in a fluidized bed gasifier significantly reduced the tar content in the product gas, while increased the CO and H_2 concentration. However, the tar yield from the gasification below 1000 °C is significantly higher than the acceptable range [157, 172, 173], and thus it needs gas cleaning.

1.6.1.2 Pressure

Gasifier operating pressure affects not only equipment cost and size but the whole plant, including the necessary gas cleanup systems. Since gas synthesis processes operate at elevated pressures, the syngas generated by low pressure gasifiers must be compressed. This favors low temperature gas cleaning since the syngas must be cooled prior to compression in any case. Biomass gasification is generally carried out in the range 1–10 bar. High-pressure gasification favors hot, pressurized cleanup of the syngas and operation of downstream equipment at high temperature and sufficiently high pressure to accommodate flow control and equipment pressure drops. Depending on the downstream application of the product gas, gasification of biomass is often conducted under atmospheric and high pressures.

In addition, an increase in the gasifier pressure reduces the tar yield in the product gas. However, some investigations conducted [174] in the fluidized bed gasifier have shown that the concentration of tar, mainly naphthalene, increased with increasing gasifier pressure from 0.1 to 0.5 MPa, and thus the concentration of CO decreased, while CH_4 and CO_2 increased. A model gasification coupled to an SOFC and gas turbine was conducted to show that a moderate pressure, for instance up to 4 bar, does not have a major impact on the gasification process. Interestingly, it affected turbine efficiency and, thus the unit's overall efficiency increased from 23 to 35 % [157].

1.6.2 Gasifying Agent

As shown in Fig. 1.2a, b, the gasification process consists of four different physical and chemical processes. In the drying zone of the gasifier, the moisture in biomass evolved as steam, while in the pyrolysis zone, the volatile organic matter distils out from the fixed carbon. The volatiles and solid carbons then introduced into the oxidation and reduction zones successively or vice versa, depending on the gasifier types, while they react with gasifying agents to produce product gases. As gasifying agents, air, steam, carbon dioxide, and pure oxygen are commonly used. Utilization of air as a single gasifying agent produces gases with lower concentration of H_2 and CO, because air also contains nitrogen.

The mass ratio of air to fuel in any combustion unit is defined as the air–fuel ratio (AFR), the gasification requires an air–fuel ratio lower than stoichiometric one. The equivalence ratio (ER) can be defined as the ratio between the air–fuel ratio of the gasification process and the air–fuel ratio for complete combustion.

Gas composition and tar content in the product gas from different biomass gasification r under different conditions are reported in Tables 1.3 and 1.4. The produced gas must have a certain percentage of burnable gas (>20 % CO and >10 % H_2), a minimum amount of tar content (<100 mg Nm^{-3}) and be completely free of dust and other poisonous gases (NH_3, SO_2, etc.). To satisfy the requirement of product gas, a comprehensive research has been done in the last decades. The entire reactor systems can be classified into two categories: (1) updraft gasifier and (2) downdraft gasifier.

1.6.3 Updraft Gasification

Updraft gasification is basically a counter current gasification system where the air and other gasifying agents are injected from the bottom, while the biomass enters from the top and moves downward under the force of gravity. The operating principle of this type of gasifier, as shown in Fig. 1.2a, is that the feedstock material is first introduced into the drying zone at the top, followed by the pyrolysis and reduction zone and finally the unconverted solid passes through the combustion zone. In the combustion zone, solid charcoal is combusted producing heat, which effectively transfers in to solid particles during counter current flow of the rising gas and descending solids. In this gasification system, the product gas exits from the low-temperature pyrolysis and drying zone and is thus assumed to be contaminated with substantial amount of tars (Table 1.3), which is the major problem of updraft gasifiers.

Updraft gasifier can be classified as updraft fixed-bed gasifiers [178–185], fluidized bed gasifiers [178–180], and circulating fluidized bed gasifiers [181]. Fluidized and circulating fluidized bed gasifiers usually operate below 900 °C under atmospheric pressure in order to avoid ash melting. Most of the researches reported that the gas from any type of updraft gasifier contains a substantial amount of tar, and thus is not suitable for an internal combustion engine.

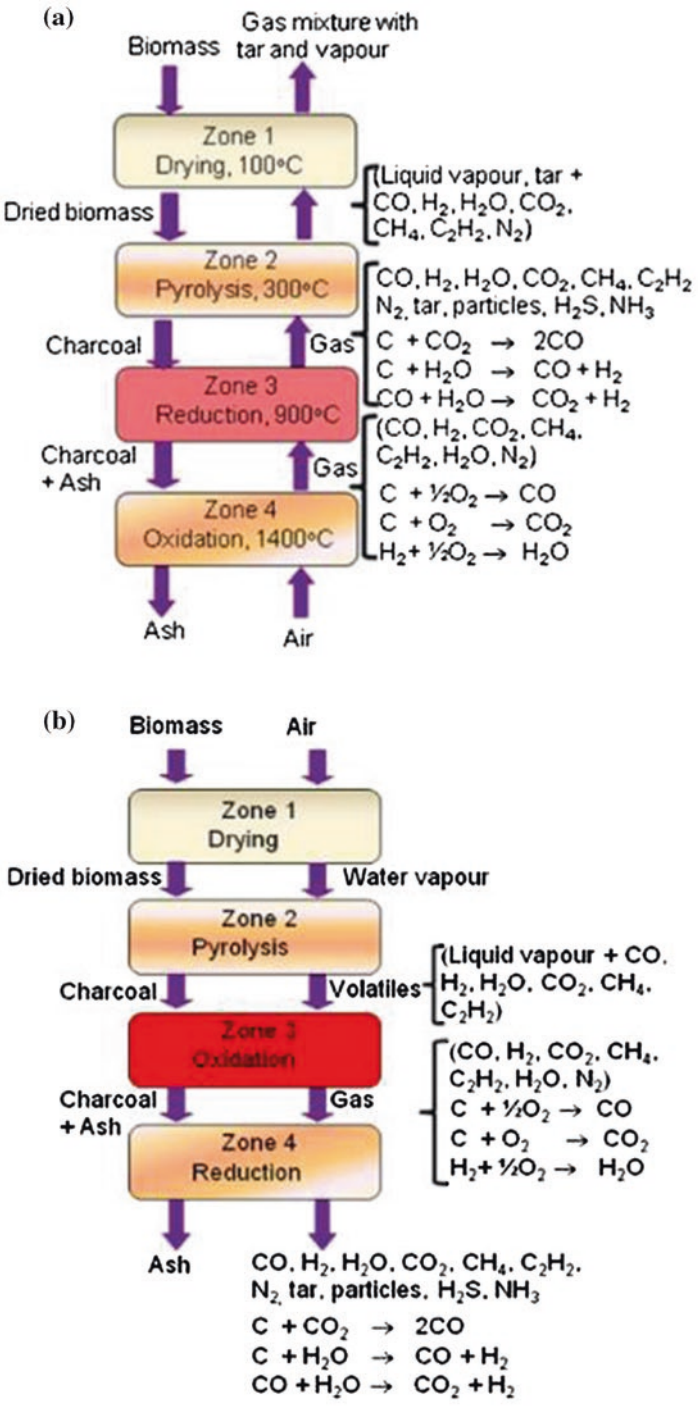

Fig. 1.2 Conceptual diagram of multiple steps in **a** updraft and **b** downdraft gasifier [174]

Table 1.3 Gas composition and tar content in the product gas from different biomass gasification in updraft gasifier under different conditions [174]

Biomass	Gasification temperature (°C)	ER	Gas composition (vol.%)	LHV (MJ Nm^{-3})	HHV (MJ Nm^{-3})	Power range (kW)	References
Cedar wood	700–900	0–0.3	–	1–33.2	–		[175]
Cedar wood	650–950	0–0.3	H_2 (30–50) CO (22–25) CO_2 (25–30) CH_4 (8–10) H_2S (35–39 ppmv) COS (<2 ppmv) N_2 free	–	6.5–12.1		[176]
Mesquite wood		2.7	CO (13–21) H_2 (1.6–3) CH_4 (0.4–6) CO_2 (11–25) N_2 (60–64)	–	2.4–3.5	10	[177]
Juniper wood		2.7	CO (21–25) H_2 (2.5–3.5) CH_4 (1.5–1.8) CO_2 (9–12) N_2 (58–61)	–	3.5–3.9	10	[177]
Rice straw	700–850	0.07–0.25	CO (10–18) H_2 (6–10) CH_4 (4) CO_2 (14–19) N_2 (46–63) NH_3 (3100 ppmv) Cl_2 (260 ppmv)	0.47–1.92	3.62–5.14	45	[178]

continued

Table 1.3 (continued)

Biomass	Gasification temperature (°C)	ER	Gas composition (vol.%)	LHV (MJ Nm^{-3})	HHV (MJ Nm^{-3})	Power range (kW)	References
–	725–925	–	CO (15–20) H_2 (55–60) CH_4 (8–10) CO_2 (15–18)	6.5–9.0	–	15	[179]
Agrol and willow and one agriculture residue Dry Distiller's Grains	800–820	0.35–0.39	CO (20–25) H_2 (30–45) CH_4 (8–12) CO_2 (15–20) H_2S (2300 ppmv) COS (200 ppmv)	2–12	–	60	[180]
Wood chip coconut shell	700–900	0.3	CO (27–40) H_2 (22–27) CH_4 (7–9) CO_2 (39–42)	–	17	15	[181]

Table 1.4 Gas composition and tar content in the product gas from different biomass gasification in downdraft gasifier under different conditions [174]

Biomass	Gasification temperature (°C)	ER	Gas composition (vol.%)	Tar content (g Nm^{-3})	HHV/LHV (MJ Nm^{-3})	Power range (kW)	References
Bagasse	1040	–	–	0.376–0.40	–	50	[182]
Hazelnut shells	1000	0.35	H_2 (13) CO (23) CO_2 (11) CH_4 (4)	–	5.0	45	[183]
Wood waste	900–1050	0.20–0–0.35	H_2 (8–12) CO (15–22) CO_2 (5–8) CH_4 (1–3) N_2 (60–70)	–	4.5–6.25	15	[184]
Biomass	–	0.27	Total combustible 45 %	0.045	6.5	10	[185]
Biomass	>900	0.26	H_2 and CO reaches 63.27–72.56 %	–	11.11	–	[160]

1.6.4 Downdraft Gasification

The operating principle of this gasifier, as shown in Fig. 1.2b, is such that the biomass and air are fed from the top, and are first introduced into the drying zone, followed by the pyrolysis, oxidation, and reduction zones, and finally the product gas is drawn out from the bottom, through the reduction zone. Since the product gas travels through the high-temperature oxidation zone and finally through the reduction zone, almost all of the organic vapors (tars) are consumed to form gas; and thus the gas is quite clean compared to the updraft gasifier. Two important requirements are needed to be maintained for this gasifier: (1) the temperature of the oxidation zone is to be kept at as high as possible (usually around 1000 °C) and (2) the distribution of the gasifying agent must be homogeneous at the throat where the oxidation of solid and vapors generated from the pyrolysis zone takes place under atmospheric pressure. Typical compositions of gas produced in downdraft gasification are reported in Table 1.4.

Agricultural waste such as bagasse was gasified in a downdraft gasifier where the effect of temperature on the tar content in the product gas was investigated [182]. The gas composition 23 % CO, 13 % H_2, 11 % CO_2, and 4 % CH_4 was achieved with HHV of 5 MJ Nm^{-3} for Hazelnut shells gasification [183]. The CO_2 concentration was reduced for wood shaving gasification, and thus the heating value slightly increased to 6.25 MJ Nm^{-3} [184]. Using an innovative two-stage downdraft gasifier, the higher heating value was achieved to 6.5 MJ Nm^3 with tar content of less than 0.045 g Nm^{-3} and total combustible gas of 45 % [185]. Utilization of steam in the gasification significantly increased the hydrogen content, thereby increasing the lower heating value to 11.11 MJ Nm^{-3} [160].

References

1. Weiland P (2010) Biogas production: current state and perspectives. Appl Microbiol Biotechnol 85:849–860
2. Andriani D, Wresta A, Atmaja TD, Saepudin A (2014) A review on optimization production and upgrading biogas through CO_2 removal using various techniques. Appl Biochem Biotechnol 172:1909–1928
3. Massé DI, Talbot G, Gilbert Y (2011) On farm biogas production: a method to reduce GHG emissions and develop more sustainable livestock operations. Anim Feed Sci Technol 166–167:436–445
4. Fehrenbach H, Giegrich J, Reinhardt G, Sayer U, Gretz M, Lanje K, Schmitz J (2008) Kriterien einer nachhaltigen Bioenergienutzung im globalen Maßstab. UBA-Forschungsbericht 206:41–112
5. Petersson A, Wellinger A (2009) Biogas upgrading technologies-developments and innovations. IEA Bioenergy
6. Yiridoe EK, Gordon R, Brown BB (2009) Nonmarket cobenefits and economic feasibility of on-farm biogas energy production. Energy Policy 37:1170–1179
7. Amon T, Amon B, Kryvoruchko V, Machmüller A, Hopfner-Sixt K, Boriroza V, Hrbek R, Friedel J, Pötsch E, Wagentristel H, Schreiner M, Zollitsch W (2007) Methane production through anaerobic digestion of various energy crop grown in sustainable crop rotations. Bioresour Technol 98:3204–3212
8. Kvasauskas M, Baltrenas P (2009) Research on anaerobically treated organic waste suitability for soil fertilisation. J Environ Eng Landsc Manage 17:205–211
9. Jeyanavagam SS, Collins ER Jr, Eldridge R (1984) Weed seed survival in dairy manure anaerobic digester. Trans Am Soc Agric Eng 27:1518–1523
10. Kramer JM, Kuzel FJ (2003) Farm-scale anaerobic digesters in the great lakes states. BioCycle 44:58–61
11. Steinfeld H, Gerber P, Wassenaar T, Castel V, Rosales M, de Haan C (2006) FAO: livestock's long shadow environmental issues and options". FAO, Rome, Italy, 416 pp
12. Kebread E, Clark K, Wagner-Riddle C, France J (2006) Methane and nitrous oxide emissions from Canadian Animal agriculture: a review. Can J Anim Sci 86:135–158 (2006)
13. Fischer JR, Iannotti EL, Sievers DM (1981) Anaerobic digestion of manure from swine fed on various diets. Agric Wastes 3:201–214
14. Stevens MA, Schulte DD (1977) Low temperature anaerobic digestion of swine manure. ASAE paper No. 77-1013. St. Joseph, MI, USA, p 19
15. Ke-Xin I, Nian-Guo L (1980) Fermentation technology for rural digesters in China. Proc. Bioenergy 80:440–442
16. Hashimoto AG (1983) Thermophilic and mesophilic anaerobic fermentation of swine manure. Agric Wastes 6:175–191
17. Wellinger A, Kaufmann R (1982) Psychrophilic methane production from pig manure. Process Biochem 17:26–30
18. Henze M, Harremoes P (1983) Anaerobic treatment of wastewater in fixed film reactors: a literature review. Water Sci Technol 15:1–101
19. Chandler JA, Hermes SK, Smith KD (1983) A low cost 75 kW covered lagoon biogas system. In: Proceedings of the Symposium on Energy from Biomass and Waste VII, Lake Buena Vista, FL, USA, pp 627–646
20. Wellinger A (1984) Anaerobic digestion: a review comparison with two types of aeration systems for manure treatment and energy production on the small scale farm. Agric Wastes 10:117–133
21. Cullimore RR, Maule A, Mansui N (1985) Ambient temperature methanogenesis from pig manure waste lagoons: thermal gradient incubator studies. Agric Wastes 12:147–157

22. Sutter K, Wellinger A (1987) ACF-system: a new low temperature biogas digester. In: Szabolcs I, Welte E (eds) Agricultural waste management and environmental protection. 4th International CIEC symposium. Braunschweig, Germany, p 554
23. Balsari P, Bozza E (1988) Fertilizers and biogas recovery installation in a slurry lagoon. In: Szabolcs I, Welte E (eds) Agricultural waste management and environmental protection, 4th International CIEC symposium. Braunschweig, Germany, pp 71–80
24. Chen TH, Shyu WH (1998) Chemical characterization of anaerobic digestion treatment of poultry mortalities. Bioresour Technol 63:37–48
25. Safley LM, Westerman PW (1992) Performance of a dairy manure anaerobic lagoon. Bioresour Technol 42:43–52
26. Safley LM, Westerman PW (1994) Low temperature digestion of dairy and swine manure. Bioresour Technol 47:165–171
27. Massé DI, Patni NK, Droste RL, Kennedy KJ (1996) Operation strategies for psychrophilic anaerobic digestion of swine manure slurry in sequencing batch reactors. Can J Civ Eng 23:1285–1294
28. Massé DI, Droste RL, Kennedy KJ, Patni NK, Munroe JA (1997) Potential for the psychrophilic anaerobic treatment of swine manure using a sequencing batch reactor. Can Agric Eng 392:5–33
29. Hansen KH, Angelidaki I, Ahring BK (1998) Anaerobic digestion of swine manure: inhibition by ammonia. Water Res 32:5–12
30. Lusk PD (1998) Methane recovery from animal manures: the current opportunities. Casebook. National Renewable Energy Laboratory US Department of Energy, Washington, DC, USA, 150 pp
31. Steffen R, Szolar O, Braun R (2000) Feedstocks for anaerobic digestion. In: Ørtenblad H (ed) Anaerobic digestion: making energy and solving modern wastes problems. AD-NETT. The European Anaerobic Digestion Network, pp 34–52
32. Hartmann H, Ahring BK (2005) Anaerobic digestion of the organic fraction of municipal waste: influence of co-digestion with manure. Water Res 39:1543–1552
33. Macias-Corral M, Samani Z, Hanson A, Smith G, Funk P, Yu H, Longworth J (2008) Anaerobic digestion of municipal solid waste and agricultural waste and the effect of co-digestion with dairy cow manure. Bioresour Technol 99:8288–8293
34. El-Mashad HM, Zhang R (2010) Biogas production from co-digestion of dairy manure and food waste. Bioresour Technol 101:4021–4028
35. Lehtomäki A, Huttunen S, Rintala JA (2007) Laboratory investigations on co-digestion of energy crops and crop residues with cow manure for methane production: effect of crop to manure ratio. Resour Conserv Recycl 51:591–609
36. Comino E, Rosso M, Riggio V (2010) Investigation of increasing organic loading rate in the co-digestion of energy crops and cow manure mix. Bioresour Technol 101:3013–3019
37. Wu X, Yao W, Zhu J, Miller C (2010) Biogas and CH_4 productivity by co-digesting swine manure with three crop residues as an external carbon source. Bioresour Technol 101:4042–4047
38. Field JA, Caldwell JS, Jeyanayagam S, Reneau RB Jr, Kroontje W, Collins ER Jr (1984) Fertilizer recovery from anaerobic digesters. Trans ASAE 27:1871–1876
39. Larsen KE (1986) Fertilizer value of anaerobic treated cattle and pig slurry to barley and beet. In: Kofoed AD, Williams JH, L'Hermite P (eds) Efficient land use of sludge and manure. Elsevier Applied Science Publishers, London, UK, pp 56–60
40. Messner H, Amberger A (1987) Composition, nitrification and fertilizing effect of anaerobically fermented slurry. In: Szabolcs I, Welte E (eds) Agricultural waste management and environmental protection. 4th International CIEC symposium. Braunschweig, Germany, pp 125–130
41. Plaixats J, Barcelo J, Garcia-Moreno J (1988) Characterization of the effluent residue from anaerobic digestion of pig excreta for its utilization as fertilizer. Agrochimica 32:236–239

42. Massé DI, Croteau F, Masse L (2007) The fate of crop nutrients during the low temperature anaerobic digestion of swine manure slurries in sequencing batch reactors. Bioresour Technol 98:2819–2823
43. Ryckebosch E, Drouillon M, Vervaeren H (2011) Techniques for transformation of biogas to biomethane. Biomass Bioenergy 35:1633–1645
44. Wellinger A, Lindberg A (2002) Biogas upgrading and utilisation. IEA Bioenergy, Task 24—Energy from biological conversion of organic waste, pp 1–20
45. Deublein D, Steinhauser A (2011) Biogas from waste and renewable resources. an introduction. Wiley-VCH, Wienheim
46. Tortora GJ, Funke BR, Case CL (2010) Microbiology, an introduction, 10th edn. Benjamin Cummings, Redwood City
47. Angelidaki I, Ellegard L, Ahring BK (1999) A comprehensive model of anaerobic bioconversion of complex substrates to biogas. Biotechnol Bioeng 63:363–372
48. Palatsi J, Viñas M, Guivernau M, Fernandez B, Flotats X (2011) Anaerobic digestion of slaughterhouse waste: main process limitations and microbial community interactions. Bioresour Technol 102:2219–2227
49. Tsavkelova EA, Netrusov AI (2012) Biogas production from cellulose containing substrates: a review. Appl Biochem Microbiol 48:421–433
50. Shin SG, Lee S, Lee C, Hwang K, Hwang S (2010) Qualitative and quantitative assessment of microbial community in batch anaerobic digestion of secondary sludge. Bioresour Technol 101:9461–9470
51. Stams AJM (1994) Metabolic interactions between anaerobic bacteria in methanogenic environments. Antonie Van Leeuwenhoek 66:271–294
52. Pöschl M, Ward S, Owende P (2010) Evaluation of energy efficiency of various biogas production and utilization pathways. Appl Energy 87:3305–3321
53. Zinder SH (1993) Physiological ecology of methanogens, In: Ferry JG (ed) Methanogenesis: ecology, physiology, biochemistry and genetics. Chapman Hall, New York, pp 128–206
54. Davies ZS, Mason D, Brooks AE, Griffith GW, Merry RJ, Theodorou MK (2000) An automated system for measuring gas production from forages inoculated with rumen fluid and its use in determining the effect of enzymes on grass silage. Anim Feed Sci Technol 83:205–221
55. Boone DR, Whitman WB, Rouviere P (1993) Diversity and taxonomy of methanogens. In: Ferry JG (ed) Methanogenesis: ecology, physiology, biochemistry and genetics. Chapman Hall, New York, pp 35–80
56. Garrity G (ed) (2001) Bergey's Manual of Systematic Bacteriology, 2nd edn. Springer, New York
57. Ferry G (2010) How to make a living by exhaling methane. Annu Rev Microbiol 64:453–473
58. Liu Y (2010) Taxonomy of methanogens. In: Timmis KN (ed) Handbook of hydrocarbon and lipid microbiology. Springer, Berlin, pp 549–558
59. Ferry JG (1993) Methanogenesis: ecology, physiology, biochemistry and genetics. Chapman Hall, New York
60. Schink B, Zeikus JG (1982) Microbial ecology of pectin decomposition in anoxic lake sediments. J General Microbiol 128:393–404
61. Pol A, Demeyer DI (1988) Fermentation of methanol in the sheep rumen. Appl Environ Microbiol 54:832–834
62. Whitman WB, Bowen TL, Boone DR (1992) The methanogenic bacteria. In: Balows A, Truper HG, Dworkin M, Harder W, Schleifer K (eds) The Prokariotes, 2nd edn. Springer, New York, pp 719–760
63. Stams AJM, Oude Elferink SJWH, Westermann P (2003) Metabolic interactions between methanogenic consortia and anaerobic respiring bacteria. Adv Biochem Eng Biotechnol 81:31–56

64. Bagi Z, Acs N, Balint B, Hovrath L, Dobo K, Perei KR, Rakhely G, Kovacs KL (2007) Biotechnological intensification of biogas production. Appl Microbiol Biotechnol 76:473–482
65. Ács N, Bagi Z, Rakhely G, Kovács E, Wirth R, Kovács KL (2011) Improvement of biogas production by biotechnological manipulation of the microbial population. In: 3rd IEEE International Symposium on Exploitation of Renewable Energy Sources. Subotica, Serbia
66. Ács N (2010) Monitoring the biogas producing microbes. Act Biologica Szegediensis 54(1):59–73
67. Ritchie DA, Edwards C, McDonald IR, Murrell JC (1997) Detection of metanogen and metanotrophs in natural environment. Glob Change Biol 3:339–350
68. Schink B (1997) Energetics of syntrophic cooperation in methanogenic degradation. Microbiol Mol Biol Rev 61:262–280
69. Gavala HN, Angelidaki I, Ahring BK (2003) Kinetics and modelling of anaerobic digestion processes. In: Scheper T, Ahring BK (eds) Biomethanation I. Springer, Berlin
70. Andara AR, Esteban JMB (1999) Kinetic study of the anaerobic digestion of the solid fraction of piggery slurries. Biomass Bioenergy 17:435–443
71. Linke B (2006) Kinetic study of thermophilic anaerobic digestion of solid wastes from potato processing. Biomass Bioenergy 30:892–896
72. Biswas L, Chowdhury R, Battacharya P (2007) Mathematical modeling for the prediction of biogas generation characteristics of an anaerobic digester based on food/vegetable residues. Biomass Bioenergy 31:80–86
73. Anhuradha S, Bakiya P, Mullai P (2013) The kinetics of biogas production in an anaerobic hybrid reactor. Int J Environ Bioenergy 7:168–177
74. Angelidaki I, Ellegaard L, Ahring B (2003) Application of the anaerobic digestion process. In: Biomethanation II. Advances in Biochemical Engineering/Biotechnology. Springer, pp 2–33
75. Nielsen HB, Agelidaki I (2008) Strategies for optimizing recovery of the biogas process following ammonia inhibition. Bioresour Technol 99:7995–8001
76. Wiegant WM, Zeeman G (1986) The mechanism of ammonia inhibition in the thermophilic digestion of livestock wastes. Agric Wastes 16:243–253
77. Abdoun E, Weiland P (2009) Optimization of monofermentation from renewable raw materials by the addition of trace elements. Bornimer Agrartechnische Berichte 68:69–78
78. Jarvis A, Nordberg A, Jarlsvik T, Mathisen B, Svensson BH (1997) Improvement of a grass-clover silage-fed biogas process by the addition of cobalt. Biomass Bioenergy 12:453–460
79. Bischoff M (2009) Erkenntnisse beim Einsatz von Zusatz- und Hilfsstoffen sowie von Spurenelementen in Biogasanlagen. VDI-Ber 2057:111–123
80. Kim IS, Hwang MH, Jang NJ, Hyun SH, Lee ST (2004) Effect of low pH on the activity of hydrogen utilizing methanogen in bio-hydrogen process. Int J Hydr Energy 29:1133–1140
81. Staley BF, Reyes III FL, Barlaz MA (2011) Effect of spatial differences in microbial activity, pH, and substrate levels on methanogenesis initiation in refuse. Appl Environ Microbiol 77, 2381–2391
82. Braun R (2007) Anaerobic digestion: a multi-faceted process for energy, environmental management and rural development. In: Ranalli P (ed) Improvement of crop plants for industrial end uses. Springer, Dordrecht, pp 335–415
83. Braun R (1982) Biogas-Methangärung organischer. Springer Wien, Abfallstoffe
84. Zubr J (1986) Methanogenic fermentation of fresh and ensiled plant materials. Biomass 11:159–171
85. Döhler H, Eckel H, Frisch J (2006) Energiepflanzen. KTBL, Darmstadt
86. Angelidaki I, Karakashev D, Batstone DJ, Plugge CM, Stams AJ (2011) Biomethanation and its potential. In: Rosenzweig, C, Ragsdale W (eds) Methanogenesis (Methods in Enzymology), vol 494. Academic Press, pp 327–351
87. Hecht C, Griehl C (2009) Investigation of the accumulation of aromatic compounds during biogas production from kitchen waste. Bioresour Technol 100:654–658

88. Ferry JG (2011) Fundamentals of methanogenic pathways that are key to the biomethanation of complex biomass. Curr Opin Biotechnol 22:351–357
89. Jones EJ, Voytek MA, Corum MD, Orem WH (2010) Stimulation of methane generation from nonproductive coal by addition of nutrients or a microbial consortium. Appl Environ Microbiol 76:7013–7022
90. Björnsson P, Mattiasson B (2008) Biogas as a resource-efficient vehicle fuel. Trends Biotechnol 26:7–13
91. Di Stefano TD, Ambulkar A (2006) Methane production and solids destruction in an anaerobic solid waste reactor due to post-reactor caustic and heat treatment. Water Sci Technol 53:43–51
92. Ferrer I, Vazquez F, Font X (2010) Long term operation of a thermophilic anaerobic reactor: Process stability and efficiency at decreasing sludge retention time. Bioresour Technol 101:2972–2980
93. Diaz EE, Stams AJM, Amils R, Sanz JL (2006) Phenotypic properties and microbial diversity of methanogenic granules from a full-scale upflow anaerobic sludge bed reactor treating brewery wastewater. Appl Environ Microbiol 72:4942–4949
94. Wang QH, Kuninobu M, Ogawa H, Kato Y (1999) Degradation of volatile fatty in highly efficient anaerobic digestion. Biomass Bioenergy 16:407–416
95. Mösche M, Jördening HJ (1999) Comparison of different models of substrate and product inhibition in anaerobic digestion. Water Res 33:2545–2554
96. Antizar-Ladislao B, Turrion-Gomez JL (2008) Biofuels Bioprod Bioref 2:455–469
97. Weiland P (2006) Biomass digestion in agriculture: a successful pathway for the energy production and waste treatment in Germany. Eng Life Sci 6:302–309
98. Yadvika S, Sreekrishnan TR, Kohli S (2004) Enhancement of biogas production from solid substrates using different techniques: a review. Biores Technol 95:1–10
99. Gladchenko MA, Gaydamaka SN, Murygina VP, Varfolomeev SD (2013) The optimization of the conversion of agricultural waste into volatile fatty acids under anaerobic conditions. Biocatalysis 69:187–193
100. Song H, Clarke P (2009) Cellulose hydrolysis by a methanogenic culture enriched from landfill waste in a semi-continuous reactor. Biores Technol 100:1268–1273
101. Pommier S, Manas LA, Lefebvre X (2010) Analysis of the outcome of shredding pretreatment on the anaerobic biodegradability of paper and cardboard materials. Biores Technol 101:463–468
102. Eleazer WE, Odle WS, Wang YS, Barlaz MA (1997) Biodegradability of municipal solid waste components in laboratory-scale landfills. Environ Sci Technol 31:911–917
103. Wolfe RS (1996) ASM News 62(10):529–534
104. Smiti N, Ollivier B, Garcia JL (1986) FEMS Microbiol Letts 35(1):93–97
105. Nozhevnikova AN, Zepp K, Vazquez F, Zehnder AJB, Holliger C (2003) Evidence for the existence of psychrophilic methanogenic communities in anoxic sediments of deep lakes. Appl Environ Microbiol 69:1832–1835
106. Li T, Mazeas Sghir A, Leblon G, Bouchez T (2009) Insights into networks of functional microbes catalysing methanization of cellulose under mesophilic conditions. Environ Microbiol 11:889–904
107. Leven L, Eriksson ARB, Schnurer A (2007) Effect of process temperature on bacterial and archaeal communities in two methanogenic bioreactors treating organic household waste. FEMS Microbiol Ecol 59:683–693
108. Gao WJ, Leung KT, Qin WS, Liao BQ (2011) Effects of temperature and temperature shock on the performance and microbial community structure of a submerged anaerobic membrane bioreactor. Bioresour Technol 102:8733–8740
109. Wijekoon KC, Visvanathan C, Abeynayaka A (2011) Effect of organic loading rate on VFA production, organic matter removal and microbial activity of a two-stage thermophilic anaerobic membrane bioreactor. Bioresour Technol 102:5353–5360
110. Teghammar A, Yngvesson J, Lundin M, Taherzadeh MJ, Sarvari HI (2010) Pretreatment of paper tube residuals for improved biogas production. Bioresour Technol 101:1206

111. Hjorth M, Christensen KV, Christensen ML, Sommer SG (2010) Solid–liquid separation of animal slurry in theory and practice: a review. Agron Sustain Dev 3:153–180
112. Mosier N, Wyman C, Dale B, Elander R, Lee YY, Holtzapple M, Ladisch M (2005) Features of promising technologies for pretreatment of lignocellulosic biomass. Bioresour Technol 96:673–686
113. Vavilin VA, Fernandez B, Palatsi J, Flotats X (2008) Hydrolysis kinetics in anaerobic degradation of particulate organic material: An overview. Waste Manage 28:939–951
114. Marañón E, Castrillón L, Quiroga G, Fernández-Nava Y, Gómez L, García MM (2012) Codigestion of cattle manure with food waste and sludge to increase biogas production. Waste Manage 32:1821–1825
115. Amon T, Amon B, Kryvoruchko V, Bodiroza V, Pötsch E, Zollitsch W (2006) Optimising methane yield from anaerobic digestion of manure: effects of dairy systems and of glycerin supplementation. Int Congr Ser 1293:217–220
116. Macias-Corral M, Samani Z, Hanson A, Smith G, Funk P, Yu H, Longworth J (2008) Anaerobic digestion of municipal solid waste and agricultural waste and the effect of co-digestion with dairy cow manure. Biores Technol 99:8288–8293
117. Boe K, Karakashev D, Trably E, Angelidaki I (2009) Effect of post-digestion temperature on serial CSTR biogas reactor performance. Water Res 43:669–676
118. Angelidaki I, Ahring BK (2000) Methods for increasing the biogas potential from the recalcitrant organic matter contained in manure. Water Sci Technol 41:189–194
119. Bougrier C, Delgenès JP, Carrere H (2006) Combination of thermal treatments and anaerobic digestion to reduce sewage sludge quantity and improve biogas yield. Process Saf Environ Prot 84:280–284
120. Lin JG, Chang CN, Chang SC (1997) Enhancement of anaerobic digestion of waste activated sludge by alkaline solubilisation. Biores Technol 62:85–90
121. Bougrier C, Battimelli A, Delgenès JP, Carrere H (2007) Combined ozone pretreatment and anaerobic digestion for the reduction of biological sludge production in wastewater treatment. Ozone Sci Eng 29:201–206
122. Xie R, Xing Y, Ghani YA, Ooi KE, Ng SW (2007) Full-scale demonstration of an ultrasonic disintegration technology in enhancing anaerobic digestion of mixed primary and thickened secondary sewage sludge. J Environ Eng Sci 6:533–541
123. Zeng X, Ma Y, Ma L (2007) Utilization of straw in biomass energy in China. Renew Sustain Energy Rev 11:976–987
124. Benabdallah El-Hadj T, Dosta J, Marquez-Serrano R, Mata-Alvarez J (2007) Effect of ultrasound pretreatment in mesophilic and thermophilic anaerobic digestion with emphasis on naphthalene and pyrene removal. Water Res 41:87–94
125. Toreci I, Eskicioglu C, Terzian N, Droste RL, Kennedy KJ (2007) Mesophilic anaerobic digestion with high temperature microwave pretreatment. Water Res 43:1273–1284
126. Eskicioglu C, Terzian N, Kennedy KJ, Droste RL, Hamoda M (2007) A thermal microwave effects for enhancing digestibility of waste activated sludge. Water Res 41:2457–2466
127. Phothilangka P, Schoen MA, Huber M, Luchetta P, Winkler T, Wett B (2006) Prediction of thermal hydrolysis pretreatment on anaerobic digestion of waste activated sludge. Water Sci Technol 58:1467–1473
128. Bougrier C, Carrere H, Delgenes JP (2005) Solubilisation of waste activated sludge by ultrasonic treatment. Chem Eng J 106:163–169
129. Bordeleau EL, Droste RL (2011) Comprehensive review and compilation of pretreatments for mesophilic and thermophilic anaerobic digestion. Water Sci Technol 63:291–296
130. Mendez JM, Jimenez BE, Barrios JA (2002) Improved alkaline stabilization of municipal wastewater sludge. Water Sci Technol 46:139–146
131. Neyens E, Baeyens J, Creemers C (2003) Alkaline thermal sludge hydrolysis. J Hazard Mater 97:295–314
132. Passos F, Carretero J, Ferrer I (2015) Comparing pretreatment methods for improving microalgae anaerobic digestion: thermal, hydrothermal, microwave and ultrasound. Chem Eng J 279:667–672

133. Ara E, Sartaj M, Kennedy K (2014) Effect of microwave pre-treatment of thickened waste activated sludge on biogas production from co-digestion of organic fraction of municipal solid waste, thickened waste activated sludge and municipal sludge. Waste Manage Res 32:1200–1209
134. Callaghan FJ, Wase DAJ, Thayanithy K, Foster CF (1999) Co-digestion of waste organic solids: batch studies. Biores Technol 67:117–122
135. Agdag ON, Sponza DT (2007) Co-digestion of mixed industrial sludge with municipal solid wastes in anaerobic simulated landfilling bioreactors. J Hazard Mater 140:75–85
136. Mata-Alvarez J, Macé S, Llabrés P (2000) Anaerobic digestion of organic solid wastes: an overview of research achievements and perspectives. Biores Technol 74:3–16
137. Kaparaju P, Ellegaard L, Angelidaki I (2009) Optimization of biogas production from manure through serial digestion: lab-scale and pilot-scale studies. Biores Technol 100:701–709
138. Wilkie AC, Castro HF, Cubisnki KR, Owens JM, Yan SC (2004) Fixed-film anaerobic digestion of flushed dairy manure after primary treatment: wastewater production and characterisation. Biosyst Eng 89:457–471
139. Jeihanipour A, Aslanzadeh S, Rajendran K, Balasubramanian G, Taherzadeh MJ (2013) High-rate biogas production from waste textiles using two-stage process. Renew Energy 52:128–135
140. Boe K, Angelidaki I (2009) Serial CSTR digester configuration for improving biogas production from manure. Water Res 43:166–172
141. Smith DP, McCarty PL (1989) Reduced product formation following perturbation of ethanol- and propionate-fed methanogenic CSTRs. Biotechnol Bioeng 34:885–895
142. Boe K (2006) Online monitoring and control of the biogas process. Ph.D. thesis, Technical University of Denmark
143. Boe K, Batstone DJ (2005) Optimisation of serial CSTR biogas reactors using modeling by ADM1. In: Proceedings of the first international workshop on the IWA Anaerobic Digestion Model No. 1 (ADM1), 2–4 Sept 2005, Lyngby, Denmark, pp 219–221
144. Ge HQ, Jensen PD, Batstone DJ (2011) Increased temperature in the thermophilic stage in temperature phased anaerobic digestion (TPAD) improves degradability of waste activated sludge. J Hazard Mater 187:355–361
145. Dyken SV, Bakken BH, Skjelbred HI (2010) Linear mixed-integer models for biomass supply chains with transport, storage and processing. Energy 35:1338–1350
146. Kaewluan S, Pipatmanomai S (2011) Gasification of high moisture rubber woodchip with rubber waste in a bubbling fluidized bed. Fuel Process Technol 92:671–677
147. Cucek L, Varbanov PS, Kleme JJ, Kravanja Z (2012) Total footprints-based multi- criteria optimisation of regional biomass energy supply chains. Energy 44:135–145
148. Gold S, Seuring S (2011) Supply chain and logistics issues of bio-energy production. J Cleaner Prod 19:32–42
149. Becker DR, Moseley C, Lee C (2011) A supply chain analysis framework for assessing state-level forest biomass utilization policies in the United States. Biomass Bioenergy 35:1429–1439
150. Chiang KY, Chien KL, Lu CH (2012) Characterization and comparison of biomass produced from various sources: suggestions for selection of pretreatment technologies in biomass-to-energy. Appl Energy 100:164–171
151. Agbor VB, Cicek N, Sparling R, Berlin A, Levin DB (2011) Biomass pretreatment: fundamentals toward application. Biotechnol Adv 29:675–685
152. Acharjee TC, Coronella CJ, Vasquez VR (2011) Effect of thermal pretreatment on equilibrium moisture content of lignocellulosic biomass. Biores Technol 102:4849–4854
153. Son Y, Yoon SJ, Kim YK, Lee JG (2011) Gasification and power generation characteristics of woody biomass utilizing a downdraft gasifier. Biomass Bioenergy 35:4215–4220
154. Wongchanapai S, Iwai H, Saito M, Yoshida H (2012) Performance evaluation of an integrated small-scale SOFC-biomass gasification power generation system. J Power Sources 216:314–322

155. Buragohain B, Mahanta P, Moholkar VS (2010) Thermodynamic optimization of biomass gasification for decentralized power generation and Fischer-Tropsch synthesis. Energy 35:2557–2579
156. Kumar A, Demirel Y, Jones DD, Hanna MA (2010) Optimization and economic evaluation of industrial gas production and combined heat and power generation from gasification of corn stover and distillers grains. Biores Technol 101:3696–3701
157. Abuadala A, Dincer I (2010) Investigation of a multi-generation system using a hybrid steam biomass gasification for hydrogen, power and heat. Int J Hydrogen Energy 35:13146–13157
158. Molino A, Giordano G, Motola V, Fiorenza G, Nanna F, Braccio G (2013) Electricity production by biomass steam gasification using a high efficiency technology and low environmental impact. Fuel 103:179–192
159. Pellegrini LF, Júnior SDO, Burbano JC (2010) Supercritical steam cycles and biomass integrated gasification combined cycles for sugarcane mills. Energy 35:1172–1180
160. Lv P, Yuan Z, Ma L, Wu C, Chen Y, Zhu J (2007) Hydrogen-rich gas production from biomass air and oxygen/steam gasification in a downdraft gasifier. Renew Energy 32:2173–2185
161. Yan F, Luo SY, Hu ZQ, Xiao B, Cheng G (2010) Hydrogen-rich gas production by steam gasification of char from biomass fast pyrolysis in a fixed-bed reactor: influence of temperature and steam on hydrogen yield and syngas composition. Biores Technol 101:5633–5637
162. Hosseini M, Dincer I, Rosen MA (2012) Steam and air fed biomass gasification: comparisons based on energy and exergy. Int J Hydrogen Energy 37:16446–16452
163. Singh RN (2004) Equilibrium moisture content of biomass briquettes. Biomass Bioenergy 26:251–253
164. Xu G, Murakami T, Suda T, Tani H, Mito Y (2008) Efficient gasification of wet biomass residue to produce middle caloric gas. Particuology 6:376–382
165. Dong L, Xu G, Suda T (2010) Murakami potential approaches to improve gasification of high water content biomass rich in cellulose in dual fluidized bed. Fuel Process Technol 91:882–888
166. Bang-Moeller C, Rokni M, Elmegaard B, Ahrenfeldt J, Henriksen UB (2013) Decentralized combined heat and power production by two-stage biomass gasification and solid oxide fuel cells. Energy 58:527–537
167. Toonssen R, Sollai S, Aravind PV, Woudstra N, Verkooijen AHM (2011) Alternative system designs of biomass gasification SOFC/GT hybrid systems. Int J Hydrogen Energy 36:10414–10425
168. Fryda LE, Panopoulos KD, Kakaras E (2008) Integrated combined heat and power with biomass gasification and SOFC-micro gas turbine. VGB PowerTech 88:66–74
169. Athanasiou C, Coutelieris F, Vakouftsi E, Skoulou V, Antonakou E, Marnellos G, Zabaniotou A (2007) From biomass to electricity through integrated gasification/SOFC system—optimization and energy balance. Int J Hydrogen Energy 32:337–342
170. Iaquaniello G, Mangiapane A (2006) Integration of biomass gasification with MCFC. Int J Hydrogen Energy 31:399–404
171. Morita H, Yoshiba F, Woudstra N, Hemmes K, Spliethoff H (2004) Feasibility study of wood biomass gasification/molten carbonate fuel cell power system-comparative characterization of fuel cell and gas turbine systems. J Power Sources 138:31–40
172. Gómez-Barea A, Leckner B, Perales AV, Nilsson S, Cano DF (2013) Improving the performance of fluidized bed biomass/waste gasifiers for distributed electricity: a new three-stage gasification system. Appl Thermal Eng 50:1453–1462
173. Kirnbauer F, Wilk V, Hofbauer H (2013) Performance improvement of dual fluidized bed gasifiers by temperature reduction: the behavior of tar species in the product gas. Fuel 108:534–542
174. Asadullah M (2014) Barriers of commercial power generation using biomass gasification gas: a review. Renew Sustain Energy Rev 29:201–215

175. Aljbour SH, Kawamoto K (2013) Bench-scale gasification of cedar wood—Part I: effect of operational conditions on product gas characteristics. Chemosphere 90:1495–1500
176. Aljbour SH, Kawamoto K (2013) Bench-scale gasification of cedar wood—Part II: effect of operational conditions on contaminant release. Chemosphere 90:1501–1507
177. Chen W, Annamalai K, Ansley RJ, Mirik M (2012) Updraft fixed bed gasification of mesquite and juniper wood samples. Energy 41:454–461
178. Calvo LF, Gil MV, Otero M, Morán A, García AI (2012) Gasification of rice straw in a fluidized-bed gasifier for syngas application in close-coupled boiler-gasifier systems. Biores. Technol. 109:206–214
179. Song T, Wu J, Shen L, Xiao J (2012) Experimental investigation on hydrogen production from biomass gasification in interconnected fluidized beds. Biomass Bioenergy 36:258–267
180. Meng X, Jong WD, Fu N, Verkooijen AHM (2011) Biomass gasification in a 100 kWth steam-oxygen blown circulating fluidized bed gasifier: effects of operational conditions on product gas distribution and tar formation. Biomass Bioenergy 35:2910–2924
181. Ngo SI, Nguyen TDB, Lim Y, Song BH, Lee UD, Choi YT et al (2011) Performance evaluation for dual circulating fluidized-bed steam gasifier of biomass using quasi-equilibrium three-stage gasification model. Appl Energy 88:5208–5220
182. Jordan CA, Akay G (2012) Occurrence, composition and dew point of tars produced during gasification of fuel cane bagasse in a downdraft gasifier. Biomass Bioenergy 42:51–58
183. Olgun H, Ozdogan S, Yinesor G (2011) Results with a bench scale downdraft biomass gasifier for agricultural and forestry residues. Biomass Bioenergy 35:572–580
184. Sheth PN, Babu BV (2009) Experimental studies on producer gas generation from wood waste in a downdraft biomass gasifier. Biores Technol 100:3127–3133
185. Jaojaruek K, Jarungthammachote S, Gratuito MKB, Wongsuwan H, Homhual S (2011) Experimental study of wood downdraft gasification for an improved producer gas quality through an innovative two-stage air and premixed air/gas supply approach. Biores Technol 102:4834–4840

Chapter 2
Fuel Cells Operating and Structural Features of MCFCs and SOFCs

2.1 Introduction

The current movement toward environmentally friendlier and more efficient power production has caused an increased interest in alternative fuels and power sources [1]. Fuel cells are one of the older energy conversion technologies, but only within the last decade have they been extensively studied for commercial use. The reliance upon the combustion of fossil fuels has resulted in severe air pollution, and extensive mining of the world's oil resources. In addition to being hazardous to the health of many species (including our own), the pollution is indirectly causing the atmosphere of the world to change (global warming). This global warming trend will become worse due to an increase in the combustion of fossil fuels for electricity because of the large increase in world population. In addition to health and environmental concerns, the world's fossil fuel reserves are decreasing rapidly [2]. The world needs a power source that has low pollutant emissions, is energy efficient, and has an unlimited supply of fuel for a growing world population. Fuel cells have been identified as one of the most promising technologies to accomplish these goals.

Many other alternative energy technologies have been researched and developed [1, 3]. These include solar, wind, hydroelectric power, bioenergy, geothermal energy, and many others. Each of these alternative energy sources have their advantages and disadvantages, and are in varying stages of development. In addition, most of these energy technologies cannot be used for transportation or portable electronics. Other portable power technologies, such as batteries and supercapacitors also are not suitable for transportation technologies, military applications, and the long-term needs of future electronics. The ideal option for a wide variety of applications is using a hydrogen fuel cell combined with solar or hydroelectric power. Compared to other fuels, hydrogen does not produce any carbon monoxide or other pollutants. When it is fed into a fuel cell, the only by-products are oxygen and heat. The oxygen is recombined with hydrogen to form water when power is needed [4, 5].

M. Turco et al., *Treatment of Biogas for Feeding High Temperature Fuel Cells*,
Green Energy and Technology, DOI 10.1007/978-3-319-03215-3_2

Fuel cells can utilize a variety of fuels to generate power—from hydrogen, methanol, and fossil fuels to biomass-derived materials. Using fossil fuels to generate hydrogen is regarded as an intermediate method of producing hydrogen, methane, methanol, or ethanol for utilization in a fuel cell before the hydrogen infrastructure has been set up. Fuels can also be derived from many sources of biomass, including methane from municipal wastes, sewage sludge, forestry residues, landfill sites, and agricultural and animal waste [6–8].

Fuel cells can also help provide electricity by working with large power plants to become more decentralized and increase efficiency [7]. Most electricity produced by large fossil fuel burning power plants is distributed through high voltage transmission wires over long distances. These power plants seem to be highly efficient because of their large size; however, a 7 to 8 % electric energy loss in Europe, and a 10 % energy loss in the United States occur during long-distance transmission [9]. One of the main issues with these transmission lines is that they do not function properly all the time. It would be safer for the population if electricity generation did not occur in several large plants, but is generated where the energy is needed. Fuel cells can be used wherever energy is required without the use of large transmission lines.

Fossil fuels are limited in supply, and are located in select regions throughout the world. This leads to regional conflicts and wars which threaten peace. The limited supply and large demand dries up the cost of fossil fuels tremendously.

Other types of alternative energy technology such as fuel cells can last indefinitely when nonfossil fuel-based hydrogen is used.

2.1.1 Fuel Cells

Fuel cells are energy conversion devices that continuously transform the chemical energy of a fuel and an oxidant into electrical energy. The fuel and oxidant gases lick the anode and cathode and are continuously fed promoting the oxidation reaction of fuel and oxidant gas reduction. Fuel cells will continue to generate electricity as long as both fuel and oxidant are available [6, 10, 11].

There are different types of fuel cells, showing a flexibility that could replace most of the devices for the production of electricity covering outputs ranging from a few W to several MW [6, 12].

A first classification distinguishes cells in high temperature (HT) up to 1100 °C, used in stationary systems for cogeneration processes, aerospace and marine applications, and low temperature (LT), from 60 to 120 °C, for low-cost portable devices and automotives.

Power can be provided by fossil fuels, coal, biogas, and biomass (for PAFC, PEMFC, MCFC, SOFC), alcohol (DMFC), and hydrogen (PEMFC and AF).

A further classification of FCs is based on the electrolyte. In PEMFC and DMFC the electrolyte is a polymeric material with cation exchange capacity; Alkaline FCs (AFCs) have a KOH solution as electrolyte; MCFCs have electrolyte

based on molten carbonate of lithium and potassium; SOFC is based on phosphoric acid.

The FCs are often presented as the solution to the problem of the future production of electricity and for transport vehicles.

Indeed, this technology presents several advantages:

- low emissions, but depend on the fuel used, especially as regards the release of NOx, CO, and particulate
- high energy efficiency, especially when compared to those of thermal machines
- weak noise
- different operating temperatures
- modular construction, so by putting in series or in parallel several elementary units you are covering the power range required
- more simple construction, and thus greater reliability and easier maintenance [10, 13].

These advantages justify the strong interest, particularly from many automotive companies, to develop the technology based on fuel cells for automotive [14, 15].

Nevertheless, there are some problems to be solved in order that fuel cells can be competitive and penetrate the market:

- the cost, due to the high value components
- the weight and volume, especially in the automotives
- the length of life, still very low (a few thousand hours for cars, about 40,000 for stationary systems)
- thermal management, for the large amount of heat exchange with an operative cooling system [16–19].

2.1.2 Comparison with Batteries

A fuel cell has many similar characteristics with batteries, but also differs in many respects. Both are electrochemical devices that produce energy directly from an electrochemical reaction between the fuel and the oxidant. The battery is an energy storage device. The maximum energy available is determined by the amount of chemical reactant stored in the battery itself. A battery has the fuel and oxidant reactants built into itself (onboard storage), in addition to being an energy conversion device. In a secondary battery, recharging regenerates the reactants. This involves putting energy into the battery from an external source. The fuel cell is an energy conversion device that theoretically has the capability of producing electrical energy for as long as the fuel and oxidant are supplied to the electrodes [11]. Figure 2.1 shows a comparison of a fuel cell and battery.

The lifetime of a primary battery is limited because when the amount of chemical reactants stored in a battery runs out, the battery stops producing electricity. In addition, when a battery is not being used, a very slow electrochemical reaction

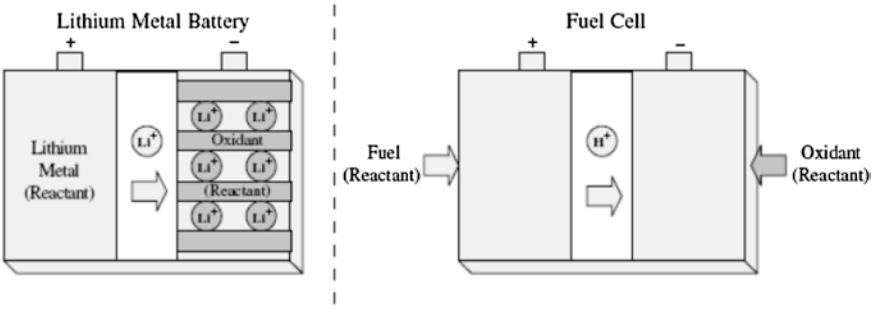

Fig. 2.1 Comparison of a fuel cell and a battery [11]

takes place that limits the lifetime of the battery. The electrode of a battery is also used in the process; therefore, the lifetime of the battery is dependent on the lifetime of the electrode. In comparison, a fuel cell is an energy conversion device where the reactants are supplied. The fuels are stored outside the fuel cell. A fuel cell can supply electrical energy as long as fuel and oxidant are supplied. The amount of energy that can be produced is theoretically unlimited as long as the fuel and oxidant are supplied. Also, no leakage occurs in a fuel cell, and no corrosion of cell components occurs when the system is not in use [11, 13, 19].

2.1.3 Comparison with Heat Engine

A heat engine converts chemical energy into electric energy like fuel cells, but through intermediate steps. The chemical energy is first converted into thermal energy through combustion, then thermal energy is converted into mechanical energy by the heat engine, and finally the mechanical energy is converted into electric energy by an electric generator.

This multistep energy process requires several devices in order to obtain electricity. The maximum efficiency is limited by Carnot's law because the conversion process is based upon a heat engine, which operates between a low and a high temperature [11, 13, 19]. The process also involves moving parts, which implies that they wear over time. Regular maintenance of moving components is required for proper operation of the mechanical components. Figure 2.2 shows a comparison between a fuel cell and a heat engine/electrical generator.

Since fuel cells are free of moving parts during operation, they can work reliably and with less noise. This results in lower maintenance costs, which make them especially advantageous for space and underwater missions. Electrochemical processes in fuel cells are not governed by Carnot's law, therefore high operating temperatures are not necessary for achieving high efficiency. In addition, the efficiency of fuel cells is not strongly dependent on operating power. It is their

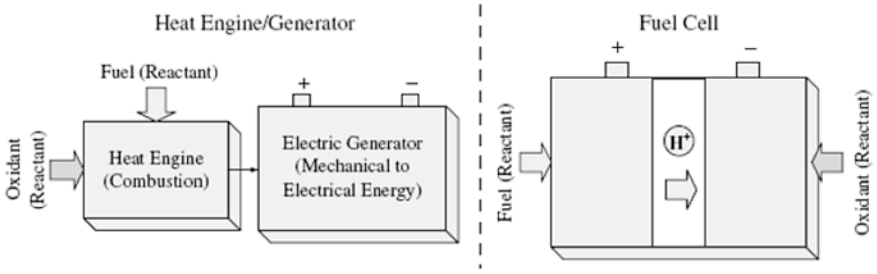

Fig. 2.2 Comparison of a fuel cell to a heat generator [11]

inherent high efficiency that makes fuel cells an attractive option for a wide range of applications, including road vehicle power sources, distributed electricity and heat production, and portable systems [11, 13, 19].

2.2 Sectors of Applications

Conventional power generation relies upon fossil fuels, which produce a significant amount of pollutants, and there is a limited supply. Many alternative energy approaches have been proposed, such as bio fuel, hydroelectric power, batteries, wind, solar, bioenergy, and geothermal energy [1]. All of these sources can provide energy, but every method has advantages and disadvantages. Fuel cells are needed because they provide electric power in applications that are currently energy limited. For example, one of the most annoying things about a laptop computer is that the battery gives out after a couple of hours.

Each market needs fuel cells for varying reasons described as follows:

- Portable sector
  In coming years, portable devices, such as laptops, cell phones, video recorders, and others, will need greater amounts of power for longer periods of time. Fuel cells are very scalable and have easy recharging capabilities compared to batteries. Cell phone technology is advancing rapidly, but the limiting factor for the new technology is the power. More power is required to provide consumers with all of the functions in devices they require and want. The military also has a need for long-term portable power for new soldier's equipment. In addition, fuel cells operate silently, and have low heat signatures, which are clear advantages for the military [20–24].
- Stationary sector
  Stationary fuel cells can produce enough electricity and heat to power an entire house or business, which can result in significant savings. These fuel cells may even make enough power to sell some of it back to the grid. Fuel cells can also power residences and businesses where no electricity is available. Sometimes

it can be extremely expensive for a house not on the grid to have the grid connected to it. Fuel cells are also more reliable than other commercial generators used to power houses and businesses. This can benefit many companies, given how much money they can lose if the power goes down for even a short time [25–29].

- Transportation sector
  Many factors are contributing to the fuel cell push in the automotive market. The availability of fossil fuels is limited, and due to this, an inevitable price increase will occur. In addition, legislation is becoming stricter about controlling environmental emissions in many countries all over the world. One of the new pieces of legislation that will help introduce the fuel cell automobile market in the United States is the Californian zero emission vehicle (ZEV) mandate, which requires that a certain number of vehicles be sold annually in California. Fuel cell vehicles also have the ability to be more fuel efficient than vehicles powered by other fuels. This power technology allows a new range of power use in small two-wheeled and four-wheeled vehicles, boats, scooters, unmanned vehicles, and other utility vehicles [30–34].

2.3 History of Fuel Cells

Fuel cells have been known to science for about 150 years. They were minimally explored in the 1800 s and extensively researched in the second half of the twentieth century. Initial design concepts for fuel cells were explored in 1800, and William Grove is credited with inventing the first fuel cell in 1839 [11, 13, 35]. Various fuel cell theories were contemplated throughout the nineteenth century, and these concepts were studied for their practical uses during the twentieth century. Extensive fuel cell research was started by NASA in the 1960s, and much has been done since then [36]. During the last decade, fuel cells were extensively researched, and are finally nearing commercialization. A summary of fuel cell history is shown in Fig. 2.3.

In 1800, William Nicholson and Anthony Carlisle described the process of using electricity to break water into hydrogen and oxygen. William Grove is credited with the first-known demonstration of the fuel cell in 1839. Grove saw notes from Nicholson and Carlisle and thought he might “recompose water” by combining electrodes in a series circuit, and soon accomplished this with a device called a “gas battery.” It operated with separate platinum electrodes in oxygen and hydrogen submerged in a dilute sulphuric acid electrolyte solution. The sealed containers contained water and gases, and it was observed that the water level rose in both tubes as the current flowed. The Grove cell, as it came to be called, used a platinum electrode immersed in nitric acid and a zinc electrode in zinc sulfate to generate about 12 A of current at about 1.8 V.

Friedrich Wilhelm Ostwald (1853–1932), one of the founders of physical chemistry, provided a large portion of the theoretical understanding of how fuel

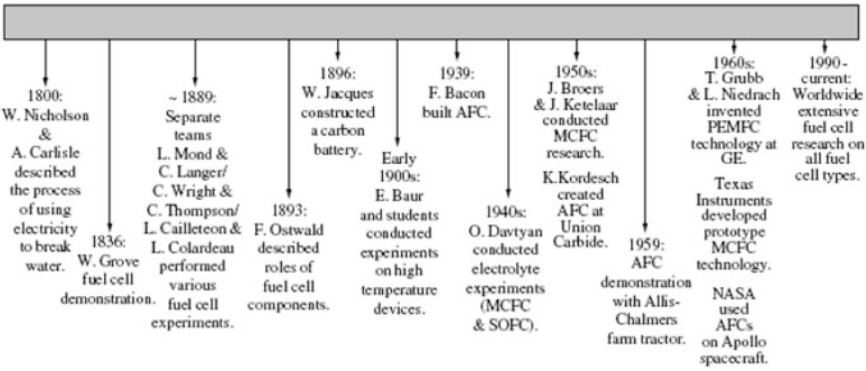

Fig. 2.3 Main milestones in the history of fuel cells [36]

cells operate. In 1893, Ostwald experimentally determined the roles of many fuel cell components.

Ludwig Mond (1839–1909) was a chemist who spent most of his career developing soda manufacturing and nickel refining. In 1889, Mond and his assistant Carl Langer performed numerous experiments using a coal-derived gas. They used electrodes made of thin, perforated platinum, and had many difficulties with liquid electrolytes. They achieved 6 A per square foot (the area of the electrode) at 0.73 V.

Charles R. Alder Wright (1844–1894) and C. Thompson developed a similar fuel cell around the same time. They had difficulties in preventing gases from leaking from one chamber to another. This and other causes prevented the battery from reaching voltages as high as 1 volt. They felt that if they had more funding, they could create a better, robust cell that could provide adequate electricity for many applications.

The French team of Louis Paul Cailleteton (1832–1913) and Louis Joseph Colardeau came to a similar conclusion, but thought the process was not practical due to needing precious metals. In addition, many papers were published during this time saying that coal was so inexpensive that a new system with a higher efficiency would not decrease the price of electricity drastically.

William W. Jacques (1855–1932), an electrical engineer and chemist, did not pay attention to these critiques, and startled the scientific world by constructing a carbon battery in 1896. Air was injected into an alkali electrolyte to react with a carbon electrode. He thought he was achieving an efficiency of 82 %, but actually obtained only an 8 % efficiency.

Emil Baur (1873–1944) of Switzerland and several of his students conducted many experiments on different types of fuel cells during the early 1900s. His work included high-temperature devices, and a unit that used a solid electrolyte of clay and metal oxides.

O.K. Davtyan of the Soviet Union did many experiments to increase the conductivity and mechanical strength of the electrolyte in the 1940s. Many of the designs did not yield the desired results, but Davtyan's and Baur's work contributed to the necessary preliminary research for today's current molten carbonate and solid oxide fuel cell devices [11, 13, 35].

2.4 Fuel Cells Fundamentals

To understand and quantify fuel cell performance, one must begin with the thermodynamic description of the fuel cell [36]. A fuel cell continuously produces electrical work and waste heat. The fuel cell can generate electricity continuously since it is an open system. The fuel cell is operated continuously for a given time period, Δt, during which reactants (fuel and oxidant) are added and products removed to maintain an electrical potential. If current is allowed to flow, a difference in electrical potential (also known as electrochemical overpotential) is maintained at the electrode interface through which charge transfer can occur. Charge carriers migrate across the cell when there is nonequilibrium between the electrical and chemical potentials across the cell. The movement occurs from a higher to lower potential energy. Thus, the chemical affinity or change in Gibbs free energy of reaction drives an electric current. The change in Gibbs free energy of reaction is available at any instant to perform electrical work.

The Gibbs free energy, G, is defined to be [13, 36, 37]

$$G = E + PV - TS \tag{2.1}$$

where P = pressure, V = volume, T = temperature, E = energy, and S = entropy.

At constant pressure and temperature (usual conditions of an electrochemical reaction), the change in the Gibbs free energy for a reaction, ΔG (J/mole) is

$$\Delta G = \Delta E + P\Delta V - T\Delta S \tag{2.2}$$

From the first law of thermodynamics, assuming the fuel cell is operated reversibly,

$$\Delta E = q + w = q + w_{electrical} - P\Delta V \tag{2.3}$$

where q = heat and w = work (J/mole). Thus, equating terms and simplifying,

$$\Delta G = q + w_{electrical} - T\Delta S \tag{2.4}$$

Again, assuming reversible operation of the fuel cell,

$$q = q_{reversible} = T\Delta S \tag{2.5}$$

Thus,

$$\Delta G = w_{electrical} \tag{2.6}$$

The change in Gibbs free energy of reaction (J/mole) is referenced to the amount of fuel. The electrical work (J) in an open system operated continuously over a given time period, Δt, where reactants (mole/s) are added and products removed to maintain the electrical potential are given for hydrogen–oxygen reaction by

$$m_{H2}\Delta G\,\Delta t = m_{H2}w_{electrical}\Delta t = W_{electrical} \tag{2.7}$$

where m_{H2} = flow rate of hydrogen for the H_2/O_2 reaction (mole/s) and Δt = operation time (s).

The average rate of work generation during the time interval, Δt, is the power (J/s).

One can mathematically demonstrate that for any direct anodic oxidation reaction for any fuel cell or hybrid system containing any fuel cell at any operating temperature and any pressure, the reversible work, $w_{electrical}$, (J/mole) is equal to the change in Gibbs free energy of reaction at the standard state (STP), ΔG^o [38, 39].

This reversible work is regarded as the maximum work. For the case of direct oxidation of hydrogen, one has

$$W_{rev} = m_{H2inlet}w_{rev} = m_{H2inlet}\Delta G^\circ\,\Delta t \tag{2.8}$$

where $m_{H2inlet}$ = flow rate of hydrogen fuel into system.

Inerts and/or water are added to or are present in a reformate with the hydrogen entering the system.

Exergy is a measure of heat quality or capability to do work. Exergetic efficiency, ζ, is the ratio of actual electrical work and the reversible work:

$$\zeta = W_{electrical}/W_{rev} \tag{2.9}$$

Using Eq. (2.8), the actual or observed electrical work for direct oxidation of hydrogen, a fuel cell is given by

$$m_{H2utilized}\Delta G_{act}\Delta t = W_{electrical} \tag{2.10}$$

where ΔG_{act} = actual change in Gibbs free energy of reaction associated with the electrical work, J/mole, $m_{H2utilized}$ = flow rate of hydrogen utilized by fuel cell (moles/s) ($m_{H2utilized}$ equals the amount in the fuel cell anode inlet; $m_{H2anode}$ inlet; minus the amount in the anode outlet; $m_{H2anode}$ outlet).

For reforming done prior to the system, $m_{H2inlet} = m_{H2anode}$ inlet. Thus, from Eqs. (2.8), (2.9), and (2.10)

$$\zeta = (m_{H2utilized}\Delta G_{act}\Delta t)/\left(m_{H2inlet}\Delta G^\circ\Delta t\right) = m_F\Delta G_{act}/\Delta G^\circ \tag{2.11}$$

where fuel utilization (μ_F) is

$$\mu_F = \mu_{H2utilized}/\,m_{H2inlet} \tag{2.12}$$

Using Eq. (2.8) for the reversible work, one can calculate the maximum thermal efficiency (maximum work for given energy input) of a fuel cell or fuel cell hybrid (fuel cell and heat engine) system for the H_2 oxidation reaction, where ΔH^o is

the reaction enthalpy for hydrogen direct oxidation (J/mole) at STP and where the inlet hydrogen is completely utilized in the fuel cell:

$$\eta_{\text{th}}\,\text{max} = \Delta G^{\circ}/\Delta H^{\circ} \tag{2.13}$$

For the H_2 oxidation reaction, $\eta_{\text{th max}}$ equals 0.83 (HHV) and 0.945 (LHV). One can also define a fuel cell intrinsic thermal efficiency at any temperature $\eta_{\text{int}}(T)$ by $\Delta G_{\text{th}}(T)/\Delta H^{o}$. One can also define for the fuel cell an intrinsic exergetic efficiency at any temperature [38, 40]:

$$\zeta_{\text{int}}(T) = \Delta G_{\text{th}}(T)/\Delta G^{\circ} \tag{2.14}$$

$\Delta G_{\text{th}}(T)$ is defined as the free energy of the reaction, here the H_2 oxidation reaction, at temperature, T, for unit concentrations of products and reactants. $\Delta G_{\text{th}}(T)$ is associated with $E^{o}(T)$. ΔG^{o} at STP with unit species concentrations is associated with E^{o}.

The actual thermal efficiency of the fuel cell is defined as the ratio of the work output to energy input, so we have

$$\eta = m_{\text{H2utilized}}\Delta G_{\text{act}}\Delta t/\left(m_{\text{H2inlet}}\Delta H^{\circ}\Delta t\right) = \mu_{\text{F}}\Delta G_{\text{act}}/\Delta H^{\circ} \tag{2.15}$$

It can be shown from Eqs. (2.11), (2.13), (2.14), and (2.15) that

$$\eta = \mu_{\text{F}}\Delta G_{\text{act}}/\Delta H^{\circ} = \eta_{\text{int}}(T)\zeta/\zeta_{\text{int}}(T) = \zeta\,\eta_{\text{th max}} \tag{2.16}$$

If one knows the reversible work which is a function of fuel, system components, and system structure, one can separate thermal efficiency into an exergetic component and a fuel component.

Exergetic performance is determined by fuel cell performance which ultimately means fuel cell voltage. The link between the macroscopic thermodynamic parameters and fuel cell voltage can be developed as follows:

The W electrical is also defined electrically as

$$W_{\text{electrical}} = -nFE \tag{2.17}$$

where

n = mole,
F = Faraday's constant (J/mole/volt),
E = fuel cell voltage (volt)

In general, from Eqs. (2.7), (2.10), and (2.17)

$$m_{\text{H2}}\Delta G\Delta t = W_{\text{electrical}} = -nFE \tag{2.18}$$

Since for the H_2 direct oxidation reaction,

$$2\,m_{\text{H2}}\Delta t = n \tag{2.19}$$

then, in general

$$\Delta G = -2FE \tag{2.20}$$

Specifically, using Eq. (2.20),

$$\Delta G_{ac} = -2FE \tag{2.21}$$

and

$$\Delta G^{\circ} = -2FE^{\circ} \tag{2.22}$$

so

$$\zeta = m_{H2utilized}\Delta G_{act}\Delta t/\left(m_{H2inlet}\Delta G^{\circ}\Delta t\right) = \mu_F(-2FE\,\Delta t)/\left(-2FE^{\circ}\,\Delta t\right) = \mu_F E/E^{\circ} \tag{2.23}$$

One of the central, steady-state fuel cell performance equations is thus given by

$$\zeta = \mu_F E/E^{\circ} \tag{2.24}$$

and combining with Eq. (2.16), one has

$$\eta = \zeta\,\eta_{th}\,max = \eta_{th}\,max\mu_F E/E^{\circ} \tag{2.25}$$

Exergetic efficiency and thermal efficiency are actually time-dependent functions describing the performance of the fuel cell at any time t.

These can be written as

$$\zeta(t) = \mu_F(t)E(t)/E^{\circ} \tag{2.26}$$

and

$$\eta(t) = \zeta(t)\eta_{th}\,max = \eta_{th}\,max\mu_F(t)E(t)/E^{\circ} \tag{2.27}$$

DR_{ζ} (t), the exergetic efficiency rate of change, is a natural and instantaneous measure of the change in fuel cell performance occurring at any time t:

$$\partial(\zeta(t))/\partial t = DR_{\zeta}(t) \tag{2.28}$$

It can be seen from Eqs. (2.26) and (2.27) that the rate of change in exergetic efficiency and rate of change of thermal efficiency are directly proportional.

Equation (2.28) is the second central equation for fuel cell performance since it is an equation that can be used in the assessment of degradation, generally defined as the change of area-specific resistance (ASR) with time [41].

2.4.1 Fuel Cell Operations

Fuel cells can be operated in a variety of modes, including constant fuel utilization, constant fuel flow rate, constant voltage, constant current, etc. For the case of constant mF and constant E, from Eq. (2.28), DRz (t) = 0, in which case the fuel cell is operating at constant exergetic efficiency. This mode of operation is achieved by lowering the current by lowering the hydrogen flow rate as the fuel cell degrades. As can be seen from Eqs. (2.26) and (2.27), to operate at constant exergetic efficiency is to operate at constant thermal efficiency.

However, efficiency is not the only important performance measure. As the current is lowered at constant voltage operation, the fuel cell power density is decreasing. Below a certain level of power or power density, given by

$$P(t) = E(t)\,J(t) \tag{2.29}$$

It is no longer economical to operate a fuel cell or fuel cell system. Power is the third central equation for fuel cell performance. General expressions can be derived for fuel cell performance involving the variables E, J, mF, pressure, and fuel flow rate to explore the full envelope of fuel cell operation.

The actual fuel cell potential is decreased from its full potential, the Nernst potential, because of irreversible losses. Multiple phenomena contribute to irreversible losses in an actual fuel cell. For the hydrogen oxidation reaction, the functionality of fuel cell voltage, E, is typically given by [42–44]

$$E(T) = E_N(T) - LJ/A\sigma - R_{ohmic}J - \eta^a_{act} - \eta^c_{act} - \eta^a_{conc} - \eta^c_{conc} \tag{2.30}$$

$$E_N(T) = E^{\circ}_{H2/O2rxn}(T) + RT/2F \ln\left(P_{H2(a)}P^{1/2}_{O2(c)}/P_{H2O(a)}\right) = \text{Nernst voltage} \tag{2.31}$$

where

F = Faraday's constant,
J = appropriate current (amperes/cm^2),
s = electrolyte charge carrier conductivity (S/cm),
L = electrolyte thickness (cm),
A = fuel cell active area (cm^2),
η^a_{act} = activation polarization for the anode,
η^c_{act} = activation polarization for the cathode,
η^a_{conc} = concentration polarization for the anode,
η^c_{conc} = concentration polarization for the anode,
R_{ohmic} = series ohmic resistance of all nonelectrolyte fuel cell components including interconnect,interlayers, and contact layers,
$E^o_{H2/O2rxn}(T)$ = voltage at unit concentrations for H_2/O_2 reaction at temperature T.

The six negative terms on the RHS of Eq. (2.30) are the usual definition of ASR. The comprehensive functionality of E and the more general definition of ASR have recently been developed for solid-state fuel cells with dense, mixed, ionic–electronic conducting electrolytes using the Wagner mass transfer model (MTM) [41, 45, 46]:

$$E = E_{MTM}\left(1-\left(J^{=}_{O} - J_{ext}\right)/J^{=}_{O}\right) - L\,J^{=}_{O}/A\sigma^{=}_{O} - R_{ohmic}J - \eta^a_{act} - \eta^c_{act} - \eta^a_{conc} - \eta_{leakage} \tag{2.32}$$

where

R_{ohmic} = series ohmic resistance of all nonelectrolyte fuel cell components, including interconnect, interlayers, and contact layers, which is multiplied by the appropriate current, J, for each type

$J_O^=$, J_e, and J_{ext} are the current terms from the Wagner MTM, $(J_O^= - J_{ext})/J_O^=$ = the shorting ratio,

$\eta_{leakage}$ = fuel leakage polarization, E_{MTM} (anode–electrolyte interface to cathode–electrolyte interface) is the reversible voltage in the Wagner MTM model

The comprehensive model for solid-state fuel cells incorporates not only the typical definition of ASR, but also electronic shorting, leakage, and other current loss mechanisms. The first term on the RHS of Eq. (2.32) is not an ASR term.

A general ASR definition for solid-state fuel cells can be defined as follows:

$$ASR = R_{ionic} + R_{ohmic} + \left(\eta_{act}^{a} + \eta_{act}^{c} + \eta_{conc}^{a} + \eta_{conc}^{c}\right)/J_O^= + R_{leakage} \quad (2.33)$$

where $R_{ionic} = L/A\sigma_o$ = ionic resistance of electrolyte and $R_{leakage} = \eta_{leakage}/J_{leakage}$ = resistance attributed to fuel leakage.

This definition of ASR is very general. However when generalized, ASR and rate of change of ASR are not broad enough concepts to describe all the phenomena affecting fuel cell performance, such as electronic shorting.

The goal of a fuel cell should be to maximize exergetic or thermal efficiency and to minimize degradation while producing as much power as possible. These three goals can be achieved by improving the fuel cell design (more conductive electrolyte, better electrocatalysts, improvement in electrode structures, thinner cell components, etc.) [10] and/or by adjusting the operating conditions (e.g., higher temperature, higher gas pressure, and change in gas composition to lower the contaminant concentration).

As shown in Fig. 2.4, the activation polarization (reaction rate loss) is significant at lower current densities [10, 11]. At this point, electronic barriers must be overcome prior to ion and current flow. Ohmic polarization (resistance loss)

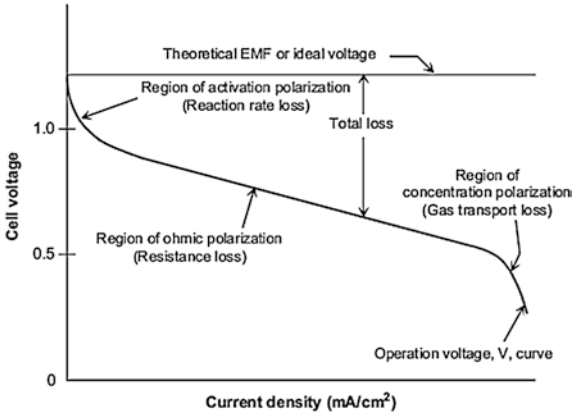

Fig. 2.4 Typical current voltage performance [10]

changes directly with current, increasing over the entire range of current because cell resistance remains essentially constant. Concentration polarization (gas transport loss) occurs over the entire range of current density, but they become significant at high limiting currents where it becomes difficult to provide enough reactant flow to the cell reaction sites.

Changing the cell operating parameters (pressure and temperature) can have an advantageous or a disadvantageous impact on fuel cell performance and compromises in the operating parameters are essential to meet the application requirements of lower system cost and acceptable cell life [10, 11].

2.5 Characteristics and Features

Fuel cells have many inherent advantages over conventional combustion-based systems, making them one of the strongest candidates to be the energy conversion device of the future (Fig. 2.5). They also have some inherent disadvantages that require further research and development to overcome them.

2.5.1 High Efficiency

The amount of heat that could be converted to useful work in a heat engine is limited by the ideal reversible Carnot efficiency, given by the following equation:

$$\eta_{\text{Carnot}} = (\text{Ti} - \text{Te})/\text{Ti} \tag{2.34}$$

where Ti is the absolute temperature at the engine inlet and Te is the absolute temperature at the engine exit. However, a fuel cell is not limited by the Carnot efficiency since a fuel cell is an electrochemical device that undergoes isothermal oxidation instead of combustion oxidation. The maximum conversion efficiency of a fuel cell is bounded by the chemical energy content of the fuel and is found by

$$\eta_{\text{rev}} = \Delta G_f/\Delta H_f \tag{2.35}$$

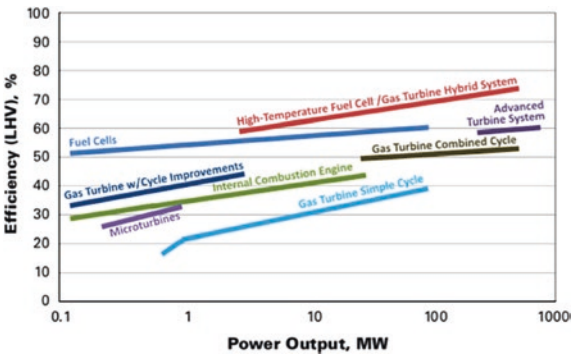

Fig. 2.5 Efficiency comparison between fuel cells and other energy conversion devices with respect to system size [6]

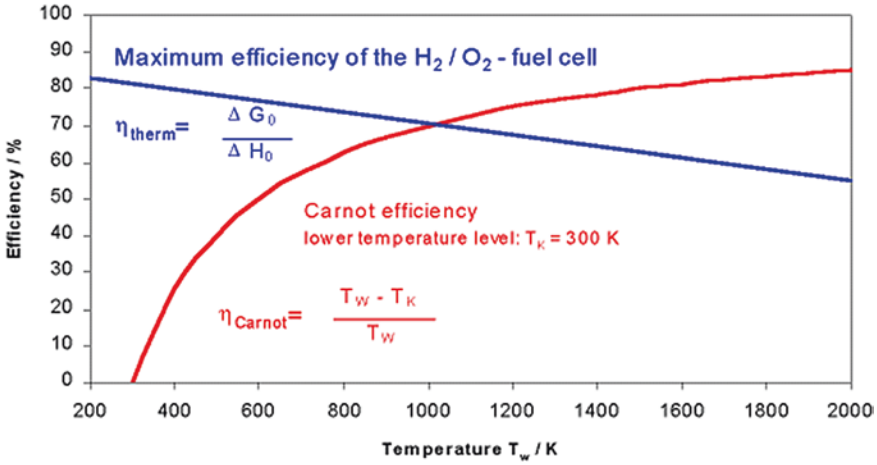

Fig. 2.6 Thermodynamic efficiency for fuel cells and Carnot efficiency for heat engines [11]

where ΔG_f is the change in Gibbs free energy of formation during the reactions and ΔH_f is the change in the enthalpy of formation (using lower heating value (LHV) or higher heating value (HHV)) [10, 11, 13].

Figure 2.6 illustrates the thermodynamic efficiency for fuel cells and Carnot efficiency for heat engines [11]. In light vehicles, for instance, the efficiency of a fuel cell-powered car is nearly twice the efficiency of an internal combustion engine-powered car. The fact that the number of energy transformations that occur within a fuel cell stack is less than that of any combustion-based device, when the required output is electricity, plays a significant role. This is because losses are associated with each energy transformation process; thus, the overall efficiency of a system generally decreases as the number of energy transformations increases.

2.5.2 Reduced Harmful Emissions

The only products from a fuel cell stack fuelled by hydrogen are water, heat, and DC electricity. And with the exception of controllable NOx emissions from high-temperature fuel cells, a hydrogen fuel cell stack is emission-free. However, the clean nature of a fuel cell depends on the production path of its fuel.

For instance, the products of a complete fuel cell system that includes a fuel reformation stage include green house emissions (e.g., CO and CO_2). When the hydrogen supplied to the fuel cell is pure (i.e., not reformation-based hydrogen which is always contaminated with CO_x), the durability and reliability of the fuel cell significantly improve in comparison to when we run the fuel cell on reformation-based hydrogen. This is one of the most important advantages of fuel cells in comparison to heat engines, i.e., fuel cells are inherently clean energy converters that ideally

run on pure hydrogen. This fact is actually pressingly driving researchers and the industry to develop efficient and renewable-based hydrogen generation technologies based on clean water electrolysis to replace the conventional reformation-based ones. Systems that integrate renewable-based hydrogen generation with fuel cells are genuinely clean energy generation and conversion systems that resemble what the energy industry is striving to achieve. It is worth mentioning that when we take into consideration the emissions from the fossil fuel reformation process, some heat engine systems appear to be less polluting than fuel cell systems [47, 48]. For non-renewable energy-based water electrolysis, the emissions and energy used for the electrolysis process make it more harmful to the environment than conventional combustion heat engines. Moreover, it is economically unfeasible since any fossil energy used for hydrogen production is going to be always more than the energy content of hydrogen. According to the studies by Argonne National Laboratory [49], 3,000,000–3,500,000 BTUs of fossil energy are used for the production of 1,000,000 BTUs of hydrogen through fossil energy-based water electrolysis. This only stresses the significance of the aforementioned conclusions regarding using renewable-based water electrolysis for hydrogen production [50].

2.5.3 Modularity

Fuel cells have excellent modularity. In principle, changing the number of cells-per-stack and/or stacks-per-system allows us to control the power output of any fuel cell system. Unlike combustion-based devices, a fuel cell's efficiency does not vary much with system size or load factor. In fact, as opposed to conventional power plants, fuel cells have higher efficiencies at part loads compared to full loads. This would prove advantageous in large-scale fuel cell systems that would normally run on part load instead of full load. Additionally, the high modularity of fuel cells means that smaller fuel cell systems have similar efficiencies to larger systems. This feature greatly facilitates the future integration of fuel cells (and hydrogen systems in general) in small-scale distributed generation systems, which hold a great potential in the power generation industry. It is worth noting, however, that reformation processors are not as modular as fuel cell stacks. This presents another reason to shift to renewable-based hydrogen production technology.

2.5.4 Prompt Load Following

Fuel cell systems generally have very good dynamic load following characteristics [51, 52]. This is partially due to the prompt nature of the electrochemical reactions that occur within a fuel cell. Again, when the fuel cell system includes a fuel reformation stage, the load following ability of the system noticeably decreases as a result of the slower nature of the reformation process.

2.5.5 Static Nature

Due to its electrochemical nature, a fuel cell stack is a static silent device. This is a very important feature that promotes the use of fuel cells for auxiliary power and distributed generation applications in addition to portable applications that require silent operation. The fact that a fuel cell system has very few dynamic parts (and hence, almost no vibrations) makes fuel cells design, manufacturing, assembly, operation, and analysis simpler than that of heat engines. Nevertheless, for fuel cell systems that use compressors instead of blowers for the oxidant supply, noise levels can noticeably increase. As such, fuel cell designers tend to avoid using compressors due to their high parasitic load, noise production, cost, weight, volume, and complexity relative to fans and blowers. The static nature of a fuel cell also reflects on its low maintenance requirements in comparison to competing technologies such as heat engines, wind turbines, and concentrated solar power plants.

2.5.6 Range of Applications and Fuel Flexibility

Fuel cells have diverse applications ranging from micro-fuel cells with less than 1 W power outputs to multi-MW prime power generation plants. This is attributed to their modularity, static nature, and variety of fuel cell types. This qualifies fuel cells to replace batteries used in consumer electronics and auxiliary vehicular power. These same properties also qualify a fuel cell to replace heat engines used in transportation and power generation. Fuel cells are also highly integrable to most renewable power generation technologies. Fuel cells that operate on low-temperature ranges require short warm-up times, which is important for portable and emergency power applications.

While for fuel cells that operate on medium-to-high temperature ranges, utilization of waste heat both increases the overall efficiency of the system and provides an additional form of power output useful for domestic hot water and space heating residential applications or CHP industrial-level applications. Fuels for a reformation-based fuel cell system include methanol, methane, and hydrocarbons such as natural gas and propane. These fuels are converted into hydrogen through a fuel reformation process. Alternatively, direct alcohol fuel cells (e.g., direct methanol fuel cells) can run directly on an alcohol. And even though fuel cells run best on hydrogen generated from water electrolysis, a fuel cell system with natural gas reformation also possesses favorable features to conventional technologies [13].

Fuel cells have been rapidly developing during the past 20 years due to the revived interest in them that started during the 1990s. However, they are still not at the widespread-commercialization stage due to many technical and sociopolitical factors, with cost and durability being the main hurdles that prevent fuel cells from becoming economically competitive in the energy market. The main challenges are detailed as follows:

2.5.7 High Cost

Fuel cells are expensive. Experts estimate that the cost-per-kW generated using fuel cells has to drop by a facto of 10 for fuel cells to enter the energy market [16, 18]. Three main reasons behind the current high cost of fuel cell stacks are: the dependence on platinum-based catalysts, delicate membrane fabrication techniques, and the coating and plate material of bipolar plates [17]. While from a system-level perspective, the BoP components such as fuel supply and storage subsystems, pumps, blowers, power and control electronics, and compressors constitute about half the cost of a typical complete fuel cell system. More specifically, whether renewable or hydrocarbon based, the current hydrogen production BoP equipment are far from being cost-effective. Technological advances in contaminate removal for hydrocarbon-based technologies are essential if the cost of fuel cell systems is to meet planned targets. Nevertheless, if fuel cells successfully enter the mass production stage, their costs are expected to significantly drop and become consumer affordable due to the fact that manufacturing and assembly of fuel cells is generally less demanding than typical competing technologies, such as heat engines.

2.5.8 Low Durability

The durability of fuel cells needs to be increased by about five times the current rates (e.g., at least 60,000 h for the stationary distributed generation sector) in order for fuel cells to present a long-term reliable alternative to the current power generation technologies available in the market. The degradation mechanisms and failure modes within the fuel cell components and the mitigation measures that could be taken to prevent failure need to be examined and tested. Contamination mechanisms in fuel cells due to air pollutants and fuel impurities need to be carefully addressed to resolve the fuel cell durability issue.

2.5.9 Hydrogen Infrastructure

One of the biggest challenges that face fuel cells commercialization is the fact that we are still producing 96 % of the world's hydrogen from hydrocarbon reformation processes [53]. Producing hydrogen from fossil fuels (mainly natural gas) and then using it in fuel cells is economically disadvantageous since the cost-per-kWh delivered from hydrogen generated from a fossil fuel is higher

than the cost-per-kWh if we were to directly use the fossil fuel. Thus, promoting renewable-based hydrogen is the only viable solution to help the shift from a fossil-based economy to a renewable-based, hydrogen-facilitated economy. Moreover, development of hydrogen storage mechanisms that provide high energy density per mass and volume whilst maintaining a reasonable cost is the second half of the hydrogen infrastructure dilemma. Any widely adopted hydrogen storage technology will have to be completely safe since hydrogen is a very light and highly flammable fuel that could easily leak from a regular container. Metal- and chemical hydride storage technologies are proving to be safer and more efficient options than the traditional compressed gaseous and liquid hydrogen mechanisms. However, more research and development are needed to reduce the relatively high cost of the hydride storage technologies and to further improve their properties.

2.5.10 Water Balance

Water transport within a fuel cell is a function of water entering with inlet streams, water generated by the cathodic reaction, water migration from one component to another, and water exiting with exit streams. Generally speaking, a successful water management strategy would keep the membrane well hydrated without causing water accumulation and blockage in any part of the MEA or flow fields. As such, maintaining this delicate water balance inside a PEMFC over different operation conditions and load requirements is a major technical difficulty the scientific community is required to fully address [54]. Flooding of the membrane; water accumulation in the pores and channels of the GDL and flow fields; dryness of the membrane; freezing of residual water inside the fuel cell; dependence between thermal, gases, and water management; and humidity of the feeding gases are all subtle and interdependent facets in the water management of a PEMFC. Improper water management within a PEMFC leads to both performance loss and durability degradations [54, 55] as a result of permanent membrane damage, low membrane ionic conductivity, nonhomogeneous current density distribution, delamination of components, and reactants starvation. As such, water management strategies range from direct water injection to reactant gases recirculation. The performance evaluation of a water management technique could be accomplished using empirical liquid water visualization or micro- and macroscale numerical simulation [44]. Nonetheless, fundamental understanding and comprehensive models of water transport phenomena within a fuel cell are highly needed in order to develop optimized component designs, residual water removal methods, and MEA materials according to application requirements and operation conditions [56].

2.5.11 Parasitic Load

The parasitic load required to run the auxiliary BoP components reduces the overall efficiency of the system. This is clearly evident when the power required to run auxiliary components such as air compressors, coolant pumps, hydrogen circulation pumps, etc., is included in the efficiency calculations. Additionally, the weight and size of fuel cell systems will need to be reduced in order for fuel cells to become compatible with onboard transportation applications and small-scale portable applications.

2.5.12 Codes, Standards, Safety, and Public Awareness

The lack of internationally accepted codes and standards for hydrogen systems in general and fuel cells in particular has a negative reflection on the public's acceptance of hydrogen power solutions. Government officials, policy makers, business leaders, and decision makers would feel more reassured about supporting early stage hydrogen power projects if general best practices and consistent safety standards in the design, installation, operation, maintenance, and handling of hydrogen equipment were established. The general public needs to be convinced that hydrogen is similar to conventional fuels in certain aspects and different in other aspects. But overall, hydrogen does not pose a safety issue if properly handled and regulated, just like any other conventional fuel. Codes and standards for hydrogen systems could be made available by the continuous collection of more real-world data and initiation of more trial projects and lab experiments, a process that could be regulated by a professional society or a government initiative (in the US, the Safety, Codes, and Standards subprogram of the Department of Energy Hydrogen and Fuel Cells Program is attempting to take this vital role) [10]. In Table 2.1 the main properties of different fuel cells are reported.

Table 2.1 Summary of the main advantages and disadvantages of fuel cells [6]

Advantages	Disadvantages
Less/no pollution	Immature hydrogen infrastructure
Higher thermodynamic efficiency	Sensitivity to contaminants
Higher part-load efficiency	Expensive platinum catalysts
Modularity and scalability	Delicate thermal and water management
Excellent load response	Dependence on hydrocarbons reforming
Fewer energy transformation	Complex and expensive BoP components
Quiet and static	Long-term durability and stability issues
Water and cogeneration applications	Hydrogen safety concerns
Fuel flexibility	High investment cost-per-W
Wide range of applications	Relatively large system size weight

2.5.13 Types

Fuel cells can be designed in various ways including many geometries, planar, tubular, radial, etc., and using many fuels and electrolyte charge carriers. Distinction of fuel cell types begins with the type of electrolyte used in the cells, the charge carrier, and the operating temperature. Low-temperature fuel cells (PEFC, AFC, and PAFC) require noble metal electrocatalysts to achieve practical reaction rates at the anode and cathode, and H_2 is the only acceptable fuel for the PEMFC. With high-temperature fuel cells (MCFC and SOFC), the requirements for catalysis are relaxed, and the number of potential fuels expands. (Other types of fuel cells are not addressed here, such as biological and enzymatic fuel cells.) For example, carbon monoxide "poisons" a noble metal anode catalyst such as platinum in low-temperature fuel cells, but it competes with H_2 as a reactant in high-temperature fuel cells where non-noble metal catalysts such as nickel can be used.

The operating temperature and required useful life of a fuel cell dictate the physicochemical and thermomechanical properties of materials used in the cell components (e.g., electrolyte, electrodes, and interconnect) [10].

Aqueous electrolytes are limited to temperatures of >200 °C because of their high water vapor pressure and/or rapid degradation at higher temperatures. The operating temperature also determines the type of fuel that can be used in a fuel cell. The low-temperature fuel cells with aqueous electrolytes are, in most practical applications, restricted to H_2 as a fuel. In high-temperature fuel cells, CO and even CH_4 can be used because of the inherently rapid electrode kinetics and the lesser need for high catalytic activity at high temperature.

Table 2.2 summarizes the main differences between the most common fuel cell types.

Table 2.2 Comparison of FCs with their performance parameters [6]

Fuel cell	Cell voltage	Start-up time	Power density (W/m^2)	Temperature (°C)
PEMFC	0.7–0.8	Seconds	3.8–6.5	60–100
AFC	1.0	Seconds	1.0	100–250
PAFC	1.0	Few minutes	0.8–1.9	150–250
MCFC	0.7–1.0	Few minutes	1.5–2.6	500–700
SOFC	0.8–1.0	Few minutes	0–0.15	700–1000
DMFC	0.2–0.4	Few seconds	1.0–2.0	60–200
DCFC	0.7–1.0	Few minutes	0.5–1.0	650–800
DFAFC	0.6–1.0	Seconds	0.5–1.2	60–100
DBFC	0.6–1.0	Seconds	0.5–1.2	70–100

2.6 Fuel Cells Types

2.6.1 Proton Exchange Membrane Fuel Cell (PEMFC)

Proton exchange membrane fuel cells (PEMFC) are believed to be the best type of fuel cell as the vehicular power source to eventually replace the gasoline and diesel internal combustion engines. PEMFCs are currently being developed and demonstrated for systems ranging from 1 W to 2 kW.

PEM fuel cells use a solid polymer membrane (a thin plastic film) as the electrolyte. The standard electrolyte material currently used in PEM fuel cells is a fully fluorinated Teflon-based material produced by DuPont for space applications in the 1960s. The DuPont electrolytes have the generic brand name Nafion, and the types used most frequently are 113, 115, and 117 [13, 57–62, 68]. The Nafion membranes are fully fluorinated polymers that have very high chemical and thermal stability. This polymer is permeable to protons when it is saturated with water, but it does not conduct electrons.

The fuel for the PEMFC is hydrogen and the charge carrier is the hydrogen ion (proton).

The best catalyst for both the anode and cathode is platinum. This catalyst was used at a content of 28 mg/cm^2 of Pt. Due to the high cost of Pt in recent years the usage has been reduced to around 0.2 mg/cm^2, yet with power increasing [13]. Platinum is dispersed on porous and conductive material, such as carbon cloth or carbon paper. PTEF will often be added also, because it is hydrophobic and so will expel the product water to the surface from where it can evaporate [13, 63–68].

At the anode, the hydrogen molecule is split into hydrogen ions (protons) and electrons. The hydrogen ions permeate across the electrolyte to the cathode while the electrons flow through an external circuit and produce electric power. Oxygen, usually in the form of air, is supplied to the cathode and combines with the electrons and the hydrogen ions to produce water. The reactions at the electrodes are as follows:

$$\text{Anode}: \quad H_{2(g)} \rightarrow 2H^{+}_{(aq)} + 2e^{-}$$

$$\text{Cathode}: \quad {}^{1}\!/_{2}\, O_{2(g)} + 2H^{+}_{(aq)} + 2e^{-} \rightarrow H_2O_{(l)}$$

$$\text{Overall}: \quad H_{2(g)} + {}^{1}\!/_{2}\, O_{2(g)} \rightarrow H_2O_{(l)}$$

Compared to other types of fuel cells, PEMFCs generate more power for a given volume or weight of fuel cell [57–62]. This high-power density characteristic makes them compact and lightweight. In addition, the operating temperature is less than 100 °C, which allows rapid start-up. These traits and the ability to rapidly change power output are some of the characteristics that make the PEMFC the top candidate for automotive power applications [57–62].

Other advantages result from the electrolyte being a solid material, compared to a liquid. The sealing of the anode and cathode gases is simpler with a solid electrolyte, and therefore, less expensive to manufacture. The solid electrolyte is also more immune to difficulties with orientation and has less problems with corrosion, compared to many of the other electrolytes, thus leading to a longer cell and stack life.

One of the disadvantages of the PEMFC for some applications is that the operating temperature is low. Temperatures near 100 °C are not high enough to perform useful cogeneration. Also, since the electrolyte is required to be saturated with water to operate optimally, careful control of the moisture of the anode and cathode streams is important.

2.6.2 Alkaline Fuel Cell (AFC)

Alkaline fuel cells (AFCs) have been used by NASA on space missions and can achieve power-generating efficiencies of up to 70 % [13, 69–72]. The operating temperature of these cells range between room temperature to 250 °C. The electrolyte is aqueous solution of alkaline potassium hydroxide (30–75 w %) soaked in a matrix [13]. (This is advantageous because the cathode reaction is faster in the alkaline electrolyte, which means higher performance).

Several companies are examining ways to reduce costs and improve operating flexibility. AFCs typically have a cell output from 300 W to 5 kW [71]. The chemical reactions that occur in this cell are as follows:

$$\text{Anode}: \quad 2H_{2(g)} + 4(OH)^{-}_{(aq)} \rightarrow 4H_2O_{(l)} + 4e^{-}$$

$$\text{Cathode}: \quad O_{2(g)} + 2H_2O_{(g)} + 4e- \rightarrow 4(OH)^{-}_{(aq)}$$

$$\text{Overall}: \quad 2H_{2(g)} + O_{2(g)} \rightarrow 2H_2O_{(l)}$$

Another advantage of AFCs are the materials such as the electrolyte and catalyst used are low cost [69, 70]. The catalyst layer can use either platinum or nonprecious metal catalysts such as nickel [72–75]. Successful achieving of very active and porous form of a metal which has been used for alkaline fuel cells from the 1960s to the present, is the use of Raney metals. These are prepared by mixing the active metal (Ni) with an inactive metal, usually aluminum. The mixture is then treated with a strong alkali that dissolves out the aluminum. This leads a porous material, with very high surface area [13]. A disadvantage of AFCs is that pure hydrogen and oxygen have to be fed into the fuel cell because it cannot tolerate the small amount of carbon dioxide from the atmosphere.

Over time, carbon dioxide degrades the KOH electrolyte which can lead to significant issues. Two commonly used solutions are refreshing the KOH electrolyte or carbon dioxide scrubbers. Due to these limitations, AFCs are not used for many power applications.

2.6.3 Phosphoric Acid Fuel Cells (PAFC)

PAFCs are very efficient fuel cells, generating electricity at more than 50 % efficiency [13]. About 85 % of the steam produced by the PAFC is used for cogeneration. This efficiency may be compared to about 35 % for the utility power grid in the United States. As with the PEMFC Pt or Pt alloys are used as catalysts at both electrodes [76]. The electrolyte is inorganic acid, concentrated phosphoric acid (100 %) which will conduct protons [77–79]. Operating temperatures are in the range of 150–220 °C. At lower temperatures, PAFC is a poor ionic conductor, and carbon monoxide (CO) poisoning of the platinum catalyst in the anode can become severe [76, 80, 81].

Two main advantages of the phosphoric acid fuel cell include a cogeneration efficiency of nearly 85 % and its ability to use impure hydrogen as fuel. PAFCs can tolerate a carbon monoxide concentration of about 1.5 % which increases the number of fuel types that can be used. Disadvantages of PAFCs include their use of platinum as a catalyst (like most other fuel cells) and their large size and weight. PAFCs also generate low current and power comparable to other types of fuel cells [13].

Phosphoric acid fuel cells are the most mature fuel cell technology. The commercialization of these cells was brought about through the Department of Energy (DOE) and ONSI (which is now United Technologies Company (UTC) Fuel Cells) and organizational linkages with Gas Research Institute (GRI), electronic utilities, energy service companies, and user groups.

The chemical reactions for PAFCs are as follows:

$$\text{Anode}: \quad H_{2(g)} \rightarrow 2H^{+}_{(aq)} + 2e^{-}$$

$$\text{Cathode}: \quad {}^{1}/_{2}\, O_{2(g)} + 2H^{+}_{(aq)} + 2e^{-} \rightarrow H_2O_{(l)}$$

$$\text{Overall}: \quad H_{2(g)} + {}^{1}/_{2}\, O_{2(g)} + CO_2 \rightarrow H_2O_{(l)} + CO_2$$

2.6.4 Direct Methanol Fuel Cells (DMFC)

A Direct Methanol Fuel Cell (DMFC) works creating an electric potential by the reaction between methanol and oxygen, specifically it produces electricity through an electrochemical process without combustion and without the need for a reformer system for the fuel [82].

The electric potential is created using a polymeric membrane that is selective to certain chemical molecules, in this case the membrane allows the passage of H^+ ions (proton conductivity). On one side of the membrane, an aqueous solution of methanol with CH_3OH concentration of around 1 M (3w%) is feed to the anode

catalyst where the catalytic decomposition of methanol molecules producing CO_2 and H_2 is oxidized to H^+ ions at the anode [13]. The protons produced can migrate to the cathode of the cell through the membrane where the electrons produced to the anode, passing through an external circuit, reduce the oxygen that is plugged in, allowing the formation of water.

The reactions occurring in the DMFC are as follows:

$$\text{Anode :} \quad CH_3OH_{(l)} + H_2O_{(l)} \rightarrow CO_2 + 6H^+_{(aq)} + 6e^-$$

$$\text{Cathode:} \quad 6H^+_{(aq)} + 3/2O_{2(g)} + 6e^- \rightarrow 3H_2O_{(1)}$$

$$\text{Overall :} \quad CH_3OH_{(l)} + 3/2O_{2(g)} \rightarrow CO_2 + 2H_2O_{(l)}$$

Because none of the methanol oxidation reaction proceeds as readily as the oxidation of hydrogen, there are considerable activation overvoltages at the fuel anode, as well as at the cathode in the DMFC. This is the main cause for the lower performance. Much work has been done to develop suitable catalysts for the anode of the DMFC. It is usually used as mixture of Pt and Ru in equal proportions. Other bimetal catalysts have been tried but this 50:50 Pt/Ru combination seems to guarantee the best performances [13, 82–84]. The cathode reaction in the DMFC is the same as that for the hydrogen fuel cells with acid electrolyte, so the same catalyst is used. There is no advantage in using the more expensive Pt/Ru bimetal catalyst used on the anode [13, 82–84].

The research and development of novel proton exchange membranes (PEMs) is known to be one of the most challenging issues regarding the direct methanol fuel cell technology [85–87]. The PEM is usually designated as the heart of the DMFC, and should ideally combine high proton conductivity (electrolyte properties) with low permeability toward DMFC species. Additionally, it should have a very high chemical and thermal stability in order to enable the DMFC operation at up to 150 °C. For this reason, a variety of PEMs have been developed by various researchers using different preparation methods [85, 88].

The different companies producing polymer electrolyte membranes have their specific patents. However, a common theme is the use a sulphonated fluoropolymers, usually fluoroethylene. The most well known and well established of these is Nafion (®Dupont), which has been developed through several variants since 1960s.

2.6.5 Molten Carbonate Fuel Cell (MCFC)

The electrolyte in the molten carbonate fuel cell uses a liquid solution of lithium, sodium, and/or potassium carbonates, soaked in a matrix. MCFCs have high fuel-to-electricity efficiencies ranging from 60 to 85 % with cogeneration, and operate

at about 620–660 °C [89–91]. The high operating temperature is an advantage because it enables a higher efficiency and the flexibility to use more types of fuels and inexpensive catalysts. This high operating temperature is needed to achieve sufficient conductivity of the electrolyte [13, 89, 90].

Molten carbonate fuel cells can use hydrogen, carbon monoxide, natural gas, propane, landfill gas, marine diesel, and coal gasification products as the fuel. MCFCs producing 10 kW to 2 MW MCFCs have been tested with a variety of fuels and are primarily targeted to electric utility applications. MCFCs for stationary applications have been successfully demonstrated in several locations throughout the world.

The reactions at the anode, cathode, and the overall reaction for the MCFC are

$$\text{Anode}: H_{2(g)} + CO_3^{2-} \rightarrow H_2O(g) + CO_{2\,(g)} + 2e^-$$

$$\text{Cathode}: \quad 1/2\, O_{2\,(g)} + CO2(g) + 2e- \rightarrow CO_3^{2-}$$

$$\text{Overall}: \quad H_{2(g)} + 1/2\, O_{2\,(g)} + CO_{2\,(g)} \rightarrow H_2O_{(g)} + CO_{2(g)}$$

The high operative temperatures and the electrolyte chemistry can be responsible of some issues. The high temperature requires significant time to reach operating conditions and responds slowly to changing power demands. These characteristics make MCFCs more suitable for constant power applications. The carbonate electrolyte can also cause electrode corrosion problems [92, 93]. Furthermore, since CO_2 is consumed at the anode and transferred to the cathode, introduction of CO_2 and its control in air stream becomes an issue for achieving optimum performance that is not present in any other fuel cell [13].

The history of Molten Carbonate Fuel Cell (MCFC) can be traced back to the late nineteenth century when W.W. Jacques had produced his carbon–air fuel cell, a device for producing "electricity from coal." This device used an electrolyte of molten potassium hydroxide at 400–500 °C in an iron pot [94]. Jacques suggested to replace molten alkali electrolytes with molten salts such as carbonates, silicates, and borates.

By the 1930s Davtyan proposed a baked mixture of 43 % calcined Na_2CO_3, 27 % monazite sand (a mixture of rare earth oxides), 20 % WO_3, and 10 % soda glass [95]. By treatment at 850 °C a mixture containing Na_3PO_4, Na_2CO_3, Na_2WO_4, Na_2SiO_3, and oxides of CeO_2, La_2O_3, and ThO_2 was obtained [95]. The mixture was constituted by a porous framework of high-melting rare earth oxides in which was constrained a eutectic mixture of molten carbonates, phosphates, tungstates, and silicates. The eutectice mixture provided the means of ionic conduction.

The works of Broers and Ketelaar [95] established that molten carbonates as the preferred electrolyte for carbon containing fuels, since other molten salts tested were decomposed by steam produced at the anode of the fuel cell. Broers and Ketelaar [95] proposed a mixture of lithium, sodium, and/or potassium carbonates

impregnated into a porous disk of magnesium oxide. Using carbonates there was no problem in replacing CO_2 at the cathode, which was effectively transferred through the molten electrolyte to the anode.

There was a general decline in interest in MCFCs during the 1970s but by the mid-1980s R&D the interest for MCFC has grow mainly in Japan and Europe [13, 95].

In recent years, MCFC development has been focused mainly on large-scale stationary and marine applications, where the relatively large size and weight of the MCFC and slow start-up time are not a problem. Molten carbonate fuel cells are under development for use with a wide range of conventional and renewable fuels.

The modern MCFC system has a high efficiency typically above 50 % and very low emissions. Since it operates at high temperature (about 650 °C) it can be used for cogeneration, combined heat and power, and distributed electricity generation. Most applications have so far been for stationary plants in hospitals, hotels, and resorts where the fuel is natural gas. The MCFC has been demonstrated to run on propane, coal gas, and anaerobic digester gas [90, 94, 96, 97]. Plants have been published for integrated coal gasifier/MCFC systems.

2.6.5.1 Components of the Molten Carbonate Fuel Cells

Materials

The heart of the molten carbonate fuel cell (MCFC) is the electrolyte, which is an ion-conducting molten salt [13, 90, 95, 96, 98–100]. This is typically a mixture of two or three alkali metal lithium, potassium, or sodium carbonates. The mixture is solid at room temperature but about 400 °C and above it becomes molten and is able to conduct carbonate (CO_3^{2-}) ions. The molten carbonate in an MCFC is constrained within a porous solid material named electrolyte matrix. An important feature of the electrolyte matrix is the chemical stability toward the molten salt that penetrates in the matrix framework and many efforts have been done in the last 20–30 years for the development of new materials [89, 94]. Alumina can be used as an MCFC matrix since it can be obtained by simple coprecipitation from an aqueous solution of aluminum nitrate, and can be made into a thin sheet. The so obtained γ-alumina, changes phase to more stable α-form at high temperatures (1200 °C). For this reason the long-term stability of the matrix could be an issue and has been investigated [101–105]. In particular lithium from the electrolyte will react over time with the alumina to form lithium aluminate ($LiAlO_2$), which also exists in two interchangeable α and γ phases: above 700 °C, γ-$LiAlO_2$ appears to be the more stable form, at 600–650 °C, the α form is more stable. The industry is directed to the use of α -$LiAlO_2$ for long-term stability [13].

The powdered matrix material is mixed with a binder to obtain sheets of 100–300 mm thickness. The carbonate electrolyte is also manufactured as similar thin sheets: cells are usually made by a sandwich of electrolyte and matrix sheets.

The stacks are assembled by building up layers of cells inserting current collectors and separator plates between one cell and the next. Once the cell or stack is assembled and mechanically clamped together, it is slowly heated up to above the melting temperature of the electrolyte. Once the electrolyte melts, it penetrates into the pores of the matrix.

Materials of anode and cathode of the MCFC are typically porous nickel and nickel oxide, respectively, in form of thin sheets [95].

Electrolyte

State-of-the-art MCFC electrolytes contain typically 60 wt% carbonate constrained in a matrix of 40 wt% Li–AlO_2. The α form of Li–AlO_2 is the most stable in the MCFC electrolyte at low temperatures and is used in the form of fibers of o1 mm diameter. Other materials (e.g., larger size particles of Li–AlO_2) may be added and many details are proprietary [99, 100].

The ohmic resistance of the MCFC electrolyte has an important and large effect on the operating voltage compared with most other fuel cells. Under typical MCFC operating conditions, it has been established that the electrolyte matrix contributes some 70 % of the ohmic losses. There is a direct relationship between the thickness of the electrolyte layer and the ionic conductivity. The thinner the electrolyte, the lower the ohmic resistance, and electrolyte matrices 0.2–0.5 mm in thickness can give better performances. However thicker materials are more stable, so low resistance and long-term stability must be optimized. For the MCFCs the typical power density at 650 °C is 0.16 Wcm^2 [13, 92, 93, 95, 106, 107].

It has been found that for the carbonates, a eutectic mixture of lithium and potassium carbonates

Li_2CO_3-K_2CO_3 (62:38 mol%) is good for atmospheric pressure operation, whereas the lithium and sodium carbonate mixture Li_2CO_3-Na_2CO_3 (60:40 mol%) is better for improved cathode stability when the cell is operated at elevated pressure [13, 95, 108–110].

An important difference between MCFC and other fuel cells is the conditioning of the electrolyte that is carried out once the stack is assembled. Layers of electrodes, electrolyte and matrix, and the various nonporous components are assembled together, and the stack is heated slowly. As the carbonate reaches its melt temperature (over 450 °C), it is absorbed into the ceramic matrix. This process can lead to some shrinkage of the components, and it is needed to pay attention to the mechanical design of the stack. An MCFC stack typically takes 14 h or more to reach the operating temperature. Another important aspect is that every time the MCFC stack is heated and cooled through the electrolyte melt temperature, stresses are set up, which can lead to cracking of the electrolyte matrix and permanent cell damage caused by fuel crossover. Thermal cycling of MCFC stacks

is therefore best avoided and MCFC systems are ideally suited to applications that need a continuous power supply.

Anode

Because the anode reaction is relatively fast at MCFC temperatures, a high surface area anode catalyst is not required [13, 95, 111–114]. State-of-the-art anodes are made of a sintered Ni–Cr/Ni–Al alloy with a thickness of 0.4–0.8 mm and porosity of 55–75 %. Fabrication is carried out usually by tape casting a slurry of the powdered material, which is subsequently sintered. Chromium is added to the basic nickel component to reduce the nickel sintering that could give rise to a decay in the MCFC, performances. However, chromium can react with lithium of the electrolyte causing some loss of electrolyte. Addition of aluminum can improve both creep resistance in the anode and electrolyte loss due to the formation of $LiAlO_2$ within the nickel particles. Ni–Cr/Ni–Al alloy are well established materials for the anodes, however nowadays the research is addressed to obtain new and less expensive materials. Moreover many efforts are addressed toward sulfur resistance materials such as $LiFeO_2$.

Cathode

One of the major problems with the MCFC is that the state-of-the-art nickel oxide cathode material shows a weak, but significant, solubility in molten carbonates [13, 95, 114–119]. Through dissolution, some Ni^{2+} ions are formed in the electrolyte and diffuse toward the anode, leading to precipitation of metallic nickel dendrites. This precipitation can cause internal short circuits with subsequent loss of power. It has been reported [13] that solubility is reduced if the more basic, carbonates are used in the electrolyte. The addition of some alkaline earth oxides (CaO, SrO, and BaO) to the electrolyte has also been found to be beneficial [13].

With state-of-the-art nickel oxide cathodes, nickel dissolution can be minimized by (1) using a basic carbonate, (2) operating at atmospheric pressure and keeping the CO_2 partial pressure in the cathode compartment low, and (3) using a relatively thick electrolyte matrix to increase the Ni^{2+} diffusion path. By these means, cell lifetimes of 40,000 h have been demonstrated under atmospheric pressure conditions. For operation at higher pressure, alternative cathode materials such as $LiCoO_2$ have been investigated. This has a dissolution rate in molten carbonate an order of magnitude lower than that of NiO at atmospheric pressure. Dissolution of $LiCoO_2$ also shows a lower dependency on the partial pressure of CO_2 than NiO.

2.6.5.2 Cell Configuration

MCFC can have different configurations depending on the flows of fuel and oxidant streams. Fuel and oxidant that flow on opposite sides of each cell can be flowing in the same direction from inlet to outlet (coflow), in opposite directions (counterflow), or at 90° to each other (crossflow) [13, 95, 114, 120–124].

If the gases supplied to the cells are connected manifold externally to the stack, then the crossflow configuration is the only option and gas inlets and outlets for the fuel and oxidant can be located on the four sides of the stack. Figure 2.7 shows the cross-flow configuration adopted by CFC Solutions.

Cross-flow has many advantages: it allows a homogeneous reactant distribution to the cell, a uniform fuel utilization over the cell, a low pressure drops through the gas channels. Moreover, simple and less expensive separator plates than other configurations can be employed.

However, the significant disadvantages of large temperature profiles across the face of the electrodes and gas leakage and migration (ion pumping) of the electrolyte must be taken into account [123, 124].

If internal manifolding is applied, then coflow or counterflow can be configured [13, 123, 124]. With coflow, the concentrations of reactants on both sides of the cells are highest at the inlet and decrease toward the outlet. Concentrations of products increase toward each outlet. Coflow produces a larger temperature gradient across the cell than counterflow, especially when internal reforming is applied. With internal reforming, counterflow is normally the best option and results in the best distribution of current density and temperature throughout the cell.

The operating temperature of the MCFC of around 650 °C provides ideal opportunities from a system design perspective. At these temperatures with a suitable catalyst, internal reforming can be carried out. Most available fuels, such as

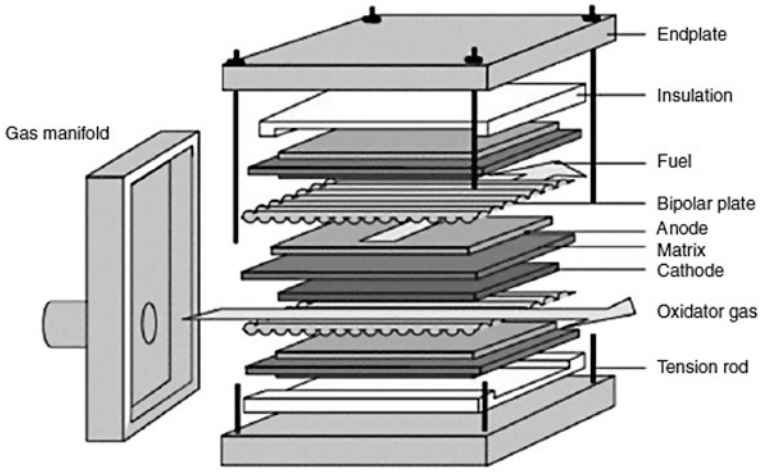

Fig. 2.7 Configuration of MCFC [13]

natural gas, liquefied petroleum gas, and biogases, need to be reformed to a hydrogen-rich gas for the fuel cell. This can be done external to the cell or stack but by carrying out the endothermic reforming reactions inside the MCFC (internal reforming), advantage is taken of the reaction to provide cell or stack cooling [13, 95, 114].

2.6.5.3 Steam Reforming

Methane reforming Eq. (2.36) is the simplest example of steam reforming (SR). This reaction is endothermic at MCFC temperatures and over an active solid catalyst the product of the reaction in a conventional reforming reactor is dictated by the equilibrium of Eq. (2.36) and the water–gas shift (WGS) reaction Eq. (2.37). This means that the product gas from a reformer depends only by the inlet steam/methane ratio (or more generally steam/carbon ratio) and the reaction temperature and pressure. Similar reaction can be written for other hydrocarbons such as natural gas, naphtha, purified gasoline, and diesel. In the case of reforming oxygenates such as ethanol [125, 126], the situation is in some way more complex, as other side reactions can occur. With simple hydrocarbons, like as methane, the formation of carbon by pyrolysis of the hydrocarbon or decomposition of carbon monoxide via the Boudouard reaction Eq. (2.38) is the only unwanted product.

$$CH_4 + H_2O = CO + 3H_2 \tag{2.36}$$

$$CO + H_2O = H_2 + CO_2 \tag{2.37}$$

$$2CO = C + CO_2 \tag{2.38}$$

In the MCFC carbon formation can be avoided by carrying out some degree of prereforming externally to the fuel cell stack. Prereforming consists of vaporizing the fuel and passing this with steam over a suitable catalyst. It converts high-molecular-weight hydrocarbons to methane, thereby reducing the risk that they pyrolyze or decompose to carbon in the MCFC stack [13, 127]. Moreover, in this way some hydrogen is present at the inlet of the fuel cell. If excess steam is used carbon monoxide decomposition is avoided due the Boudouard equilibrium. A hydrocarbon fuel such as diesel may be represented by the empirical formula CH_2 and prereforming of this fuel may be represented as

$$3CH_2 + 2H_2O \rightarrow 2CH_4 + CO_2 + H_2 \text{ (prereforming)} \tag{2.39}$$

Prereforming is usually carried out at modest temperatures (i.e., 320 °C) over a supported nickel catalyst in an adiabatic reactor [13].

Any fuel, including gases produced by the gasification of coal, wood waste, or other organic waste or biogas from digesters, that is fed to either the anode compartment directly or to an external reformer or prereformer must contain low sulfur to avoid poisoning of the reforming or prereforming catalyst [128].

2.6.5.4 MCFC Internal Reforming and Steam Reforming Catalyst

One of the advantages of the MCFC over low-temperature fuel cells is the ability to internally convert fuels such as methane or natural gas directly into hydrogen via internal steam reforming [127, 129–132]. The reforming reaction is endothermic, therefore by cooling the stack can reduce the heat that is removed out of the stack in the cathode exhaust stream. So the flow of air to the cathode (which normally provides the cooling for the stack) can be reduced. In this way the CO_2 partial pressure through the cathode compartment is raised, leading to a higher cell voltage, moreover it reduces the parasitic electrical load on the system related the cathode air compressor. For these reasons an internal reforming MCFC system has a higher efficiency than an external reforming system.

There are two approaches to internal reforming. Indirect internal reforming (IIR): the reforming reaction takes place in channels or compartments within the stack that are adjacent to the anode compartments, the heat generated in the cell is transferred to the reforming channels, and the product from the reforming is fed to the anode channels.

In direct internal reforming (DIR) the reforming reaction is carried out on the fuel cell anode itself (or as close to it as possible); in this way hydrogen produced by reforming is immediately consumed by the electrochemical cell reaction allowing to shift the equilibrium of the reforming and WGS reactions to the right as product is consumed by the electrochemical reaction [13, 95, 133–135]. The DIR approach is best carried out at low pressures with catalyst inside the anode compartment close to the anode of the cell.

In the IIR configuration, commercial reforming catalyst (e.g., nickel/alumina) exhibits little deactivation because the cell temperature is generally much lower than in a conventional reforming plant (usually above 800 °C) [13, 136–139]. The stability of a DIR catalyst, however, is strongly affected by the anode environment. Conventional catalysts decay usually via two mechanisms—sintering of the metal particles or support leading to a loss of catalytic surface area, or poisoning of catalyst active sites by sulfur [13, 128].

Carbonate retention has been the biggest issue for MCFC developers. There are two mechanisms for loss of carbonate from the cells, namely, creepage and loss by vapor phase transport [140, 141].

Steam reforming of ethanol has been demonstrated in the MCFC and proceeds rather differently to the reforming of hydrocarbons [125, 126]. Rinaldi et al. [121] studied ethanol reforming over supported metal catalyst (nickel on doped magnesium oxide). They concluded that acetaldehyde is the main unwanted product. Further catalyst optimization may improve the selectivity in the MCFC.

Some tests have been carried out recently with catalysts of titanium dioxide promoted with lanthanum or samarium oxides [13].

2.6.6 Solid Oxide Fuel Cell (SOFC)

The SOFC is a complete solid-state device that uses an oxide ion-conducting ceramic material as the electrolyte. The electrolyte is a nonporous solid, such as Y_2O_3 stabilized ZrO_2 with conductivity-based oxygen ions [122, 128, 142–144]. Yttria-stabilized zirconia (YSZ) is the most commonly used material for the electrolyte. It was first used as a fuel cell electrolyte by Baur and Preis in 1937 [145]. The anode is usually made of a Co-ZrO_2 or Ni-ZrO_2 cement [13, 95, 146, 147], while the cathode is made of Sr-doped $LaMnO_3$ (LSM) [13, 148–150].

The anode, cathode, and overall cell reactions are

$$\text{Anode}: \quad H_{2(g)} + O^{2-} \rightarrow H_2O_{(g)} + 2e^-$$

$$\text{Cathode}: \quad {}^1\!/_2\, O_{2(g)} + 2e- \rightarrow O^{2-}$$

$$\text{Overall}: \quad H_{2\,(g)} + {}^1\!/_2 O_{2\,(g)} \rightarrow H_2O_{(g)}$$

SOFCs efficiency is lower than MCMF although the operating temperature (850–1000 °C) is higher. The high operating temperatures imply that precious metal electrocatalysts are not needed, hence reducing the cost of cell components; it is also possible to use carbon-based fuels directly, removing the need for external reformers, further reducing the cost [13]. The high operating temperature of SOFC enables relatively inexpensive electrode materials to be used. Moreover, SOFC has high tolerance to impurities due to the catalytic properties of the nickel anode catalyst unlike PEMFC. The conductivity of the fuel cell materials increases with temperature [151, 152]. The dominant losses in SOFCs is mainly due to the ohmic resistance losses, thus increasing the temperature enhances the SOFC efficiency. Noticeable interest to develop electrolytes that are able to operate at lower temperatures is ongoing for several reasons: lowering the operating temperature would reduce the costs and improve cell lifetime [153].

The main configurations of SOFC are tubular, bipolar, and a planar, this last being developed more recently [13, 154–156]. SOFCs can operate at a high enough temperature to incorporate an internal fuel reformer that uses heat from the fuel cell. The recycled steam and a catalyst can convert the natural gas directly into a hydrogen-rich fuel. The waste heat allows the developmet of cogenerative processes enhancing energy efficiency to very attractive levels.

Power-generating efficiencies could reach 60 to 85 % with cogeneration [13, 128, 142–144, 146–150, 154–158]. Tubular SOFC technology has produced as much as 220 kW [154, 155]. Japan has two 25-kW units online, and a 100 kW plant is being tested in Europe [6, 159]. SOFCs coupled with small gas turbines are high-efficiency systems that have a combined rating in the range of 250 kW to 25 MW, and are expected to fit into grid support or industrial onsite generation markets [6, 13, 159].

2.6.6.1 Components of the Solid Oxide Fuel Cells

Electrolyte

In an SOFC the electrolyte is exposed to both oxidizing (air side) and reducing species (fuel side) at high temperatures. Several properties of the SOFC electrolyte are required: (1) Sufficient ionic conductivity (the electronic conductivity of the electrolyte must be sufficiently low in order to provide a high energy conversion efficiency); also the oxide ion conductivity must be high to minimize the ohmic loss. (2) Dense structure, in order to produce maximum electrochemical performance. (3) Stability since the electrolyte is exposed to the air and the fuel at elevated temperatures. This requires that the thermal expansion coefficients must match at the interfaces.

Typical electrolyte materials for SOFCs are oxides with low valence element substitutions, sometimes named acceptor dopants [13, 95] which create oxygen vacancies through charge compensation. For SOFC applications, there are various materials that have been explored as electrolyte, yttria-doped zirconia (YSZ) and gadolinium-doped ceria (GDC) are the most common materials used for the oxide-conducting electrolyte. Above 800 °C, YSZ becomes a conductor of oxygen ions (O^{2-}); zirconia-based SOFC operates between 800 and 1100 °C. The ionic conductivity of YSZ is 0.02 S m^{-1} at 800 °C and 0.1 S cm^{-1} at 1000 °C. A thin electrolyte (25–50 μm) ensures that the contribution of electrolyte to the ohmic loss in the SOFC is kept to a minimum.

Zirconium oxide-based electrolyte (YSZ)

Yttria-doped zirconia (YSZ) is stable under reducing and oxidizing conditions. It is a pure ionic conductor, completely nonreactive with anode and cathode at operating and production temperatures. Above 800 °C, YSZ becomes a conductor of oxygen ions (O^{2-}) and typically operates at 800–1100 °C. The ionic conductivity of YSZ is 0.02 S m^{-1} at 800 °C and 0.1 Scm^{-1} at 1000 °C. A thin electrolyte (25–50 μm) ensures that the contribution of electrolyte to the ohmic loss in the SOFC is kept to a minimum. Its thermal expansion has to be close to other fuel cell components and it must be gas tight to prevent direct combination of fuel and oxidant. Pure zirconia is not used, as its ionic conductivity is too low for fuel cell use [160].

Cerium oxide-based electrolyte

Doped cerium dioxide materials are candidates for the electrolyte for cell operation at T ≤ 600 °C, because of their higher oxide ion conductivity ($Ce_{0.9}Gd_{0.1}O_{-1.95}$: $0.025O^{-1}$ cm^{-1} at 600 °C) compared to YSZ (<0.005 Ω^{-1} cm^{-1}). Gadolinium- or samarium-doped cerium dioxide provides the highest ionic conductivity in cerium dioxide-based materials owing to similar ionic radii of Gd^{3+}/Sm^{3+} and Ce^{4+}. The main issue of doped cerium dioxide is the onset of electronic

conduction in reducing conditions at T ≥ 650 °C owing to the reduction of Ce^{4+} to Ce^{3+} to compensate the formation of oxygen vacancies [13].

Perovskite electrolytes

The perovskite structure (ABO_3) offers an opportunity for a material scientist to selectively substitute either the A or the B ion by introducing isovalent or aliovalent cations. The compound (La, Sr)(Mg, Ga)O_3 (LSMG) has been developed as an oxide ion conductor. The use of LSMG is attractive because it has reasonable oxide ion conductivity and is compatible with a variety of cathodes, in particular the highly active ones. Other interesting materials, such as $Bi_4V_2O_{11}$ (BIMEVOX (bismuth metal vanadium oxide)), have also been mentioned in the literature.

Cathode

The cathode electrode operates in an oxidizing environment of air at 1000 °C. The cathode electrode is a porous structure that allows mass transport of reactants and products.

Materials suitable for an SOFC cathode have to satisfy the following requirements: high electronic conductivity; stability in oxidizing atmospheres at high temperature; thermal expansion match with other cell components; compatibility and minimum reactivity with different cell components; sufficient porosity to allow transport of the fuel gas to the electrolyte/electrode interface [148–150].

LSM, (La0.84Sr0.16)MnO_3, a p-type semiconductor, is most commonly used for the cathode material. Although adequate for most SOFCs, other materials may be used, particularly attractive being p-type conducting perovskite structures that exhibit mixed ionic and electronic conductivity [13]. The advantages of using mixed conducting oxides become apparent in cells operating at around 650 °C. As well as the perovskites, lanthanum strontium ferrite, lanthanum strontium cobalite, are proposed in literature [13, 160–162].

LaMnO3 can react with the YSZ electrolyte at high temperature producing insulating phases of lanthanum zirconate [13].

Anode

The key requirements for the anode are high conductivity, stability in reducing atmospheres, and sufficient porosity to allow good mass transport. The most common anode for SOFCs is the Ni/YSZ cermet. Ni is chosen among other components because of its high electronic conductivity and stability under reducing conditions. Moreover, Ni activates both direct oxidation and steam reforming. The use of YSZ has multiple purposes: to inhibit sintering of the nickel [160, 161], to guarantee thermal expansion coefficient (TEC) comparable with other fuel cell components (mainly the electrolyte), and to increase the triple phase boundary

(TPB) [163, 164]. The anode porosity (20–40 %) ensures good mass transport and improves the triple boundary by allowing O^{2-} ion movement within the anode electrode [13, 160]. A small amount of ceria is added to the anode cermet to improve ohmic polarization loss at the interface between the anode and the electrolyte. This also improves the tolerance of the anodes to temperature cycling and redox changes within the anode gas [13, 160].

The TPB is a key area and it is important to increase this surface area since in this point the oxygen ions and the hydrogen gas are brought together to react at the surface of the nickel site [160, 165–167].

2.6.6.2 Fuel Reforming

The high operational temperature of SOFCs has two benefits: high efficiency and fuel flexibility. The high operating temperature allows the production of high-quality off-gases, which can be used for cogeneration processes [122, 154–156, 168], or to heat the reformer for endothermic steam reforming reactions, or even to fire a secondary gas turbine. Therefore, SOFCs have a high electrical efficiency, higher than other fuel cells [13, 95]. Moreover, a variety of fuels can be reformed within the cell stack (internal reforming) or through a separate fuel reformer (external reforming). This flexibility allows use of fuels such as biogas [169], liquid hydrocarbon fuels, and landfill gas. These fuels can be reformed to a mixture of hydrogen and carbon monoxide.

In the internal reforming arrangement, two configurations are employed: the direct internal reforming (DIR), and indirect internal reforming (IIR).

In the DIR the fuel reforming occurs directly on the fuel cell anode where the fuel is converted into a hydrogen-rich mixture directly inside the anode compartment: electrochemical reaction and fuel reforming reactions simultaneously take place at the anode. This is a simple and very efficient design and involves low capital costs. However, some issue must be taken into account: the anode compartment must be equipped with a proper catalyst for the steam reforming; carbon deposition is favored due to the larger content of fuel at the anode side; temperature distribution should not be homogeneous due to cooling caused by the endothermic reaction [170–175].

The problems of DIR can be in some way overcame by the indirect internal reforming (IIR) configuration. IIR uses a separate fuel reforming catalyst that is integrated within the SOFC stack upstream of the anode side, and typically utilizes heat and water from the SOFC stack. Therefore, in this case only a thermal coupling between the reformer and the SOFC stack exists. Obviously, the IIR configuration results in a higher system complexity and in higher capital costs [127, 133].

IIR should not be as efficient as DIR, however t it allows a more stable cell performance. Since the external reformer is physically separated from the fuel cell stack it can be operated at different pressures and temperatures if necessary. This is of particular importance because in this way it is possible to eliminate the problem of carbon deposition via fuel decomposition that deactivates the anode [13, 133, 168, 169].

2.6.6.3 Solid Oxide Fuel Cell Configurations

The most common SOFC designs are planar and tubular, and their many variants.

In the planar SOFC, cell components are thin and flat plates electrically connected in series. A generic schematic of a planar SOFC design is shown in Fig. 2.8 [176]. The planar cells can be electrolyte supported, electrode supported, or metal supported. For instance, the cell may be in the form of a circular disk fed with fuel from the central axis, or it may be in the form of a square plate fed from the edges. Planar designs offer several potential advantages, including simpler and less expensive manufacturing processes and higher power densities, than tubular cells. However, planar designs need high-temperature gas-tight seals between the components in the SOFC stack; but these still remain a challenging area for the successful commercialization of planar SOFCs [177, 178]. The electrochemical performance is highly dependent on cell materials, electrode microstructures, and cell geometric parameters. The cell was optimized with an anode of thickness 0.5 mm and porosity ~57 %. The anode interlayer was ~20 mm. The electrolyte was ~8 mm and cathode interlayer ~20 mm. The flow rates of humidified hydrogen and air were 300 and 550 mL min^{-1}, respectively. The maximum power density obtained is about 1.8 Wcm^2 at 800 °C [179–181].

In the tubular SOFC design, components are flat tubes and joined together to give higher power density and easily printable surfaces for depositing the electrode layers. It may be of a large diameter (>15 mm), or a microtubular cells with a smaller diameter (<5 mm) [44, 179, 182]. Figure 2.9 illustrates a tubular SOFC in which the oxidant (air or oxygen) is introduced through an alumina injector tube positioned inside the cell. The oxidant is discharged near the closed end of the cell and flows through the annular space formed by the cell and the coaxial injector tube. The fuel flows on the outside of the cell from the closed end and is electrochemically oxidized while flowing to the open end of the cell generating

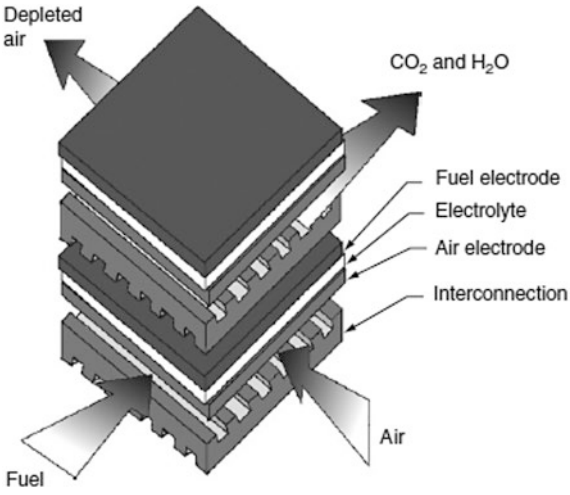

Fig. 2.8 Planar SOFC design [176]

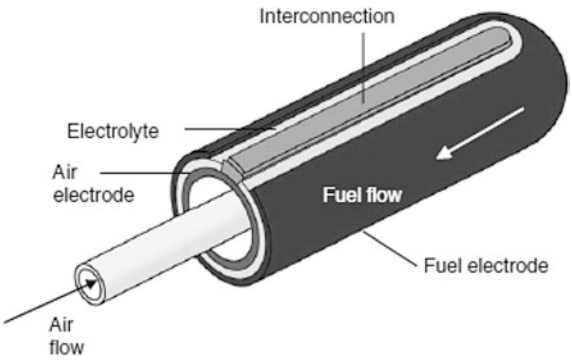

Fig. 2.9 Tubular SOFC design [176]

electricity. Part of the fuel is recirculated in the fuel stream and the rest combusted to preheat the incoming air and/or fuel. The exhaust gas from the fuel cell is at 600–900 °C depending on the operating conditions. The single biggest advantage of tubular cells over planar cells is that they do not require any high-temperature seals to isolate the oxidant from the fuel, and this leads to very stable performance of tubular cell stacks over long periods of time (several years). However, their areal power density is much lower (about 0.2 Wcm^{-2}) compared to planar cells, and manufacturing costs are high [183–185].

A single planar or tubular SOFC generally produces a low voltage and power and the connection into a stack is needed in order to give higher power. Electrochemical performance, structural and mechanical integrity gas manifold and ease of fabrication are important targets for the improvements of cell performances [176, 186].

References

1. Dincer I, Zamfirescu C (2014) Advanced power generation systems. In: Chapter 3—Fossil fuels and alternatives, 95–141
2. Shafiee S, Topal E (2009) When will fossil fuel reserves be diminished? Energy Policy 37:181–189
3. Abas N, Kalair A, Khan N (2015) Review of fossil fuels and future energy technologies. Futures 69:31–49
4. Ball M, Weeda M (2015) The hydrogen economy—Vision or reality? Int J Hydrogen Energy 40:7903–7919
5. Andrews J, Shabani B (2012) Where does hydrogen fit in a sustainable energy economy? Procedia Eng 49:15–25
6. Sharaf OZ, Orhan MF (2014) An overview of fuel cell technology: fundamentals and applications. Renew Sustain Energy Rev 32:810–853
7. Elmer T, Worall M, Wu S, Riffat SB (2015) Fuel cell technology for domestic built environment applications: state of-the-art review. Renew Sustain Energy Rev 42:913–931
8. Alves HJ, Bley C, Niklevicz RR, Pires Frigo E, Sato Frigo M, Coimbra-Araújo CH (2013) Overview of hydrogen production technologies from biogas and the applications in fuel cells. Int J Hydrogen Energy 38:5215–5225

9. The Department of Energy hydrogen and fuel cells program plan: an integrated strategic plan for the research, development, and demonstration of hydrogen and fuel cell technologies US Department of Energy (2011)
10. National Energy Technology Laboratory, U.S. Department of Energy Fuel Cell Handbook 7th ed. Morgantown, 1–35 (2005)
11. O'Hayre R, Cha SW, Colella W, Prinz FB (2006) Fuel cell fundamentals. Wiley, New York
12. Carter D, Ryan M, Wing J (2012) The fuel cell industry review 2012. Fuel Cell Today
13. Larminie J, Dicks A (2003) In: Fuel Cell Systems Explained, 2nd edn, Wiley
14. Park SY, Kim JW, Lee DH (2011) Development of a market penetration forecasting model for hydrogen fuel cell vehicles considering infrastructure and cost reduction effects. Energy Policy 39:3307–3315
15. Simons A, Bauer C (2015) A life-cycle perspective on automotive fuel cells. Appl Energy 157:884–896
16. Hellmana HL, van den Hoedb R (2007) Characterising fuel cell technology: challenges of the commercialisation process. Int J Hydrogen Energy 32:305–315
17. Wang J (2015) Barriers of scaling-up fuel cells: cost, durability and reliability. Energy 80:509–521
18. Lewis J (2014) Stationary fuel cells insights into commercialisation. Int J Hydrogen Energy 39:21896–21901
19. Xianguo L (2006) Principles of fuel cells. Taylor & Francis Group, New York
20. Cowey K, Green KJ, Mepsted GO, Reeve R (2004) Portable and military fuel cells. Curr Opin Solid State Mater Sci 8:367–371
21. Patil AS, Dubois TG, Sifer N, Bostic E, Gardner K, Quah M (2004) Portable fuel cell systems for America's army: technology transition to the field. J Power Sources 136:220–225
22. Wang Y, Chen KS, Mishler J, Cho SC, Adroher XC (2011) A review of polymer electrolyte membrane fuel cells: technology, applications, and needs on fundamental research. Appl Energy 88:981–1007
23. Breakthrough Technologies Institute Fuel cell technologies market report US Department of Energy (2011)
24. Abdullah MO, Yung VC, Anyi M, Othman AK, Hamid KBAb, Tarawe J (2010) Review and comparison study of hybrid diesel/solar/hydro/fuel cell energy schemes for a rural ICT Telecenter. Energy 35:639–646
25. Bauen A, Hart D, Chase A (2003) Fuel cells for distributed generation in developing countries: an analysis. Int J Hydrog Energy 28:695–701
26. Munuswamy S, Nakamura K, Katta A (2011) Comparing the cost of electricity sourced from a fuel cell-based renewable energy system and the national grid to electrify a rural health centre in India: a case study. Renew Energy 36:2978–2983
27. Santarelli M (2004) Design and analysis of stand-alone hydrogen energy systems with different renewable sources. Int J Hydrog Energy 29:1571–1586
28. Kazempoor P, Dorer V, Weber A (2011) Modelling and evaluation of building integrated SOFC systems. Int J. Hydrog Energy 36:13241–13249
29. Alcaide F, Cabot PL, Brillas E (2006) Fuel cells for chemicals and energy cogeneration. J Power Sources 153:47–60
30. Agnolucci P (2007) Prospects of fuel cell auxiliary power units in the civil markets. Int J Hydrog Energy 32:4306–4318
31. Lutsey N, Brodrick CJ, Sperling D, Dwyer HA (2002) Markets for fuel cell auxiliary power units in vehicles: a preliminary assessment. Institute of Transportation Studies. UCD-ITS-RP-02-44
32. Hochgraf C (2009) Application: transportation: electric vehicles: fuel cells. In: Garche J (ed) Encyclopedia of electrochemical power sources. Elsevier, Amsterdam
33. Bradley TH, Moffitt BA, Mavris D, Parekh DE (2009) Applications: transportation: aviation: fuelcells. In Garche J (ed) Encyclopedia of Electrochemical Power Sources, Elsevier Amsterdam

34. Saxe M, Folkesson A, Alvfors P (2008) Energy system analysis of the fuel cell buses operated in the project: clean urban transport for Europe. Energy 33:689–711
35. Collecting the History of Fuel Cells (2006). http://americanhistory.si.edu/fuelcells/index.htm. Smithsonian Institution. Accessed 30 Oct 2015
36. Shekhawat D, Spivey JJ, Berry DA (2011) Fuel cells: technologies for fuel processing, Elsevier (2011)
37. Wark K (1977) Applied thermodynamics for engineers. McGraw-Hill, New York
38. Williams MC, Yamaji K, Yokokawa H, Fundamental thermodynamic studies of fuel cells using MALT2. J Fuel Cell Sci Technol 6:97–102 and 113–116 (2009)
39. Winkler W (2003) High temperature solid oxide fuel cells: fundamentals, design, and applications Thermodynamics. In: Singhal SC, Kendall K (eds) Oxford. Elsevier, UK, pp 53–82
40. Winkler W (1994) SOFC integrated power plants for natural gas. In: Proceedings of first European solid oxide fuel cell forum, Lucerne, Switzerland, 821–848, 3–7 Oct 1994
41. Williams M, Yamaji K, Horita T, Sakai N, Yokokawa H (2009) Exergetic studies of intermediate temperature, solid oxide fuel cell electrolytes. J Electrochem Soc 156:546–551
42. Virkar A, Williams MC, Singhal SC (2007) Concepts for ultrahigh power density solid oxide fuel cells In: Williams M, Krist K (eds) ECS Transactions, vol 5. pp 401–422
43. Virkar AV (2005) Theoretical analysis of the role of interfaces in transport through oxygen ion and electron conducting membranes. J Power Sources 147:8–31
44. Zhao, Virkar AV (2005) Dependence of polarization in anode-supported solid oxide fuel cells on various cell parameters. J Power Sources 141:79–95
45. Yokokawa H, Sakai N, Horita T, Yamaji K, Brito ME (2005) Electrolytes for solid-oxide fuel cells. MRS Bull 30(8):591–595
46. Choudhury NS, Patterson JW (1970) Steady-state chemical potential profiles in solid electrolytes. J Electrochem Soc 117:1384–1388
47. Space applications of hydrogen and fuel cells (2015) National Aeronautics and Space Administration. http://www.nasa.gov/topics/technology/hydrogen/hydrogen_2009.html. Accessed 30 Oct 2015
48. Sheffield JW (2007) Assessment of hydrogen energy for sustainable development. In: Sheffield Ç (ed) Springer, Netherlands (2007)
49. Gaines LL, Elgowainy A, Wang MQ (2008) Full fuel-cycle comparison of forklift propulsion systems. In: Argonne National Laboratory. ANL/ESD/08-3
50. Wang M, Elgowainy A, Han J (2010) Life-cycle analysis of criteria pollutant emissions from stationary fuel cell systems. US Department of Energy Hydrogen and Fuel Cells Program AN012
51. El-Sharkh MY, Rahman A, Alam MS, Byrne PC, Sakla AA, Thomas T (2004) A dynamic model for a stand-alone PEM fuel cell power plant for residential applications. J Power Sources 138:199–204
52. Zhu Y, Tomsovic K (2002) Development of models for analyzing the load—following performance of microturbines and fuel cells. Electr Power Syst Res 62:1–11
53. Grimes CA, Varghese OK, Ranjan S (2008) Light, water, hydrogen: the solar generation of hydrogen by water photoelectrolysis. Springer, New York
54. Jiao K, Li X (2011) Water transport in polymer electrolyte membrane fuel cells. Prog Energy Combust Sci 37:221–291
55. Ous T, Arcoumanis C (2013) Degradation aspects of water formation and transport in proton exchange membrane fuel cell: a review. J Power Sources 240:558–582
56. Tsushima S, Hirai S (2011) In situ diagnostics for water transport in proton exchange membrane fuel cells. Prog Energy Combust Sci 37:204–220
57. Zhang Y, Li J, Ma L, Cai W, Cheng H (2015) Recent developments on alternative proton exchange membranes: strategies for systematic performance improvement. Energy Technol 3:675–691
58. Dubau L, Castanheira L, Maillard F, Chatenet M, Lottin O, Maranzana G, Dillet J, Lamibrac A, Perrin JC, Moukheiber E et al (2014) A review of PEM fuel cell durability:

materials degradation, local heterogeneities of aging and possible mitigation strategies. Wiley Interdisc Rev Energy Environ 3:540–560
59. Banham D, Feng F, Furstenhaupt T, Pei K, Ye S, Birss V (2015) Novel mesoporous carbon supports for PEMFC catalysts. Catalysts 5:1046–1067
60. Anstrom JR (2014) Hydrogen as a fuel in transportation. Energy 63:499–524
61. Chirachanchar S, Pangon A, Jarumaneeroj C (2013) High temperature performance polymer electrolyte membranes. Membr Process. Sustain. Growth 247–287
62. Sim V, Han W, Poon HY, Lai YT, Yeung KL (2014) Confinement as a new architecture for self-humidifying proton-exchange membrane for PEMFC Abstracts of Papers. In: 248th ACS National Meeting & Exposition, San Francisco, CA, United States, 10–14 Aug 2014
63. Moilanen D E, Piletic IR, Fayer MD (2007) Dynamics of water in Nafion fuel cell membranes: the effects of confinement and structural changes on the hydrogen bonding network. In: NSTI Nanotech 2007, Nanotechnology Conference and Trade Show, Santa Clara, CA, United States, vol 4, pp 712–715 20–24 May 2007
64. Narayanan SR, Valdez TI, Firdosy S (2009) Analysis of the performance of Nafion-based hydrogen-oxygen fuel cells. J Electrochem Soc 156:B152–B159
65. Tian JH, Gao PF, Zhang ZY, Luo WH, Shan ZQ (2008) Preparation and performance evaluation of a Nafion-TiO2 composite membrane for PEMFCs. Int J Hydrogen Energy 33:5686–5690
66. Tsai CH, Wang CC, Chang CY, Lin CH, Chen-Yang YW (2014) Enhancing performance of Nafion-based PEMFC by 1-D channel metal-organic frameworks as PEM filler. Int J Hydrogen Energy 39:15696–15705
67. Matolin V, Fiala R, Vaclavu M, Matolinova I (2014) Thin film catalysts for PEMFCs. In: Abstracts of Papers, 248th ACS National Meeting & Exposition, San Francisco, CA, United States. 2014 ENFL-211, pp 10–14 (2014)
68. Boyaci SFC, Isik-Gulsac I, Osman OO (2013) Analysis of the polymer composite bipolar plate properties on the performance of PEMFC (polymer electrolyte membrane fuel cells) by RSM (response surface methodology). Energy 55:1067–1075
69. Lin BYS, Kirk DW, Thorpe SJ (2006) Performance of alkaline fuel cells: a possible future energy system. J Power Sources 161:474–483
70. Aremo B, Adeoye MO, Obioh IB (2015) A simplified test station for alkaline fuel cell. J Fuel Cell Sci Technol 12:1–7
71. Fuel Cell Basics (2000). Fuel Cells. http://www.fuelcells.org/basics/how.html. Accessed 30 Oct 2015
72. Marino MG, Kreuer KD (2015) Alkaline stability of quaternary ammonium cations for alkaline fuel cell membranes and ionic liquids. ChemSusChem 8:513–523
73. Ishimoto T, Hamatake Y, Kazuno H, Kishida T, Koyama M (2015) Theoretical study of support effect of Au catalyst for glucose oxidation of alkaline fuel cell anode. Appl Surf Sci 324:76–81
74. Geng F, Zeng WM, Ma YL (2013) Preparation and characterization of foam-Ni deposit Pt and Pd catalysts for alkaline fuel cell. Dianyuan Jishu 37:387–389
75. Aziznia, Oloman CW, Gyenge EL (2013) Platinum- and membrane-free swiss-roll mixed-reactant Alkaline Fuel cell. ChemSusChem 6:847–855
76. Fuller TF, Perry M, Reiser C (2006) Applying the lessons learned from PAFC to PEM fuel cells. ECS Trans 1:337–344
77. Fuller TF, Gallagher KG (2008) Phosphoric acid fuel cells. Mater Fuel Cells 209–247
78. Sammes N, Bove R, Stahl K (2004) Phosphoric acid fuel cells: fundamentals and applications. Curr Opin Solid State Mater Sci 8:372–378
79. Steele BCH (2001) Material science and engineering: the enabling technology for the commercialisation of fuel cell systems. J. Mater Sci 36:1053–1068
80. Antolini E, Salgado JRC, Gonzalez ER (2006) The stability of Pt-M (M = first row transition metal) alloy catalysts and its effect on the activity in low temperature fuel cells. J Power Sources 160:957–968

81. Stonehart P, Wheeler D (2005) Phosphoric acid fuel cells (PAFCs) for utilities: electrocatalyst crystallite design, carbon support, and matrix materials challenges. Mod Aspects Electrochem 38:373–424
82. Hogarth M, Hards G (1996) Direct methanol fuel cells: technological advances and further requirements. Plat Met Rev 40:150–159
83. Hamnett A, Kennedy BJ (1988) Bimetallic carbon supported anode for the direct methanol-air fuel cell. Electrochim Acta 33:1613–1618
84. Hamnett A (1997) Mechanism and electrocatalysis in the direct methanol fuel cell. Catal Today 38:445–457
85. Libby B, Smyrl WH, Cussler EL (2003) Polymer-Zeolite composite membranes for direct methanol fuel cells. AIChE J 49:991–1001
86. R. F. Service (2002) Fuel cells. Shrinking fuel cells promise power in your pocket. Science 296:1222–1224
87. Lu GQ, Wang CY, Yen TJ, Zang X (2004) Development and characterization of a silicon-based micro direct methanol fuel cell. Electrochem Acta 49:821
88. Li X, Roberts EPL, Holmes SM (2006) Evaluation of composite membranes for direct methanol fuel cells. J Power Sources 154:115–123
89. Tomczyk P (2006) MCFC versus other fuel cells—characteristics, technologies and prospects. J Power Sources 160(2006):858–862
90. Zhu XJ, Huang B (2012) Molten carbonate fuel cells. Electrochem Technol Energy Storage Convers 2:729–775
91. Rossi et al C (1999) In: Proceedings of Micro Nanotechnology for Space Applications, vol 1, Apr (1999)
92. Blomen L, Leo JMJ, Mugerwa M (1993) Fuel cell systems. Plenum Publishing, New York
93. Kunz HR (1987) Transport of electrolyte in molten carbonate fuel cells. J Electrochem Soc 134:195–113
94. Perry ML, Fuller TF (2002) A historical perspective of fuel cell technology in the 20th century. J Electrochem Soc 149:S59–S67
95. Fuel Cell Technology Handbook (2002) In: Hoogers G (ed), CRC Press
96. McPhail SJ, Hsieh PH, Selman JR (2013) Molten carbonate fuel cells. Mater High-Temp Fuel Cells 341–371
97. Chen B (2011) Research and development of fuel cell technology in China. In: Asia-Pacific Power and Energy Engineering Conference, Wuhan, China, (Pt. 1), 529–532, 25–28 Mar 2011
98. Mirahmadi A, Akbari H (2012) A noble method for molten carbonate fuel cells electrolyte manufacturing. J Solid State Electrochem 16:931–936
99. Maru HC, Pigeaud A, Chamberlin R, Wilemski G (1986) Electrolyte management in molten carbonate fuel cells. Proc Electrochem Soc 86:398–422
100. Ang PGP, Sammells AF (1980) Influence of electrolyte composition on electrode kinetics in the molten carbonate fuel cell. J Electrochem Soc 127:1287–1294
101. Albin V, Goux A, Ringuede A, Belair S, Lair V, Cassir M (2007) Screening and properties of new materials for MCFC application. ECS Trans 3:205–213
102. Park E, Hong M, Lee H, Kim M, Kim K (2005) A new candidate cathode material as (Co/Mg)-coated Ni powder for molten carbonate fuel cell. J Power Sources 143:84–92
103. Wijayasinghe A, Lagergren C, Bergman B (2003) New cathode materials for molten carbonate fuel cells. Fuel Cells 2:181–188
104. Fang B, Chen H (2001) A new candidate material for molten carbonate fuel cell cathodes. J Electroanal Chem 501:128–131
105. Nguyen HVP, Kang MG, Ham HC, Choi SH, Han J, Nam SW, Hong SA, Yoon SP (2014) A new cathode for reduced-temperature molten carbonate fuel cells" J. Electrochem Soc 161:F1458–F1467
106. Li S, Sun J (2010) Electrochemical performances of NANOCOFC in MCFC environments. Int J Hydrogen Energy 35:2980–2985

107. Selman JR (2006) Molten-salt fuel cells-Technical and economic challenges. J Power Sources 160:852–857
108. Kaun TD, Schoeler A, Centeno CJ, Krumpelt M (1999) Improved MCFC performance with Li/Na/Ba/Ca carbonate electrolyte. Proc Electrochem Soc 99:219–227
109. Makkus RC, Sitters EF, Nammensma P, Huijsmans JPP (1997) MCFC electrolyte behavior; Li/K versus Li/Na carbonate. Proc Electrochem Soc 97:344–352
110. Ketelaar JAA (1987) Molten carbonate fuel cells. From Fuel Cells Trends Res Appl [Proc. Workshop] 161–72
111. Cigolotti V, McPhail S, Moreno A, Yoon SP, Han JH, Nam SW, Lim TH (2011) MCFC fed with biogas: Experimental investigation of sulphur poisoning using impedance spectroscopy. Int J Hydrogen Energy 36:10311–10318
112. Lee D, Kim J, Jo K (2011) A Study on In-Situ Sintering of Ni-10 wt % Cr Anode for MCFC. J Electrochem Soc 158:B500–B504
113. Devianto H, Yoon SP, Nam SW, Han J, Lim TH (2006) Study on ceria coating effect of H_2S tolerance in the anode of molten carbonate fuel cell. Stud Surf Sci Catal 159:601–604
114. Hirschenhofer JH, Stauffer DB, Hengelman RR (1998) Fuel cell handbook 4th edn. Passons Co. for US Department of Energy
115. Melendez-Ceballos A, Albin V, Ringuede A, Fernandez-Valverde SM, Cassir M (2014) Electrochemical behavior of Mx-1Ox (M = Ti, Ce and Co) ultra-thin protective layers for MCFC cathode. Int J. Hydrogen Energy 39:12233–12241
116. Bozzini B, Maci S, Sgura I, Lo Presti R, Simonetti E (2011) Elisabetta Numerical modelling of MCFC cathode degradation in terms of morphological variations. Int J Hydrogen Energy 36:10403–10413
117. Matsuzawa K, Akinaga Y, Mitsushima S, Ota KI (2011) Solubilities of NiO and $LaNiO_3$ in Li/Na eutectic carbonate with rare-earth oxide. J Power Sources 196:5007–5011
118. Escudero MJ, Ringuede A, Cassir M, Gonzalez-Ayuso T, Daza L (2007) Porous nickel MCFC cathode coated by potentiostatically deposited cobalt oxide. J Power Sources 171:261–267
119. Matsuzawa K, Tatezawa G, Matsuda Y, Ryoke H, Mitsushima S, Kamiya N, Ota KI (2006) Effect of rare earth addition to molten carbonate on the solubility of NiO. Proc Electrochem Soc 24:666–678
120. Sciavovelli A, Verda V, Amelio C, Repetto C, Diaz G (2012) Performance improvement of a circular MCFC through optimal design of the fluid distribution system. J Fuel Cell Sci Technol 9:041011/1–041011/8
121. Rinaldi G, McLarty D, Brouwer J, Lanzini A, Santarelli M (2015) Study of CO2 recovery in a carbonate fuel cell tri-generation plant. J Power Sources 284:16–26
122. Minutillo M, Perna A, Jannelli E (2014) SOFC and MCFC system level modeling for hybrid plants performance prediction. Int J Hydrogen Energy 39:21688–21699
123. Kim YJ, Chang IG, Lee TW, Chung MK (2010) Effects of relative gas flow direction in the anode and cathode on the performance characteristics of a Molten Carbonate Fuel Cell. Fuel 89:1019–1028
124. Law MC, Lee VC-C, Tay CL (2015) Dynamic behaviors of a molten carbonate fuel cell under a sudden shut-down scenario: the effects on temperature gradients. Appl Therm Eng 82:98–109
125. Zanchet D, Santos JBO, Damyanova S, Gallo JMR, Bueno JMC (2015) Toward Understanding Metal-Catalyzed Ethanol Reforming ACS Catalysis 5:3841–3863
126. Guerrero L, Castilla S, Cobo M (2014) Martha Advances in ethanol reforming for the production of hydrogen. Quimica Nova 37:850–856
127. Vatani A, Khazaeli A, Roshandel R, Panjeshahi MH (2013) Thermodynamic analysis of application of organic Rankine cycle for heat recovery from an integrated DIR-MCFC with pre-reformer. Energy Convers Manag 67:197–207
128. Vahc ZY, Jung CY, Yi SC (2014) Performance degradation of solid oxide fuel cells due to sulfur poisoning of the electrochemical reaction and internal reforming reaction. Int J Hydrogen Energy 39:17275–17283

129. Dimopoulos G G, Stefanatos IC, Kakalis NMP (2015) Exergy analysis and optimisation of a marine molten carbonate fuel cell system in simple and combined cycle configuration. Energy Convers Manag (2015). in press
130. Gharieh K, Jafari MA, Guo Q (2015) Investment in hydrogen tri-generation for wastewater treatment plants under uncertainties. J Power Sources 297:302–314
131. Zhang X, Liu H, Ni M, Chen J (2015) Performance evaluation and parametric optimum design of a syngas molten carbonate fuel cell and gas turbine hybrid system. Renewable Energy 80:407–414
132. Zhang J, Zhang X, Liu W, Liu H, Qiu J, Yeung KL (2014) A new alkali-resistant Ni/Al2O3-MSU-1 core-shell catalyst for methane steam reforming in a direct internal reforming molten carbonate fuel cell. J Power Sources 246:74–83
133. Moon HD, Lim TH, Lee HI (1999) Chemical poisoning of Ni/MgO catalyst by alkali carbonate vapor in the steam reforming reaction of DIR-MCFC. Bull Korean Chem Soc 20:1413–1417
134. Tanaka J, Saiai A, Sakurada S, Nakajima T, Miyake Y, Saitoh T, Sasaki M, Yanaru H (1993) Design of 30 kW class DIR-MCFC system. Proc Electrochem Soc 93:37–47
135. Baker B, Burns D, Lee C, Maru H, Patel P (1981) Internal reforming for natural gas-fueled molten-carbonate fuel cells. Report 107. (90-6194-(13), GRI-80/0126; Order No. PB82-200676)
136. Kim H, Cho JH, Lee KS (2013) Detailed dynamic modeling of a molten carbonate fuel cell stack with indirect internal reformers. Fuel Cells 13:259–269
137. Pfafferodt M, Heidebrecht P, Sundmacher K, Wuertenberger U, Bednarz M (2008) Multiscale Simulation of the Indirect Internal Reforming Unit (IIR) in a Molten Carbonate Fuel Cell (MCFC). Ind Eng Chem Res 47:4332–4341
138. Freni S, Aquino M, Passalacqua E (1994) Molten carbonate fuel cell with indirect internal reforming. J Power Sources 52:41–47
139. Miyazaki M, Okada T, Ide H, Matsumoto S, Shinoki T, Ohtsuki J (1992) Development of an indirect internal reforming molten carbonate fuel cell stack. In: Proceedings of the Intersociety Energy Conversion Engineering Conference, 27th(3), vol 3. 287–3.292
140. Huijsmans JPP, Kraaij GJ, Makkus RC, Rietveld G, Sitters EF, Reijers HThJ (2000) An analysis of endurance issues for MCFC. J Power Sources 86:117–121
141. Williams MC, Maru HC (2006) Distributed generation—Molten carbonate fuel cells. J Power Sources 160:866–867
142. Coddet P, Liao HL, Coddet C (2014) A review on high power SOFC electrolyte layer manufacturing using thermal spray and physical vapour deposition technologies. Adv Manufact 2:212–221
143. Patakangas J, Ma Y, Jing Y, Lund P (2014) Review and analysis of characterization methods and ionic conductivities for low-temperature solid oxide fuel cells (LT-SOFC). J Power Sources 263:315–331
144. Zhu B (2009) Solid oxide fuel cell (SOFC) technical challenges and solutions from nano-aspects. Int J Energy Res 33:1126–1137
145. Ishihara S, Yamamoto T (2003) High temperature solid oxide fuel cells fundamentals, design and applications. In: Singhal SC, Kendal K (eds) Elsevier
146. Mukhopadhyay M, Mukhopadhyay J, Basu RN (2013) Functional anode materials for solid oxide fuel cell—a review. Trans Indian Ceram Soc 72:145–168
147. Tao SW, Cowin PI, Lan R (2012) Novel anode materials for solid oxide fuel cells. Energy 35:445–477
148. Grenier JC, Bassat JM, Mauvy F (2012) Novel cathodes for solid oxide fuel cells. Energy 35:402–444
149. Ding D, Li X, Lai SY, Gerdes K, Liu M (2014) Enhancing SOFC cathode performance by surface modification through infiltration. Energy Environ Sci 7:552–575
150. Backhaus-Ricoult M (2008) SOFC—a playground for solid state chemistry. Solid State Sci 10:670–688

151. Vielstich W (1970) In: Fuel Cells, Modern Processes for the Electrochemical Production of Energy Chichester, Wiley-Interscience, UK
152. Yamamoto O (2000) Solid oxide fuel cells: fundamental aspects and prospects. Electrochim Acta 45:2423–2435
153. Huijsmans JPP, van Berkel FPF, Christie GM (1998) Intermediate temperature SOFC—A promise for the 21st century. J Power Sources 71:107–110
154. Singh P, Minh NQ (2004) Solid oxide fuel cells: technology status. Int J Appl Ceramic Technol 1:5–15
155. Veyo SE, Vora SD, Lundberg WL, Litzinger KP (2003) Tubular SOFC hybrid power system status. ASME Turbo Expo: Power for Land, Sea & Air, Atlanta, GA, United States, 708-714, 16–19 June 2003
156. Hishinuma M, Kawashima T, Yasuda I, Matsuzuki Y, Ogasawara K (1995) Current status of planar SOFC development at Tokyo Gas. Proc Electrochem Soc 1:153–162
157. Singhal SC (2000) Advances in solid oxide fuel cell technology. Solid State Ionics 135:305–313
158. Winkler W, Lorenz H (2002) The design of stationary and mobile solid oxide fuel cell-gas turbine systems. J Power Sources 105:222–227
159. Horiuchi K (2013) Current status of national SOFC projects in Japan. ECS Trans 57:3–10
160. Jones FGE, Casting T (2005) Co-Firing and Electrical Characterisation of Novel Design Solid Oxide Fuel Cell SOFCROLL PhD thesis, University of St Andrews
161. Minh NQ (1993) Ceramic fuel-cells. J. American Ceramic Soc 76:563–588
162. Lee HM (2003) Electrochemical characteristics of $La_{1-x}Sr_xMnO_3$ for solid oxide fuel cell. Mater Chem Phys 77:639–646
163. Tanner CW, Fung KZ, Virkar AV (1997) The effect of porous composite electrode structure on solid oxide fuel cell performance. 1. Theoretical analysis. J Electrochem Soc 144:21–30
164. Gorte RJ et al (2000) Anodes for direct oxidation of dry hydrocarbons in a solid-oxide fuel cell. Adv Mater 12:1465–1469
165. Ivers-Tiffee E, Weber A, Herbstritt D (2001) Materials and technologies for SOFC-components. J Eur Ceram Soc 21:1805–1811
166. Dees DW et al (1987) Conductivity of porous Ni/ZrO_2-Y_2O_3 cermets. J Electrochem Soc 134:2141–2146
167. Jiang SP, Callus PJ, Badwal SPS (2000) Fabrication and performance of Ni/3 mol% Y_2O_3-ZrO_2 cermet anodes for solid oxide fuel cells. Solid State Ionics 132:1–14
168. Buonomano A, Calise F, Dentice d'Accadia M, Palombo A, Vicidomini M (2015) Hybrid solid oxide fuel cells–gas turbine systems for combined heat and power: a review. Appl Energy 156:32–85
169. Doherty W, Reynolds A, Kennedy D (2015) Process simulation of biomass gasification integrated with a solid oxide fuel cell stack. J Power Sources 277:292–303
170. Zabihian FA (2009) A review on modeling of hybrid solid oxide fuel cell systems. Int J Eng 3:85–119
171. McPhail SJ, Aarva A, Devianto H, Bove R, Moreno A (2011) SOFC and MCFC: commonalities and opportunities for integrated research. Int J Hydrogen Energy 36:10337–45.9
172. Calise F, Dentice d Accadia M, Vanoli L, von Spakovsky MR (2007) Full load synthesis/design optimization of a hybrid SOFC GT power plant. Energy 32:446–458
173. Zhang X, Chan SH, Li G, Ho HK, Li J, Feng Z (2010) A review of integration strategies for solid oxide fuel cells. J Power Sources 195:685–702
174. Calise F, Dentice d Accadia M, Vanoli L, von Spakovsky MR (2006) Single-level optimization of a hybrid SOFC GT power plant. J Power Sources 159:1169–1185
175. Calise F, Ferruzzi G, Vanoli L (2009) Parametric exergy analysis of a tubular solid oxide fuel cell (SOFC) stack through finite-volume model. Appl Energy 86:2401–2410
176. Zhou XD, Singhal SC, Fuel Cells—Solid Oxide Fuel Cells, pp 1–16
177. Amarasinghe S, Ammala P, Aruliah S, Mizusaki J (2005) Solid Oxide Fuel Cells IX (SOFC-IX). In: Singhal SC (ed) The Electrochemical Society, Inc, 184—190

178. Singhal SC, Kendall K (2003) High temperature solid oxide fuel cells: fundamentals, design and applications. Elsevier, Oxford
179. Mukerjee S, Haltiner K, Kerr R et al (2007) Solid oxide fuel cell development: latest results. In: Eguchi K, Singhal SC, Yokokawa H, Mizusaki J (eds) Solid oxide fuel cells-X. The Electrochemical Society, New Jersey, pp 59–65
180. Brandon NP, Blake A, Corcoran D et al (2004) Development of metal supported solid oxide fuel cells for operation at 500–600 °C. J Fuel Cell Sci Technol 1:61–65
181. van Gerwen RJF (2003) High temperature solid oxide fuel cells, fundamentals, design and applications, systems and applications. In: Singhal SC, Kendall K (eds.) Elsevier, New York, 364–392
182. Atkinson A, Barnett S, Gorte RJ et al (2004) Advanced anodes for high-temperature fuel cells. Nat Mater 3:17–27
183. Suzuki M, Sogi T, Higaki K et al (2007) Development of SOFC residential cogeneration system at Osaka Gas and Kyocera. In: Eguchi K, Singhal SC, Yokokawa H, Mizusaki J (eds) Solid Oxide Fuel Cells-X, The Electrochemical Society, 27–30
184. Tanner CW, Fung KZ, Virkar AV (1997) The effect of porous composite electrode structure on solid oxide fuel cell performance: theoretical analysis. J Electrochem Soc 144:21–30
185. Vora SD (2007) Development of high power density seal-less SOFCs. In: Eguchi K, Singhal SC, Yokokawa H, Mizusaki J (eds) Solid oxide fuel cells-X. Electrochem Soc, New Jersey, pp 149–154
186. Stevenson JW, Singh P, Singhal SC (2005) The secrets of SOFC success. Fuel Cell Rev 2:15–21

Chapter 3
Fuel Cells Challenges

3.1 Introduction

Despite many successfully specialized applications of fuel cells, such as UAV (unmanned aerial vehicles), submarines and the Apollo and Shuttle space missions [1–5], these applications are not the primary markets for fuel cell and hydrogen industries. To date the cost and quality of fuel cells are not comparable to those of the IC engines or gas turbines.

Over the past 50 years, a large number of research institutes, private companies and government labs have conducted research and development on fuel cell products because of its high efficiency and environmental-friendly operation. More than US$22 billion has been invested in research and development of fuel cell technology in Japan, USA and Europe over the past 18 years [6]. The results from these efforts are reflected by a rapid growth in the number of publications and patents. However, progress has been incremental, resulting in only slightly improved performance, but durability and reliability have shown no major progress or real competitive benefits. The process of commercializing any new technology is fraught with a multitude of challenges. A widespread adoption of fuel cells must start because of their unacceptably low durability and reliability and, in many cases, unacceptably high cost.

Throughout the history of the development of the fuel cell, many companies, investors and governments believed that the technology was just a few years away from commercial success and the investment of a little more time and money would lead to a progress [7]. Recently, the EU has launched a new framework program [8], (2014–2020), in which 2.8 billion was allocated to the development of fuel cell and hydrogen technology that leans heavily upon the development of a hydrogen fuelling infrastructure [8]. Mr. Hancock (Minister

M. Turco et al., *Treatment of Biogas for Feeding High Temperature Fuel Cells*,
Green Energy and Technology, DOI 10.1007/978-3-319-03215-3_3

of Business, UK) announced funding of £11 million for a pilot project of public sector hydrogen vehicles and an initial network of up to 15 hydrogen refueling stations by the end of 2015 [9]. These ambitious goals are perfectly defensible and indeed desirable if we have the means to achieve them, although they long on ambition and short on scientific detail [10–12]. So far, fuel cells have not achieved reliable operation or cost benefits comparable to IC engines. Thus, the resulting disappointment has led to a breakdown of the initial high expectations of governments and the general public. As a result, in spite of their many claimed successes, the fuel cell industry has serious problems [13]. It is a top priority to produce high-quality fuel cells with high reliability and long-term durability at a low cost in R&D.

3.2 The Hydrogen Economy, Hydrogen Fuelling Infrastructure, and Fuel Cell Technology

Hydrogen fuelling infrastructure and fuel cell technology are parts of the Hydrogen economy. Therefore, hydrogen fuelling infrastructure and fuel cell technology are assumed to have a close relationship [14]. There are major challenges for the hydrogen economy and fuel cell technology causing them to be viewed as post 2030 technologies [10, 12, 15, 16]. However, the fuel cell itself is independent of the hydrogen economy. As engines, fuel cells can use different fuels, such as natural gas, methanol and ethanol, and can have different applications [17]. There are two main flaws in the relationship between hydrogen and fuel cell technology: the chicken-egg problem; and the barriers to scaling-up fuel cells.

3.2.1 Chicken-Egg Issue

The chicken-egg issue with regard to fuel cells is a longstanding assumption that the hydrogen fuelling infrastructure would lead to a substantial reduction in the costs of fuel cells through mass-manufacturing, and the performance of fuel cells would be improved definitely as planned steps [18, 19]. The commercialization of fuel cells has intentionally created a chicken-egg relationship between hydrogen fuelling infrastructure and fuel cell vehicles [18–24]. The absence of hydrogen fueling infrastructure and the consequent absence of hydrogen vehicles does not incentive to build a hydrogen fueling infrastructure [25].

The technical problems could be overcome by a displacement of hydrogen fuelling infrastructure and mass vehicle purchases under government support, and over time, the cost of fuel cell vehicles and hydrogen would be comparable or even lower than current IC engine vehicles [24, 26]. However, a hydrogen fuelling

infrastructure cannot solve the technical issues of fuel cells. Over the past few decades, pilot hydrogen fuelling infrastructures have been built for demonstration, such as CaFCP and the California mandate on zero emission vehicles [27, 28], the CUTE (Clean Urban Transport for Europe) [25] and the Whistler's hydrogen fuel cell buses [16, 29]. Numerous studies of hydrogen fuelling infrastructures have been carried out [18, 20, 23, 24, 30, 31]. However, most of these studies focused on strategy and economic analysis of a hydrogen fuelling infrastructure and deployment of numerous fuel cell vehicles [24, 32–37], and not on the analysis of the technical feasibility of how a hydrogen fuelling infrastructure would reduce the costs of the fuel cell itself and solve the fundamental problems of durability and reliability of fuel cells.

A hydrogen fuelling infrastructure can improve fuel supply for vehicles, reducing some of the cost of hydrogen fuel cells through massive manufacturing, but the importance of the hydrogen fuelling infrastructure on fuel cell costs has been overestimated for several reasons:

- Hydrogen is not the only energy source for fuel cells. There are many different types of fuel cells (e.g., solid oxide fuel cells and direct ethanol fuel cells) which do not use hydrogen.
- Hydrogen has no actual relationship to manufacturing costs, robustness, durability or reliability of the fuel cell. It only relates to operational costs.
- Hydrogen is not currently considered renewable energy as it comes from fossil fuels [30, 32, 37–40] and a hydrogen fuelling infrastructure is not necessary because natural gas can be converted locally into hydrogen.
- Hydrogen fuelling infrastructure is to ensure a reliable hydrogen supply to vehicles rather than reduce costs and technical problems of fuel cells.

Investments in a hydrogen fuelling infrastructure do not substantially reduce costs of the fuel cell itself or answer the key questions of durability, reliability and robustness [25, 35].

3.2.2 Independence of Fuel Cell Technology

It is established that the fuel cell itself is independent of a hydrogen economy. Thus, it is important clarify the difference between commercialization of fuel cells and a hydrogen economy. Figure 3.1 shows two ways to achieve commercialization of fuel cells. One is commercialization of fuel cell itself (Black color), and the other is a hydrogen economy including commercialization of fuel cells (Blue color). The former has no any relation to a hydrogen fuelling infrastructure. Therefore, the commercialization of fuel cells can start with the fuel cell itself rather than the hydrogen economy. Many successful special applications of fuel cells have demonstrated this possibility.

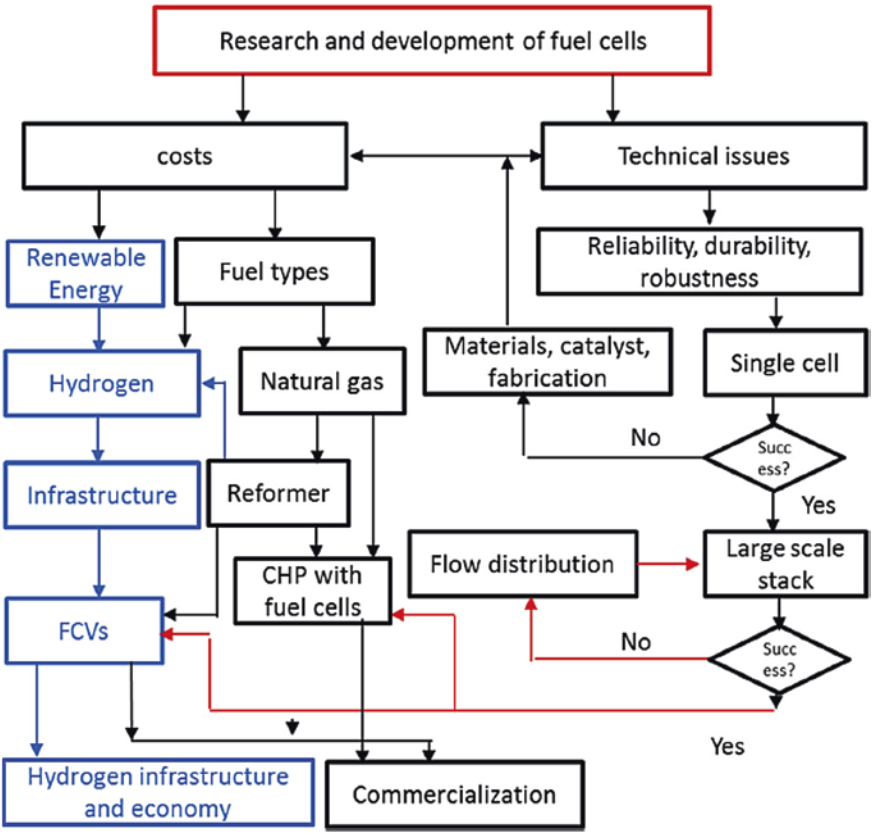

Fig. 3.1 Ways to achieve commercialization of fuel cells [114]

3.3 Major Barriers for Commercialization of Fuel Cells

Generally, commercialization of any new product has three challenges: costs, quality and acceptance by end-users. However, unlike other new products, fuel cells have no natural opposition [40]. Given their quality and price being comparable to IC engines and gas turbines, fuel cell would be accepted by end-users and the public as an environment-friendly technological alternative. This public acceptance has been reflected by large investments in fuel cells under subsidies over the past 20 years. Thus, the largest single impediment of fuel cells is the high costs (e.g., hydrogen production and manufacturing), and technical issues (e.g., low robustness, reliability, and durability) compared to IC or turbine engines.

A large number of private companies and government research labs have conducted major R&D and product development activities over the past 50 years in this technology [6, 41, 42], however, the challenges lie in the difficulty of fuel cell

technology, which involves highly complex mechanisms, related to multiple chemical and physical interactions [6, 43].

3.3.1 Costs of Fuel Cell Itself

Fuel cell costs can be broken into three areas: the material and component costs, labor (i.e., design, fabrication, and transport), and capital cost of the manufacturing equipment [44]. It should be mentioned that only labor and capital costs can be reduced through mass-manufacturing. Material and component costs, such as catalysts, membrane, and bipolar plates, are dependent on technological innovations and the market [30, 45]. With a clear advantage of having no moving-parts, the fabrication and operation of fuel cells should be less expensive than IC engines and turbines. However, the fuel cells are more expensive and less durable and reliable than IC engines [41, 46]. Thus, the manufacturers of fuel cells have to continue to collect subsidies from governments to scale these units up for commercial applications with limited success because of the challenges of cost, durability, robustness or reliability. One method of reducing costs is to develop cheaper materials, catalysts or sealing with higher tolerances to higher operating temperatures. As a result, research and development of fuel cells has been directed to solve the issues of materials, chemistry, water and hotspots control [46]. Several measures have been considered, such as associated systems for water and heat management [43, 47], high temperature PEM fuel cell [48, 49], and cheaper catalysts [50–52].

3.3.2 Key Technical Barriers

The U.S. Department of Energy has established targets for fuel cell durability [41, 42, 53]. The durability for automotive use will be of 5000 h by 2017 and for micro-CHP of 40,000 h, respectively. Durability is a lifetime within the repair rate and cost in the planned repair, overhaul and maintenance. However, this durability target is not sufficient as the key targets for acceptance by end users. Reliability and availability may be more important than durability for end-users since an unplanned repair and maintenance can cause delay in home, work or business activities, but is not recognized in the targets [7]. A higher availability is an indicator of reliability and durability, which means fewer repairs and maintenance. Therefore, the major technical barriers for fuel cells are not only low durability but also low reliability. Availability and reliability must be taken into account for the targets of fuel cell scaling-up since end-users require a warranty of use as well as less maintenance and repair and a low operating cost. Both low durability and reliability are caused by accumulated degradation of materials and catalysts [43, 54–58].

The identical individual cells are stacked together through flow field designs. It is a challenge to keep all the cells of the stack at a uniform flow rate and pressure drop [59, 60].

Whilst reliability, robustness and durability in the stack cannot reproduce the performance of a singular working cell, it is understood that failure of a stack can occur because of the failure of any one individual cell.

The failure of an individual cell generally occurs because the cell did not work as it was designed due to higher or lower flow rates.

The change of the flow rates lead to fast or slow reaction of the local cell, resulting in a higher or lower temperature and water production, even in a hotspot or flood. The hotspot temperature can greatly exceed the design capacity of materials or catalyst, leading to accelerated degradation or failure. Furthermore, the uneven distribution of temperature results in thermal stresses, which are the primary causes of mechanical failure. The failure of a catalyst may result from flooding and the failure of seals may result from high mechanical stress due to extreme pressure differences. Further, the uneven reaction may be amplified because of a blockage of some cells, leading to the serious degradation of materials and catalyst, water and heat. Thus, the failure of fuel cell scaling-up is generally caused when some cells deviate from design conditions within the stack, resulting in uneven electrochemical reactions, although the outward appearance of the failure is still one of materials, chemistry, water and hotspot issues. As a result, the system performance deteriorates the designed performance, reliability and durability.

For example, the loss of power output due to an individual cell failure is only 1 % in a stack of 100 cells. However, the very small deviation caused by the cell failure may be amplified in multiple level manifolds due to water blockage of the cell. This effect of amplification may be serious enough to lead to various other degradations or failure of materials and catalysts or local hotspot or flooding.

It has been observed that individual cells in a stack often exhibit heterogeneities in cell performance and a fuel cell stack was drastically more susceptible to performance degradation compared to a single cell fuel cell [61–65]. A fuel cell stack performs different compared to single cells [66–69]. A larger stack has a shorter lifespan due to early failure of some individual cells. A failure of the operation of a fuel cell stack ultimately occurs due to the loss of structural integrity of one or several of the cells, even in short-stack experiments [70–72].

3.3.3 Theoretical Solutions of Fuel Cell Scaling-Up Issues

One theory to address the scaling-up issue is to ensure that each of the cells work at its optimal design flow and temperature conditions. The flow distribution and

pressure drop can be significantly improved using appropriate configurations of bipolar plates [59, 60, 73], operating conditions [66, 68] and channel sizes [74].

Major technical barriers of fuel cells are not only durability but also reliability. The reliability may be more important than durability for acceptance by end-users but receives a little attention. The integration of fuel cell technology with other areas of science such as materials, catalyst and process control is highly needed [6, 43, 75].

There are two key steps to achieve the commercialization of fuel cells. The first step is to solve the issues of cost, reliability and durability of fuel cells. The second step is to build a new business model and develop standards for the industry.

The pre-commercialisation phase of FC technologies is challenging and uncertain. A new market development phase is said to be near, as FC firms are developing and unveiling prototypes and pre-commercial products at an increasing rate. However, widespread commercialisation has been announced several times and subsequently postponed an equal number of times. Illustrative are statements by Daimler Chrysler in 2000 that by 2004 a few thousand FC vehicles would be introduced for a targeted price of $18.000 [76].

Market application decisions appear critical for commercialisation success. The market application of a new technology requires some kind of "match" between technology and market opportunities (e.g., [77, 78]). Additionally, the difficulty of making decisions on technology and market matches is recognized. For example, customer needs may not be explicitly known and firms may be uncertain about the function of their technology with respect to diverse market segments [79]. To what degree is the selection of market applications challenging in the case of FC technology?

It can be expected that FC technology will initially be applied in various niche markets such as specialized or professional segments and eventually applied in mass markets. As Geels [80] suggests, the diffusion of innovations needs to be understood as a trajectory of niche-cumulation, i.e., new technologies are first used in particular niches or application domains then in other niches and eventually also in mainstream markets. A niche market is a market portion that may accept the relative high cost and low performance of a new technology because the technology fulfills a demand that is not addressed by mainstream technologies. The ability to recognize and exploit such market opportunities requires both technical and market expertise [81, 82].

According to the recent paper of Penrose [83] and Barney [84], resources are determinant for competitive decision-making. Critical resources include (1) basic scientific or technological research, (2) financing mechanisms, and (3) a pool of competent human resources [85]. Considering that young firms are characterized by a scarcity of resources, it can be assumed that resource acquisition and allocation are particularly challenging for the firms of an emerging industry. In the case of FC technology resource and competence development are expected to be critical issues with respect to decisions on the development of FC technology and FC market applications.

3.4 The Market for FC Products

A characterisation of the market for FC products highlights the performance indicators of the technology that matter to the end user.

Van der Meer [86] explains that despite the abundance of customer interest, there is no observable market demand. Current high costs and the predicted gradual cost reduction are likely to imply slow market acceptance. Mallant [87], Heijboer [88] Kammerer [89] evidenced the demonstrative phase of development and the significance of practical application experience to communicate the state of the art to market actors.

The lack of cost and performance competitiveness, due to the current immaturity of the technology, poses uncertainty about if, when and which markets will adopt the technology. The lack of competitiveness increases the importance of finding premium markets and applications with added value on other performance metrics. At the same time FC technology requires optimisation and product development to meet traditional performance indicators and to enhance new qualities of the technology.

FC technology offers new qualities and non-traditional performance indicators such as zero emission and quiet performance. However, consumers tend to judge the technology based on traditional indicators [90]. Consumers assume that the new technology will perform as their current product [88]. Additionally, due to the novelty of the technology, cultural and psychological factors, consumers may not understand or accept the new qualities of FC technology [91]. For example, motorists may prefer loud engine sounds above the quiet propulsion of a FC electric or battery electric vehicles. The historic development of battery electric vehicles has shown that a superior environmental performance (zero emission) does not out way a lack of traditional performance (low range). However, new values of the technology may provide market opportunities for niche market applications. FC firms target early adopter niche markets in which the new and non-traditional indicators provide sufficient added value to outweigh the limited traditional performance.

Demonstration projects prove to be effective for explaining the novel values to customers [92]. Communicating the technology through demonstrations has two functions: to create excitement at a mass level and to explain the technology and persuade stakeholders at an individual level. It is, however, challenging to create pull, without creating interest without unrealistic expectations [81].

An additional challenge lies in understanding to what degree customers really value the new qualities of FC technology [93]. Due to the clean and sustainable nature of the technology the interest of the public opinion is increasing the market research may not be representative when customers are unfamiliar with the technology and its values [94]. Heijboer [88] and Geels [80] suggest that traditional marketing techniques cannot be applied when the final shape of the product and market are uncertain. The evaluation of market opportunities and customer interest is challenging.

Concluding, the market for FC products can be characterized by a (i) lack of cost and performance competitiveness and (ii) non-traditional performance indicators. An additional characteristic is the commodity business, related to the lack of cost competitiveness: consumers generally do not consider the power source of a product, as long as the product functions, whilst the replacement of the current power source may result in higher costs for the consumer without necessarily providing higher performance or quality. These characteristics indicate that FC developers are challenged to find and evaluate niche markets and understand customers to develop competitive FC products according to both traditional performance indicators and new qualities. Beside the technological and market characteristics, the contextual factors also influence the commercialisation process of FC technology.

3.5 Contextual Characteristics

The development and commercialisation of FC technology is related to numerous contextual factors, like as for example policy issues and the development of a fuel infrastructure.

Complementary Technologies and Network Externalities

The implementation of FC technology strongly depends on the development of complementary technology and network externalities such as refueling stations and the distribution of fuel storage tanks [91, 95]. Infrastructure investment payback depends on the number of FC vehicles in operation and the usability of a FC vehicle depends on the number of available fuelling stations. Smith [96] describes the significance of a firm's compatibility with complementary products and network externalities for the successful commercialisation of a technology. FC storage and fuelling products must, for example, complement the FC developments of a FC firm. Complementary products are likely to give rise to network externalities: the attractiveness of FC technology to potential customers depends on the size of installed fuelling infrastructure and available storage tanks. Subsequently, the development of network externalities will partly depend on the emergence of FC standards and certification codes.

Regulatory Support

Additional contextual characteristics include the formation of regulatory support. There is a steady increase in regulatory support in terms of investment programs, financial possibilities and good will, in the US, EU and Japan. For example, in 2003 President Bush announced the Freedom Fuel initiative of 1.2 billion research funding for hydrogen powered automobile development. In 2004, the European research commissioner Philippe Busquin presented an EU funding program of some ¥100 million [97].

The development of complementary standards and the availability of regulatory support are characteristics of the FC technology commercialisation context.

The implications for FC developers are (i) the consideration of complementary technologies in competence development and (ii) the consideration of resource acquisition through regulatory support.

There is a dynamic relationship among FC innovation, the market and the FC firms that emerge and compete on the basis of this new technology. Historical cases have shown that the development of a new technology brings about the development of a new industry in which entrepreneurs get opportunities to innovate [98] although historical cases of new technology emergence show that only a small percentage will survive [99, 100].

FC industry is not self-supporting and considering the long-term process of implementation, return on investment will take time. FC firms are faced with a long payback period and depend on subsidized projects, new venture funding or OEMs for capital to invest in further R&D.

The low return on the required high investments pose challenges on the acquisition and allocation of resources. Niche markets will enable short- and near-term sales. With the lack of observable demand, it is challenging to decide when to invest in which project or market application. FC firms depend on investors over a long period of time, in which the firms are required to show progress and initiate revenue generation.

The FC industry is characterized by a high degree of business to business (B&B) collaboration. The FC firms have formed and are looking for both long and short-term strategic alliance and partnerships for direct use or market access. For example, Ballard, Nuvera, and Hydrogenics have alliances and are partly owned by the automotive firms Daimler Chysler/Ford, Renault and GM, respectively.

Concluding, the FC industry can be characterized as an (i) emerging industry, (ii) with low return on investment, (iii) collaborative, and (iv) heterogeneous technology application strategies. The consequent implications on decision-making in the process of FC technology commercialisation for FC developers are: (i) dependence on external resources for R&D and market development, (ii) resource acquisition and market access through inter-firm partnerships, and (iii) technology supply and market breadth.

Stationary Fuel Cell Systems potentially offer solutions to the varied energy issues that face Europe, and other regions of the world. The European Union's 20–20–20 targets for emissions, efficiency and energy sources point to a need to do things differently, and stationary fuel cell systems can be part of the solution. The stationary fuel cell value proposition is complex. Costs are clearly important, but so are the other benefits: the environmental benefits of lower emissions, the relatively quiet operation and the promise of autonomy from mainstream power suppliers for end users. Such benefits need to be matched by three key operational and economic criteria: reliability, durability and affordability.

Fuel cell systems must be able to offer reliability of supply equal to centralized power grids; they should have an operational lifetime equivalent to existing domestic and commercial boilers and generators; and they need to be 'competitive' in terms of cost of delivered power and heat (and cooling where applicable). Stationary fuel cell systems have made steady progress toward reliability and

durability targets over the past decade; the greatest challenge remains that of cost, but even here progress is being made.

Costs

The prospect of wide scale commercialisation of stationary fuel cell systems will ultimately depend on cost. Evidence available in the market place suggests that the costs of stationary fuel cell systems are currently available for between €25,000 and €4000/kWe.

In assessing the commercialisation potential of stationary fuel cell systems emphasis is placed upon cost targets which need to be met to achieve mass market success. These are most developed for the domestic micro-CHP products, and they have often been set by the public sector. METI in Japan has reiterated the 2008 estimate that micro-CHP fuel cell systems must meet a target of ¥500,000e¥600,000 by 2020 (€3700–€4450) in the period from 2020 to 2030 [101]; in the USA the DoE sees a figure of $1000/kWe by 2020 for a 2 kWe unit [102] released in 2011, whilst the European FCH JU in Europe has a target of €5000/kWe plus household heating by 2020 as set out in the revised Multi-Annual Implementation Plan [103]. In assessing the commercialisation potential of stationary fuel cell systems emphasis is placed upon cost targets which need to be met to achieve mass market success. These are most developed for the domestic micro-CHP products, and they have often been set by the public sector. METI in Japan has reiterated the 2008 estimate that micro-CHP fuel cell systems must meet a target of ¥500,000-¥600,000 by 2020.

(€3700–€4450) in the period 2020–2030 [101]; in the USA the DoE sees a figure of $1000/kWe by 2020 for a 2 kWe unit [102] released in 2011, whilst the European FCH JU in Europe has a target of V5000/kWe plus household heating by 2020 as set out in the revised Multi-Annual Implementation Plan [103].

Of interest is the view that the majority of the cost is dominated by the fuel cell stack and the fuel processing subsystems. Further, the primary cost reduction for smaller SOFC units will stem from improvements to the fuel cell subsystem, whilst cost reductions for the fuel processing system will be difficult: balance of plant component costs reduction opportunities, such as compressors, pumps, sensors and heat exchangers, are considered to be fairly small. Similarly, other subsystems such as power electronics are considered fairly stable cost wise.

3.5.1 Fuel Cell System Cost Reduction

Identifying real examples of cost reductions in the fuel cell field is difficult given the limited numbers of units in service and the increase in production experience to date. However, evidence from the Japanese Ene-Farm project over the past few years provides examples of what has been achieved by leading businesses in the field. Both Panasonic and Toshiba have made public announcements in the past

few years about the costs of their products and progress in reducing these costs alongside product improvements.

Panasonic, with Tokyo Gas, announced in January 2013 that it had reduced the price (excluding installation) of its domestic PEM fuel cell system to ¥1,995,000 by approximately ¥760,000, a reduction of 27.5 % from its 2011 model. This itself was a reduction from its 2009 model (selling at ¥3,465,000 [104]) of 20 %. A year or so earlier in January 2012 Toshiba, with Osaka Gas, announced that it had reduced the price of its domestic fuel cell system by ¥650,000–¥2,604,000, a 25 % reduction in cost [105]. In both cases sales increases were anticipated and further cost reductions expected. The Panasonic announcement also included further information on the performance and other aspects of the unit. The cost reduction was associated with an improvement of lifetime from 50,000 to 60,000 h; a reduction in components by 20 %; reduced weight by 10 % and reduced size overall. Of significance was a reduction in noble metals in the fuel processing subsystem by 50 % and platinum catalyst by 50 %. Total efficiency, both heat and power, was calculated at 95 % LHV.

It is evident that cost reductions are possible over time, but that they are not simply a function of numbers of units produced and installed, or technology improvements, but a mix of both production increases and technology and product improvements, made by it should be added, experienced and capable businesses.

Public Support

One means to address the issue of the current overly expensive stationary fuel cell systems is to provide some form of financial support from the public sector. Public support is an important early market incentive for stationary fuel cells systems, be this in the form of capital subsidies (e.g., North Rhine-Westphalia in Germany [106]); or capital support and feed-in-tariff style pricing (e.g., South Korea [107]); or capital and other incentives available in the USA, usually at the State level, where incentives vary up to $5500/kWe. This support goes some way toward negating the higher prices of stationary fuel cell systems when compared with competitive systems.

Market

Fuel cell systems with grid gas connections have proven to be highly reliable in terms of power and heat provision [108] for end users. Similarly, stationary fuel cell systems offer end users the prospect of better control over their energy costs. As energy costs continue to rise, for example in Europe, the attractiveness to large energy users of autonomy from the grid is likely to prove increasingly attractive.

There are markets where the relatively high cost of fuel cell systems, be it residential or commercial, can be justified on the basis of the additional value associated with “green” credentials or other benefits. In Japan under the Ene-Farm program subsidies are available for the sale of residential CHP fuel cell systems.

Credible cost reduction pathways are necessary for stationary fuel cell systems to achieve the longer term aim of mass market adoption. Developers therefore face the challenge of both addressing market segmentation, but also of defining

achievable cost reductions over, if not the short term, at least the medium term. Cost reduction strategies therefore become critical.

Fuel cell technology is a feasible technological option for domestic CHP built environment applications.

Currently there is no conclusive set of figures concerning the CO_2 emission savings achievable from fuel cell CHP operating in the domestic built environment; however, they are achievable and have the potential to be size able depending upon the situation. Currently, the main barriers for fuel cell CHP systems in the domestic built environment include [109]: 1. Cost—future systems will need to use using fewer parts and more mass produced components. 2. Reliability—future systems will need to look for simpler design solutions and quality control mechanisms. 3. Current performance—for the more promising SOFC technology this will be the use of lower temperature catalysts and novel materials.

3.6 Fuel Cell Combined Heat and Power Systems

Elmer et al. [110] have evidenced the significant operational advantages fuel cells offer compared to conventional micro-CHP technologies, such as; higher electrical efficiencies, lower H:P ratios, reduced noise and vibrations during operation and flexibility of fuel use. The use of fuel cell technology can lead to significant reductions in CO_2 emissions and operating costs for the user. With regards to the type of fuel cells being used, the low temperature PEMFC and the intermediate to high temperature SOFC currently show the greatest promise, with most building integrated projects focussing on these two technological variants. The PEMFC offers quick start up time, power modulation, and useful direct hot water output, whilst the SOFC provides high electrical efficiency, ability to internally reform hydrocarbon fuels and a high temperature heat output which can be utilized in another cycle.

It has been reported that in 2012 fuel cell technology outsold conventional combustion-based systems for micro-CHP applications for the first time. This signifies a significant shift in the market and shows an exciting future for fuel cell technology.

Issues of fuel cell CHP optimisation, particularly thermal, has been addressed, with district scale fuel cell operation and interaction being cited as an effective way to optimize the use of fuel cell technology in the domestic built environment.

Fuel Cell Tri-generation

Domestic scale tri-generation has the potential to produce higher energy conversion efficiency and hence reduce net fuel cost and CO_2 emissions compared to a conventional combustion-based CHP system. Currently there is very limited literature regarding fuel cell tri-generation systems, however, three core topics can be recognized: (1) commercial scale systems, which illustrate high system efficiency and reduced primary energy demand, (2) combustion-based systems,

which would benefit from a prime move technology with a higher electrical efficiency, such as a fuel cell, and (3) fuel cell tri-generation systems, although only simulation-based work, they show high energy utilization and future potential [111, 112]. A common conclusion is that the cost of the fuel cell needs to fall in order to effectively facilitate the uptake of fuel cell tri-generation systems. By sharing the capital cost of the fuel cell in the CHP or tri-generation system it would make the current use of fuel cell technology a much more viable prospect. Decentralized energy generation from fuel cells in the domestic built environment can lead to emission reductions, reduced operational cost for the user and increased energy security, all essential objectives for the future built environment. Economic profitability is an essential criterion for any form of sustainable development [113]. Fuel cell CHP and tri-generation systems can offer significant economic benefit [110]. However, as with any novel technology, a major challenge facing fuel cell technology is its capital cost. Until significant reductions in the capital cost of the technology can be made, be it through government support or technological innovation, the wider use of fuel cell technology in the domestic built environment cannot be expected.

References

1. Gross D (2010) Fuel cells: 170 years of technology development e and space age experience! Cleantech Mag Fuel Cell. http://www.cleantechinvestor.com/portal/fuel-cells/6455-fuel-cell-history.html. Special Sept/Oct 2010
2. Johnson B (2012) Power sources for space exploration. http://large.stanford.edu/courses/2012/ph240/johnson1/. 11 Dec 2012
3. Naval-Technol. U212/U214 submarines. Germany (2014). http://www.navaltechnology.com/projects/type_212
4. Perry ML, Fuller TF (2002) A historical perspective of fuel cell technology in the 20th century. J Electrochem Soc 149:S59–S67
5. Warshay M, Prokopius PR (1990) The fuel cell in space: yesterday, today and tomorrow. J Power Sources 29:193–200
6. Behling N (2012) Solving the fuel cell dilemma. Fuel Cells Bull 11:12–14
7. Zegers P (2006) Fuel cell commercialization: the key to a hydrogen economy. J Power Sources 154:497–502
8. Horizon (2020) http://www.sciencebusiness.net/OurReports/ReportDetail.aspx?ReportId¼450. Accessed 29 Jan 2014
9. ITM Power (2014) Government funding to help prepare the UK for the arrival of hydrogen FCEVs. http://www.itm-power.com/news-item/government-funding-to-help-prepare-the-uk-for-the-arrival-of-hydrogenfcevs/
10. Bossel U (2006) Does a hydrogen economy make sense? In: Proceedings of IEEE vol 94, pp 1826–1837
11. Blanchette S Jr (2008) A hydrogen economy and its impact on the world as we know it. Energy Policy 36:522–530
12. Bakker S (2010) The car industry and the blow-out of the hydrogen hype. Energy Policy 38:6540–6544
13. Adamson KA (2012) Fuel cell industry faces a precipice. Forbes Mag 25. www.forbes.com/sites/pikeresearch/2012/10/25/fuel-cellindustryfaces-a-precipice/. Accessed 29 Jan 14

14. Haeseldonckx D, D'haeseleer W (2011) Concrete transition issues towards a fullyfledged use of hydrogen as an energy carrier: methodology and modelling. Int J Hydrogen Energy 36:4636–4652
15. Romm JJ (2004) The hype about hydrogen: fact and fiction in the race to save the climate. Island Press, Washington (2004)
16. Sinoski K (2013) Whistler's hydrogen fuel cell bus program in jeopardy. http://www.vancouversun.com/technology/Whistlerþhydrogenþfuelþcellþprogramþjeopardy/9212028/story.html. Accessed 22 Dec 2014. Vancouver Sun Nov 25 2013
17. EC (2013) Hydrogen energy and fuel cells: a vision of our future. European Commission, Brussels, Belgium
18. Mercuri R, Bauen A, Hart D (2002) Options for refuelling fuel cell vehicles in Italy. J Power Sources 106:353–363
19. Hardman S, Steinberger-Wilckens R (2014) Mobile phone infrastructure development: lessons for the development of a hydrogen infrastructure. Int J Hydrogen Energy 39:8185–8193
20. Agnolucci P (2007) Hydrogen infrastructure for the transport sector. Int J Hydrogen Energy 32:3526–3544
21. Oi T, Wada K (2004) Feasibility study on hydrogen refueling infrastructure for fuel cell vehicles using the o0-peak power in Japan. Int J Hydrogen Energy 29:347–354
22. Stephens-Romero SD, Brown TM, Kang JE, Recker WW, Samuelsen GS (2010) Systematic planning to optimize investments in hydrogen infrastructure deployment. Int J Hydrogen Energy 35:4652–4667
23. Baufum S, Grüger F, Grube T, Krieg D, Linssen J, Weber M et al (2013) GIS-based scenario calculations for a nationwide German hydrogen pipeline infrastructure. Int J Hydrogen Energy 38:3813–3829
24. Yang C, Ogden JM (2013) Renewable and low carbon hydrogen for California e modeling the long term evolution of fuel infrastructure using a quasi-spatial TIMES model. Int J Hydrogen Energy 38:4250–4265
25. Stolzenburga K, Tsatsamib V, Grubel H (2009) Lessons learned from infrastructure operation in the CUTE project. Int J Hydrogen Energy 34:7114–7124
26. NRC (2008) Transitions to alternative transportation technologies e a focus on hydrogen. National Research Council of the National Academies (2008)
27. CaFCP (2014) California fuel cell partnership. http://www.fuelcellpartnership.org/
28. Van den Hoed R (2005) Commitment to fuel cell technology? How to interpret carmakers' efforts in this radical technology. J Power Sources 141:265–271
29. Ballard Power System (2013). Ballard wins extra funding to advance bus fuel cell modules. Fuel Cells Bull 3:9
30. Sun Y, Delucchi M, Ogden J (2011) The impact of widespread deployment of fuel cell vehicles on platinum demand and price. Int J Hydrogen Energy 36:11116–11127
31. Industry Canada (2008) Canadian fuel cell commercialization roadmap update. ISBN: 978-1-100-10468-3
32. Chiesa P, Consonni S, Kreutz T, Williams RH (2005) Co-production of hydrogen, electricity, and CO_2 from coal with commercially ready technology. Part A: performance and emissions. Int J Hydrogen Energy 30:747–767
33. Feng W, Wang S, Ni W, Chen C (2004) The future of hydrogen infrastructure for fuel cell vehicles in China and a case of application in Beijing. Int J Hydrogen Energy 29:355–367
34. Hua T, Ahluwalia R, Eudy L, Singer G, Jermer B, Asselin-Miller N et al (2014) Status of hydrogen fuel cell electric buses worldwide. J Power Sources 269:975–993
35. BC Transit (2014) http://gofuelcellbus.com/index.php/project/bc-transit. Accessed 22 Dec 14
36. Mayer T, Kreyenberg D, Wind J, Braun F (2012) Feasibility study of 2020 target costs for PEM fuel cells and lithium-ion batteries: a two-factor experience curve approach. Int J Hydrogen Energy 37:14463–14474

37. Ogden JM (1999) Developing a refueling infrastructure for hydrogen vehicles: a Southern California case study. Int J Hydrogen Energy 24:709–730
38. Blok K, Williams RH, Katofsky RE, Hendriks CA (1997) Hydrogen production from natural gas, sequestration of recovered CO_2 in depleted gas wells, and enhanced natural gas recovery. Energy Int J 22:161–168
39. Kreutz T, Williams RH, Consonni S, Chiesa P (2005) Co-production of hydrogen, electricity, and CO_2 from coal with commercially ready technology, part B: economic analysis. Int J Hydrogen Energy 30:769–784
40. Sperling D, Ogden J (2004) The hope for hydrogen, issues in science and technology, pp 82–86
41. DOE (2012) Technical plan d fuel cells 2012. Department of Energy. https://www1.eere.energy.gov/hydrogenandfuelcells/mypp/pdfs/production.pdf. Accessed 29 Jan 14
42. DOE (2011) An integrated strategic plan for the research, development, and demonstration of hydrogen and fuel cell technologies. Department of Energy. http://www.hydrogen.energy.gov/guiding_documents.html. Accessed 29 Jan 14
43. Wang Y, Chen KS, Mishler J, Cho SC, Adroher XC (2011) A review of polymer electrolyte membrane fuel cells: technology, applications, and needs on fundamental research. Appl Energy 88:981–1007
44. Marcinkoski J, James BD, Kalinoski JA, Podolski W, Benjamin T, Kopasz J (2011) Manufacturing process assumptions used in fuel cell system cost analyses. J Power Sources 196:5282–5292
45. Odeh AO, Osifo P, Noemagus H (2013) Chitosan: a low cost material for the production of membrane for use in PEMFC: a review. Energy Sources, Part A: Recovery Util Environ Eff 35:152–163
46. DOE (2013) Annual merit review proceedings by Department of Energy. In: http://www.hydrogen.energy.gov/annual_review13_proceedings.html. Accessed 29 Jan 14
47. Dai W, Wang HJ, Yuan XZ, Martin JJ, Yang DJ, Qiao JL et al (2009) A review on water balance in the membrane electrode assembly of proton exchange membrane fuel cells. Int J Hydrogen Energy 34:9461–9478
48. Carter D (2013) A turning point for high-temperature PEM fuel cells. Fuel Cell Today 28. http://www.fuelcelltoday.com/analysis/analystviews/2013/13-08-28-a-turning-point-for-high-temperature-pem-fuel-cells. Accessed 22 Dec 14
49. Shao Y, Yin GP, Wang ZB, Gao YZ (2007) Proton exchange membrane fuel cell from low temperature to high temperature: material challenges. J Power Sources 167:235–242
50. Wu G, More KL, Johnston CM, Zelenay P (2011) High-performance electrocatalysts for oxygen reduction derived from polyaniline, iron, and cobalt. Science 332:443–447
51. Su DS, Su GQ (2011) Non precious-metal catalysts for low-cost fuel cells. Angew Chem Int Ed Angew Chem Int Ed 50:11570–11572
52. Cerri I, Nagami T, Davies J, Mormiche C, Vecoven A, Hayden B (2013) Innovative catalyst supports to address fuel cell stack durability. Int J Hydrogen Energy 38:640–645
53. Papageorgopoulos D (2011) U.S. DOE activities related to fuel cell durability. In: 2nd International Workshop on Degradation Issues of Fuel Cells, Thessaloniki, Greece, Sept 21 2011
54. Bae SJ, Kim SJ, Lee JH, Song I, Kim NI, Seo Y et al (2014) Degradation pattern prediction of a polymer electrolyte membrane fuel cell stack with series reliability structure via durability data of single cells. Appl Energy 131:48–55
55. Ji M, Wei Z (2009) A review of water management in polymer electrolyte membrane fuel cells. Energies 2:1057–1106
56. Pei P, Chen H (2014) Main factors affecting the lifetime of proton exchange membrane fuel cells in vehicle applications: a review. Appl Energy 125:60–75
57. Tu H, Stimming U (2004) Advances, aging mechanisms and lifetime in solid-oxide fuel cells. J Power Sources 127:284–293
58. Wu JF, Yuan XZ, Martin JJ, Wang HJ, Zhang JJ, Shen J et al (2008) A review of PEM fuel cell durability: degradation mechanisms and mitigation strategies. J Power Sources 184:104–119

59. Wang JY, Wang HL (2012) Flow field designs of bipolar plates in PEM fuel cells: theory and applications. Fuel Cells 12:989–1003
60. Wang JY, Wang HL (2012) Discrete approach for flow-field designs of parallel channel configurations in fuel cells. Int J Hydrogen Energy 37:10881–10897
61. Mennola T, Mikkola M, Noponen M, Hottinen T, Lund P (2002) Measurement of ohmic voltage losses in individual cells of a PEMFC stack. J Power Sources 112:261–272
62. Miller M, Bazylak A (2011) A review of polymer electrolyte membrane fuel cell stack testing. J Power Sources 196:601–613
63. Radev I, Koutzarov K, Lefterova E, Tsotridis G (2013) Influence of failure modes on PEFC stack and single cell performance and durability. Int J Hydrogen Energy 38:7133–7139
64. Wasterlain S, Candusso D, Harel F, Hissel D, François X (2011) Development of new test instruments and protocols for the diagnostic of fuel cell stacks. J Power Sources 196:5325–5333
65. Yuan X, Sun JC, Wang H, Zhang J (2006) AC impedance diagnosis of a 500 W PEM fuel cell stack part II: individual cell impedance. J Power Sources 161:929–937
66. Jang JH, Chiu HC, Yan WM, Sun WL (2008) Effects of operating conditions on the performances of individual cell and stack of PEM fuel cell. J Power Sources 180:476–483
67. Rodatz P, Büchi F, Onder C, Guzzella L (2004) Operational aspects of a large PEFC stack under practical conditions. J Power Sources 128:208–217
68. Urbani F, Barbera O, Giacoppo G, Squadrito G, Passalacqua E (2008) Effect of operative conditions on a PEFC stack performance. Int J Hydrogen Energy 33:3137–3141
69. Weng F, Jou B, Su A, Chan SH, Chi P (2007) Design, fabrication and performance analysis of a 200 W PEM fuel cell short stack. J Power Sources 171:179–185
70. Nakajo A, Mueller F, Brouwer J, Van Herle J, Favrat D (2012) Mechanical reliability and durability of SOFC stacks. Part I: modelling of the effect of operating conditions and design alternatives on the reliability. Int J Hydrogen Energy 37 (2012) 9249–9268
71. Nakajo A, Mueller F, Brouwer J, Van Herle J, Favrat D (2012) Mechanical reliability and durability of SOFC stacks. Part II: modelling of mechanical failures during ageing and cycling. Int J Hydrogen Energy 37:9269–9286
72. Diethelm S, Van Herle J, Wuillemin Z, Nakajo A, Autissier N, Molinelli M (2008) Impact of materials and design on solid oxide fuel cell stack operation. J Fuel Cell Sci Technol 5:1–6
73. Carton JG, Olabi AG (2010) Design of experiment study of the parameters that affect performance of three flow plate configurations of a proton exchange membrane fuel cell. Energy 35:2796–2806
74. Carton JG, Lawlor V, Olabi AG, Hochenauer C, Zauner G (2012) Water droplet accumulation and motion in PEM (Proton Exchange Membrane) fuel cell mini-channels. Energy 39:63–73
75. Neef HJ (2009) International overview of hydrogen and fuel cell research. Energy 34:327–333
76. Fuel cells 2000 (2006). www.fuelcells.org
77. Dougherty D, Heller T (1994) The illegitimacy of sustainable product innovation in established firms. Organ Sci 2:200–218
78. Jolly VK (1997) Commercialising new technologies, getting from mind to market. Harvard Business School Press, Boston (1997)
79. Friar JH, Balachandra R (1999) Spotting the customers for emerging technologies. J Prod Innovation Manage 7–43
80. Geels FW (2002) Understanding the dynamics of technological transitions: a co-evolutionary and socio-technical analysis. Dissertation, Twente University Press, Enschede (2002)
81. Bond EU, Houston MB (2003) J Prod Innovation. Manage 20:120–135
82. Kakati M (2003) Success criteria in high-tech new ventures. Technovation 23:447–457
83. Penrose E (1959) The theory of the growth of the firm. Wiley, New York
84. Barney JB (1991) Resource-based theories of competitive advantage: a ten year retrospective on the resource-based view. J Manage 27:643–650

85. Mowery D, Rosenberg N (1979) The influence of market demand upon innovation, a critical review of some recent empirical studies. Res Policy 8:102–153
86. Van der Meer JP (2005) Open interview at fuel cell firm Ned. stack. Arnhem
87. Mallant R (2006) Open interview at energy research center the Netherlands. Petten
88. Heijboer W (2005) Open interview at electric vehicle manufacturer Spijkstaal. Pernis
89. Kammerer M (2006) Open interview with fuel cell firm hydrogenics
90. Von Hippel E (1998) The sources of innovation. Oxford University Press, New York (1988)
91. Hall J, Kerr R (2003) Innovation dynamics and environmental technologies: the emergence of fuel cell technology. J Cleaner Prod 11:459–471
92. Koppel T (2001) Powering the future: the Ballard fuel cell and the race to change the world. Wiley, New York
93. Van der Heyden J (2006) Open interview at plug power. Amersfoort
94. De Waterstof (2005) Report feasibility study for transition coalitions. Senter Novem Petten
95. Schneider MT, Schade B, Grupp H (2004) Innovation process 'fuel cell vehicle': what strategy promises to be most successful? Technol Anal Strategic Manage 16:147–172
96. Smith CG (1996) Design competition in young industries: an integrative perspective. J High Technol Manage Res 7:227–243
97. Fuel cell today (2005). www.fuelcelltoday.com
98. Utterback JM (1994) Mastering the dynamics of innovation; how companies can seize opportunities in the face of technological change. Harvard Business School, Boston
99. Olleros FJ (1996) Emerging industries and the burnout of pioneers. J Prod Innovation Manage 1:5–18
100. Balachandra R, Goldschmitt M, Friar JH (2004) The evolution of technology generations and associated markets: a double helix model. IEEE Trans Eng Manage 51:3–13
101. FC Expo 2013 (2013) Presentation by METI
102. Micro-CHP Fuel Cell System Targets (2011). DoE hydrogen and fuel cell progress report, Oct 2011
103. FCH JU (2012) Revised multi-annual implementation plan
104. Panasonic press release, Feb 2013
105. Toshiba press release (2012)
106. Ceramic fuel cells press release (2012)
107. Fuel cell today (2009)
108. US DoE (2013) Energy efficiency and renewable energy case study. First National Bank of Omaha
109. Takami H (2011) Development of fuel cell at JX. DOE Hydrogen and Fuel Cell Technical Advisory Committee 2011. http://www.hydrogen.energy.gov/pdfs/htac_02_2011_jx_eneos_takami.pdf
110. Elmer T, Worall M, Wu S, Riffat SB (2015) Fuel cell technology for domestic built environment applications: State of-the-art review. Renew Sustain Energy Rev 42:913–931
111. Sadeghi M, Chitsaz A, Mahmoudi SMS, Rosen MA (2015) Thermoeconomic optimization using an evolutionary algorithm of a trigeneration system driven by a solid oxide fuel cell. Energy 89:191–204
112. Li X, Ogden J, Yang C (2013) Analysis of design and economics of molten carbonate fuel cell tri-generation systems providing heat and power for commercial buildings and H2 for FC vehicles. J Power Sources 241:668–679
113. Sonar D, Soni SL, Sharma D (2014) Micro-trigeneration for energy sustainability: technologies, tools and trends. Appl Therm Eng 71:790–796
114. Wang J (2015) Barriers of scaling-up fuel cells: cost, durability and reliability. Energy 80:509–521

Chapter 4
The Use of Biogas in MCFCs and SOFCs Technology: Adsorption Processes and Adsorbent Materials for Removal of Noxious Compounds

4.1 Introduction

Fuel cells are highly efficient, cost effective, and ultra low emission power generation systems. The major application for FCs are stationary electric power plants, including cogeneration units, as motive power for vehicles and as on-board electric power for space vehicles or other closed environments [1]. The most promising progress on which European or worldwide programs [2–8] have concentrated concerns mainly polymer membranes fuel cells (PEMFCs). Nevertheless the molten carbonate (MCFCs) and solid oxide fuel cells (SOFCs) are competitors for the development of high power units due to the possibility of heat and electricity cogeneration. They can be fed with different kinds of fuels: natural gas, LPG, gaseous carbon, and liquid fuels (such as gasoline and diesel) and biogas [9, 10].

European environment agency (EEA) identified and prioritized five environmental and sectorial areas for energy production which the European Union has included in its Sixth Environment Action Programme as well as in its sustainable development strategy. Regarding climate change, there is a great interest to reduce greenhouse gases as well as to enhance the rational use of fossil fuels (energy efficiency and renewable and sustainable energy sources) [11].

One of the main guide lines for renewable energy in the European Union is the Renewable Energy Roadmap [12] which has the goal of raising the share of renewable energy in total energy consumption to 20 % by 2020. In 2004 that share amounted to 109 million tons oil equivalent (MTOE), or 6.25 % of the 1747 MTOE of energy consumed in the 25 EU member states, about two thirds of that, or 72 MTOE caming from biomass mainly the agricultural ones.

Biomethane may play an important role in an integrated strategy to achieve ambitious targets for biofuels within Europe (25 % of total road transport in 2030) and worldwide. European market of the biomethane production is essentially developed in Germany where the first plants were started in 2007 and there were

M. Turco et al., *Treatment of Biogas for Feeding High Temperature Fuel Cells*,
Green Energy and Technology, DOI 10.1007/978-3-319-03215-3_4

Table 4.1 Classification of biogas substrate according to power plant capacity [20]

Plant size	Installed power	Biogas substrate
S small size	10−100 kWel	Livestock effluents energy crops agricultural waste organic waste
M medium size	<1 MWel	Livestock effluents + energy crops + agricultural waste agro-industrial waste small wastewater treatment units
L large size	1−10 MWel	Large-scale wastewater treatment units landfills

more efforts for regulatory the technical standard for its grid injection, furthermore other countries, as Austria, Switzerland, Sweden and the Netherland, have developed several plants for biomethane production [13].

Biomethane can be obtained from anaerobic decomposition of organic matter, and the most important sources are digestors (manure and agro-forest matter) and landfills (municipal solid waste).

Biogas composition is strongly dependent on the source and is within (50–75) % CH_4, where the main contaminants are CO_2 (up to 50 %) which lowers the calorific value of the gas and sulfuric acid (H_2S) which could cause several problem on the plants and for human health: on the plants it causes corrosion (compressors, gas storage tank and engines), while it is toxic after its inhalation [14–19].

Feedstocks used for biogas production and the corresponding composition and type of contaminants are reported in Table 4.1.

4.2 Substrates

Three different plant categories are identified and classified as a function of installed power capacity of the biogas user. Connected to each category substrates considered for biogas production varied: the larger the power rating, the larger the biogas resources which have to be harvested.

In the following, the different substrates are specified in more details:

- Livestock effluents: manure from farm animals is used in most agricultural biogas plants; in practice manure is mixed with straw, bedding material fodder, and other residues from animal husbandry;
- Energy crops; such crops are grown to be specifically used for energetic valorization whereas anaerobic digestion is one option; energy crops include (among others) cereals, corn, and grasses;
- Agricultural waste: any kind of biological residue and green waste generated on a farm is considered in this substrate group; more precisely it includes plant residues, side products of agricultural production processes, sawdust, and other wastes;
- Organic waste: small municipalities gather and separate waste from restaurants, abattoirs, other small-scale businesses, and households in order to utilize the organic waste fraction.

Depending on the substrate used for biogas production the type and amount of impurities vary largely, according to Tables 4.2 and 4.3.

The main contaminants in biogas produced from agricultural wastes and biological substrates are sulfur compounds among which hydrogen sulfide (H_2S) is the most dominant one [22–24].

In biogas stemming from food and animal waste as well as waste water halogenated compounds are present in very small trace amounts.

Organic silicon compounds are only detected in landfill gas and from WWTU [24, 25].

Sulfur is present in nearly all biological compounds as part of amino acids such as methionine and cysteine [26]. In addition biomass itself is made by up to <2 % (on weight basis of dry and ash-free biomass) of sulfur taken up through soil and air [27]. During digestion sulfur is converted into gaseous compounds including H_2S, carbonyl sulpfde (COS), mercaptans, and disulfides among which H_2S is the most common one [24].

Concentration levels of H_2S in biogas along with the overall chemical buildup of biogas vary significantly depending not only on substrate but also on operating conditions. Sklorz et al. [28] observed the H_2S concentration fluctuations in a 45 kWe biogas plant using a gas engine for power generation due to microorganism or chemical reactions of H_2S in coordination with galvanized steel tubing, mechanical stirring, to the injection of new batch of fresh sulfur-containing matter.

Not only H_2S is present in biogas but other sulfur compounds [29] such as methanethiol (CH_3SH) propanethiol (C_3H_7SH), butanethiol (C_4H_9SH), and dimethylsulfide (DMS), with levels that at time even surpass those of H_2S. As a

Table 4.2 Biogas composition for different biogas plant types [21]

Composition	Natural gas	Waste water	Food waste	Animal waste	Landfill
CH_4 (vol.%)	80–100	50–60	50–70	45–60	40–55
CO_2 (vol.%)	<3	30–40	25–45	35–50	35–50
N_2 (vol.%)	<3	<4	<4	<4	<20
O_2 (vol.%)	<0.2	<1	<1	<1	<2
H_2S (ppm)	<0.1	<400	<10,000	<100	<200
Non H_2S sulfur (ppm)	<10	<1	<1000	<30	<30
Halogens (ppm)	<0.1	<0.2	<0.2	<0.2	<100
Moisture (%)	<0.02	~3	~3	~3	~3

Table 4.3 Average and maximum values of the main contaminants in biogas from WWTU [20]

Species	Contaminants	Average value (ppm)	Maximum value (ppm)
sulfur compounds	H_2S	400	2987
Siloxanes	D4	0.825	20.144
	D5	1.689	18.129
Halogens	Dichloromethane	0.082	0.052
	Chlorobenzene	0.255	0.693
	Dichlorobenzene	0.254	0.61

consequence at least two gas-cleaning steps are needed for effective biogas cleaning: one step to remove bulk H_2S concentration and a second step to remove remaining sulfur compounds because H_2S removal should be not enough to remove other sulfur compounds [24]. Halogens are contained in waste in the form of kitchen salts and polymers (polytetrafluoroethylene PTFE polyvinyl chloride PVC) As such these compounds are mostly found in biogas from landsfill [24, 25, 30]. The presence of halogens in biological substances is due to the uptake by the plants through salts which are washed out of the soils. On average chlorine build up in plants amounts to <1 $\%_{wtdb}$(20). The quantities of halogens reported in literature are below 1 ppm [18, 29, 31, 32].

4.3 Biogas to Biomethane

The biogas has different applications, such as a source for heat, steam, and electricity, household fuel for cooking, fuel cell, and can be further upgraded to vehicle fuel, or for production of chemicals and is a very promising technology for generating bioenergy [17, 33, 34].

The presence of CO_2 is a major problem in the biogas and its removal is needed to improve the calorific value and the relative density according to the specifications of the Wobbe index [35]. However, it is well assessed that the removal of H_2S (that can be performed both during digestion (in situ) or after digestion) [36] can be of crucial point to the technological and economic feasibility of upgrading process of the gas.

The removal of CO_2 from biogas to obtain biomethane with purity above 98 % is the most expensive step in the upgrading. Depending on the extraction method employed in landfills, nitrogen can also be found as a contaminant with contents up to 10 %. Water washing, amine scrubbing, pressure swing adsorption (PSA), and membranes are commercial technologies already available to remove CO2 from biogas, although it is recognized that the energy consumption of actual technologies can be improved.

In order to convert biogas into biomethane two major steps are performed: (1) a cleaning process to remove the trace components and (2) an upgrading process to adjust the calorific value. Upgrading is generally performed in order to meet the standards for use as vehicle fuel or for injection in the natural gas grid [18].

The basic gas upgrading steps include: water vapor removal, H_2S removal, CO_2 removal, and siloxane, and trace gas removal.

A number of techniques have been developed to remove H_2S from biogas. Air dosing to the biogas and addition of iron chloride into the digester tank are two procedures that remove H_2S during digestion. Techniques such as adsorption on probe materials or absorption in liquids remove H_2S after digestion. Subsequently, trace components like siloxanes, hydrocarbons, ammonia, oxygen, carbon monoxide, and nitrogen can require extra removal steps, if not sufficiently removed by other treatment steps. Finally, CH_4 must be separated from CO_2 using pressure swing adsorption, membrane separation, physical, or chemical CO_2-absorption [18].

4.3.1 Biogas Upgrading

4.3.1.1 Removal of Oxygen/Air

Oxygen and in part also nitrogen indicate that air has intruded the digester or landfill gas collector. This occurs quite often in landfills where the gas is collected through permeable tubes by providing a slight vacuum. Small concentrations (0–4 %) of oxygen are harmless. Biogas in air with a methane content of 60 % is explosive between 6 and 12 %, depending on the temperature [18].

4.3.1.2 Removal of Water

Physical Drying Methods (Condensation)
The simplest way of removing excess water vapor is the refrigeration. This method can only lower the dew point to 0.5 °C due to problems with freezing on the surface of the heat exchanger. To achieve lower dew points the gas has to be compressed before cooling and then later expanded to the desired pressure. The lower the dew point, the higher pressure is needed to be applied [35].

The condensed water droplets are entrapped and removed. The physical drying methods prevent water contact with downstream equipment like compressors, pipes, activated carbon beds, and other parts of the process, thus avoiding the problem of corrosion.

Techniques using physical separation of condensed water include:

- demisters in which liquid particles are separated with a wired mesh (0.5–2 nm). A dewpoint of 2–20 °C (atmospheric pressure) can be reached;
- cyclone separators in which water droplets are separated using centrifugal forces;
- moisture traps in which the condensation takes place by expansion, causing a low temperature that condenses the water;
- water taps in the biogas pipe from which condensed water can be removed [18, 37].

Chemical Drying Methods (Adsorption or Absorption)
These techniques are usually applied at elevated pressures. At atmospheric pressure only a small amount of water is removed by the absorption and adsorption techniques.

Adsorption using alumina or zeolites/molecular sieves is the most common technique [38–42].

Methods based on gas drying include:

Adsorption of water vapor on silica [43] or alumina [44, 45] or equal chemical components that can bind water molecules (adsorption dryer).

The gas is pressurized and led through a column filled with silica (CAS# 63231-67-4). Usually two columns are used in parallel: one column adsorbs water, while the other is being regenerated. Regeneration is achieved by evaporating the water through decompression and heating.

Absorption of Water in Triethylene Glycol
Drying takes place by using the water binding component triethylene glycol. Used glycol is pumped into a regeneration unit, where a temperature of 200 °C is used to regenerate the glycol. Dew points from −5 to −15 °C (atmospheric pressure) can be reached [37].

Absorption of Water with Hygroscopic Salts
The salt is dissolved as it absorbs water from the biogas. The saturated salt solution is withdrawn from the bottom of the vessel. The salt is not regenerated and new salt granules have to be added to replace the dissolved salt [35].

4.3.1.3 Removal of CO_2

Upgrading biogas to natural gas quality needs the removal of CO_2 in order to obtain the quality that meets the Wobbe Index [18, 35].

Depending on its use (pipeline or vehicle fuel), biomethane consists typically of 97–99 % methane and 1–3 % CO_2. Typical pipeline specifications require a CO_2 content of less than 3 % whereas vehicle fuel specifications require a combined CO_2N_2 content of 1.5–4.5 % [37]. One of the following techniques can be used to remove CO_2 from the biogas: (1) physical and chemical CO_2-absorption, (2) pressure swing adsorption (PSA) and vacuum swing adsorption (VSA), (3) membrane separation, (4) cryogenic separation, and (5) biological methane enrichment (Table 4.4) [17, 35, 37, 46–57].

Physical and Chemical CO_2-Absorption

This technique is based on the separation of CO_2 and CH_4 by using an absorbent. One of the methods is the use of water as physical absorbent: CO_2 is separated from the biogas by washing with water at high pressure. Alternatively, biogas can be upgraded by chemical absorption with alkanol amines. CO_2 is absorbed in the liquid and reacts at quasi atmospheric pressure with the chemical substance in the absorption column [58, 59].

Pressure Swing Adsorption (PSA), Vacuum Swing Adsorption (VSA)

PSA and VSA use a column filled with a molecular sieve, typically activated carbon, silicagel, alumina, or zeolite, for differential adsorption of the gases CO_2 and H_2O, alloeing CH_4 pass through [47, 49]. The molecules are adsorbed loosely in the cavities of the molecular sieve and not irreversible bound [46]. It is a cyclic batch process where adsorption is performed on a relatively higher pressure (around 800 kPa) and desorption (regeneration) at lower pressure [51]. H_2S,

Table 4.4 Advantages and disadvantages of techniques for removal of CO_2 [18]

Method	Advantages	Disadvantages
Absorption with water	High efficiency (>97 % CH_4)	Expensive investment
	Simultaneous removal of H_2S	Expensive operation
	When $H_2S < 300$ cm^3 m^{-3}	Clogging due to bacterial growth
	Easy in operation	Foaming possible
	Capacity is adjustable by changing pressure or temperature	Low flexibility toward variation of input gas
	Regeneration possible	
	Low CH_4 losses (<2 %)	
	Tolerant for impurities	
Absorption with polyethylene glycol	High efficiency (>97 % CH_4)	Expensive investment
	Simultaneous removal of organic S components,	Expensive operation
	H_2S, NH_3, HCN and H_2O	Difficult in operation Incomplete regeneration when stripping/vacuum (boiling required)
	Energetic more favorable than water	Reduced operation when dilution of glycol with water
	Regenerative	
	Low CH_4 losses	
Chemical absorption with amines	High efficiency (>99 % CH_4)	Expensive investment
	Cheap operation	Heat required for regeneration
	Regenerative	Corrosion
	More CO_2 dissolved per unit of volume (compared to water)	Decomposition and poisoning of the amines by O_2 or other chemicals
	Very low CH_4 losses (<0.1 %)	Precipitation of salts
		Foaming possible
PSA/VSA	Highly efficient (95–98 % CH_4)	Expensive investment
Carbon molecular sieves	H_2S is removed	Expensive operation
Molecular sieves (zeolites)	Low energy use: high pressure, but regenerative	Extensive process control needed
Alumina silicates	Compact technique	CH_4 losses when malfunctioning of valves
	Also for small capacities	
	Tolerant to impurities	
Membrane technology	H_2S and H_2O are removed	Low membrane selectivity: compromise between purity of CH_4 and amount of upgraded biogas
	Simple construction	
	Simple operation	
	High reliability	

(continued)

Table 4.4 (continued)

Method	Advantages	Disadvantages
Gas/gas	Small gas flows treated without proportional increase of costs	Multiple steps required (modular system) to reach high purity
	Gas/gas	
	Removal efficiency: <92 % CH_4 (1 step) or >96 % CH_4	CH_4 losses
	H_2O is removed	
Gas/liquid	Gas/liquid	Little operational experience
	Removal efficiency: >96 % CH_4	
	Cheap investment and operation	
	Pure CO_2 can be obtained	
Cryogenic separation	90−98 % CH_4 can be reached	Expensive investment and operation
	CO_2 and CH_4 in high purity	CO_2 can remain in the CH_4
	Low extra energy cost to reach liquid biomethane (LBM)	
Biological removal	Removal of H_2S and CO_2	Addition of H_2
	Enrichment of CH_4	Experimental e not at large scale
	No unwanted end products	

adsorbing irreversibly, must be removed before the PSA or VSA unit to prevent poisoning of the molecular sieve. PSA and VSA are similar systems, but VSA has a supplementary vacuum pump: the differential pressure is situated at lower absolute pressure. Adsorption takes place on a gas under pressure, desorption at vacuum [50].

4.3.1.4 Membrane Separation

Membrane separation is based on the selective permeability property of membranes. Two systems are proposed: (1) gas–gas separation with a gas phase at both sides of the membrane and (2) gas–liquid absorption separation with a liquid absorbing the diffused molecules. Due to imperfect separation, multiple stages may be required [46]. Because of this, an increase in methane loss is obtained. This can be partly prevented by recirculation [60].

A demonstration plant that use membranes for biogas upgrading through has been installed at Bruck/Leitha in the south of Austria [61]; the membranes used are hollow fiber type and the operative pressure is of about 8–9 bar. The process is carried out in two stages and biomethane concentration was of about 98 %

in volume that is injected into the local gas grid. This technology is capable of removing also small concentrations of H_2S.

Several literature studies show the industrial applicability of the processes in polymeric membranes for the separation of carbon dioxide from biogas [62–78]. At the actual state polymeric membranes show a good level of competitiveness with conventional technologies for CO_2 and H_2S separation from biogas. Biogas upgrading plant and other equipment used are located at the ENEA Trisaia (Italy) research centre [69]. The polymer membranes is PEEK and works up to 48 bar, with a differential pressure 41 bar in a range of temperature 5–70 °C in line with the operational regimes of the biogas plants. The H_2S presence in the biogas do not represents a problem in term of separative stage using PEEK polymeric membrane, but its selectivity was of about 50 %. Best performing could be carried out using multiple stage separative processes where is possible to work with low operative pressure in the feed stream.

4.3.1.5 Cryogenic Separation

Taking into account that CH_4, CO_2, and other impurities liquefy in different temperature/pressure areas, it is possible to produce biomethane by cooling and compressing the biogas. The liquid CO_2 should also dissolve and thus separate the remaining impurities from the gas. The raw biogas is compressed till 8000 kPa. Compression is done in different stadia with interim refrigeration. The compressed gas needs to be dried in advance, to prevent freezing in the following cooling steps. The dried and compressed biogas is eventually cooled till −45 °C. The condensed CO_2 is removed and treated in a next step to recover the remaining CH_4. The biogas is cooled further to −55 °C and afterward expanded to 800–1000 kPa in an expansion tank, reaching a temperature of about −110 °C. In these conditions, there is a gas–solid phase balance, with the solid phase being CO_2 and the gaseous phase containing more than 97 % CH_4. The CH_4 gas stream is collected and heated before leaving the plant [35, 79].

4.3.1.6 Biological Methane Enrichment

Biological methane enrichment was recently studied [57, 80, 81].

Strevett et al. [57] investigated the mechanism and kinetics of chemoautotrophic biogas upgrading. Different methanogens using only CO_2 as a carbon source and H_2 as an energy source were examined. The selection between mesophilic and thermophilic operation temperatures must be properly chosen. Thermophilic methanogens exhibit rapid methanogenesis, while mesophilic bacteria give more complete conversion of the available CO_2 [57]. The authors selected Methanobacterium thermoautotrophicum that works optimally at temperatures of 65−70 °C and has a specific requirement for H_2S, so leading to the removal of further unwanted compounds.

4.4 Removal of H_2S

Due to the damage that H_2S can cause in several parts of the plants, it is typically removed in an early state of the biogas upgrading process. Several techniques are applied: (1) removal of H_2S during digestion and (2) removal of H_2S after digestion (Table 4.5) [35, 46–50, 79].

Table 4.5 Advantages and disadvantages of techniques for removal of H_2S [18]

Method	Advantages	Disadvantages
Biological with O_2/air (in filter/scrubber/digester)	Cheap investment and exploitation: low electricity and heat requirements, no extra chemicals or equipment required	Concentration H_2S still high (100–300 cm3 m^{-3})
		Excess O_2/N_2 in biogas implies difficult upgrading or additional cleaning
	Simple operation and maintenance	Overdosing air results in explosive mixture
$FeCl_3/FeCl_2/FeSO_4$ (in digester)	Cheap investment: storage tank and dosing pump	Low efficiency (100–150 cm^3 m^{-3})
	Low electricity and heat requirements	Expensive operation (iron salt)
	Simple operation and maintenance	Changes in pH/temp not beneficial for the digestion process
	Compact technique	
	H_2S not in biogas wire	Correct dosing is difficult
	No air in biogas	
$Fe_2O_3/Fe(OH)_3$-bed	High removal efficiency: >99 %	Sensitive for water
Rust steel wool impregnated wood chips or pellets	Mercaptanes are also captured	Expensive operation costs
		Regeneration is exothermic: risk of ignition of chips
	Cheap investment	Reaction surface reduced each cycle
	Simple	Released dust can be toxic
Absorption in water	$H_2S < 15$ cm^3 m^{-3}	Expensive operation: high pressure, low temperature
	Cheap when water is available (not regenerative)	Difficult technique
	CO_2 is also removed	Clogging of the absorption column possible
Chemical absorption	Low electricity requirement	Expensive investment and operation
NaOH	Smaller volume, less pumping, smaller vessels (compared to absorption in H_2O)	More difficult technique
$FeCl_3$	Low CH_4 losses	Not regenerative

(continued)

Table 4.5 (continued)

Method	Advantages	Disadvantages
Chemical absorption	High removal efficiency: 95−100 %	Difficult technique
	Cheap operation	Regeneration through oxygenation
$Fe(OH)_3$	Small volume required	$CO_2 \rightarrow H_2CO_3$ (using EDTA) leads to precipitation
Fe-EDTA	Regenerative	Build up of thiosulfates from chelates + H_2S (using EDTA)
Cooab	Low CH_4 losses	
Membranes	Removal of >98 % is possible	Expensive operation and maintenance
	CO_2 is also removed	Complex
Biological filter	High removal possible: >97 %	Extra H_2S-treatment to reach pipeline quality
	Low operational cost	O_2/N_2 in biogas implies difficult and additional upgrading steps
Adsorption on activated carbon (Impregnated with KI 1−5 %)	High efficiency ($H_2S < 3$ cm^3 m^{-3})	Expensive investment and operation
	High purification rate	CH_4 losses
	Low operation temperature	H_2O and O_2 needed to remove H_2S
	Compact technique	H_2O can occupy the binding places of H_2S
	High loading capacity	Regeneration at 450 °C
		Residue present till 850 °C

4.4.1 Removal of H_2S During Digestion

To choose an appropriate technique for H_2S removal, the technique to remove CO_2 should be considered first. A technique such as absorption in water or selexol, membranes or PSA/VSA that removes H_2S as well as CO_2, will make an additional technique for the removal of H_2S unnecessary, unless H_2S is present in high concentrations (>300 cm^3m^{-3}). A CO_2 removal technique such as absorption with amines, that does not explicitly eliminate H_2S, will necessitate an additional removal step such as absorption in a NaOH solution, absorption on hygroscopic salt and reaction in a Fe_2O_3-bed.

H_2S can be treated directly in the digester vessel. The sulfide either reacts with a metal ion to form an insoluble metal sulfide or is oxidized to elementary sulfur [35, 79].

(a) *Air/oxygen dosing to the biogas system*

This technique is based on the biological aerobic oxidation of H_2S to elemental sulfur by a group of specific bacteria [18].

Most of sulfide oxidizing microorganisms (Thiobacillus) are autotrophic [82–85] and use CO_2 from the biogas as source of carbon. They grow on the surface of the digestate or on the framework of the digester and do not require inoculation. The following reaction occurs in the biogas:

$$2H_2S + O_2 \rightarrow 2S + 2H_2O \tag{4.1}$$

not only elemental sulfur, but also sulfate is formed, which can cause corrosion in solutions. A certain amount (2−6 %) of O_2 required for the reaction is introduced in the biogas. A reduction of H_2S concentrations down to 20−100 cm^3m^{-3} and a removal efficiency of 80−99 % can be achieved [46, 47] but the remaining concentrations may still be too large [37]. Safety measures have to be taken to avoid overdosing of air since biogas in air (6–12 %) is an explosive mixture. Moreover, care has to be taken to guarantee anaerobic conditions.

(b) *Addition of iron chloride into the digester*

Commonly, $FeCl_2$/$FeCl_3$ is added during digestion to reduce the concentration of H_2S to a few hundred cm^3m^{-3}. Precautions should be taken to prevent O_2 and N_2 from entering the biogas, rather than to remove them [35, 46, 47, 79].

Iron chloride can be dosed directly into the digester or through the influent mixing tank. It reacts with the H_2S present in the biogas to form FeS (particles) according to Eqs. (4.2) and (4.3). The precipitation reaction of the iron salt can be written as follows:

$$2Fe^{3+} + 3S^{2-} \rightarrow 2FeS + S \tag{4.2}$$

$$Fe^{2+} + S^{2-} \rightarrow FeS \tag{4.3}$$

This method is very efficient in reducing high concentrations of H_2S, since a reduction of H_2S concentration down to 100 cm^3 m^{-3} can be achieved [37], but does not allow the attainment of a low and stable level of hydrogen sulfide [47].

4.4.2 Removal of H_2S After Digestion

4.4.2.1 Adsorption Using Iron Oxide or Hydroxide

Hydrogen sulfide reacts easily with iron oxide, iron hydroxide, and zinc oxide and forms iron sulfide or zinc sulfide, respectively [18]. This process is often referred to as “iron sponge” because rust-covered steel wool may be used to form the reaction bed.

Iron oxide and iron hydroxide react with H_2S in the biogas according to following reactions

$$Fe_2O_3 + 3H_2S \rightarrow Fe_2S_3 + 3H_2O \tag{4.4}$$

$$2Fe(OH)_3 + 3H_2S \rightarrow Fe_2S_3 + 6H_2O \tag{4.5}$$

The reaction is slightly endothermic: a temperature minimum of about 12 °C is required, but the optimal conditions are between 25 and 50 °C. Condensation of water on the iron oxide should be avoided since the iron oxide material will link together with water which reducing the surface [3]. The iron oxide can be regenerated with oxygen according to the following reaction:

$$2Fe_2S_3 + 3O_2 \rightarrow 2Fe_2O_3 + 6S \tag{4.6}$$

4.4.2.2 Physical and Chemical Absorption with Liquids

Physical absorption removes H_2S by absorption in water or an organic solvent [18, 37, 86–88]. The most common solvent is water although operational problems due to the growth of microorganisms on the packing occur.

Two types of water absorption processes are commonly used for the upgrading of biogas: single pass absorption and regenerative absorption [48]. A high consumption of water is needed in the case of absence of regeneration steps.

Chemical absorption liquids that can be used are:

- Diluted NaOH-solution: NaOH reacts with H_2S to form Na_2S or NaHS which precipitates. The formed sodium salts are not regenerative and have to be disposed of;
- $FeCl_2$-solution: $FeCl_2$ f reacts with H_2S to form insoluble FeS that needs to be removed;
- $Fe(OH)_3$-solution: H_2S is removed using $Fe(OH)_3$ resulting in the formation of Fe_2S_3. Regeneration is done with oxygen or air (closed system) [18, 37, 89, 90].

Horikawa et al. [91] investigated chemical absorption of H_2S in an Fe(III)-EDTA catalyst solution. In this process, H_2S is dissolved in an aqueous solution and catalytically removed by a chelated iron according to the following reaction:

$$S^{2-} + 2Fe^{3+} = S + 2Fe^{2+} \tag{4.7}$$

The sulfur produced is easily separated by sedimentation or filtration from the Fe-EDTA-solution. Regeneration of the aqueous Fe-EDTA-solution is done by oxygenation according to Eq. (4.8):

$$O_2(aq) + 2Fe^{2+} = 2Fe^{3+} + 2OH \tag{4.8}$$

The regeneration the Fe-EDTA-solution allows a large consumption of chemicals. The process can be carried out at ambient temperature and is highly selective in removing H_2S: the volumes CH_4 and CO_2 present in biogas remain nearly constant. A removal of 90−100 % can be obtained for biogas containing 2.2 % H_2S at a gas flow of 1 $dm^3\ min^{-1}$, and at a solution flow of 83.6 $cm^3\ min^{-1}$ and an inlet biogas pressure of 220 kPa [91]. At lower catalytic solution flow, lower absorption efficiency is obtained. At lower inlet H_2S concentration higher absorption efficiency is obtained. Therefore, the total removal of H_2S depends on the use of the adequate ratio of gas to liquid flow rates [91].

4.4.2.3 Separation of H_2S with Membrane

H_2S can be separated from the gas by the use of semi-permeable membranes. H_2S (and CO_2) can pass the membrane whereas CH_4 cannot [18, 37]. In addition, gas–liquid absorption membranes can be used. The membranes are micro porous and have hydrophobic properties: the molecules in the gas stream, flowing in one direction, diffuse through the membrane and are absorbed on the other side by the liquid, flowing in counter current. At a temperature of 25−35 °C the H_2S concentration of the raw gas of 2 % could be reduced to less than 250 cm^3m^{-3} thus yielding an efficiency of more than 98 %. NaOH is used as the absorbent in liquid [18, 46].

4.4.3 Biological Filter

This method is similar to the technique where air/O_2 was added to the digestion tank. It is based on the use of specific bacteria that are able to oxidize H_2S. Air (4−6 %) is added to the biogas the filter bed; H_2S is absorbed in the liquid phase that is gas condensate and liquid from effluent slurry separation. After absorption, H_2S is oxidized by the bacteria, growing on the filter bed. The temperature is about 35 °C which promotes the biological process. Sulfur is retained in the liquid of the filter [18, 35, 37, 79]. Biological filtration is required in several plants for removing odors (oxygen rich situation) [47] and in some cases to remove H_2S from biogas. This technique has the advantage of low costs in comparison to chemical cleaning. The method is also able to remove ammonia from the biogas. With addition of air to the biological filters, the H_2S content can be decreased from 2000−3000 to 50−100 $cm^3\ m^{-3}$. Some works reported H_2S reduction from 800 to 10 $cm^3\ m^{-3}$ [35, 79].

Among the several gas purification processes proposed to eliminate H_2S, such as chemical scrubbing, physical adsorption [92], electrochemical treatment [93], and biofiltration [94, 95] the physical and chemical treatments suffers the disadvantages of high costs and secondary pollutants production although are rapid and efficient. On the contrary biological treatment that directly metabolizes H_2S into sulfate has receiving increasing attention. It is reported that the drop in pH caused by sulfate accumulation has negative effects [96–101], therefore, studies on biological processes have focused on removing low H_2S concentrations (10–50 ppm) to prevent rapid pH drop [102–106].

Other studies that combined chemical and biological processes for both H_2S elimination and ferric iron regeneration by Acidithiobacillus ferrooxidans have been reported [107–109]. These processes are based on two reactions as follows: the inlet H_2S is first oxidized with a ferric iron solution and yields elemental sulfur, and the reduced ferrous iron is then reoxidized by A. ferrooxidans in the biological process.

Separate studies that focused on chemical absorption [110, 111] and biological oxidation [109, 112] were proposed. For instance, when the inlet H_2S

concentration is lower than 300 ppm, the rate-limiting step for the chemical absorption process is the mass-transfer limitation, as revealed by model validation [113]. When the system has a high inlet H_2S concentration (e.g., above 1500 ppm), the H_2S removal efficiency is significantly maintained via long GRT (gas retention time) and stable ferric iron concentration in the chemical reactor [114]. In the biological reaction, Mesa et al. [115] investigated the continuous oxidation efficiency of ferrous iron by using immobilized A. ferrooxidans. However, studies that focused on the combined and continuous operation are limited.

In the present study, the chemical absorption reactor and the biological oxidation reactor with immobilized A. ferrooxidans CP9 were connected and then examined in both laboratory and pilot scales to evaluate the performance of H_2S elimination. In the laboratory-scale study, optimal operating parameters, such as GRT, temperature, and H2S inlet loading were examined. In the pilot-scale study, the biogas with an average H_2S concentration of 1645 ppm was introduced into the chemical–biological system. The long-term performance was examined, and the results demonstrate that the chemical–biological process effectively removed H_2S from the biogas.

Biotrickling filters work by passing a stream of contaminated air through a chemically inert packing material over which an aqueous phase is continuously trickled. Microorganisms grow as biofilms on the surface of the packing material by using pollutants transferred from the gas to the biofilm as energy and/or carbon sources. The effect of CH_3SH in the removal of H_2S in biogas in biotrickling filters has not been explored yet although there are few references in the co-treatment of low loads of CH_3SH and H_2S for odor removal [106, 116].

The biological oxidation of H_2S in aerobic (Eqs. 4.9, 4.10) and anoxic (Eq. 4.11) biotrickling filters occurs according the following scheme [100, 117]

$$H_2S + O_2 \rightarrow S^\circ + H_2O \tag{4.9}$$

$$H_2S + 2O_2 \rightarrow SO_4^{-2} + 2H^+ \tag{4.10}$$

$$15NO_3^- + 12H_2S \rightarrow 9H_2O + 6S^\circ + 6SO_4^{-2} + 5NO_2^- + 5N_2 + 2OH^- + 4H^+ \tag{4.11}$$

Equation (4.3) involves both complete and partial denitrification coupled to complete and partial H_2S oxidation [118]. In both cases the principal products are sulfate and elemental sulfur.

The risk of clogging by elemental sulfur formation is the most important bottleneck for stable, long-term operation in biotrickling filters.

The ratio between the available electron acceptor and H_2S, i.e., O_2/H_2S and NO^{3-}/H_2S in aerobic and anoxic biotrockling filter are the key parameters to end up with a certain SO_4^{-2}/S° produced ratio [100, 119].

The biological oxidation of CH_3SH under aerobic conditions produces formaldehyde and H_2S intermediate product [120]. The overall reaction can be expressed by Eq. (4.12) [121].

$$2CH_3SH + 7O_2 \rightarrow 2CO_2 + 2H_2SO_4 + H_2O \tag{4.12}$$

Chemical oxidation of CH_3SH to DMDS in an aerobic reactor has been reported according to Eq. (4.13) [122]

$$2CH_3SH + 1/2O_2 \rightarrow CH_3SSCH_3 + H_2O \tag{4.13}$$

Recently van Leerdam [122, 123] have found that CH_3SH also reacts chemically with biosulfur particles at pH 8.7 to form DMDS and other polysulfide according to

$$2CH_3S^- + H^+ + 1/8S_8 = HS^- + CH_3SSCH_3 \tag{4.14}$$

$$2CH_3S^- + S8 = S_y^{2-} + CH_3S_xCH_3 (\text{with } x + y = 10) \tag{4.15}$$

The main products of these reactions are dimehyl polisulfides (DMDS and dimethyl trisulfide (DMTS)) and some longer-chain dimethyl polysulfides.DMDS and DMTS are less inhibitory than CH_3SH on biological (poly)sulfide oxidation [124].

H_2S and methylmercaptan (CH_3SH) are the most common sulfur compounds found in biogas. Montebello et al. [99] studied the simultaneous removal of H_2S and CH_3SH was tested at neutral pH in two biotrackling filters one operated under aerobic conditions and the other one under anoxic conditions. Both reactors were run for several months treating H_2S concentration of around 2000 ppm and CH_3SH in the range 10−75 ppm. Maximum removal capacities of around 1.8 gS-CH_3SH $m^{-3}h^{-1}$ were observed by stepwise increasing CH_3SH concentrations from 0 to 75−90 ppm(v) at a constant H_2S loading rate of 53–63 gS-H_2S $m^{-3}h^{-1}$. Maximum H_2S elimination capacities for both reactors were between 100 and 140 gS-H_2S $m^{-3}h^{-1}$.

A negative influence was found in the elimination capacities of CH_3S by the presence of high H_2S in both biotrckling filters. CH_3SH chemically reacts with elemental sulfur at neutral pH enhancing the overall reactors performance by reducing the impact of sulfur accumulation. Both reactors were also able to treat CH_3S without prior inoculation because of the already existing sulfide-oxidazing microorganisms grown in the reactors during H_2S treatment. Co-treatment of H_2S and CH_3SH under aerobic and anoxic conditions was considered as a feasible operation for concentrations commonly found in biogas (2000 ppm of H_2S and below 20 ppm of CH_3SH).

A chemical–biological process was propose by Ho et al. [107] to remove a high concentration of H_2S in biogas. The high iron concentration tolerance (20 g L^{-1}) of Acidithiobacillus ferrooxidans CP9 provided sufficient ferric iron level for stable and efficient H_2S removal. The results showed that the H_2S removal efficiency reached 98 % for 1500 ppm H_2S. The optimal ferric iron concentration was kept between 9 and 11 g L^{-1} with a cell density of 108 CFU g^{-1} granular activated carbon and a loading of 15 g S m^{-3} h^{-1}. In pilot-scale studies for biogas purification, the average inlet H_2S concentration was 1645 ppm with a removal efficiency of up to 97 % for a 311 days operation and an inlet loading 40.8 g S m^{-3} h^{-1}.

Removal of H_2S up to <100 ppm by in situ precipitation was reported by several authors [20, 125, 126]. The remaining content of H_2S which is not removed by bacterial activity is cleaned by adsorption on ZnO ideally reaching concentrations levels of <1 ppm [127].

Trace impurities are removed in a final step by an adsorption bed of activated carbon aiming for concentration levels <1 ppm [128].

4.5 Adsorption on Activated Carbon

H_2S can also be removed by using activated carbon, which is often dosed with KI or sulfuric acid (H_2SO_4) to increase the reaction rate. Before entering the carbon bed 4−6 % air is added to the biogas and H_2S is catalytically converted to elemental sulfur and water in biological filters, according to Eq. (4.16):

$$2H_2S + O_2 \rightarrow 2S + 2H_2O \tag{4.16}$$

The elementary sulfur is adsorbed by the activated carbon. Best efficiency is obtained at pressures of 700−800 kPa and temperatures of 50−70 °C that can be achieved through heat generation during compression. In continuous process the system consists of two vessels [35, 46, 79]: one vessel for adsorption and the other for regeneration. Regeneration can be performed with hot nitrogen (inert gas) or steam. The sulfur is vaporized and, after cooling, liquefied at approximately 130 °C. Typically, the activated carbon is replaced rather than regenerated [18, 35, 46, 79].

4.6 Ammonia Stripping

Anaerobic digestion effluent typically contains high amounts of ammonium, phosphate, suspended solid (SS), and persistent organic substrate, which has been generally applied as a fertilizer for recycling the nutrients in agricultural field [129]. However, the excessive application of digested effluent in agricultural areas is the probable cause of nitrogen pollution in farming areas [130]. The high ammonia, phosphate, and SS contents of anaerobic digestion effluent are generally difficult of access to conventional biological treatment processes, such as activated sludge process [131, 132], soil trench system, etc. [133]. In addition, the relatively low chemical oxygen demand/total nitrogen (COD/TN) ratio [129–131] is insufficient to facilitate efficient TN removal. Meinhold et al. [134] suggested that the COD/TN ratio for efficient TN removal by nitrification and denitrification in an activated sludge process should be between 4 and 5. Hence, physicochemical pretreatments such as ammonia stripping, ion exchange, membrane processes, and chemical precipitation are required to lower the concentration of ammonia, phosphate, and SS prior to application to biological treatment processes. Ammonia stripping has been

successfully applied in pretreating pig slurry [135, 136], landfill leachate [137], urea fertilizer plant wastes [138], etc. However, researches on the application of ammonia stripping to anaerobic digested effluent are limited. Further, the optimal $Ca(OH)_2$ dosage must also be studied because of the different C, N, and P concentrations and pH buffer capacity of anaerobic digested effluent.

Lei et al. [139] showed that an overdose of calcium hydroxide, i.e., 27.5 g/L wastewater, achieved higher ammonia, phosphorus, chemical oxygen demand, suspended solids, and turbidity removal efficiency. The pH of the anaerobic digestion effluent can be increased from about 7 to about 9 by CO_2 stripping. It was roughly estimated that 43 m^3 of biogas (CH_4:CO_2 ≈ 60:40 %) produced daily could be purified to CH_4:CO_2 ≈ 74:26 % by neutralizing the pH of the 5 m^3 anaerobic digestion effluent pretreated by ammonia stripping.

4.7 Materials for Sulfur Removal: Activate Carbons and Zeolites

At present adsorption technology is recognized to be the most common technology applied to reach ultra-low sulfur levels for fuel cells applications. Activated carbon is one of the most versatile adsorbents known with high removal efficiency, low costs reusability, and possible product recovery [16, 140–155]. However, there are many other commercial adsorbents used for fuels desulfurization at ambient temperature and pressure, such as silica, alumina, zeolites and some metal oxides [156–166].

Aslam et al. [147] reported the study of activated carbon (AC) made from waste oil fly ash (OFA) which is produced in large quantities from power generation plants through combustion of heavy fuel oil. OFA contains ~80 % C that makes it suitable for producing AC by physicochemical treatments using a mixture of HNO_3, H_2SO_4, and H_3PO_4 acids to remove non-carbonaceous impurities. The physicochemical treatments of OFA increased the surface area from 4 to 375 m^2/g. The materials are characterized by combined SEM and EDX techniques. The AC is further treated with HNO_3 and NH_4OH solutions in order to attach the carboxylic and amine groups on the surface, respectively. FTIR characterization is used to confirm the presence of the functional groups on the surface of AC at different stages of its development. The performance of functionalized AC samples is tested for the removal of H_2S from a synthetic natural gas by carrying out breakthrough curves. The results showed maximum adsorption capacity of 0.3001 mg/g for NH_4OH functionalized AC with 86.43200B % regeneration efficiency. The NH_4OH-treated AC is more effective for H_2S removal than acid-treated AC.

Phooratsamee et al. [146] reported the preparation of activated carbon from palm oil shells by chemical activation using $ZnCl_2$ impregnated with NaOH, KI, and K_2CO_3 for H_2S absorption from biogas. The production of activated carbon involved three stages; (i) carbonization of raw material at 600 °C; (ii) activation of char product from the first stages; (iii) alkali impregnation of activated carbon

NaOH, KI, and K_2CO_3 solutions. The result showed that the highest surface area and the pore volume (741.71 m^2/g and 0.4210 cc g^{-1}) was obtained on K_2CO_3-AC activated carbon. The best performances were obtained with K_2CO_3-AC in comparison to KI-AC and NaOH. Therefore, K_2CO_3-AC impregnated activated carbon has a high surface area and showed be an efficient adsorbent for removal of H_2S from biogas product.

Cu and Zn modified 13X zeolites prepd. by ion exchange or impregnation and activated carbons (ACs) treated with KOH, NaOH, or Na_2CO_3 solutions were studied by Micoli et al. [149] as H_2S sorbents for biogas purification for fuelling molten carbonate fuel cells. H_2S sorption was studied in a new experimental apparatus equipped with a high sensitivity potentiometric system for the analysis of H_2S. Breakthrough curves were obtained at 40° with a fixed bed of 20 mg of the samples under a stream (6 L h^{-1}) of 8 ppm H_2S/He mixt. The adsorption properties of 13X zeolite improved with addn. of Cu or Zn:Cu exchanged zeolite showed the best performances with a breakthrough time of 580 min at 0.5 ppm H_2S, that is 12 times longer than the parent zeolite. In general, unmodified and modified ACs were more effective H_2S sorbents than zeolites. Treating ACs with NaOH, KOH, or Na_2CO_3 solutions. improved the H_2S adsorption properties: active carbons treated with Na_2CO_3 was the most effective sorbent, showing a breakthrough time of 1222 min at 0.5 ppm, that is twice the time of the parent AC.

The influence of modification conditions and operation conditions on the H_2S adsorption performance on AC samples was also study by Liang et al. [150]. The authors reported that a combinatory method of high pressure hydrothermal treatment followed by alkaline solution impregnation could promote the H_2S adsorption performance remarkably.

Monteleone et al. [153] studied anaerobic H_2S adsorption on activated carbons, with particular attention to the influence of thermal treatment on adsorption capacity, to feasibility of regeneration and the competitive adsorption of H_2S and CO_2. The selected materials were characterized before and after adsorption tests, using sorption of N, XRPD, TGA-DTA, SEM, and EDX. All tested carbons showed a better adsorption capacity before thermal treatment, confirming the crucial role of H_2O in absorption mechanism. Activated C impregnated with metal salts, revealed the highest adsorption capacity due to the combination of microporosity and oxidative properties.

Osorio et al. [167] reported a study dealing with biogas purification coming from the anaerobic digestion of sludges in a wastewater treatment plant. The purification apparatus contains scrubbing towers and filters of activated carbon at the end of the line. The H_2S inflow concentrations were quite high (up tp 2000 ppm). The effluent biogas from the scrubbing towers presented an H_2S concentration less than 1 ppm and zero or undetectable values after adsorption of active carbons filters.

An et al. [151] investigate the performance of activated carbon fiber (ACF) modified by impregnation with transition metals. The differences of the performance between original and modified ACF and the effects of type and concentration of impregnants were studied. It was observed that the adsorption capacity of

ACF was significantly improved by modification and that sulfur capacity increased with the concentration of impregnant initially, and then decreased. The adsorption of H_2S was in the order: 5 % $Cu(NO_3)_2$-ACF > 5 % $Co(NO_3)_2$-ACF > 5 % $Mn(NO_3)_2$-ACF. The modified ACF by 5 % $Cu(NO_3)_2$-3 % $Co(NO_3)_2$ solutions has the best performance with the sulfur capacity of 166.7 mg/g. The modified ACF by 5 % $Cu(NO_3)_2$-3 % $Co(NO_3)_2$-1 % $Mn(NO_3)_2$ solution has the worst performance with a sulfur capacity of 83.3 mg/g.

Huang and Chen [152] propose a dynamic adsorption model to simulate removal of H_2S by a fixed-bed packed with copper impregnated activated carbon (IAC). After diffusion into the interior of a pellet, H_2S species either may be physical adsorbed on carbon surface or may react with the copper impregnated on the IAC.

Hernandez et al. [141] studied a system for both the desulfurization and dehalogenation of landfill biogas at ambient temperature. The principal aim of the work was to identify a multifunctional adsorption bed that would be able to purify the landfill biogas to sulfur and chlorine concentrations of below 1 ppmv, with a high removal efficiency (>99 %). Two commercial activated carbons were studied. Moreover activated carbon, functionalized by ZnO nanoparticles, was tested at ambient temperature for the simultaneous removal of H_2S and organochlorinated mols. The biogas desulfurization results have shown that the ZnO (10 %) modified commercial active carbon has a higher adsorption capacity than the commercial material due to the presence of well dispersed ZnO nanoparticles on the surface. Moreover, the biogas dehalogenation results confirm that the use of two adsorbent beds in series improves the performance of the abatement of high molecular weight halogenated.

Riberio et al. [14] reported a study of adsorption of carbon dioxide, methane, and nitrogen on an activated carbon honeycomb monolith supplied by Mast Carbon (United Kingdom). A very interesting property of honeycomb monoliths is that the pressure drop is almost negligible [168]. Kinetics of adsorption (diffusion rates) of pure gases was measured by diluted breakthrough curves of the pure gases diluted in helium. A mathematical model using one lumped resistance was employed to determine diffusivity coefficients from experimental data. The results were correlated with the Langmuir and multisite Langmuir models.

Chang [142] reported the study of high-silica/alumina ratio (>10) zeolite including MCM-4 and Y-type zeolite or high-silica zeolite and Mg^{2+} or Cu^{2+} modified activated carbons.

Yazdanbakhsh et al. [158] reported the H_2S breakthrough capacity of copper-exchanged Engelhard Titanosilicate-2 (ETS-2). The adsorbent efficiency remains unchanged up to 950 °C. Below 750 °C, the adsorption capacity at breakthrough is 0.7 mol of H_2S per mol of copper while >750 °C the capacity of the adsorbent is halved. The change in H_2S capacity is due to Cu^{2+} reduction by the H_2 which is formed through the thermal dissociation of H_2S.

Liu et al. [157] studied an efficient hybrid adsorbent/photocatalytic composite (TiO_2/zeolite) for the H_2S removal and SO_2 capture by coating TiO_2 on the surface of cheap natural zeolite with an ultrasonic-calcination way. The TiO_2/zeolite

showed the highest H_2S removal capacity and lowest SO_2 emission, compared with the single zeolite adsorption and TiO_2 photocatalysis. H_2S removal capacity and SO_2 capture capacity of TiO_2/zeolite were enhanced in the presence of moisture in the biogas.

Papurello et al. [29] reported the use of with Na-X zeolites combined with a ZnO guard bed (heated at 300 °C) before feeding the reformer unit in order to guarantee a durable and stable operation.

Tomadakis et al. [162] proposed pressure swing adsorption method using as adsorbent materials 4A, 5A, and 13X molecular sieves was studied by Tomadakis et al. [162]. It was found that 13X and 5A materials give high purity methane (98 % or more) of zero or nearly zero H_2S concentration for short periods of time. High methane recovery rates were obtained in most adsorption experiments, averaging at 60−70 % for all sieves, and topped by 100 % in certain 13X runs. Similarly, high H_2S recovery rates were typically achieved in desorption tests averaging at 72 % with sieve 4A, and reaching 100 % in some 13X and 4A runs.

A theoretical approach to describe the adsorption fenomena of H_2S on zeolites was reported in literature. Shah et al. [156] studied the adsorption behavior of binary mixtures of H_2S and CH4 on different all-silica zeolite frameworks using Gibbs ensemble Monte Carlo simulations at 25 and 70 °C and pressures in the range 1−50 bar. The simulations demonstrate high selectivities that increase with increasing H_2S concentration due to favorable sorbate–sorbate interactions. The simulations indicate significant inaccuracies using unary adsorption data and ideal adsorbed theory. Cosoli et al. [160] used coupled grand canonical–canonical Monte Carlo and mol. dynamics (MD) simulation techniques to investigate in details the adsorption of low-pressure hydrogen sulfide (H_2S) in zeolites, and the selective adsorption behavior toward carbon dioxide and methane, the main biogas constituents. Results from Monte Carlo (MC) simulations indicated, among many others, zeolite NaY as the best option for H_2S removal. Thermodynamic evaluations confirm the results obtained from Monte Carlo simulations, evidencing the greater affinity for H_2S to NaY zeolite framework.

A theoretical approach was also reported by Qiu et al. [161] to investigate the interactions between H_2S and HZSM-5 zeolites. The results showed that the nature of interactions lead to the formation of the zeolite cluster-H_2S and silanol-H_2S complexes was van der Waals force confirmed by a little change of geometric structures and properties.

Recently, the removal of sulfur and chlorinated compounds has received more and more attention but only few reports are focused on the selectivity of different adsorbent materials respect to these different molecules [15].

Ryckebosch et al. [18] described the removal of halogenated carbon hydrates that are mainly found in landfill gas. These compounds cause the corrosion in engines and can be removed with activated carbon. Generally, are used two tubes in parallel for the treatment and for the regeneration, respectively. Regeneration is done by heating the activated carbon to 200 °C, thus evaporating the adsorbed components which are thereafter removed by an inert gas flow [46].

Hernandez et al. [141] report a study on the removal of sulfur and halogenated compounds from a model landfill biogas through adsorption. SCL3 Recently Papapdias et al. [30] performed a detailed analysis of impurities contained in digester and landfill gas combined with a sensitivity analysis of electricity costs of a fuel cell system focusing on establishing a fitting gas-cleaning unit SC L3.

The landfill was in Pianezza (Turin) performed with the company Asja Ambiente Italia S.p.A.

The authors [141] reported the results obtained on six commercial adsorbents (Table 4.6) to compare their selectivity and their uptake capacity toward nine different sulfur compounds (including mercaptanes). In Table 4.7 the analysis of the biogas is reported.

Norit activated carbon presented the highest adsorption capacities for COS MM, EM tBM, and sBM. Conversely zeolite 13X had the highest uptake capacity for DMS and iPM and the ST material showed the highest capability to adsorb MES and THT; almost the same performance was observed for MES adsorption on zeolite 13X.

Moisture and other sulfur-free hydrocarbons (C2 to C5) are indeed present in the real biogas and may influence the adsorption process. Since activated carbons and zeolites can adsorb water this capability can significantly reduce their selectivity and uptake capacity toward sulfur compounds [169–172]. When RGM3 was tested in the presence of moisture its uptake capacity towards some sulfur compounds was greatly reduced (from 58.892 to 22.164 %). Reduction of up to 100 % for COS, 57 % for DMS-iPM, 89 % for MES and 60 % for THT were observed.

It was found that each halogenated compound is adsorbed on the activated carbon in a different manner: Norit R1540 W and Norit RB4 W could remove the majority of the chlorinated species but with different breakthrough times. The adsorptive capacity for the smaller molecular weight species (chloromethane and chloroethane) is practically zero but it is the highest for the 1,1,2,2-tetrachloroethane (6.79 and 7.76 wt%, for the R1540 W and RB4 W, respectively). Hence, these activated carbons have an uptake capacity that increase with the molecular weight (MW) of the halogenated molecules, although this trend is not absolute: the adsorption capacity can be explained as a function of the adsorbate molecular weight, degree of unsaturation, polarization and symmetry as well. The authors

Table 4.6 Adsorbents tested [141]

Use	Active component	Supplier	Product name
Desulfurization	Activated carbon with Cr and Cu salts	Norit	RGM-3
	Zeolite 13X	Grace Davison	554HP
	Molecular sieve	Grace Davison	Sylobead 522
	Molecular sieve	Grace Davison	Sylobead 534
	Metal oxides	Non disclosable	ST
	Metal oxides	ECN	SulfCath
Dehalogenation	Activated carbon	Norit	R1540 W
	Activated carbon	Norit	RB4 W

Table 4.7 Analysis of the Pianezza MSW landfill biogas [171]

Parameter	Measure unit	Minimum value	Maximum value
Temperature	°C	9	26
Humidity	% v	0.6	1.1
O_2	% v t.q.	1.5	2.8
CO_2	% v t.q.	34	40.9
CO	% v t.q	<0.001	0.003
N_2	% v t.q.	11.4	16.0
H_2	% v t.q.	<0.1	<0.1
CH_4	% v t.q.	42.8	50.2
Hydrocarbons > C5 (as hexane)	mg/m^3	337.3	1178.0
Aromatic hydrocarbons	mg/m^3	101.4	128.0
Total organic carbon (as C)	mg/m^3	306	790.1
Siloxanes	mg/m^3	<0.05	<0.2
NH_3	mg/m^3	<0.5	15.7
HCl	mg/m^3	<0.6	2.0
Organochlorurated compounds	$mgCl/m^3$	20	30.6
Total chlorine	$mgCl/m^3$	17.4	32.0
HF	mg/m^3	<0.5	0.8
Organofluorinated compounds	mgF/m^3	1.2	6
Total fluorine	mgF/m^3	1.2	<6,6
H_2S	p.p.m.	114.3	205
H_2SO_4	p.p.m.	<0.3	1.0
Mercaptanes (C_2H_5SH)	p.p.m.	0.7	27.7

concluded that none the tested adsorbents could remove the wide variety of sulfur compounds and the chlorinated compounds with low molecular weight that could be present into the landfill biogas, such as chloromethane and chloroethane.

The authors [141] proposed a multistep desulfurization process with two adsorption beds so that the species not adsorbed in the first bed could be trapped in the second one. The first bed is based on molecular sieves; the second one contains activated carbons that are able to remove all the S-compounds present in the biogas. Tests that have been performed on the SOFC power generation system at the Turbocare site in Turin [171]. A two component arrangement of 130 kg zeolite-X followed by 90 kg activated carbon provided an acceptable solution for large-scale SOFC unit. After 4 months of operation no sulfur breakthrough was observed.

4.8 Removal of Sulfur Compounds in Fuels by Adsorption Processes

Organic sulfurs in natural gas and liquid fuels are poison to both the reforming catalyst and fuel cell's electrocatalysts. Many zeolites adsorb organic sulfurs and can efficiently remove these impurities from fuels. Sulfur removal by adsorption

Table 4.8 Zeolites and mesoporous materials used for the removal of sulfur compounds [210]

Material	Sulfur compounds or fuel	Temperature (K)	Results	Results	Regeneration method	Ref.
			Sulfur content (ppm)	Adsorption capacity (mg S g^{-1})		
Cu(I)Y, AgY	Commercial diesel	RT	430 → < 0.2	N	Air-calcination at 623 K and at 723 K, washing with dimethylformamide or carbon tetrachloride	[173]
Cu(I)Y	Commercial gasoline	RT	335 → < 0.28	12.5	N	[174]
Ni/KY	Benzothiophene, 2-methyl benzothiophene, 5-methylbenzothiophene	RT and 353	510 → < 1	5	Air-calcination at 573 K	[175]
$AgNO_3$/BEA, $AgNO_3$/MCM-41, $AgNO_3$/SBA-15	Tetrahydrothiophene, tert-butylmercaptane	RT-353	80 → 0.1	41.1 (AgNO3/BEA)	N	[176]
AgY CuZnY	Thiophene, dibenzothiophene, 4,6-dimethyldibenzothiophene	293–353	700 → 22 (Ag-Y) 700 → 36 (CuZn-Y)	44.9 (at 1500 ppm) 17.5 (at 500 ppm)	Air-calcination at 723 K	[177]
Ce(IV)Y	HDS-treated diesel	353	1.87 → < 0.01	N	N	[178]
Ga/AlY	Thiophene, tetrahydrothiophene, 4,6-dimethyldibenzothiophene	293–333	500 → 15	7.0, 17.4, 14.5	Air-calcination at 573 K N2-calcination at 623 K	[202]
CuY, NiY, NaY, and USY	Benzothiophene	303	N	54.1(NaY), 53.8(USY), 57.6(NiY), 63(CuY)	N	[203]
Cu(I)Y	Thiophene, benzothiophene, dibenzothiophene,	RT	300 → < 0.1	3.1	N	[204]
Cu(I)Y	Commercial jet fuel	RT	364 → 0.071	25.5	Air-calcination at 623 K calcination in 5 vol. % H2/He at 504 K	[205]

(continued)

Table 4.8 (continued)

Material	Sulfur compounds or fuel	Temperature (K)	Results	Results	Regeneration method	Ref.
			Sulfur content (ppm)	Adsorption capacity (mg S g^{-1})		
Cu(I)Y Cu(I)/ZSM-5	Commercial diesel	RT	297 → 0.06 (AC/Cu(I)Y)	12.2 (Cu(I)Y) 2.6 (Cu(I)/ZSM-5)	Air-calcination at 700–923 K	[206]
Ni(II)X, Ni(II)Y	Commercial diesel	RT and 353	297 → 0.22	10.6	Air-calcination at 623 K	[207]
AgBeta CuBeta	Dimethyl disulfide	333	20 → 1	7.1 8.7	N	[208]
Cu(I)/ETS-10	Tert-butylmercaptan tetrahydrothiophene	303	N	80	N	[209]
Cu_2O/MCM-41	JP-5 light fraction	RTa	841 → 50	12.8	Air-calcination at 723 K He-calcination at 973 K	[189]
Ni/SBA-15	Commercial diesel	RT-473	240 → 10 11.7 → 0.1	1.7 (at 240 ppm) 0.47 (at 11.7 ppm)	N[b]	[190]
CuCl($PdCl_2$)/MCM-41(SBA-15)	JP-5 light fraction	RT	841 → 50 (PdCl2/SBA-15)	38.4 (PdCl2/SBA-15)	Purge with benzene at 343 K	[191]
Cu(I)/Mesoporous aluminosilicate	Diesel	303	315 → 54	N	N	[192]
$AgNO_3$/mesoporous silica	Benzothiophene, dibenzothiophene, 4,6-dimethyldibenzothiophene	RT	N	20.5	Purge with diethyl ether	[193]
CuO/SBA-15	Thiophene	RT	N	6.4	N	[194]
Ni/MCM-41	4-Methyldibenzothiophene	RT	N	1.5	H2-calcination at 773 K	[195]
Fe_3O_4/MAS Fe_3O_4/MCM-41	Hydrotreated diesel	303	37 → 6	N	N	[196]

has obvious advantages over hydrodesulfurization. The process can be carried out at room temperature and does not require hydrogen, which is an important advantage. Table 4.8 lists some zeolites and mesoporous materials used for the removal of sulfur compounds. Yang and coworkers [173, 174] prepared Ag and Cu ion-exchanged NaY zeolites that selectively adsorbed sulfur compounds via π-complexation between thiophene and the ion-exchanged metals. Other researchers reported high degree of desulfurization using Ni/KY [175], $AgNO_3$/Beta [176], and CuZn/Y [177] adsorbents. These adsorbents were regenerated by washing with solvents at room temperature without loss of capacity. Feng and coworkers [178] used Ce(IV)Y zeolite to produce diesels with unprecedented low S (i.e., <0.01 ppm S). Mesoporous materials with their extremely high surface area and highly accessible pores are also efficient adsorbents [179–188]. Metal oxides and salts supported on mesoporous materials [189–196] had been used to remove sulfur from fuels, but were less able to attain the same level of ultra-deep desulfurization seen in the zeolite counterparts. Metal cations in zeolite appear to be the key in achieving ultra-deep desulfurization and it might be possible to replicate the same zeolite environment in mesoporous silica by incorporating zeolite framework structure on the pore wall, which has been demonstrated by several researchers [197–201].

References

1. Evers AA (2003) Go to where the market is! Challenges and opportunities to bring fuel cells to the international market. Int J Hydrogen Energy 28:725–733
2. http://www.fch.europa.eu/access. Accessed 20 Oct 2015
3. http://www.verticale.net/un-centro-di-competenza-permanente-per-7463. Accessed 20 Oct 2015
4. http://www.now-gmbh.de/en/about-now/funding-programmes/national-innovation-programme-nip.html. Accessed 20 Oct 2015
5. http://www.iphe.net/partners/republicofkorea.html. Accessed 20 Oct 2015
6. http://www.iphe.net/partners/japan.html. Accessed 20 Oct 2015
7. http://www.iphe.net/partners/china/research.html. Accessed 20 Oct 2015
8. http://www.hydrogen.energy.gov/access. Accessed 20 Oct 2015
9. Levin DB, Chahine R (2010) Challenges for renewable hydrogen production from biomass. Int J Hydrogen Energy 35:4962–4969
10. Bensaid S, Specchia S, Federici F, Saracco G, Specchia V (2009) MCFC-based marine APU: comparison between conventional ATR and cracking coupled with SR integrated inside the stack pressurized vessel. Int J Hydrogen Energy 34:2026–2042
11. European Environment Agency (2005) Climate change and a European low-carbon energy system. Report 1/2005. EEA (European Environment Agency) and OPOCE (Office for Official Publications of the European Communities)
12. Feige AK (2007) Effect of the growing bioenergy market on the availability of agricultural raw materials and products. Zuckerindustrie 132:687–693
13. Petterson A, Wellinger, A Biogas upgrading—developments and innovations. IEA Bioenergy. www.iea-biogas.net/publicationspublic.htm
14. Ribeiro RP, Sauer TP, Lopes FV, Moreira RF, Grande CA, Rodrigues AE (2008) Adsorption of CO_2, CH_4, and N_2 in activated carbon honeycomb monolith. J Chem Eng 53:2311–2317

15. Hernandez S, Scarpa F, Fino D, Conti R (2011) Biogas purification for MCFC application. Int J Hydrogen Energy 36:8112–8118
16. Fangmark IE, Hammarstrom LG, Stromqvist ME, Ness AL, Norman PR, Osmond NM (2002) Estimation of activated carbon adsorption efficiency for organic vapours I. A strategy for selecting test compounds. Carbon 40:2861–2869
17. Andriani D, Wresta A, Atmaja TD, Saepudin A (2014) A review on optimization production and upgrading biogas through CO_2 removal using various techniques. Appl Biochem Biotechnol 172:1909–1928
18. Ryckebosch E, Drouillon M, Vervaeren H (2011) Techniques for transformation of biogas to biomethane. Biomass Bioenergy 35:1633–1645
19. Wheless E, Pierce J (2004) Siloxanes in landfill and digester gasupdate. Los Angeles Country Sanitation Districts andSCS Energy, Whittier (Canada) and Long Beach (California)
20. Tjaden B, Gandiglio M, Lanzini A, Santarelli M, Jarvinen M (2014) Small-scale biogas-SOFC plant: technical analysis and assessment of different fuel reforming options. Energy Fuels 28:4216–4232
21. Wolak F (2012) Fuel cell power plants: biofuel case study—Tulare, CA. In: DOE-NREL Workshop, Golden, Colorado, June11−13. http://www1.eere.energy.gov/hydrogenandfuelcells/wkshp_biogas_fuel_cells.html
22. Van Herle J, Marechal F, Leuenberger S, Membrez Y, Bucheli O, Favrat D (2004) Process flow model of solid oxide fuel cell system supplied with sewage biogas. J Power Sources 131:127–141
23. Trendewicz A, Braun R (2013) Techno-economic analysis of solid oxide fuel cell-based combined heat and power systems for biogas utilization at wastewater treatment facilities. J Power Sources 233:380–393
24. Arnold M (2009) Reduction and monitoring of biogas trace compounds. VTT Research Notes 2496, VTT Technical Research Centre of Finland, Espoo, Finland (2009)
25. Pfeifer T, Nousch L, Lieftink D, Modena S (2013) System design and process layout for a SOFC micro-CHP unit with reduced operating temperatures. Int J Hydrogen Energy 38:431–439
26. Du W, Parker W (2012) Modeling volatile organic sulphur compounds in mesophilic and thermophilic anaerobic digestion of methionine. Water Res 46:539–546
27. Vassilev S, Baxter D, Andersen L, Vassileva C (2010) An overview of the chemical composition of biomass. Fuel 89:913–933
28. Sklorz M, Schnelle-Kreis J, Gottlieb A, Kuhner N, Schmid B (2003) Untersuchungen zum Einsatz von Oxidationskatalysatoren an landwirtschaftlichen Biogas-Verbrennungsmotoren. Bayerisches Institut fur Angewandte Umweltforschung und –technik, Augsburg, Germany (2003)
29. Papurello D, Soukoulis C, Schuhfried E, Cappellin L, Gasperi F, Silvestri S, Santarelli M, Biasioli F (2012) Monitoring of volatile compound emissions during dry anaerobic digestion of the organic fraction of municipal solid waste by proton transfer reaction time-offlight mass spectrometry. Bioresour Technol 126:254–265
30. Papadias D, Ahmed S, Kumar R (2012) Fuel quality issues with biogas energy—An economic analysis for a stationary fuel cell system. Energy 44:257–277
31. Rasmussen JFB, Hagen A, Thyden K (2011) Durability of solid oxide fuel cells using sulfur containing fuels. J Power Sources 196:7271–7276
32. Cheng Z, Wang JH, Choi Y, Yang L, Lin MC, Liu M (2011) From Ni–YSZ to sulfur-tolerant anode materials for SOFCs: electrochemical behavior, in situ characterization, modeling, and future perspectives. Energy Environ Sci 4:4380–4409
33. Jeihanipour A, Aslanzadeh S, Rajendran K, Balasubramanian G, Taherzadeh MJ (2013) High-rate biogas production from waste textiles using two-stage process. Renew Energy 52:128–135
34. Weiland P (2010) Biogas production: current state and perspectives. Appl Microbiol Biotechnol 85:849–860

35. Persson M (2003) Utvardering av uppgraderingstekniker for biogas, 85 pp. Report SGC 142, Svenskt Gastekniskt Center, Malmo, Sweden, Nov 2003
36. Iovane P, Nanna F, Ding Y, Bikson B, Molino A (2014) Experimental test with polymeric membrane for the biogas purification from CO_2 and H_2S. Fuel 135:352–358
37. Schomaker, AHHM, Boerboom AAM, Visser A, Pfeifer AE (2000) Anaerobic digestion of agro-industrial wastes: information networks e technical summary on gas treatment. AD-NETT, Nijmegen, Nederland, Report No.: FAIR-CT 96-2083 (DG12-SSMI)31 Aug 2000
38. Bteuten S, Pasel C, Luckas M, Bathen D (2013) Trace level adsorption of toxic sulfur compounds, carbon dioxide, and water from methane. J. Chemical Engineering 58:2465–2473
39. Ferreira D, Magalhaes R, Taveira P, Mendes A (2011) Effective adsorption equilibrium isotherms and breakthroughs of water vapor and carbon dioxide on different adsorbents. Ind Eng Chemist Res 50:10201–10210
40. Li G, Xiao P, Webley PA, Zhang J, Singh R (2009) Competition of CO2/H2O in adsorption based CO2 capture. Energy Procedia 1:1123–1130
41. Iwai Y, Oka N, Yamanishi T (2009) Influence of framework silica-to-alumina ratio on the water adsorption and desorption characteristics of MHI-CaX/CaY zeolite. J Phys Chemist Solids 70:881–888
42. Ribeiro AM, Sauer TP, Grande CA, Moreira RFPM, Loureiro JM, Rodrigues AE (2008) Adsorption equilibrium and kinetics of water vapor on different adsorbents. Ind Eng Chem Res 47:7019–7026
43. Lee YC, Weng LC, Tseng PC, Wang CC (2015) Effect of pressure on the moisture adsorption of silica gel and zeolite 13X adsorbents. Heat Mass Transf 51:441–447
44. Ozensoy E, Szanyi J, Peden CHF (2005) Interaction of water with ordered θ-Al2O3 ultrathin films grown on NiAl(100). J Phys Chemist B 109:3431–343
45. Kittaka S, Yamaguchi K, Takahara S (2012) High physisorption affinity of water molecules to the hydroxylated aluminum oxide (0 0 1) surface. J Colloid Interface Sci 368:552–557
46. Wellinger A, Lindberg A (2005) Biogas upgrading and utilisation. IEA Bioenergy Task 24: Energy From Biological Conversion of Organic Waste (2005)
47. Krich K, Augenstein A, Batmale J, Benemann J, Rutledge B, Salour D (2005) Upgrading dairy biogas to biomethane and other fuels. In: Andrews K (ed) Biomethane from dairy waste—a sourcebook for the production and use of renewable natural gas in California. Clear Concepts, California, pp 47–69
48. Jonsson O (2004) Biogas upgrading and use as transport fuel. Swedish Gas Center, Malmo Sweden, 5 pp. Report
49. Bourque H (2006) Use of liquefied biogas in transport sector. In: Conference sur les credits CO_2 et la valorisation du biogaz, 20 Apr 2006. www.apcas.qc.ca
50. Enggas. Gilbertsville: Engineered Gas Systems. Worldwide Inc. (2003). November 2007. http://www.enggas.com
51. Gomes VG, Hassan MM (2001) Coalseam methane recovery by vacuum swing adsorption. Separ Purif Technol 24:189–196
52. Welink JH, Dumont M, Kwant K (2014) Groen Gas: Gas van aardgaskwaliteit uit biomassa: update van de studie uit, Jan 2007, Senternovem, Nederland 2004, 34 p [Report]
53. Kim TJ, Li B, Hagg MB (2004) Novel fixed-site-carrier polyvinylamine membrane for carbon dioxide capture. J Polym Sci, Part B Polym Phys 42:4326–4336
54. Roks MFM, Luning L, Coops O (1997) Feasibility of applying new membrane for processing landfill gas to natural gas quality at low pressure (8 bar) [Haalbaarheid toepassing nieuw membraan voor opwerking stortgas naar aardgaskwaliteit bij lage druk (8 bar)]. Aquilo Gas Separation bv, Nederland, 57 p. Report
55. Guha AK, Majumdar S, Sirkar KK (1992) Gas separation Modes in a hollow fiber contained liquid membrane permeator. Ind Eng Chem Res 31:593–604
56. Esteves IAAC, Mota JPB (2002) Simulation of a new hybrid membrane/pressure swing adsorption process for gas separation. Desalination 148:275–280

57. Strevett KA, Vieth RF, Grasso D (1995) Chemo-autotrophic biogas purification for methane enrichment: mechanism and kinetics. Chem Eng J Biochem Eng J 58:71–79
58. Persson M (2003) Evaluation of upgrading techniques for biogas. School of Environmental Engineering, Lund. http://www.sgc.se/dokument/Evaluation.pdf
59. Tynell A (2005) Microbial growth on pall-rings—A problem when upgrading biogas with the technique absorption with water wash. Svenska Biogas for eningen and Swedish Gas Center, Stockholm, Sweden, 53 p. Report No.: 610408
60. Rutledge B (2005) California biogas industry assessment white paper. WestStart-Calstart, Pasadena, USA, 38 p. Report
61. Miltner M, Makaruk A, Harasek M (2008) Application of gas permeation for biogas upgrade—operational experiences of feeding biomethane into the Austrian gas grid. In: 16th European biomass conference and exhibition. Valencia, Spain, pp. 1905–1911
62. Makaruk A, Miltner M, Harasek M (2010) Membrane biogas upgrading processes for the production of natural gas substitute. Sep Purif Technol 74:83–92
63. Di Natale F, Erto A, Lancia A, Musmarra D (2009) A descriptive model for metallic ions adsorption from aqueous solutions onto activated carbons. J Hazard Mater 169:360–369
64. Schell WJ, Houston CD (1983) Use of membranes for biogas treatment. Energy Prog 3:96–100
65. Roehr M, Wimmerstedt R (1990) A comparison of two commercial membranes used for biogas upgrading. Desalination 77:331–345
66. Rautenbach R, Welsch K (1993) Treatment of landfill gas by gas permeation—pilot plant results and comparison to alternatives. Desalination 90:193–207
67. Favre E, Bounaceur R, Roizard D (2009) Biogas, membranes and carbon dioxide. J Membr Sci 328:11–14
68. Sridhar S, Smitha B, Aminabhavi TM (2007) Separation of carbon dioxide from natural gas mixtures through polymeric membranes: a review. Membrane separations division, center of excellence in polymer science, Karnatak University—India. Sep Purif Rev 36:113–174
69. Stern SA, Krishnakumar B, Charati SG, Amato WS, Friedman AA, Fuess DJ (1998) Performance of a bench-scale membrane pilot plant for the upgrading of biogas in a waste-water treatment plant. J Membr Sci 151:63–74
70. Bhide BD, Stern SA (1993) Membrane processes for the removal of acid gases from natural gas. Process configurations and optimization of operatine conditions. J Membr Sci 81:209–237
71. Bhide BD, Stern SA (1993) Membrane processes for the removal of acid gases from natural gas. II. Effects of operating conditions, economic parameters, and membrane properties. J Membr Sci 81:239–252
72. Hao J, Rice PA, Stern SA (2002) Upgrading low-quality natural gas with H_2S- and CO_2-selective polymer membranes: Part I. Process design and economics of membrane stages without recycle streams. J Membr Sci 209:177–206
73. Hao J, Rice PA, Stern SA (2008) Upgrading low-quality natural gas with H_2S- and CO_2-selective polymer membranes: Part II. Process design, economics, and sensitivity study of membrane stages with recycle streams. J Membr Sci 320:108–122
74. Persson M, Jönsson O (2006) Wellinger "Biogas upgrading to vehicle fuel standards and grid injection. IEA Bioenergy Task 37—Energy from biogas and landfill gas. Sweden & Switzerland. www.iea-biogas.net
75. Miltner M, Makaruk A, Krischan J, Harasek M (2012) Chemical-oxidative scrubbing for the removal of hydrogen sulphide from raw biogas: potentials and economics. Water Sci Technol 66:1354–1360
76. Baker WR, Lokhandawa K (2008) Natural gas processing with membranes: an overview. Membrane Technology and Research, Inc. 1360 Willow Road, Suite 103, Menlo Park, California 94025. Inf Eng Chem Res 47:2109–2121
77. Bernardo P, Drioli E, Golemme G (2009) Membrane gas separation: a review/state of the art. Ind Eng Chem Res 48:4638–4663

78. Bhide BD, Voskericyan A, Stern SA (1998) Hybrid processes for the removal of acid gases from natural gas. J Membr Sci 140:1–7
79. Hagen M, Polman E, Jensen J, Myken A, Jonsson O, Dahl A (2001) Adding gas from biomass to the gas grid. Swedish Gas Center, Malmo Sweden, July 2001, pp 144. Report SCG 118
80. Arimi MM, Knodel J, Kiprop A, Namango SS, Zhang Y, Geissen SU (2015) Strategies for improvement of biohydrogen production from organic-rich wastewater: a review. Biomass Bioenergy 75:101–118
81. Luo G, Angelidaki I (2012) Integrated biogas upgrading and hydrogen utilization in an anaerobic reactor containing enriched hydrogenotrophic methanogenic culture. Biotechnol Bioeng 109:2729–2736
82. Tsang YF, Wang L, Chua H (2015) Simultaneous hydrogen sulfide and ammonia removal in a biotrickling filter: crossed inhibitory effects among selected pollutants and microbial community change. Chem Eng J 281:389–396
83. Liu C, Zhao D, Yan L, Wang A, Gu Y, Lee DJ (2015) Elemental sulfur formation and nitrogen removal from wastewaters by autotrophic denitrifiers and anammox bacteria. Biores Technol 191:332–336
84. Xu G, Peng J, Feng C, Fang F, Chen S, Xu Y, Wang X (2015) Evaluation of simultaneous autotrophic and heterotrophic denitrification processes and bacterial community structure analysis. Appl Microbiol Biotechnol 99:6527–6536
85. Mora M, Dorado AD, Gamisans X, Gabriel D (2015) Investigating the kinetics of autotrophic denitrification with thiosulfate: modeling the denitritation mechanisms and the effect of the acclimation of SO-NR cultures to nitrite. Chem Eng J 262:235–241
86. Robinson PJ, Luyben WL (2010) Integrated gasification combined cycle dynamic model: H_2S absorption/stripping, water-gas shift reactors, and CO_2 absorption/stripping. Ind Eng Chem Res 49:4766–4781
87. Huang X, Zhu D (2004) Review of technologies for removal of H_2S. Huaxue Gongye Yu Gongcheng Jishu 25:47–49
88. Hix R, Marshall LS (1990) Reactive absorption of hydrogen sulfide by a solution of sulfur dioxide in polyglycol ether. Preprints of Papers—Am Chem Soc, Division of Fuel, Chem 35:128–135
89. Park D, Lee DS, Joung JY, Park JM (2005) Comparison of different bioreactor systems for indirect H_2S removal using iron-oxidizing bacteria. Process Biochem 40:1461–1467
90. Nasr MRJ, Abedinzadegan M (1995) Performance of a venturi jet scrubber for H_2S removal by iron-complex solution. Chem Eng Technol 18:166–170
91. Horikawa MS, Rossi F, Gimenes ML, Costa CMM, da Silva MGC (2004) Chemical absorption of H_2S for biogas purification. Braz J Chem Eng 21:415–422
92. Belmabkhout Y, De Weireld G, Sayari A (2009) Amine-bearing mesoporous silica for CO_2 and H_2S removal from natural gas and biogas. Langmuir 25:13275–13278
93. Chang M, Tseng T (1996) Gas-phase removal of H_2S and NH_3 with dielectric barrier discharges. J Environ Eng 122:41–46
94. Duan H, Yan R, Koe LCC, Wang X (2007) Combined effect of adsorption and biodegradation of biological activated carbon on H_2S biotrickling filtration. Chemosphere 66:1684–1691
95. Ho KL, Chung YC, Lin YH, Tseng CP (2008) Microbial populations analysis and field application of biofilter for the removal of volatile-sulfur compounds from swine wastewater treatment system. J Hazard Mater 152:580–588
96. Lee EY, Lee NY, Cho KS, Ryu HW (2006) Removal of hydrogen sulfide by sulfate-resistant Acidithiobacillus thiooxidans AZ11. J Biosci Bioeng 101:309–314
97. González-Sánchez A, Revah S, Deshusses MA (2008) Alkaline biofiltration of H_2S odors. Environ Sci Technol 42:7398–7404
98. Jiang X, Yan R, Tay JH (2009) Simultaneous autotrophic biodegradation of H_2S and NH_3 in a biotrickling filter. Chemosphere 75:1350–1355

99. Montebello AM, Fernández M, Almenglo F, Ramírez M, Cantero D, Baeza M, Gabriel D (2012) Simultaneous methylmercaptan and hydrogen sulfide removal in the desulfurization of biogas in aerobic and anoxic biotrickling filters. Chem Eng J 200–202:237–246
100. Fortuny M, Baeza JA, Deshusses MA, Gamisans X, Casas C, Lafuente J, Gabriel D (2008) Biological sweetening of energy gases mimics in biotrickling filters. Chemosphere 71:10–17
101. Fernández M, Ramírez M, Perez RM, Rovira R, Gabriel D, Gomez JM, Cantero D (2010) Hydrogen sulfide removal from biogas using biofiltration under anoxic conditions. In: Proceedings of the 2010 Duke-UAM Conference on Biofiltration, CD-ROM, Washington, USA (2010)
102. Gabriel D (2003) Retrofitting existing chemical scrubbers to biotrickling filters for H_2S emission control. Proc Natl Acad Sci 100:6308–6312
103. Kim JH, Rene ER, Park HS (2008) Biological oxidation of hydrogen sulfide under steady and transient state conditions in an immobilized cell biofilter. Bioresour Technol 99:583–588
104. Goncalves JJ, Govind R (2009) Enhanced biofiltration using cell attachment promoters. Environ Sci Technol 43:1049–1054
105. Ryu HW, Yoo SK, Choi JM, Cho KS, Cha DK (2009) Thermophilic biofiltration of H_2S and isolation of a thermophilic and heterotrophic H_2S-degrading bacterium, Bacillus sp. TSO3. J Hazard Mater 168:501–506
106. Ramírez M, Fernández M, Granada C, Le Borgne S, Gómez JM, Cantero D (2011) Biofiltration of reduced sulphur compounds and community analysis of sulphur-oxidizing bacteria. Bioresour Technol 102:4047–4053
107. Ho KL, Lin WC, Chung YC, Chen YP, Tseng CP (2013) Elimination of high concentration hydrogen sulfide and biogas purification by chemical-biological process. Chemosphere 92:1396–1401
108. Giro MEA, Garcia O Jr, Zaiat M (2006) Immobilized cells of Acidithiobacillus ferrooxidans in PVC strands and sulfite removal in a pilot-scale bioreactor. Chem Eng J 28:201–207
109. Alemzadeh I, Kahrizi E, Vossoughi M (2009) Bio-oxidation of ferrous ions by Acidithioobacillus ferrooxidans in a monolithic bioreactor. J Chem Technol Biotechnol 84:504–510
110. Asai S, Konishi Y, Yabu T (1990) Kinetics of absorption of hydrogen sulfide into aqueous ferric sulfate solutions. AIChE J 36:1331–1338
111. Ebrahimi S, Kleerebezem R, van Loosdrecht M, Heijnen J (2003) Kinetics of the reactive absorption of hydrogen sulfide into aqueous ferric sulfate solutions. Chem Eng Sci 58:417–427
112. Mousavi SM, Yaghmaei S, Vossoughi M, Roostaazad R, Jafari A, Ebrahimi M, Chabok OH, Turunen I (2008) The effects of Fe(II) and Fe(III) concentration and initial pH on microbial leaching of low-grade sphalerite ore in a column reactor. Bioresour Technol 99:2840–2845
113. Chung YC, Ho KL, Tseng CP (2003) Hydrogen sulfide gas treatment by a chemical–biological process: chemical absorption and biological oxidation steps. J Environ Sci Health, Part B 38:663–679
114. Chung YC, Ho KL, Tseng CP (2006) Treatment of high H_2S concentrations by chemical absorption and biological oxidation process. Environ Eng Sci 23:942–953
115. Mesa M, Andrades J, Macias M, Cantero D (2004) Biological oxidation of ferrous iron: study of bioreactor efficiency. J Chem Technol Biotechnol 79:163–170
116. Pinjing H, Liming S, Zhiwen Y, Guojian L (2001) Removal of hydrogen sulfide and methyl mercaptan by a packed tower with immobilized micro-organism beads. Water Sci Technol 44:327–333
117. Soreanu G, Béland M, Falletta P, Edmonson K, Seto P (2008) Laboratory pilot scale study for H_2S removal from biogas in an anoxic biotrickling filter. Water Sci Technol 57:201–207
118. Soreanu G, Béland M, Falletta P, Edmonson K, Seto P (2008) Investigation on the use of nitrified wastewater for the steady-state operation of a biotrickling filter for the removal of hydrogen sulfide in biogas. J Environ Eng Sci 7:543–552

119. Manconi I, Carucci A, Lens P, Rossetti S (2006) Simultaneous biological removal of sulfide and nitrate by autotrophic denitrification in an activated sludge system. Water Sci Technol 53:91–99
120. Bentley R, Chasteen TG (2004) Environmental VOSCs—formation and degradation of dimethyl sulfide, methanethiol and related materials. Chemosphere 55:291–317
121. Sipma J, Svitelskaya A, van der Mark B, Hulstoff Pol LW, Lettinga G, Buisman CJN, Janssen AJH (2004) Potentials of biological oxidation processes for the treatment of spent sulfidic caustics containing thiols. Water Res 38:4331–4340
122. van Leerdam RC, Bonilla-Salinas M, de Bok FAM, Bruning H, Lens PNL, Stams AJM, Janssen AJH (2008) Anaerobic methanethiol degradation and methanogenic community analysis in an alkaline (pH 10) biological process for liquefied petroleum gas desulfurization. Biotechnol Bioeng 101:691–701
123. van Leerdam RC, van den Bosch PLF, Lens PNL, Janssen AJH (2011) Reactions between methanethiol and biologically produced sulfur particles. Environ Sci Technol 45:1320–1326
124. van den Bosch PLF, de Graaff M, Fortuny-Picornell M, van Leerdam RC, Janssen AJH (2009) Inhibition of microbiological sulfide oxidation by methanethiol and dimethyl polysulfides at natron-alkaline conditions. Appl Microbiol Biotechnol 83:579–587
125. Goyal R, Babu V, Patel GK (2014) Biomethane production. In: Babu V, Thapliyal A, Patel, GK (eds) Biofuels production, pp 333–356
126. Krich K, Augenstein D, Batmale J, Benemann J, Rutledge B, Salour D (2005) Biomethane from dairy waste: a sourcebook for the production and use of renewable natural gas in California. California, Western United Dairymen
127. Rasi S, Lantela J, Rintala J (2011) Trace compounds affecting biogas energy utilisation—A review. Energy Convers Manage 52:3369–3375
128. Papurello D, Schuhfried E, Lanzini A, Romano A, Cappellin L, Mark T, Silvestri S, Biasioli F (2014) Influence of co-vapors on biogas filtration for fuel cells monitored with PTR-MS (Proton Transfer Reaction-Mass Spectrometry). Fuel Process Technol 118:133–140
129. Salminen E, Rintala J, H¨ark¨onen J, Kuitunen M, Hogmander H, Oikari A (2001) Anaerobically digested poultry slaughterhouse wastes as fertilizer in agriculture. Bioresour Technol 78:81–88
130. Woli KR, Nagumo T, Kuramochi K, Hatano R (2004) Evaluating river water quality through land use analysis and N budget approaches in livestock farming areas. Sci Total Environ 329:61–74
131. Li XZ, Zhao QL (1999) Inhibition of microbial activity of activated sludge by ammonia in leachate. Environ Int 25:961–968
132. Battistoni P, Fava G, Pavan P, Musacco A, Cecchi F (1997) Phosphate removal in anaerobic liquors by struvite crystallization without addition of chemicals: preliminary results. Water Res 31:2925–2929
133. Bouwer H, Chaney RL (1974) Land treatment of wastewater. Adv Agron 26:133–176
134. Meinhold J, Pedersen H, Arnold E, Issacs S, Henze M (1998) Effect of continuous addition of an organic substrate to the anoxic phase on biological phosphate removal. Water Sci Technol 38:97–105
135. Bonmati A, Flotats X (2003) Air stripping of ammonia from pig slurry: characterisation and feasibility as a pre- or post-treatment to mesophilic anaerobic digestion. Waste Manage 23:261–272
136. Liao PH, Chen A, Lo KV (1995) Removal of nitrogen from swine manure wastewaters by ammonia stripping. Bioresour Technol 54:17–20
137. Cheung KC, Chu LM, Wong MH (1997) Ammonia stripping as a pretreatment for landfill leachate. Water Air Soil Pollut 94:209–220
138. Minocha VK, Prabhakar AVS (1988) Ammonia removal and recovery from urea fertilizer plant waste. Environ Technol Lett 9:655–664
139. Lei X, Sugiura N, Feng C, Maekawa T (2007) Pretreatment of anaerobic digestion effluent with ammonia stripping and biogas purification. J Hazard Mater 145:391–397

140. Esteves IAAC, Lopes MSS, Nunes PMC, Mota JPB (2008) Adsorption of natural gas and biogas components on activated carbon. Sep Purif Technol 62:281–296
141. Hernandez SP, Chiappero M, Russo N, Fino D (2011) A novel ZnO-based adsorbent for biogas purification in H2 production systems. Chem Eng J 176–177:272–279
142. Chang FT (2010) Apparatus and method for purification of sulfur-containing waste gas and methane recovery from biogas. Faming Zhuanli Shenqing. CN 101884870 A 20101117
143. Sakanishi K, Matsumura A, Saito I, Hanaoka T, Minowa T, Tomoaki (2004) Removal of hydrogen sulfide and carbonyl sulfide for purification of biomass-gasified synthetic gas using active carbons. Prepr Symp-Am Chem Soc, Div Fuel Chem 49:580–581
144. Richter E, Henning KD, Knoblauch K, Juntgen H (1985) Utilization of activated carbon and carbon molecular sieves in biogas purification and methane recovery. Comm Eur Communities, [Rep.] EUR, (EUR 10024, Energy Biomass), pp 621–624
145. Shi L, Yang K, Zhao Q, Wang H, Cui Q (2015) Characterization and mechanisms of H_2S and SO_2 adsorption by activated carbon. Energy Fuels. Ahead of Print
146. Phooratsamee W, Hussaro K, Teekasap S, Hirunlabh J (2014) Increasing adsorption of activated carbon from palm oil shell for adsorb H_2S from biogas production by impregnation. Am J Env Sci 10:431–445
147. Aslam Z, Shawabkeh RA, Hussein IA, Al-Baghli N, Eic M (2015) Synthesis of activated carbon from oil fly ash for removal of H_2S from gas stream. Appl Surf Sci 327:107–115
148. Sisani E, Cinti G, Discepoli G, Penchini D, Desideri U, Marmottini F (2014) Adsorptive removal of H_2S in biogas conditions for high temperature fuel cell systems. Int J Hydrogen Energy 39:21753–21766.|
149. Micoli L, Bagnasco G, Turco M (2014) H_2S removal from biogas for fuelling MCFCs: new adsorbing materials. Int J Hydrogen Energy 39:1783–1787
150. Liang M, Zhang C, Zheng H (2014) The removal of H_2S derived from livestock farm on activated carbon modified by combinatory method of high-pressure hydrothermal method and impregnation method. Adsorption 20:525–531
151. An H, Zhao D, Zhao C, Xue J, Li X, Xiuling (2011) Study on removal of H_2S by modified ACF with impregnation of transition metal. Huanjing Gongcheng Xuebao 5:1581–1585
152. Huang CC, Chen CH (2013) Dynamic adsorption model of H_2S in a fixed bed of copper impregnated activated carbon. Separation Sci Technol 48:148–155
153. Monteleone G, De Francesco M, Galli S, Marchetti M, Naticchioni V (2011) Deep H_2S removal from biogas for molten carbonate fuel cell (MCFC) systems. Chem Eng J 173:407–414
154. Yan B, Jiang W, Li F, Liu L (2010) Study on adsorbents from sewage sludge to removal of NH3 and H_2S. Harbin Shangye Daxue Xuebao, Ziran Kexueban 26:662–666
155. Polster A, Brummack J (2009) Desulfurization in biogas plants. VDI-Berichte 2057 (Biogas 2009), pp 185–193
156. Shah M, Tsapatsis M, Siepmann JI, Ilja J (2015) Monte carlo simulations probing the adsorptive separation of hydrogen sulfide/methane mixtures using all-silica zeolites. Langmuir. Ahead of Print
157. Liu C, Zhang R, Wei S, Wang J, Liu Y, Li M, Liu R, Rutao (2015) Selective removal of H_2S from biogas using a regenerable hybrid TiO_2/zeolite composite. Fuel 157:183–190
158. Yazdanbakhsh F, Blasing M, Sawada JA, Rezaei S, Muller M, Baumann S, Kuznicki SM (2014) Copper Exchanged Nanotitanate for High Temperature H_2S Adsorption. Ind Eng Chem Res 53:11734–11739
159. Izumi J, Wang H (2010) Methane recovery and purification from biogasses using vacuum pressure swing adsorption. In: Pacifichem 2010, International Chemical Congress of Pacific Basin Societies, Honolulu, HI, United States, AETECH-264, Dec 15–20 2010
160. Cosoli P, Ferrone M, Pricl S, Fermeglia M (2008) Hydrogen sulfide removal from biogas by zeolite adsorption. Part II. MD simulations. Chem Eng J 145:93–99
161. Qiu G, Huang B, Wang X, Li X, Xiangtong (2006) Theoretical study of H_2S adsorption on HZSM-5 zeolite. Shiyou Yu Tianranqi Huagong 35:107–109

162. Tomadakis MM, Heck HH, Howell M. Hall, Merilyn (2006) Use of molecular sieves to remove H_2S and CO_2 from landfill gas, producing a high-energy content methane stream. In: AIChE Spring National Meeting, Conference Proceedings, Orlando, FL, United States, Apr 23–27 2006, P43008/1-P43008/6
163. Gong J, Jiao YF, Su QQ, Mi WL (2015) Deep removal of carbonyl sulfide in biogas. Gaoxiao Huaxue Gongcheng Xuebao 29:443–451
164. Liu Y, Guo BB, Zhu YQ (2013) Research progress in desulfurizers. Dangdai Huagong 42:827–829, 840
165. Sun T, Shen Y, Jia J (2014) Gas cleaning and hydrogen sulfide removal for COREX coal gas by sorption enhanced catalytic oxidation over recyclable activated carbon desulfurizer. Environ Sci Technol 48:2263–2272
166. Hyung-Tae K, Seung-Moon K, Ki-Won J, Young-Seek Y, Jin-Hong K (2007) Desulphurisation of odorant-containing gas: removal of t-butylmercaptan on $Cu/ZnO/Al_2O_3$. Int J Hydrogen Energy 32:3603–3608
167. Osorio F, Torres JC (2009) Biogas purification from anaerobic digestion in a wastewater treatment plant for biofuel production. Renew Energy 34:2164–2171
168. Li YY, Perera SP, Crittenden BD (1998) Zeolite monoliths for air separation, part 2: oxygen enrichment, pressure drop and pressurization. Trans I Chem E 76:931–941
169. Gordon Israelson PE (2009) Hydrocarbon condensation heating of natural gas by an activated carbon desulfurizer. J Fuel Cell Sci Technol 6:34506–34518
170. Gordon Israelson PE (2004) Results of testing various natural gas desulphurisation adsorbents. J Mater Eng Perform 13:282–286
171. Hernandez S, Solarino L, Orsello G, Russo N, Fino D, Saracco G et al (2008) Desulphurization process for fuel cells systems Int. J. Hydrogen Energy 33:3209–3214
172. Gordon Israelson PE (2008) Water vapor effects on fuel cell desulfurizer performance—a decade of field experience. In: Proceedings of Fuel Cell 200 Sixth Int Fuel Cell Science Eng Tech; Conference Denver, Colorado, USA
173. Yang RT, Hernandez-Maldonado AJ, Yang FH (2003) Desulfurization of transportation fuels with zeolites under ambient conditions. Science 301:79–81
174. Hernandez-Maldonado AJ, Yang RT (2003) Desulfurization of diesel fuels by adsorption via π-complexation with vapor-phase exchanged Cu(I)−Y zeolites. Ind Eng Chem Res 42:3103–3110
175. Velu S, Song CS, Engelhard MH, Chin YH (2005) Adsorptive removal of organic sulfur compounds from jet fuel over K-exchanged NiY zeolites prepared by impregnation and ion exchange. Ind Eng Chem Res 44:5740–5749
176. Ko CH, Song HI, Park JH, Han SS, Kim JN (2007) Selective removal of sulfur compounds in city-gas by adsorbents. Korean J Chem Eng 24:1124–1127
177. Zhang ZY, Shi TB, Jia CZ, Ji WJ, Chen Y, He MY (2008) Adsorptive removal of aromatic organosulfur compounds over the modified Na-Y zeolites. Appl Catal B 82:1–10
178. Xue M, Chitrakar R, Sakane K, Hirotsu T, Ooi K, Yoshimura Y, Toba M, Feng Q (2006) Preparation of cerium-loaded Y-zeolites for removal of organic sulfur compounds from hydrodesulfurizated gasoline and diesel oil. J Colloid Interface Sci 298:535–542
179. Lam KF, Yeung KL, Mckay G (2006) An investigation of gold adsorption from a binary mixture with selective mesoporous silica adsorbents. J Phys Chem B 110:2187–2194
180. Lam KF, Yeung KL, Mckay G (2006) A rational approach in the design of selective mesoporous adsorbents. Langmuir 22:9632–9641
181. Lam KF, Fong CM, Yeung KL (2007) Separation of precious metals using selective mesoporous adsorbents. Gold Bull. 40:192–198
182. Lam KF, Yeung KL, Mckay G (2007) Efficient approach for Cd^{2+} and Ni^{2+} removal and recovery using mesoporous adsorbent with tunable selectivity. Environ Sci Technol 41:3329–3334
183. Parida KM, Dash SK (2010) Adsorption of Cu^{2+} on spherical Fe-MCM-41 and its application for oxidation of adamantine. J Hazard Mater 179:642–649

184. Arruebo M, Ho WY, Lam KF, Chen XG, Arbiol J, Santamaria J, Yeung KL (2008) Preparation of magnetic nanoparticles encapsulated by an ultrathin silica shell via transformation of magnetic Fe-MCM-41. Chem Mater 20:486–493
185. Lam KF, Chen XQ, Mckay G, Yeung KL (2008) Anion Effect on $Cu2^{+}$ Adsorption on NH2-MCM-41. Ind Eng Chem Res 47:9376–9383
186. Lam KF, Fong CM, Yeung KL, Mckay G (2008) Selective adsorption of gold from complex mixtures using mesoporous adsorbents. Chem Eng J 145:185–195
187. Lam KF, Chen XQ, Fong CM, Yeung KL (2008) Selective mesoporous adsorbents for Ag^{+}/$Cu2^{+}$ separation. Chem Commun 17:2034–2036
188. Chen XQ, Lam KF, Zhang QJ, Pan BC, Arruebo M, Yeung KL (2009) Synthesis of highly selective magnetic mesoporous adsorbent. J Phys Chem 113:9804–9813
189. Wang YH, Yang RT, Heinzel JM (2009) Desulfurization of jet fuel JP-5 light fraction by MCM-41 and SBA-15 supported cuprous oxide for fuel cell applications. Ind Eng Chem Res 48:142–147
190. Park JG, Ko CH, Yi KB, Park JH, Han SS, Cho SH, Kim JN (2008) Reactive adsorption of sulfur compounds in diesel on nickel supported on mesoporous silica. Appl Catal B 81:244–250
191. Wang Y, Yang RT, Heinzel JM (2008) Desulfurization of jet fuel by π-complexation adsorption with metal halides supported on MCM-41 and SBA-15 mesoporous materials. Chem Eng Sci 63:356–365
192. Li WL, Liu QF, Xing JM, Gao HS, Xiong XC, Li YG, Li X, Liu HZ (2007) High-efficiency desulfurization by adsorption with mesoporous aluminosilicates. AIChE J 53:3263–3268
193. Yang LM, Wang YJ, Huang D, Luo GS, Dai YY (2007) Preparation of high performance adsorbents by functionalizing mesostructured silica spheres for selective adsorption of organosulfur compounds. Ind Eng Chem Res 46:579–583
194. Yin Y, Jiang WJ, Liu XQ, Li YH, Sun LB (2012) Dispersion of copper species in a confined space and their application in thiophene capture. J Mater Chem 22:18514–18521
195. Samadi-Maybodi A, Teymouri M, Vahid A, Miranbeigi A (2011) In situ incorporation of nickel nanoparticles into the mesopores of MCM-41 by manipulation of solvent-solute interaction and its activity toward adsorptive desulfurization of gas oil. J Hazard Mater 192:1667–1674
196. Li WL, Tang H, Zhang T, Li Q, Xing JM, Liu HZ (2010) Ultra-deep desulfurization adsorbents for hydrotreated diesel with magnetic mesoporous aluminosilicates. AIChE J 56:1391–1396
197. Tao YS, Kanoh H, Abrams L, Kaneko K (2006) Mesopore-modified zeolites: preparation, characterization, and applications. Chem Rev 106:896–910
198. Xiao FS, Wang LF, Yin CY, Lin KF, Di Y, Li JX, Xu RR, Su DS, Schlogl R, Yokoi T, Tatsumi T (2006) Catalytic properties of hierarchical mesoporous zeolites templated with a mixture of small organic ammonium salts and mesoscale cationic polymers. Angew Chem Int Ed 45:3090–3093
199. Wang H, Pinnavaia TJ (2006) MFI zeolite with small and uniform intracrystal mesopores. Angew Chem Int Ed 45:7603–7606
200. Choi M, Cho HS, Srivastava R, Venkatesan C, Choi DH, Ryoo R (2006) Amphiphilic organosilane-directed synthesis of crystalline zeolite with tunable mesoporosity. Nat Mater 5:718–723
201. Zhang XY, Liu DX, Xu DD, Asahina S, Cychosz KA, Agrawal KV, Wahedi YA, Bhan A, Hashimi SA, Terasaki O, Thommes M, Tsapatsis M (2012) Synthesis of Self-Pillared Zeolite Nanosheets by Repetitive Branching. Science 336:1684–1687
202. Tang K, Song LJ, Duan LH, Li XQ, Gui JZ, Sun ZL (2008) Deep desulfurization by selective adsorption on a heteroatoms zeolite prepared by secondary synthesis. Fuel Process Technol 89:1–6
203. Jiang M, Ng FTT (2006) Adsorption of benzothiophene on Y zeolites investigated by infrared spectroscopy and flow calorimetry. Catal Today 116:530–536

204. Jayaraman A, Yang FH, Yang RT (2006) Effects of nitrogen compounds and polyaromatic hydrocarbons on desulfurization of liquid fuels by adsorption via π-complexation with Cu(I)Y Zeolite. Energy Fuels 20:909–914
205. Hernandez-Maldonado AJ, Yang RT, Cannella W (2004) Desulfurization of commercial jet fuels by adsorption via π-complexation with vapor phase ion exchanged Cu(I)-Y zeolites. Ind Eng Chem Res 43:6142–6149
206. Hernandez-Maldonado AJ, Yang RT (2004) New sorbents for desulfurization of diesel fuels via π-complexation. AIChE J 50:791–801
207. Hernandez-Maldonado AJ, Yang RT (2004) Desulfurization of diesel fuels via π-complexation with nickel(II)-exchanged X- and Y-zeolites. Ind Eng Chem Res 43:1081–1089
208. Lee J, Beum HT, Ko CH, Park SY, Park JH, Kim JN, Chun BH, Kim SH (2011) Adsorptive removal of dimethyl disulfide in olefin rich C4 with ion-exchanged zeolites. Ind Eng Chem Res 50:6382–6390
209. Jung GS, Park DH, Lee DH, Lee HC, Hong SB, Woo HC (2010) Adsorptive removal of tert-butylmercaptan and tetrahydrothiophene using microporous molecular sieve ETS-10. Appl Catal 100:264–270
210. Yeung KL, Han W (2014) Zeolites and mesoporous materials in fuel cell applications. Catal Today 236:182–205

Chapter 5
The Effect of Sulfur Compounds on MCFC

5.1 Sulfur Poisoning on the MCFC Components

Molten carbonate fuel cells (MCFC) are composed of a porous nickel-based anode, a porous nickel oxide-based cathode and molten carbonate salts as electrolyte within a porous lithium aluminate matrix. Molten carbonate fuel cells with internal reforming can be fed directly with light hydrocarbons rich gas such as biogas.

Though MCFCs have the advantage of not requiring noble metal catalysts for the electrochemical reactions, some species have a poisoning effect on the catalytic properties of the electrodes.

The harmful effect of impurities may depend on the partial pressure of other species in the gas (e.g., hydrogen, water, carbon dioxide), the current density at which the fuel cell is operated, the temperature, and the fuel utilization.

Hydrogen sulfide is the most important contaminant and even few parts-per-million concentrations the fuel gas at the anode side strongly affect cell performance. H_2S has an immediate effect on cell performance, also at 1 ppm [1]. The effect of sulfur poisoning was observed at the initial H_2S addition, even though the concentration was very low.

The limit of H_2S concentration accepted for fuel gas is less than 1 ppm. Sulfur poisoning of the electrode is irreversible upon long-term exposure to concentrations of more than about 10 ppm since surface structure changes take place and cause permanent damage and deactivation of the anode [2–11]. At low concentrations the effects of H_2S are generally reversible by passing over H_2S-free hydrogen and water vapor.

Poisoning mechanisms depend on many factors, such as applied current density, inlet anodic gas composition, operating temperature and pressure.

In many studies various causes have been identified for the immediate decrease in MCFC performance upon introduction of H_2S [6–9, 11–16]. This problem has

M. Turco et al., *Treatment of Biogas for Feeding High Temperature Fuel Cells*,
Green Energy and Technology, DOI 10.1007/978-3-319-03215-3_5

been widely studied but no assessment on the mechanisms of the poisoning by H_2S has been reached.

There are two main interactions of H_2S with cell components, with the electrolyte and with the anode and cathode [11].

H_2S can react chemically with carbonates of the electrolyte to form either sulfide or sulfate ions (Eqs. 5.1 and 5.2) reducing electrochemically active charge carriers which would otherwise be available for the hydrogen oxidation mechanism [5, 13, 17]. The cell performances decay, even if the ion conductivity of the electrolyte does not appreciably changes because carbonate ions are replaced by the same equivalent number of sulfur-based anions.

$$H_2S + CO_3^{2-} \rightarrow H_2O + CO_2 + S^{2-} \tag{5.1}$$

$$H_2S + CO_3^{2-} + 3H_2O \rightarrow SO_4^{2-} + CO_2 + 4H_2 \tag{5.2}$$

H_2S can react with carbonates also via electrochemical processes [5, 14, 18] (Eqs. 5.3 and 5.4) yielding harmful, ionized sulfate compounds forming either sulfide S^{2-} or sulfate $SO_4{}^{2-}$ ions.

$$5CO_3^{2-} + 4H_2 + H_2S \rightarrow S^{2-} + 5CO_2 + 5H_2O + 8e^- \tag{5.3}$$

$$5CO_3^{2-} + H_2S \rightarrow SO_4^{2-} + 5CO_2 + H_2O + 8e^- \tag{5.4}$$

Standard potentials of above reactions are, respectively, − 1.037 V and −0.986 V with respect to O_2:CO_2 = 33:67 vol.% reference electrode.

When the above reactions occur instead of the hydrogen oxidation, the overall cell reactions are respectively as follows:

$$H_2S + M_2CO_3 \rightarrow M_2S + H_2O + CO_2 \tag{5.5}$$

$$H_2S + M_2CO_3 + 3H_2O \rightarrow M_2SO_4 + CO_2 + 4H_2 \tag{5.6}$$

where M is a metal such as lithium or potassium.

Hydrogen sulfide is a poison for the nickel catalyst and the negative effect on fuel cell performance is well documented [3, 8, 9, 13, 18, 19].

H_2S reacting with nickel can block electrochemically active sites for the hydrogen oxidation, can change the wettability of the anode toward carbonates, can modify the anode surface and its porous structure, can alter the anode conductivity, can change the carbonate conversion to sulfate and can poison catalytic sites for the water gas shift reaction.

The affected sites give rise to morphological changes in the anode structure, and can thereby cause further deterioration of cell performance through secondary effects like impeded gas diffusion, volume change or reduced wetting by the electrolyte [20].

Possible reactions of hydrogen sulfide with nickel can have different natures: formation of bulk nickel sulfides via chemical reactions, reaction (5.7); surface sulfuration either via physical adsorptions of hydrogen sulfide molecules, reaction (5.8), or via chemisorptions of sulfur atoms, reaction (5.9) [18].

$$xNi + yH_2S \rightarrow Ni_xS_y + yH_2 \tag{5.7}$$

$$Ni(s) + H_2S(s) \rightarrow Ni{-}H_2S(ads) \tag{5.8}$$

$$\begin{aligned} &2Ni(s) + H_2S(g) \rightarrow Ni{-}HS(ads) + Ni{-}H(ads) \rightarrow Ni{-}S(ads) + Ni{-}H_2(ads) \\ &\rightarrow Ni{-}S(ads) + Ni + H_2(g) \end{aligned} \tag{5.9}$$

With the anode, H_2S can be chemisorbed on nickel surfaces or can react chemically with nickel to form nickel sulfide. Nickel sulfides can be formed also electrochemically by oxidation of sulfide ions in the electrolyte.

$$Ni + H_2S \rightarrow NiS + H_2 \tag{5.10}$$

$$Ni + S^{2-} \rightarrow NiS + 2e^- \tag{5.11}$$

Electrochemical poisoning reactions occur when the anodic potential reach electrode potentials for nickel sulfides formation: the standard electrode potential for the half-reaction forming NiS and Ni3S2 are respectively −0.756 V and −0.829 V [13, 18]. At open circuit voltage conditions, the anodic potential is more negative than electrode potentials necessary for either NiS or Ni_3S_2 formation.

At low H_2S levels just two poisoning reaction types occur: physical and chemical absorptions on nickel surface by reactions (5.8) and (5.9); replacement of carbonate ions with sulfide and sulfate ions by reactions (5.1)–(5.4). In fact, formations of bulk nickel sulfides by reaction (5.7) are thermodynamically forbidden.

Devianto et al. [21] investigated the poisoning effect of H_2S on Ni-based anodes in MCFC at low H_2S concentrations, simulating biogas impurity. A conventional Ni-Cr anode was coated with ceria using dip coating to form a rare earth metal oxide thin layer on the surface of the anode. Electrochemical studies of the Ni-based samples were performed in symmetric cells under anode atmosphere (H_2, CO_2, H_2O, and N_2 as balance) with 2, 6, 12, and 24 ppm of H_2S by means of electrochemical impedance spectroscopy.

The results showed that the poisoning resistance was enhanced at low coating percentages of ceria; the effects depend on H_2S concentration and the applied load. These results were confirmed by electrochemical impedance tests where the cerium oxide addition appears through stable polarization behavior up to 6 ppm of H_2S, particularly in the mass transfer region. The protection is explained by the depression of poisoned Ni active sites and formation of a layer to the metal surface. The ceria coating layer is a potential solution to reduce H_2S poisoning of MCFCs fuelled with biogas.

Higher water content accelerated the effect of corrosion and the poisoning resistance was enhanced at low coating percentages of ceria; effects depend on

H_2S concentration and the applied load. The ceria coating layer is a potential solution to reduce H_2S poisoning of MCFCs fuelled with biogas.

The research to obtain new advanced anode materials with high sulfur tolerance and effective recovery capability is largely discussed in literature [7, 17, 22]. Zaza et al. [18] studied the H_2S poisoning mechanisms of conventional nickel-based anode MCFCs in order to determine sulfur tolerant advanced anodes for MCFC fed with biogas. Proposed anode materials include two different categories: anodes made of an electrocatalyst and a hydrogen sulfide trap such as NiCr covered with either CeO_2 or CeO_2–ZrO_2; anodes made of a hydrogen sulfide resistance electrocatalyst such as NiAl.

5.2 Effect of SO_2 on Cathode and H_2S on Anode

Recently Rexed et al. [23] studied the effect of contamination of MCFC with low concentrations of both SO_2 at the cathode and H_2S at the anode. The poisoning mechanism of SO_2 is due to sulfur transfer through the electrolyte and formation of H_2S at the anode. Measurements were performed with SO_2 in the oxidant gas at concentrations up to 24 ppm, for short-term (90 min) and long-term (100 h) contaminant exposure. The poisoning effect of H_2S (up to 12 ppm) was studied for gas compositions with high and low concentrations of H_2 in fuel gas. Sulfur poisoning by SO_2 of MCFC has been considered as a result of anode exhaust gas recirculation to the anode. Any H_2S present in the exhaust gas will be oxidized to SO_2 (reaction 5.12) together with residual fuel in a catalytic burner before entering the cathode.

$$H_2S + 3/2\,O_2 \rightarrow H_2O + SO_2 \tag{5.12}$$

$$CO_3^{2-} + SO_2 + 1/2\,O_2 \rightarrow CO_2 + SO_4^{2-} \tag{5.13}$$

H_2S causes poisoning of the Ni-anode surface by formation of NiS which kinetically hinders the oxidation of hydrogen [3, 7, 18]. It may react chemically to form NiS (reaction 5.14), or electrochemically as sulfide in the electrolyte (reaction 5.15), with the nickel anode to form nickel sulfide.

$$xNi + yH_2S \rightarrow Ni_xS_y + yH_2 \tag{5.14}$$

$$xNi + yS^{2-} \rightarrow Ni_xS_y + 2xe \tag{5.15}$$

SO_2 added to the cathode immediately affects also the anode, indicating a transfer mechanism of sulfur from anode to cathode. It can be hypothesized that SO_2 dissolves into the electrolyte as sulfate ions which migrate to the cathode where are released as H_2S, causing the poisoning of the anode catalyst by interactions with nickel H_2S. Increased polarization of both anode and cathode was observe after longterm exposure to 8 ppm SO_2 at the cathode increasing at high current

density. The short-term tests show anode polarization for concentrations higher than 12 ppm SO_2 suggesting that the transfer mechanism of sulfur from the cathode to the anode is fast, although no detailed data on transfer kinetics are reported. The anode poisoning effects were largely reversible by regeneration with clean gas, however, the cathode evidenced irreversible polarization. The increase in cell resistance after long-term exposure was attributed to the cathode. This could be due to carbonate being replaced by sulfate by reaction with SO_2 dissolved in the electrolyte, or the formation of a layer at the electrode–current collector interface.

Ciccoli et al. [5] discuss the possibility of regeneration of the fuel cell.

In fact in the case of nickel transformation to nickel sulfide (reaction 5.10), passing pure gas over the poisoned anode can regenerate the electrochemically inert metal sulfide to the original, active catalyst:

The conditions and limits for the above reaction to be reversible are under investigation in and could provide a crucial, added operating parameter to guarantee long-term reliability of the MCFC stack. In this study [5], it is observed that, at different currents and concentrations of H_2S, the cell voltage drops can be partially recuperated. At higher degrees of poisoning and current load, the performance degradation is permanent.

Zaza et al. [18] reported that cell performances recovery levels depend on water vapor amounts in inlet anode gas. Irreversible poisoning effects are due to stable nickel sulfide formations, Ni_3S_2.

References

1. Cigolotti V, McPhail S, Moreno A, Yoon SP, Han JH, Nam SW, Lim T (2011) MCFC fed with biogas: experimental investigation of sulphur poisoning using impedance spectroscopy. Int J Hydrogen Energy 36:10311–10318
2. Hoffmann J (2005) Applications of molten carbonate fuel cells with biofuels. In: Lens P, Westermann P, Haberbauer M, Moreno A (eds) Cells biofuels for fuel. IWA Publishing, pp. 478–94
3. Vogel WM, Smith SW (1982) The effect of sulfur on the anodic H_2 (Ni) electrode in fused Li_2CO_3-K_2CO_3 at 650 °C. J Electrochem Soc 129(7):1441–1445
4. Cigolotti V, McPhail S, Moreno A (2009) Non-conventional fuels for high-temperature fuel cells: status and issue. ASME J Fuel Cell Sci Tech 6(2)
5. Ciccoli R, Cigolotti V, Lo Presti R, Massi E, McPhail S, Monteleone G et al (2010) Molten carbonate fuel cells fed with biogas: combating H_2S. Waste Manag 30(6):1018–1024
6. Sammells AF, Nicholson SB, Ang PGP (1980) Development of sulphur-tolerant components for the molten carbonate fuel cell. J Electrochem Soc 127(2):350–357
7. Devianto H, Yoon SP, Nam SW, Han J, Lim T-H (2006) The effect of ceria coating on the H_2S tolerance of a molten carbonate fuel cell. J Power Sources 159:1147–1152
8. Kawase M, Mugikura Y, Watanabe T (2000) The effects of H_2S on electrolyte distribution and cell performance in the molten carbonate fuel cell. J Elect Soc 147(4):1240–1244
9. Uchida, Ohuchi S, Nishina T (1994) Kinetic studies of the effects of H2S impurity on hydrogen oxidation in molten (Li + K)CO_3. J Elect Chem 369:161–168
10. Jablonski G, Hamm JR, Alvin MA, Wenglarz RA, Patel B (1982) Evaluation of Gasification and Gas Cleanup Process for Use in Molten Carbonate Fuel Cell Power Plants. Department of Energy, Morgantown Energy Technology Center, Report DOE/MC/16220-1306 (DE83003821)

11. Zaza F, Paoletti C, Lo Presti R, Simonetti E, Pasquali M (2008) Effects of hydrogen sulfide impurities on MCFC performance. In: Fundamentals and developments of fuel cells conference—FDFC2008, Nancy, France, 10–12 Dec 2008
12. Kawase M, Mugikura Y, Izaki Y, Watanabe T (1999) Effects of H_2S on the performance of MCFC. II. Behavior of sulfur in the cell. Electrochemistry 4:67
13. Weaver D, Winnik J (1989) Sulphuration of molten carbonate fuel cell anode. J Electrochem Soc 136(6):1679–1686
14. Townley D, Winnick J, Huang HS (1980) Mixed potential analysis of sulphuration of molten carbonate fuel cells. J Electrochem Soc 125(5):1104–1106
15. Marianowski LG, Anderson GL, Camara EH (1991) Use of sulphur containing fuel in molten carbonate fuel cells. United States Patent, No 5,071,718
16. Dong J, Cheng Z, Zha S, Liu M (2006) Identification of nickel sulphides on Ni-YSZ cermet exposed to H_2 fuel containing H_2S using Raman spectroscopy. J Power Sources 156:461–465
17. Gong M, Liu X, Trembly J, Johnson C (2007) Sulfur-tolerant anode materials for solid oxide fuel cell application. J Power Sources 168:289–298
18. Zaza F, Paoletti C, LoPresti R, Simonetti E, Pasquali M (2010) Studies on sulfur poisoning and development of advanced anodic materials for waste-to-energy fuel cells applications. J Power Sources 195:4043–4050
19. Watanabe T, Izaki Y, Mugikura Y, Morita H, Yoshikawa M, Kawase M et al (2006) Applicability of molten carbonate fuel cells to various fuels. J Power Sources 160:868–871
20. Hernandez S, Scarpa F, Fino D, Conti R (2011) Biogas purification for MCFC application. Int J Hydrogen Energy 36:8112–8118
21. Devianto H, Simonetti E, McPhail SJ, Zaza F, Cigolotti V, Paoletti C, Moreno A, La Barbera A, Luisetto I (2012) Electrochemical impedance study of the poisoning behaviour of Ni-based anodes at low concentrations of H_2S in an MCFC. Int J Hydrogen Energy 37:19312–19318
22. Cheng Z, Zha S, Liu M (2006) Stability of materials as candidates for sulfur-resistant anodes of solid oxide fuel cells. J Electrochem Soc 153(7):A1302–A1309
23. Rexed, Lagergren C, Lindbergh G (2014) Effect of sulfur contaminants on MCFC performance. Int J Hydrogen Energy 39:12242–12250

Chapter 6
The Effect of Biogas Impurities on SOFC

6.1 Introduction

Biogas contains several substances (Table 6.1) that have negative impact on the process converting the biogas into energy. So the biogas should be converted into biomethane stream having proper characteristics.

The treatment of biogas generally aims at: (1) a cleaning process, in which the trace components harmful to the natural gas grid, appliances, or end users are removed, (2) an upgrading process, in which CO_2 is removed to adjust the calorific value and relative density in order to meet the specifications of the Wobbe Index. This latter parameter is dependent on both the calorific value and the relative density [1, 2].

After transformation, the final product is referred to as 'biomethane', typically containing 95–97 % CH_4 and 1–3 % CO_2. Biomethane can be used as an alternative for natural gas. In general, the type of end use of the biogas sets its quality demands [3].

An interesting alternative to conventional technology can be based on SOFC due to their high biogas to electricity conversion efficiency (around 50–60 %). Conversely to thermal engines, SOFC can operate with diluted biogas, differently from while internal combustion engines (ICE) that cannot operate if the CH_4 content in biogas falls below 40–45 %. Essentially two main concerns come from direct biogas feeding in an SOFC: carbon deposition and the detrimental effects of contaminants on the Ni anode electrode [5–9]. Carbon deposition can be easily managed provided that a proper steam-to-carbon or oxygen ratio in guaranteed at the SOFC inlet so that C build up is thermodynamically unfeasible. Carbon deposition has been investigated by several authors [7, 10–13]. Memelstein et al. [10] reported that thermodynamic calculations do not indicate C deposition from a typical biomass gasification syngas at SOFCs operating temperatures >750 °C. However, intermediate temperatures <650 °C require threshold current densities

M. Turco et al., *Treatment of Biogas for Feeding High Temperature Fuel Cells*,
Green Energy and Technology, DOI 10.1007/978-3-319-03215-3_6

Table 6.1 Biogas impurities and their consequences [4]

Impurity	Possible impact
Water	Corrosion in compressors, gas storage tanks and engines due to reaction with H_2S, NH_3 and CO_2 to form acids
	Accumulation of water in pipes
	Condensation and/or freezing due to high pressure
Dust	Clogging due to deposition in compressors, gas storage tanks
H_2S	Corrosion in compressors, gas storage tanks and engines
	Toxic concentrations of H_2S ($>5 cm^3 m^{-3}$) remain in the biogas
	SO_2 and SO_3 are formed due to combustion, which are more toxic than H_2S and cause corrosion with water
CO_2	Low calorific value
Siloxanes	Formation of SiO_2 and microcrystalline quartz due to combustion; deposition at spark plugs, valves and cylinder heads abrading the surface
Hydrocarbons	Corrosion in engines due to combustion
NH_3	Corrosion when dissolved in water
O_2/air	Explosive mixtures due to high concentrations of O_2 in biogas
Cl^-	Corrosion in combustion engines
F^-	Corrosion in combustion engines

well above what is achievable to inhibit the effects of C deposition. Zheng et al. [11] observed that C deposition depends on temperature, gas composition, (CO or CH_4), and presence of $Ce_{0.8}Gd_{0.2}O_{1.9}$ electrolyte in the composite-type electrode. Stable fuel cell performance, without C deposition, was obtained for $SrFe_{0.75}Mo_{0.25}O_{3-\delta}$-based SOFC in 10 vol.% of CO in CO_2. Also for SOFC operating with CH_4 at temperatures $\leq$700 °C no coking was obtained. Singh et al. [12] reported thermodynamic analysis of the carbon deposition in a SOFC fueled by a biomass gasifier. The carbon deposition is shown to decrease with steam in the feed stream, while the amount of carbon first decreases and then increases with temperature. Gunji et al. [13] studied a SOFC using Ni/scandia-stabilized zirconia (Ni-ScSZ) anodes under internal reforming conditions. A single cell achieved a maximum power density of 0.64 W/cm^2 at 900 °C with a 97% CH_4/3% H_2O fuel. With this fuel composition the cell voltage during power generation at 0.5 A/cm^2 was stable at 900 °C for $\geq$150 h. However, under the same conditions degradation of anode performance and C deposition occurred at 800 °C.

The as produced biogas from AD contained several contaminants like as sulfur, aromatic, siloxane, and halogenated compounds that can in principle affect the SOFC performance and the electrode stability. Sulfur compounds are present in the range from tens to thousands of ppm(v) (sulfur) while halogens and siloxanes vary from 0.1 to 10 ppm(v). Sulfur compounds are generally the most abundant in biogas and decompose to H_2S at the SOFC operating temperature. Moreover H_2S is a well-known poison for Ni-based ceramic cells [6, 14]. Sulfur compounds decompose to H_2S at the SOFC operating temperature as shown from equilibrium thermodynamic calculation [5]. H_2S adsorbs on the Ni active sites preventing H_2

and CO oxidation as well as also methane reforming [15]. The effect of chlorine compounds, generally decomposed to HCl in the H_2 rich anode environment, is less understood than sulfur compounds. However, a deactivation mechanism similar to that of sulfur (dissociative chemisorption on the Ni surface) but less severe was generally observed [16]. Aromatic compounds are probably the less dangerous ones as they are catalytically converted to H_2 and CO within the SOFC. Siloxanes are instead the most critical ones for durability of the fuel cell. For instance a study by Ruokomaki et al. [17] showed how the siloxane compounds already affect the SOFC performance at 10 ppb(v) whereas chlorine compounds concentration above 5000 ppb(v) are required. Haga et al. [18] also showed how an amount of 10 ppm(v) of D5 in the H_2 feed quickly leaded to a cell failure.

6.2 Effect of Halogenated Compounds

Halogenated compounds lead to corrosion in delicate power plant components and measures have to be taken in order to keep low the concentrations [4]. In connection to SOFC the effect of chlorine gas are analyzed in several articles: experiments show that fuel gas containing 5 ppm of Cl does not cause cell degradation or voltage drop in the SOFC [19–21]. Blesznowski et al. [21] investigated the effect of HCl-contamined fuel gas and concluded that at 10 ppm a recoverable voltage drop is identified. When increasing concentration levels to 1000 ppm the cell voltage starts to decrease continuously at a rate of 9.4 % over 100 h.

Recently, Trembly et al. [22] have investigated the effect of HCl on the SOFC at 800 and 900 °C. The study has indicated that introduction of 20–160 ppm HCl leads to a performance loss of about 13–52 %. It was also shown that the cell performance loss at 800 °C is mostly associated with the increase in charge-transfer resistance whereas at 900 °C the performance losses are affected by increases in the ohmic resistance and charge-transfer resistance across the SOFC [22, 23].

In the chlorine poisoning, the reaction of Ni with chlorine is crucial to understand the poisoning mechanism. According to Haga et al. [18] the formation of $NiCl_2$ may be described by reaction (6.1):

$$Cl_2(g) + Ni(s) = Nicl_2(s\,or\,g) \tag{6.1}$$

Haga et al. [18] observed low but still measurable degradation in cell voltage for H_2-based fuels containing 5 ppm Cl_2, whereas fuels containing 100 ppm and 1000 ppm Cl_2 caused continuous degradation of cell voltage with an almost constant degradation rate. The degradation rates were 1.7 and 13 % per 100 h for H_2-based fuels containing 100 ppm and 1000 ppm Cl_2, respectively. In addition, significant microstructural change of cermet anode surfaces was confirmed by the FESEM observations.

Haga et al. [18] suggested that contrary to sulfur, chlorine can easily react with Ni: nickel chloride ($NiCl_2$) is stable even when only ca. 100 ppb and 10 ppm Cl_2 are contained in fuel gases at 800 °C and 1000 °C, respectively. Furthermore the

formation of $NiCl_2$ should be paid careful attention in durability of SOFC anodes, as the sublimation temperature of $NiCl_2$ is 985 °C, near the typical SOFC operational temperatures [18].

The interaction of Cl_2 with Ni was also proposed by Tjaden et al. [24] that suggested the subliming of $NiCl_2$ at Cl concentration >100 ppm. Low levels of halogens compounds typically observed in biogas are not dangerous for the SOFC system. However, halogen compounds have to be considered when applying adsorptive gas-cleaning methods: adsorption efficiency of active carbon decrease in the presence of halogenated and aromatic co-vapors. Absolute breakthrough times of various sulfur compounds decrease by up to 14 % when halogen containing co-vapors are added to the gas stream [25].

Poisoning effects by various fuel impurities, including H_2S, CH_3SH, COS, Cl_2, and siloxane, to Ni–ScSZ cermet anodes have been analyzed and compared by Haga et al. [18] with the aim to study the poisoning mechanisms for typical SOFC fuel impurities (sulfur compounds, chlorine, and siloxane).

Haga et al. [18] studied degradation of cell performance by measuring cell voltage and anode polarization at a constant current density of 0.2 Acm^{-2} for humidified H_2 and CH_4 fuels. Cell voltage was measured at a constant current density of 0.2 Acm^{-2}, at temperatures 800–1000 °C and, by changing the carrier gas from pure N_2 to impurity-containing N_2. Gradual and continuous degradation was verified in Cl_2 poisoning, associated with a microstrucutural change to form Ni precipitates in the Ni-Sc-SZ cermet anodes. Poisoning for hydrogen-based fuels containing 5 ppm sulfur compounds, H_2S, CH_3SH, and COS, caused an initial cell voltage drop of about 15 mV at 1000 °C. The initial voltage drop was independent of the kind of sulfur compounds, whereas in the case of poisoning by CH_3SH, an additional gradual decrease in cell voltage was clearly detected after the initial voltage drop. It is known that a few ppm levels of H_2S as well as sulfide-based odorants are typically contained in commercial natural gas [26], and thus the major impurity in SOFC anode poisoning may be H_2S so far [19, 27–32].

6.3 Effect of Sulfur Compounds on SOFC

Depending on its production source and the stage of the upgrading process biogas can contain a number of sulfur compounds that have the capability to corrode processing equipment and gas pipeline, to inhibit the performance of vehicle catalysts and to damage fuel cells..

It is widely recognized that sulfur compounds are the major poisons for fuel cell systems [28, 33–38] Most common reduced sulfur compounds found in biogas are H_2S and methylmercaptan (CH_3SH) Also ethylmercaptan, dimethyl sulfide (DMS) and dimethyldisulfide (DMDS) are found [39–41]. Brown et al. [40] reported as an example a study measuring sulfur-containing compounds in biogas from a plant in Linkoping, Sweden [42]: the biogas before upgrading contained hydrogen sulfide (at a volume fraction of up to 32.4 $\mu mL\ L^{-1}$) carbonyl

sulfide (1.2 μmL L^{-1}) methanethiol (up to 0.75 μmL L^{-1}) dimethyl sulfide (up to 9.2 μmL L^{-1}) carbon disulfide (up to 0.02 μmL L^{-1}), 2-propanethiol (up to 0.05 μmL L^{-1}) ethylmethyl sulfide (up to 1.2 μmL L^{-1}) diethyl sulfide (up to 0.58 μmL L^{-1}) and dimethyl disulfide (up to 1.0 μmL L^{-1}).

Typically H_2S content in biogas ranges 1000–20,000 ppm, while CH_3SH is normally present in trace levels of around 1–20 ppm, with maximum values reported around 100 ppm [43–45].

In terms of process performance impact Van de Bosch et al. [43] reported that CH_3SH severely inhibits biological sulfide oxidation (50 % reduction of the biological oxidation rate) at concentrations above 0.05 mM under natron-alkaline-aerobic conditions. Complete inhibition was found at CH_3SH of concentration of 0.65 nM. Thus, potential accumulation of CH_3SH in aerobic and anoxic biotrickling filters may hinder H_2S removal.

6.3.1 Levels of Sulfur-Containing Compounds in Biogas

The accurate quantification of low concentration of sulfur-containing compounds in gases is essential to ensure compliance with legislation in a number of industrial and environmental sectors. These measurements are very arduous due to the reactivity of such compounds [40]. The actual European Directives of promote the diversification gas supply [46, 47] and European Commission targets specify that 20 % of EC energy consumption should come from renewable sources by 2020 [48]. As a direct result of these drivers the European biogas industry has strongly increased starting from 2012, more than 20 Mtoe of biogas was produced in the European Union [49]. The key uses for biogas (as biomethane) are for the injection into natural gas network and for vehicle fuel [40].

CEN (The European Committee for Standardization) Technical Committee 408 (Natural gas and biomethane for injection in the natural gas grid) is currently working in response to the ECs Mandate M/475 [50] to develop specifications for the permissible levels of a range of compounds.

The concentrations of sulfur-containing compounds in biogas can vary substantially depending on the source of the gas, but mass concentrations of hydrogen sulfide as high as 7000 mg m^{-3} are possible [51]. However, typically hydrogen mass concentrations are <600 mg m^{-3} for biogas produced by anaerobic digestion and <100 mg m^{-3} for biogas from landfill [52]. Biogas is usually desulfurized whilst still in the bioreactor in order to avoid damage to downstream processing equipment [40].

The maximum gas concentrations of sulfur-containing compounds permissible in European countries [53] are shown in Table 6.2.

H_2S is the most stable sulfur compound under SOFC operational conditions and the equilibrium concentration of other sulfur compounds such as COS is relatively low [18].

Table 6.2 Maximum mass concentrations of sulfur-containing compounds specified in European gas transmission network [40]

Country	Maximum mass concentration mgm^{-3}		
	Total sulfur-containing compounds	Hydrogen sulfide	Thiols
Austria	100	5	15
Belgium	150	5*	15
France	30	5*	6
Germany	30	5	6
Italy	150	6.6	15.5
Netherland	45	5	–
Poland	40	7	16
Spain	50	15*	17
Sweden	23	10	–
Switzerland	10	5	–
United Kingdom	50	5	–

An Asterix (*) indicates the specification is for the sum of hydrogen sulfide and carbonyl sulfide; a dash (–) indicates that no specification exists [40]

Tjaden et al. [24] reported chemical equilibrium calculations showing that H_2S is the most stable sulfur compound at the operating temperature of SOFC [24, 33].

Sasaki et al. [33] reported equilibrium concentration of minor sulfur-based impurities in the fuel cell fuels in the temperature range 400–1000 °C. As sulfur-based impurities in the fuel cell gases, H_2S, elementary sulfur, inorganic sulfur compounds, mercaptans alkyl (di-)sulfides, thiophenes, and related compounds have been taken into account.

The authors considered various types of fuels including H_2, H_2-CO, CO, CH_4, biogas, LPG, gasoline kerosene, and diesel fuel. COS can also coexist, but even in CO riche gases and in hydrocarbon-based fuels COS concentration in equilibrium is one order of magnitude lower than H_2S concentration. Other sulfur compounds, such as CH_4S at intermediate temperatures and $HS_{(g)}$ and SO_2 at high temperature are also expected to coexist but their concentrations are less that 1 ppb assuming thermochemical equilibrium. As a solid carbon, only the graphite was taken into account for simplicity. Thermochemical calculations at 400–1000 °C clearly indicates that H_2S is the predominant sulfur species at the elevated temperatures the typical operational temperatures of fuel processors for low temperature fuel cells PEFC as well as of high temperature fuel cell such as SOFC.

As the poisoning by H_2S with a concentration less than approximatively 100 ppm, a typical sulfur concentration of practical fuel, is associated with an increase in anodic overvoltage: the tolerance concentration of sulfur can be determined by the tolerant cell voltage drop. Concentration of sulfur will also be limited by irreversible poisoning process such as oxidation of Ni to NiO and Ni sulfide in SOFC [26].

Initial cell voltage drop due to sulfur contamination is temperature dependent and decrease with increasing temperature [24, 54]. The extent and nature of cell degradation is dependent on applied cell materials and microstructural characteristics and thus the phenomenon of degradation cannot be generalized. It is assumed that any kind of sulfur compound has to be removed to a level <1 ppm to ensure long-term performance of the SOFC.

Haga et al. [18] studied the poisoning by sulfur compounds and observed that it occurs generally in the following way: cell voltage decreases rapidly after adding each impurity to fuel gas, followed by a quasi steady state with a constant cell voltage [19, 28]. In this study, the initial voltage drops by three types of sulfur impurities were compared under various conditions. Similar results are reported by Tjaden et al. [24] that concluded that long-term exposure to mercapatanes can be however, more critical than H_2S or COS contamination.

The initial voltage drops by CH_3SH and COS were almost identical to the initial voltage drop by H_2S. Initial voltage drops at a constant current density of 0.2 Acm^{-2} were approximately 80, 35, and 15 mV at 800, 900, and 1000 °C.

Degradation behavior by CH_3SH was different from that by H_2S, as cell voltage gradually decreased with time after operation beyond ca. 2 h.

Ni particles with the size of 50–70 nm^{Φ} were deposited on ScSZ surfaces in the anodes.

In a recent paper [55] SOFC cells with YSZ electrolyte and anodes of LaSrCrMn oxide (LSCrM perovskite) or LSCrM impregnated with Ni/CeO_2 are tested with H_2 fuel containing 50 ppm H_2S. Ni and CeO_2 particles with diameter of about 100 nm are distributed on the surface of LSCrM. XRD, XPS measurements showed that the anode poisoned with H_2S is covered by adsorbed sulfur, metal sulfides and sulfate radical. Sulfides are produced by the reaction of sulfur with the anode rather than the direct reaction between H_2S gas and anode. This seems to contradict previous studies on Ni/YSZ anodes [56], where absorbed sulfur is the sole poisoning product. According to thermodynamic analysis [14], the sulfide Ni_3S_2 can be formed only when H_2S concentration (in H_2) is higher than 3600 and 4700 ppm at 750 °C and 800 °C, respectively. Formation of other sulfides such as NiS and Ni_3S_4 need a higher equilibrium pressure of H_2S. However, Ni_3S_2 is detected on the anode with a low H_2S concentration of 50 ppm. The formation of sulfides can take place at a lower H_2S concentration through the reaction of absorbed sulfur with nickel considering the higher adsorption energy of S compared to H_2S on the anode surface, as confirmed by DFT calculations.

Thermodynamic calculations [57–59] were reported on the stability of nickel sulfides as a function of temperature, PO_2 (or $P(H_2)/P(H_2O)$), and H_2S content. At low H_2S conc. (~10 ppm), sulfides were not observed [60–62]. For higher (100 ppm) H_2S concentrations, nickel sulfides were generally observed [63–65]. Ni sulfide formed in H_2 containing 100 ppm H_2S at 727 °C [65] although it is not thermodynamically stable. Haga et al. [18] reported no formation of Ni sulfide under the condition with 5 ppm sulfur compounds.

These results outline the importance of in situ techniques to study the sulfidation process.

Thi et al. [57] studied the kinetics of the reactions between H_2S and Ni or Ni-CGO (ceria doped with gadolinium) by using Raman spectra in situ. Ni_3S_2 is formed at low temperature (200–500 °C) and remains stable at 800 °C while no Ni_3S_2 is formed on clean nickel at 800 °C. It is important to avoid contact of a working SOFC with H_2S during heating and cooling. Probably, the first step of Ni_3S_2 formation is adsorption of sulfur onto Ni that is fast at low temperature, but much more difficult at high temperature [66, 67]. At high temperature, a Ni_3S_2 film is formed at the surface of the Ni-CGO pellet, due to a diffusion of nickel toward the H_2S atmosphere. Moreover, H_2S reacts with the support CGO to produce $Ce_4O_5S_2$.

SOFC anodes Ni-gadolinium doped ceria (Ni/GDC) are studied for sulfur poisoning under operando conditions by Nurk et al. [62]. The molecular structure of sulfur species formed on the anodes in the temperature range 250–550 °C is studied by XANES (K shell). With H_2 fuel containing 5 ppm H_2S, several sulfur species in different oxidation states (6+ , 4+ , 0, −2) are detected: the species could either relate to $–SO_4^{2-}$ or SO_3 (g), $–SO_3^{2-}$ or SO_2 (g), S_2 (g) or surface-adsorbed S atoms, and Ni or Ce sulfides. These results do not agree with thermodynamic phase calculations, in particular the formation of sulfate species is not expected at the highest temperatures: this can be related to the difference between equilibrium conditions and the steady-state conditions in the fuel cell that are determined by kinetic-controlled processes.

Ni anodes exposed to H_2S undergo a reversible or partially reversible degradation for few minutes [39, 60, 68], followed by a slow non-reversible degradation [39, 60, 68]. It is generally accepted that the initial rapid decrease of performance is due to adsorption of sulfur species with inhibition of the three-phase-boundary (TPB) for hydrogen oxidation [39, 60]. On the other hand, different hypotheses have been proposed to explain the following slow degradation: (i) the formation of a volatile NixSy phase, leading to degradation of the electrode structure [56, 59, 69]; (ii) adsorption of sulfur on nickel particles that are in less accessible sites, such as pores with bottlenecks [69]; (iii) surface reconstruction of Ni that leads to catalytically less active form [69]; (iv) bulk phase diffusion of sulfur into Ni grains [69].

Nickel sulfide formation is reported with $H_2S > 2500$ ppm at 850 °C with 50 % H_2 fuel, and therefore, cannot explain the generally observed power degradation of SOFCs with few ppm H_2S: the sulfur poisoning of nickel-based anodes is generally explained by dissociative adsorption of H_2S on nickel [62]. Two stage poisoning of Ni/8YSZ (8 mol% Y_2O_3 doped ZrO_2) anodes was reported [39, 59, 71]. Singhal [71] found that at 1000 °C with constant current density, adding H_2S to the fuel, the cell voltage decreased rapidly (11.5 % with 10 ppm H_2S). A slow decrease of cell voltage (3.5 %) occurred in the following 100 h. The effect of H_2S was reversible. Sasaki et al. [39] also found a two phase poisoning with 5 ppm H_2S in 5 % H_2O/95 % H_2 fuel at 1000 °C. The cell voltage was almost recovered after removing H_2S. The poisoning was more severe and not reversible when the temperature was lowered to 850 °C. It was hypothesized that the chemisorption of sulfur caused a decrease of electrochemical sites thus increasing the anodic polarization.

Increasing pH_2S to 20 ppm led to increased chemisorption of sulfur on nickel and thus further increase in anodic polarization and cell voltage loss. However, no sulfur but NiO traces were found in the poisoned anode. Wang et al. [59] studied the effect of adding 2–50 ppm H_2S to a fuel containing 50 % H_2/1.5 %H_2O in N_2. The cell voltage dropped rapidly in the first minutes and slowly in the next 120 h. After removing H_2S, the cell voltage was recovered to 96 % in 50 h. The irreversible poisoning was explained with a microstructural change of the nickel surface. Fewer studies are reported on the poisoning of Ni/CGO (Gd_2O_3 doped CeO_2) anodes. Tests with syngas (34.8 % H_2/35.7 % N_2/40 % CO) containing 207 ppm H_2S at 850 °C showed a rapid drop of power of 6–8 % then a slow degradation up to 10–12.5 % (Trembly et al. [30]). The power recovered to 97 % after H_2S removal. After the tests the amount of nickel decreased and morphological change was observed. NiS formation was the proposed mechanism. Lohsoontorn et al. [61] reported that the performance of a Ni-CGO/YSZ/Ni-CGO symmetrical cell decreases with decreasing pH_2 (9.7–97 %), decreasing temperature (600–557 °C) and increasing pH_2S (1–3 ppm). The recovery of the cell after removal of H_2S increased with increasing pH_2. The performance loss was due to the increase of the resistance due to charge transfer. Zhang et al. [72] compared Ni/YSZ and Ni/10CGO anodes in the presence of H_2S (5–00 ppm in H_2) at 800 °C. The drop of cell voltage was much higher with Ni/YSZ than with Ni/CGO anode. The positive effect of CGO was attributed to its mixed ionic electronic conductivity. Ni surface of both anodes appeared rougher after contamination with H_2S but no sulfur was found with EDX. Smaller CGO particles were observed after the experiment.

In the work of Schubert et al. [70] Ni/YSZ and Ni/10CGO anodes are compared for the effect of H_2S, using an $H_2/H_2O/N_2$ fuel mixture at 850 °C. The degradation of cell voltage is noticeable even with 2 ppm H_2S. The cell with Ni/8YSZ anode showed two poisoning stages: the first stage occurred in few minutes while the following degradation was slower and lasted more than 10 h. The degradation of cell with Ni/10CGO occurred in one step and was slighter. The drop of performance cannot be explained by sulfide formation because it is not thermodynamically possible under these conditions. Dissociative H_2S adsorption on Ni is assumed on the base of DFT calculations (Eq. 6.2) [73]:

$$Ni_{(s)} + H_2S_{(g)} \rightarrow Ni - S_{(s)} + 2H_{(s)} \tag{6.2}$$

where the subscript (s) indicates species on the surface of metallic Ni. The heat of adsorption of H_2S on different forms of metallic Ni was found more favorable than the heat of formation of Ni sulfides [74, 75]. The authors propose a Temkin-like equation to describe the adsorption of H_2S and a mechanism of poisoning that explains the time progress of sulfur contamination of the Ni anode. On the basis of this mechanism, it is possible to calculate the nickel anode surface area from the duration of the first step of decrease of the cell voltage. The higher sulfur resistance of Ni/10CGO compared to Ni/YSZ is explained with the high mixed ionic electronic conductivity of the CGO phase and its ability to adsorb H_2.

SOFC degradation due to H_2S is studied by a mathematical modeling approach by Vahc et al. [76]. Electrolyte-supported and anode-supported SOFC are considered. Both contain five layers: anode gas diffusion layer (AGDL), anode active layer (ACL), electrolyte (ELEC), cathode active layer (CCL), and cathode gas diffusion layer (CGDL). The electrochemical reaction occurs at each active layers and the internal reforming reaction occurs only at AGDL. The model is based on a Temkin-like isotherm of sulfur adsorption. The sulfur coverage and cell polarization are related to the cell temperature, H_2S concentration, and electrochemical performance. Vahc et al. [76] concluded that the effect of sulfur poisoning on the internal reforming reaction is dominant over its impact on the electrochemical reaction.

References

1. Jurgensen L, Ehimen EA, Born J, Holm-Nielsen JB (2015) Dynamic biogas upgrading based on the Sabatier process: Thermodynamic and dynamic process simulation. Biores Technol 178:323–329
2. Hagen M, Polman E, Jensen J, Myken A, Jonsson O, Dahl A (2001) Adding gas from biomass to the gas grid. Swedish Gas Center, Malmö, Sweden, July 2001, Report SCG 118, p 144
3. Wellinger A, Lindberg A (2001) Biogas upgrading and utilisation. IEA Bioenergy Task 24: Energy from biological conversion of organic waste 24, pp 1–20
4. Ryckebosch E, Drouillon M, Vervaeren H (2011) Techniques for transformation of biogas to biomethane. Biomass Bioenergy 35:1633–1645
5. Papurello D, Lanzini A, Leone P, Santarelli M, Silvestri S (2014) Biogas from the organic fraction of municipal solid waste: dealing with contaminants for a solid oxide fuel cell energy generator. Waste Manag 34:2047–2056
6. Rasmussen JFB, Hagen A, Thyden K (2011) Durability of solid oxide fuel cells using sulfur containing fuels. J Power Sources 196:7271–7276
7. Lanzini A, Leone P (2010) Experimental investigation of direct internal reforming of biogas in solid oxide fuel cells. Int J Hydrogen Energy 35:2463–2476
8. Shiratori Y, Ijichi T, Oshima T, Sasaki K (2010) Internal reforming SOFC running on biogas. Int J Hydrogen Energy 35:7905–7912
9. Sasaki K, Haga K, Yoshizumi T, Minematsu D, Yuki E, Liu R, Uryu C, Oshima T, Ogura T, Shiratori Y, Ito K, Koyama M, Yokomoto K (2011) Chemical durability of solid oxide fuel cells: influence of impurities on long-term performance. J Power Sources 196:9130–9140
10. Mermelstein J, Millan M, Brandon NP (2011) The interaction of biomass gasification syngas components with tar in a solid oxide fuel cell and operational conditions to mitigate carbon deposition on nickel-gadolinium doped ceria anodes. J Power Sources 196:5027–5034
11. Zheng K, Swierczek K, Polfus JM, Sunding MF, Pishahang M, Norby T, Truls (2015) Carbon Deposition and Sulfur Poisoning in SrFe0.75Mo0.25O3-δ and SrFe0.5Mn0.25Mo0.25O3-δ Electrode Materials for Symmetrical SOFCs. J Electrochem Soc 162:F1078–F1087
12. Singh D, Hernandez-Pacheco E, Hutton PN, Patel N, Mann MD (2005) Carbon deposition in an SOFC fueled by tar-laden biomass gas: a thermodynamic analysis. J Power Sources 142:194–199
13. Gunji A, Wen C, Otomo J, Kobayashi T, Ukai K, Mizutani Y, Takahashi H (2004) Carbon deposition behaviour on Ni-ScSZ anodes for internal reforming solid oxide fuel cells. J Power Sources 131:285–288

14. Cheng Z, Wang JH, Choi Y, Yang L, Lin MC, Liu M (2011) From Ni–YSZ to sulfur-tolerant anode materials for SOFCs: electrochemical behavior, in situ characterization, modeling, and future perspectives. Energy Environ Sci 4:4380–4409
15. Rostrup-Nielsen JR, Hansen JB, Helveg S, Christiansen N, Jannasch AK (2006) Sites for catalysis and electrochemistry in solid oxide fuel cell (SOFC) anode. Appl Phys A Mater Sci Process 85:427–430
16. Bao J, Krishnan GN, Jayaweera P, Perez-Mariano J, Sanjurjo A (2009) Effect of various coal contaminants on the performance of solid oxide fuel cells: part I. Accelerated testing. J Power Sources 193:607–616
17. Ruokomäki J (2009) Biogas criteria for SOFC. Product Centre Ecotech. Wärtsilä. http://www.vtt.fi/inf/pdf/tiedotteet/2009/T2496.pdf. Accessed 07 July 2013
18. Haga K, Adachi S, Shiratori Y, Itoh K, Sasaki K (2008) Poisoning of SOFC anodes by various fuel impurities. Solid State Ionics 179:1427–1431
19. Sasaki K, Adachi S, Haga K, Uchikawa M, Yamamoto J, Iyoshi A, Chou J, Shiratori Y, Ito K (2007) Fuel impurity tolerance of solid oxide fuel cells. ECS Trans 7:1675–1683
20. Arnold M (2009) Reduction and monitoring of biogas trace compounds. VTT Research Notes 2496; VTT Technical Research Centre of Finland: Espoo, Finland
21. Błesznowski M, Jewulski J, Zieleniak A (2013) Determination of H_2S and HCl concentration limits in the fuel for anode supported SOFC operation. Cent Eur J Chem 11:960–967
22. Trembly JP, Gemmen RS, Bayless DJ (2007) The effect of coal syngas containing HCl on the performance of solid oxide fuel cells: investigations into the effect of operational temperature and HCl concentration. J Power Sources 169:347–354
23. Cayana FN, Zhia M, Pakalapatia SR, Celika I, Wua N, Gemmenb R (2008) Effects of coal syngas impurities on anodes of solid oxide fuel cells. J Power Sources 185:595–602
24. Tjaden B, Gandiglio M, Lanzini A, Santarelli M, Jarvinen M (2014) Small-scale biogas-SOFC plant: technical analysis and assessment of different fuel reforming options. Energy Fuels 28:4216–4232
25. Papurello D, Schuhfried E, Lanzini A, Romano A, Cappellin L, Mark T, Silvestri S, Biasioli F (2014) Influence of co-vapors on biogas filtration for fuel cells monitored with PTR-MS (Proton Transfer Reaction-Mass Spectrometry). Fuel Process Technol 118:133–140
26. Larminie J, Dicks A (2003) Fuel cell systems explained, 2nd edn. John Wiley & Sons Ltd., England
27. Matsuzaki Y, Yasuda I (2000) The poisoning effect of sulfur-containing impurity gas on a SOFC anode: Part I. Dependence on temperature, time, and impurity concentration. Solid State Ion. 132:261–269
28. Riegraf M, Schiller G, Costa R, Friedrich KA, Latz A, Yurkiv V (2015) Elementary kinetic numerical simulation of Ni/YSZ SOFC anode performance considering sulfur poisoning. J Electrochem Soc 162:F65–F75
29. Aguilar L, Zha S, Li S, Winnick J, Liu M (2004) A solid oxide fuel cell operating on hydrogen sulfide (H2S) and sulfur-containing fuels. J Power Sources 135:17–24
30. Trembly JP, Marquez AI, Ohrn TR, Bayless DJ (2006) Effects of coal syngas and H_2S on the performance of solid oxide fuel cells: single-cell tests. J Power Sources 158:263–273
31. Sasaki K, Teraoka Y (2003) equilibria in fuel cell gases. J Electrochem Soc 150(11):A885–A888
32. Jess A (1996) Catalytic upgrading of tarry fuel gases: A kinetic study with model components. Chem Eng Process 35:487–494
33. Sasaki K (2008) Thermochemical stability of sulfur compounds in fuel cell gases related to fuel impurity poisoning. J Fuel Cell Sci Technol 5, 031212-1/031212-8
34. Lima da Silva A, Heck NC (2015) Thermodynamics of sulfur poisoning in solid oxide fuel cells revisited: the effect of H_2S concentration, temperature, current density and fuel utilization. J Power Sources 296:92–101
35. Sapountzi FM, Tsampas MN, Zhao C, Boreave A, Retailleau L, Montinaro D, Vernoux P (2015) Triode operation for enhancing the performance of H2S-poisoned SOFCs operated under CH_4-H_2O mixtures. Solid State Ionics 277:65–71

36. Hagen A, Johnson GB, Hjalmarsson P (2014) Electrochemical evaluation of sulfur poisoning in a methane-fuelled solid oxide fuel cell: Effect of current density and sulfur concentration. J Power Sources 272:776–785
37. Ma J, Jiang C, Connor PA, Cassidy M, Irvine JTS (2015) Highly efficient, coking-resistant SOFCs for energy conversion using biogas fuels. J Mater Chemist A: Mater Energy Sustain 3:19068–19076
38. Escudero MJ, Gomez de Parada I, Fuerte A (2015) Performance evaluation of WNi-CeO_2 as anode in a solid oxide fuel cell fed by simulated biogas mixtures. Int J Hydrogen Energy 40:11303–11314
39. Sasaki K, Susuki K, Iyoshi A, Uchimura M, Imamura N, Kusaba H, Teraoka Y, Fuchino H, Tsujimoto K, Uchida Y, Jingo N (2006) H_2S poisoning of solid oxide fuel cells. J Electrochem Soc 153:A2023–A2029
40. Brown AS, van der Veen AMH, Arrhenius K, Murugan A, Culleton LP, Ziel PR, Li J (2015) Sampling of gaseous sulfur-containing compounds at low concentrations with a review of best-practice methods for biogas and natural gas applications. Trends Anal Chem 64:42–52
41. Montebello AM, Fernández M, Almenglo F, Ramírez M, Cantero D, Baeza M, Gabriel D (2012) Simultaneous methylmercaptan and hydrogen sulfide removal in the desulfurization of biogas in aerobic and anoxic biotrickling filters. Chem Eng J 200–202:237–246
42. Anderson FAT, Karlsson A, Svensson BH, Ejlertsson J (2004) Occurrence and abatement of volatile sulphur compounds during biogas production. J Air Waste Manag Assoc 54:855–861
43. van den Bosch PLF, de Graaff M, Fortuny-Picornell M, van Leerdam RC, Janssen AJH (2009) Inhibition of microbiological sulfide oxidation by methanethiol and dimethyl polysulfides at natron-alkaline conditions. Appl Microbiol Biotechnol 83:579–587
44. Parker T, Dottridge J, Kelly S (2002) Investigation of the composition and emissions of trace components in landfill gas, R&D Technical Report P1-438/TR Environment Agency, Bristol, UK
45. Deublein D, Steinhauser A (2008) Biogas from waste and renewable resources. Wiley-VCH Verlag GmbH & Co. KGaA, Weinheim
46. Directive 2009/28/EC on the promotion of the use of energy from renewable sources (2009). Off J Eur Union L140:16–62
47. Directive 2003/55/EC concerning the common rules for the internal market in natural gas (2003). Off J Eur Union L176:57–78
48. COM (2010) 639 Energy 2020: a strategy for competitive sustenaible and secure energy, European Commission, Bruxelles
49. Biomass barometer ObservER (2012). http://www.eurobserv-er.org/pdf/baro212.pdf. Accessed 08 February 2014
50. European Commission Mandate M/475, Mandate to CEN for standard for biomethane for use in transport and injection in natural gas pipeline (2010)
51. Deublein D, Steinhhauser A (2011) Biogas from waste and renewable resources, 2nd edn. Wiley-VCH Verlag, Weinheim (2011)
52. Injection of gases from non-conventional sources into gas networks, Marcogaz report D497 (2006)
53. Gas quality harmonisation: cost benefit analysis, GL Noble Denton and Poyry Management Consulting (2012)
54. Haga K, Adachi S, Shiratori Y, Ito K, Sasaki K (2008) Poisoning of SOFC anodes by various fuel impurities. In: Solid State Ionics 16: Proceedings of the 16th International Conference on Solid State Ionics (SSI-16), Part II, vol 179, pp 1427–1431. Shanghai, China, July 1−6 2008
55. Li Y, Zhang Y, Zhu X, Wang Z, Lü Z, Huang X, Zhou Y, Zhu L, Jiang W (2015) Performance and sulfur poisoning of Ni/CeO2 impregnated La0.75Sr0.25Cr0.5Mn0.5O3-δ anode in solid oxide fuel cells. J Power Sources 285:354–359
56. Cheng Z, Liu M (2007) Characterization of sulfur poisoning of Ni-YSZ anodes for solid oxide fuel cells using in situ Raman microspectroscopy. Solid State Ionics 178:925–935

57. Thi HHM, Saubat B, Sergent N, Pagnier T (2015) In situ Raman and optical characterization of H_2S reaction with Ni-based anodes for SOFCs. Solid State Ionics 272:84–90
58. Lohsoontorn P, Brett DJL, Brandon NP (2008) Thermodynamic predictions of the impact of fuel composition on the propensity of sulphur to interact with Ni and ceria-based anodes for solid oxide fuel cells. J Power Sources 175:60–67
59. Wang J-H, Liu M (2007) Computational study of sulfur-nickel interactions: A new S-Ni phase diagram. Electrochem Commun 9:2212–2217
60. Zha S, Cheng Z, Liu M (2007) Sulfur poisoning and regeneration of Ni-based anodes in solid oxide fuel cells. J Electrochem Soc 154:B201–B206
61. Lohsoontorn P, Brett DJL, Brandon NP (2008) The effect of fuel composition and temperature on the interaction of H_2S with nickel-ceria anodes for solid oxide fuel cells. J Power Sources 183:232–239
62. Nurk G, Huthwelker T, Braun A, Ludwig C, Lust E, Struis RPWJ (2013) Redox dynamics of sulphur with Ni/GDC anode during SOFC operation at mid- and low-range temperatures: an operando S K-edge XANES study. J Power Sources 240:448–457
63. Harris WM, Lombardo JJ, Nelson GJ, Lai B, Wang S, Vila-Comamala J, Liu M, Liu M, Chiu WKS (2014) Three-dimensional microstructural imaging of sulfur poisoning-induced degradation in a Ni-YSZ anode of solid oxide fuel cells. Sci Rep 4:5246
64. Lussier A, Sofie S, Dvorak J, Idzerda YU (2008) Mechanism for SOFC anode degradation from hydrogen sulfide exposure. Int J Hydrog Energy 33:3945–3951
65. Dong J, Cheng Z, Zha S, Liu M (2006) Identification of nickel sulfides on Ni-YSZ cermet exposed to H_2 fuel containing H_2S using Raman spectroscopy. J Power Sources 156:461–465
66. Monder DS, Karan K (2010) Ab initio adsorption thermodynamics of H2S and H2 on Ni(111). The importance of thermal corrections and multiple reaction equilibria. J Phys Chem C 114:22597–22602
67. Bartholomew CH, Agrawal PK, Katzer JR (1982) Sulfur poisoning of metals. Adv Catal 31:135–242
68. Kurokawa H, Sholklapper TZ, Jacobson CP, Jonghe LCD, Visco SJ (2007) Ceria nanocoating for sulfur tolerant Ni-based anodes of solid oxide fuel cells. Electrochem Solid-State Lett 10:B135–B138
69. Siriwardane RV, Poston JA Jr, Fisher EP (2005) Interaction of hydrogen sulfide with Zr0.92Y0.08O2-δ/40 % Ni cermet. Appl Surf Sci 243:40–54
70. Schubert SK, Kusnezoff M, Michaelis A, Bredikhin SI (2012) Comparison of the performances of single cell solid oxide fuel cell stacks with Ni/8YSZ and Ni/10CGO anodes with H_2S containing fuel. J Power Sources 217:364–372
71. Singhal SC, Ruka RJ, Bauerle JE, Sprengler CJ (1986) US Department of Energy Report No. DOE/MC/22046-237 I, Washington D.C
72. Zhang L, Jiang SP, He HQ, Chen X, Ma J, Song XC (2010) A comparative study of H_2S poisoning on electrode behavior of Ni/YSZ and Ni/GDC anodes of solid oxide fuel cells. Int J Hydrog Energy 35:12359–12368
73. Choi YM, Compson C, Lin MC, Liu ML (2006) A mechanistic study of H2S decomposition on Ni- and Cu-based anode surfaces in a solid oxide fuel cell. Chem Phys Lett 421:179–183
74. McCarty JG, Wise H (1980) Thermodynamics of sulfur chemisorption on metals. I. Alumina-supported nickel. J Chem Phys 72:6332–6337
75. Oliphant JL, Fowler RW, Pannell RB, Bartholomew CH (1978) Chemisorption of hydrogen sulfide on nickel and ruthenium catalysts: I. Desorption isotherms. J Catal 51:229–242
76. Vahc ZY, Jung CY, Yi SC (2014) Performance degradation of solid oxide fuel cells due to sulfur poisoning of the electrochemical reaction and internal reforming reaction. Int J Hydrogen Energy 39:17275–17283

Chapter 7
The Effects of Siloxanes on High-Temperature Fuel Cells

7.1 Siloxanes in Biogas

The second largest family of biogas contaminants is volatile organic silicon compounds, namely silanes and siloxanes [1].

Siloxanes are a group of components that contain a Si-O bond and organic radicals (methyl, ethyl, and other organic groups) bound to the silicon atom. Siloxanes are used in cosmetics, pharmaceuticals as antifoam products and have useful properties like high compressibility, low flammability, low surface tension and water repelling properties, high thermal stability, low toxicity (nonallergenic), and biodegradability [2, 3].

Siloxanes are a class of compounds formed by linear or closed chains of functional groups $(R_2SiO)_n$ where R is either a hydrogen or alkyl group.

Cyclic siloxanes are designed with the letter D, whereas the linear compounds are designated with the letter L. The number following the letter refers to the quantity of Si atoms in the molecules [4].

The linear species L2-L5 and cyclic species D3-D6 are the most commonly found in biogases in significant concentrations (1–400 mg m^{-3}) [5, 6].

The total volatile siloxanes content and their relative volumetric percentage in biogas vary largely depending on biogas origin: as they are largely used mainly in cosmetics and detergent products their content is extremely low in biogas from agricultural wastes whilst biogas deriving from human activities can contain siloxane contents as large as 3–25 mg/m^3 (0.6 ppm).

Sigot et al. [7] reported typical total volatile organic silicon compounds (VOSiCs) including siloxane concentrations in the 0–60 mg/Nm^3 [8] but higher concentrations up to 400 mg/Nm^3 have also been measured [9–13]. VOCSiCs are suspected to come either from direct volatilization of low molecular weight siloxanes [14] or from chemical and/or biological degradation of higher molecular weight silicones [15, 16].

M. Turco et al., *Treatment of Biogas for Feeding High Temperature Fuel Cells*,
Green Energy and Technology, DOI 10.1007/978-3-319-03215-3_7

Cyclic siloxanes, octamethyltetrasiloxane (D4) and decamethylcyclopentasiloxane (D5), are the most common compounds in waste treatment plants (WWTP), D4 and hexamethyildisiloxane (L2) in landfills [1, 12, 17, 18].

For waster and landfills the majority of the siloxane compounds are in the D4 (61 %) and D5 (24 %) category, total siloxane ranged from 5.03 to 9.91 mg/m^3.

Wheless and Gary [19] reported siloxanes in digester for 15 different sites with an average of 27.7 mg/m^3 and a range from 3.8 to 122 mg/m^3 for categories D4 and D5. In comparison the results for landfills indicate a mean value 4.1 mg/m^3 and a range from 1.6 to 6.23 mg/m^3 for D4 and D5. This indicates that digester gas tends to have significantly higher siloxane concentrations than landfilll biogas.

Siloxanes in the biogas from WWTPs originate from the sewage sludge digestion, where soaps and other silicon-based cosmetics are contained. Their concentration in biogases has been reported to be in the range of 2–30 mg/Nm^3 [20] and 4–80 mg/Nm^3 [21] according to site and season variability. Other studies report average concentrations between 30 and 50 mg/Nm^3 with peaks up to 400 mg/Nm^3 [22, 23]. On the other hand, Vesterager and Matthiesen [24] report that the general concentration range lies typically below 10 mg/Nm^3 and that the higher values reported in literature concern sites facing troubles with biogas trace compounds. In particular, cyclic siloxanes (D3, D4, D5, etc.) have been reported to be in larger concentrations in WWTP biogas streams.

The sources of volatile methylsiloxanes (VMSs) and poly dimethylsiloxanes (PDMSs) in biogas are largely increasing [25]. For example, VMS solvents have importance because they are aroma free, are available from natural sources and are not covered in the VOC regulations.

The VMSs are representing replacements for solvents such as 111-TCA. Other uses for VMSs are as carrying agents in applications such as skin cream and stick deodorants [26]. Volatile methylsiloxanes are also common components in products such as shampoo, cosmetics, detergents, pharmaceutics, ink, lubricants, and adhesives. To put the magnitude in context a solid antiperspirant may contain 50 % siloxanes. In industrial applications siloxanes are the basic building blocks of silicones used as universal sealant. Polydimethylsiloxanes are used to lubricate hypodermic needles and to coat bottle stoppers and room temperature vulcanizing silicones are used for other medical and pharmaceutical equipments.

As a consequence of these and further uses the growth in the use of VMSs and PDMs over that last 15 years has been dramatic and is resulting in the presence of siloxanes in both wastewater and landfills wastes. In WWTP hydrophobic siloxanes [27, 28] accumulate in the sewage sludge and given the anaerobic conditions and high temperatures in the digesters (mesophilic digesters in the range 30–38 °C and thermophilic digesters in the 45–60 °C range) generate biogases containing siloxanes. Similarly, siloxanes are contained in the refuse placed in the landfills and subsequently with the anaerobic conditions and relatively high temperatures (approximatively 25 °C) in landfilled refuse also generate biogases containing siloxanes.

Table 7.1 [25] summarizes the chemical properties of the more prevalent siloxane compounds.

Table 7.1 Chemical properties of the siloxane compounds mainly present in biogas [25]

Siloxane compound	Abbreviation	Molecular weight (g/mol)	Boiling point (°C)	Melting point (°C)	Vapor pressure at 25°C (kPa)
Hexamethylcyclotrisiloxane $C_{12}H_{18}O_3Si_3$	D3	222.46	134	65	1.14
					1.83
Octamethylcyclotetrasiloxane $C_8H_{24}O_4Si_4$	D4	296.61	175	17.4	0.13
					0.17
Decamethylcyclopentasiloxane $C_{10}H_{30}O_5Si_5$	D5	370.77	210	−44	0.05
					0.02
Dodecamethylcyclohexasiloxane $C_{12}H_{36}O_6Si_6$	D6	445.00	245	−3	0.003
Hexamethyldisiloxane $C_6H_{18}Si_2O$	L2	162.40	100	−67	4.12
Octamethyltrisiloxane $C_8H_{24}Si_3O_2$	L3	236.50	153	−82	0.52
Decamethyltetrasiloxane $C_{10}H_{30}Si_4O_3$	L4	310.70	194	−68	0.073
Dodecamethylpentasiloxane $C_{12}H_{36}Si_5O_4$	L5	384.80	230	−81	0.009
Benzene		78.11	80.1	5.5	0.12

It is well evident that siloxane compounds have higher vapor pressure at temperatures typical of biogas in digesters and in many landfills. Because they have relatively high vapor pressures and low water solubilities they also have high Henry's law constants [26]. For example, siloxane compound D4 has an Henry's law constants in the range 3–17 that are values very high for a chemical compound with a molecular weight of 296.6 mg/mol. This indicates D4 has a strong tendency to volatilize to air [29] and hence into biogas from wastewater and landfills. The high molecular weight siloxanes volatilize and thus are transported in the biogas because of the low water solubility (in the ppb range) [25].

A large number of siloxanes are found in trace in biogas. Siloxanes, which mostly arise from hydrolysis of polydimethylsiloxanes [8, 17], represent troublesome impurities for biogas upgrading equipments [3, 9, 10, 12, 14, 30, 31].

The major issue for utilization of biogases is that the high molecular weight volatile forms convert during combustion to silica and form amorphous silica ash [7, 32, 33]. Crystalline SiO_2 produced from the oxidation of siloxanes during combustion represent the so-called "sand in the transmission" [12, 25, 34].

Several studies have been carried out on the poisoning by siloxanes in the fields of gas turbines and gas engines [14, 17, 35–37]. Microcrystalline silica, a very firm substance which has similar properties to that of glass coats and grazes metal surfaces, e.g., the spark plugs, cylinders, valves, and emission catalyst with white deposits and acts as a thermal insulator.

Engine manufacturers claim maximum limits of siloxanes in biogas, ranging from 0.03 mg m^{-3} (Capstone Microturbines) to 28 mg m^{-3} (Caterpillar) [2, 6].

No extensive studies are reported on the effect of siloxanes on MCFC.

Siloxanes also have a poisoning effect on SOFCs performances. Segregated silica can deposit in porous cermet anodes [7, 38, 39], also on steam reforming catalysts and FC anodes, causing their silication and consequent deactivation. [17]. Moreover it also affects many other components of the fuel cell system, such as heat exchangers, catalysts, and sensors [3, 40].

For these reasons siloxane removal is highly recommended [7]. It has been recognized that the presence of siloxane needs to be kept below 1 ppm in order to avoid damages [12].

They however are considered as the most difficult contaminants to remove from biogas [14, 15, 38, 41–43]. And the presence of siloxanes makes also more complex the issue of purification of biogases from sulfide and halide compounds [17] due to competitive adsorption of different biogas contaminants [42]. For instance, the adsorption of the different compounds follows the ranking: water > aromatics > siloxanes > halocarbons, halocarbons. Finally, other gas trace compounds (i.e., linear, aromatic, and halogenated hydrocarbons), typically found in waste-derived fuels, are also known to cause detrimental effects in the fuel cell catalysts [3, 44, 45].

7.2 Effect of Siloxanes on SOFC

Siloxane impurities can reach downstream SOFCs and could cause degradation of cell performance. In general, degradation mechanisms can be classified as intrinsically or extrinsically sourced [42, 46, 47]. Intrinsically sourced degradation occurs because of microstructure coarsening, impurities in raw materials, etc. The initial degradation was assumed as intrinsic due to the grain growth of Ni particles [5]. Extrinsically sourced degradation occurs when a foreign or unexpected material is introduced into the cell to induce degradation. Extrinsic type degradations are also all conditions inducing Ni redox cycles, carbon formation, or secondary phase formation.

It must be taken into account that silica contamination in the SOFC does not only originate from a contamination of the fuel stream but silicon compounds can be also contained in the water used for the steam reformer upstream of the SOFC or can derive from stack sealants.

Madi et al. [42] report the study of the impact of silica contamination on the performance of SOFC Ni anodes. Haga et al. [48] observed the effect of feeding 10 ppm of D5 on a Ni anode showing how the SOFC performance is rapidly falling (within hours). The analysis revealed the plugging of the anode structure with SiO_2 deposits [47]. They concluded that the presence of siloxane can cause

deposition-type degradation, associated with the formation of SiO_2(s) according to the following reactions:

$$[(CH3)_2SiO]_5 + 25H_2O = 5Si(OH)4 + 10CO + 30H_2 \quad (7.1)$$

$$Si(OH)_4 = SiO_2 + 2\,H_2O \quad (7.2)$$

In this paper [42] the software Factsage® was employed to calculate the thermochemical equilibrium decomposition of siloxanes at the SOFC operating temperature of 700 °C. In particular, the equilibrium phase diagram for the quaternary system Ni-Si-O-H was calculated showing the probable formation of solid Ni-Si solution. However, the presence of solid Ni-Si phases has not been reported in the literature [42]. Instead, silica deposition was widely observed on the blades of microturbines fed with biogas rich in organic silicon compounds [21] and operating with inlet temperature quite similar to the operating one of an SOFC stack. The study of Hauch et al. [49] reports on the degradation phenomena involving the segregation of silicates at the anode three-phase boundary during electrolysis operation. They observed that the raw materials used in the anode manufacturing processes and the albite ($NaAlSi_3O_8$) glass sealant can cause Si contamination. The sealant was responsible for the initial passivation of the tested cell, caused by the formation of glassy phase from gaseous $Si(OH)_4$ evaporated from the sealant silicates that can precipitate at the triple phase boundaries in the Ni/YSZ electrode.

Madi et al. [42] also investigated the effect of D4 (octamethylcyclotetrasiloxane) siloxane (at ppb(v) level) on the performance of the SOFC Ni anode. The mechanism of Ni anode degradation was hypothesized. The study was extended to the cell stack. A commercial Ni-YSZ anode-supported SOFC, with the active area of 12.5 cm^2 (TOPSOE Fuel Cell) was used. The cell was heated from room temperature to 800 °C at a rate of 100 °C/h.

SOFC stacks consisting of a series of 11 cells each were used for the experiments. All the stacks were provided by TOPSOE Fuel Cell (Denmark). Anode-supported type cells with a Ni anode are used in these stacks.

Upon the introduction of 1 ppm D4 at 495 h, the cell voltage started to decrease gradually from 0.785 V with an average degradation rate of 0.25 mV h^{-1} at constant current density of 0.25 A/cm^2. At 2 and 3 ppm D4, the cell performance strongly decreased with an average degradation rate of 0.34 mV h^{-1} and 0.39 mV h^{-1}, respectively.

The effect of D4 was tested on a single cell that was exposed to siloxane concentrations in the range of 0.1–2 ppm. A marked degradation was observed, and a partial performance recovery was observed when feeding clean gas at the end of the experiment.

The effect of D4-siloxane on the stack performance was studied by varying the D4 concentration from 69 ppb (v) up to 1.0 ppm(v) and strong voltage degradation even at the lowest concentrations was observed. The effect of the contaminant starts immediately suggesting the poisoning of the electrochemically active

sites rather than the pore blocking. A voltage degradation (~5 % per 1000 h) is observed with 69 ppb(v) of D4 and at 1 ppm(v) the degradation rate is as high as 32 % per 1000 h. The degradation rate of the stack was comparable to that of the single cell, for the same concentration of D4 (1 ppm), a consistent degradation rate results.

The authors concluded that cell degradation is caused by Si deposition on the anode support down to the electrolyte interface at the three phase boundary.

Madi et al. [42] hypothesized that the deposition took place due to the decomposition of the siloxane as given by Eqs. (7.3) and (7.4), where it is converted into SiO_2(s)

$$[(CH_3)_2SiO]_5(g) + 25H_2O = 5\,Si(OH)_4(g) + 10CO + 30H_2 \tag{7.3}$$

$$Si(OH)_4(g) = SiO_2(s) + 2H_2O \tag{7.4}$$

According to the proposed degradation mechanism, the siloxane is fast decomposed to SiO_2 as it reaches the fuel cell anode chamber, thus depositing silica both on the interconnect and anode current collector. Some Si remains in the vapor phase as $Si(OH)_4$ that further diffuses to the triple phase boundary (TPB) region where it can precipitates too.

Haga et al. [48] studied the influence of $[SiO(CH_3)_2]_5$ (decamethylcyclopentasiloxane: D5), the major siloxane species in a digester gas, on electrochemical activity of SOFC anodes by measuring cell voltages and anodic polarizations as a function of operational temperature.

They observed that cell voltages decrease in the presence of 10 ppm siloxane (D5) in 3 %-humidified H_2 at 800, 900, and 1000 °C. Poisoning by siloxane for 30–50 h resulted in a fatal degradation of cell performance. This degradation is associated with the formation of SiO_2 (s) in porous cermet anodes.

The formation of SiO_2 (s) under SOFC operational conditions may be described by reactions (7.5) and (7.6):

$$[(CH_3)_2SiO]_5(g) + 25H_2O \rightarrow 5\,Si(OH)_4(g) + 10CO + 30H_2 \tag{7.5}$$

$$Si(OH)_4(g) \rightarrow SiO_2(s) + 2\,H_2O \tag{7.6}$$

Silica precipitation may cause a decrease in the active TPB areas, simultaneously leading to an increase in nonohmic anodic polarization and in ohmic loss on the anode side.

7.3 Siloxanes Removal Techniques

Several techniques have been developed, also at the industrial level [6, 41, 42, 50–52] to purify biogases from siloxanes, such as condensation, absorption in liquids, adsorption on solids at room temperature and decomposition [39, 53, 54] (Table 7.2 [6]) or combination of refrigeration and adsorption on active carbons [25].

Table 7.2 Techniques for removing siloxanes in biogas [6]

Method	Advantages	Disadvantages
Absorption with organic solvents	High removal efficiency (97 %)	Complete removal not possible
Absorption in strong acid	High removal efficiency (<95 %)	Corrosion
		Environmental issues
		Hazardous chemicals
Absorption in strong base	n.da	Corrosion
		$CO3^{2-}$ precipitation
		Hazardous chemicals
Adsorption on silica gel	High removal efficiency (<95 %)	High pressure needed
	Higher removal capacity versus activated carbon (50 % extra)	Moisture decreases efficiency
	Regeneration possible (95 % desorption at 250 °C)	
Adsorption on activated carbon	High removal efficiency (95 %)	Moisture decreases removal efficiency
	Regeneration possible (desorption < desorption with silica gel at 250 °C)	High pressure needed (higher adsorption capacity)
Cryogenic separation	High removal efficiency (99.3 % at −70 °C)	Expensive investment and operation (high pressure and low temperature)
	Removal of several impurities	

Siloxanes can be removed by physical absorption with long carbon chain organic solvents in a spraying device or a packed column. A complete removal of siloxanes is difficult to obtain because siloxanes are highly volatile and they are stripped from the solvent at elevated gas flow rates. This problem does not arise when siloxanes are absorbed chemically, since they are converted to components of low volatility.

Both cyclic and linear siloxanes are stable against chemical and biochemical degradation. Strong bases and acids catalyze the cleavage of Si-O bonds. However, strong bases cannot be used because large amounts of precipitated carbonates are formed due to the high content of CO_2 in biogas.

The practical application of acids as absorbent must be evaluated with care because of the corrosive potential and the potential risk to health and environment [41]. Cryogenic separation of siloxanes is also a possibility. Hagman et al. [55] reported removal efficiency of 25.9 % when cooled to −25 °C and of 99.3 % when frozen to −70 °C.

High temperature treatment with solids, such as alumina [17, 53] allows complete siloxane removal [52, 56]. This technique can be applied to treat biogases prior to steam reforming and/or to utilization with high-temperature fuel cells [54], heat produced by the fuel cell being used to preheat the landfill gas. Biological removal or deep chilling are also recently proposed [12], but at present are still a challenge [12, 56].

7.3.1 Adsorption Processes

Although high-temperature treatment with solids may be efficient for siloxane removal, [57, 58] room-temperature adsorption in solids is the most practical technique today. Several adsorbent materials are reported to be active in siloxane adsorption. Earlier Schweigkofler and Niessner [41] tested inorganic materials like silica and 13X molecular sieves concluding that silica is cost-effective and efficient material, although its regeneration is incomplete also at high temperature. Similar results were reported by Matsui and Imamura that observed a more effective adsorption on some ACs [40].

The most used solids to remove siloxanes are activated carbons (ACs), although other solids, such as inorganics (silica and zeolites) or polymeric resins, may also give interesting results.

To make adsorption practical from an economic point of view, regeneration of the adsorbent by desorption is needed. This is, however, a major problem with the adsorption of siloxanes on solids, in particular ACs that can be ACs can only be partially regenerated from siloxanes after use [52, 57].

Adsorption on high surface area materials, namely silica gel, zeolites, and activated carbons (ACs) is a well-assessed method for siloxane removal [1, 2, 6, 8, 13, 30, 31, 39–41, 52, 56, 58–66] due to the very large internal surface area (500–1500 m^2/g) including macropores (pore diameter > 20 nm) and micropores (pore diameter < 20 nm). Due to the contemporary presence of siloxanes and H_2S in biogas stream several commercial high surface area materials useful for H_2S removal can be efficiently employed to reduce siloxanes concentration down to less than 1 ppm.

As biogas contains a broad range of different compounds in varying concentrations, high selectivity for siloxanes is essential due to competitive adsorption [6].

ACs are frequently used as adsorbent materials to remove siloxanes. The chemical backbone of siloxanes is very stable and chemical reaction of siloxane bonds (Si–O–Si) with the surface is unexpected. Therefore, siloxane removal mainly occurs through physical adsorption [58]. Other possible adsorbents are molecular sieves and polymeric pellets [2]. The temperature and humidity of the gas affect the efficiency of activated carbon separation; hence before activated carbon filtration the gas should be dried, otherwise the filter quickly saturates with water [21].

Ryckebosch et al. [6] reported polymer beds (Tenax TA 60/80 mesh and Amberlite XAD II 20/60 mesh), inorganic adsorbents (Molecular sieve 13X 45/60 mesh en silica gel particle size 1–3 mm), and two adsorbents with carbon as the major component (activated charcoal, particle size 2.5 mm en Carbopack B 60/80 mesh).

Silica gel and activated charcoal showed the best performances since the absence of initial breakthrough concentration of siloxanes in the effluent unlike the other adsorbents. Thermal regeneration of silica gel and activated charcoal is performed at 250 °C for about 20 h. Silica gel gives excellent regeneration (more than 95 %) while activated coal regeneration was less effective. Humidity plays an important role in the removal of siloxanes with silica gel, since its presence

decreases the removal efficiency and a dehumidification step should be required before siloxane adsorption. Silica gel beds can be operated at elevated pressure, achieving simultaneously a very effective biogas drying and a quantitative siloxane removal. Experiments with silica gel show that its removal capacity is larger than with activated carbon.

Cheremisinoff and Ellerbush [67] have experimented with graphite-based activated carbon and coconut shell activated carbon. Niessner [41] compared the effectiveness of various technologies for the removal of siloxanes in digester gas from bench-scale conditions. They reported that silica gel was very promising and cost-effective material for removal of siloxanes (adsorption capacity more than 100 mg/g). Liang et al. [68] used a polymorphous porous graphic adsorption system to remove siloxanes from biogas from an anaerobic digester but did not report any quantitative removal efficiency. Huppmann et al. [69] suggested based on bench-scale testing that adsorption using resins may be cost-effective approach.

Sigot et al. [7] described a dynamic laboratory scale experiments on a synthetic polluted gas to compare three adsorbents for removal of octamethyltetrasiloxane (D4): activated carbon (AC), zeolite (Z), and silica gel (SG).

Octamethyltetrasiloxane (D4) was chosen as a representative of VOSiCs because it is present in both landfill gas and sewage gas [9, 62, 70] D4 content was 30 ppm(v) (400 mg/Nm^3) that is high compared to field concentrations, but allows to set a low and stable siloxane concentration and enable shorter experiments to reach saturation. A similar experimental approach was frequently reported. Schweigkofler and Niessner [41] adjusted siloxane (hexamethylsisiloxane L2 or decamethylciclopentasiloxane D5) concentration to 4 g/m^3 in most experiments involving silica gel; Matsui and Imamura [40] set the concentration of D4 in their model gas at 4.5 g(m^3); Finocchio et al. [39] investigated hexamethylcyclotrisiloxane (D3) at a concentration of 5000 g/m^3.

Sigot et al. [7] tested three commercial adsorbents: a coconut-based activated carbon (AC) obtained from Chemviron Carbon (930 m^2/g BET surface), 13X zeolite obtained from CECA (700 m^2/g BET surface) (Z), Chameleon silica gel obtained from BDH Prolabo (690 m^2/g BET surface) (SG).

The adsorption capacity of D4 was estimated from the integration of the area above the breakthrough curve and by gravimetric method. SG proved to be the most efficient adsorbent for D4 removal compared to active carbon and zeolite.

Dynamic adsorption tests at 27 °C showed adsorbed quantities of 52–53 mgD4/g for AC, 113–139 mgD4/g for Z, and 216–259 mgD4/g for SG. This result was explained by the surface chemistry of SG which exposes surface siloxane (Si-O-Si) and silanol (Si-O-H) groups that show affinity for the compounds of the same family such as D4; indeed there is a strong affinity of silicon for oxygen [71].

The SG adsorption capacity as expected decreases in the presence of humidity due to competitive adsorption: at 70 % relative humidity was 21 mgD4/gSG, that is, 10 times lower than in the absence of water. Similar result is reported by Schweigkofler and Niessner [41] who studied L2 or D5 removal on SG at relative humidity in the range 10–15 %. Tests conducted at 45 °C (that is a condition

comparable to thermophilic conditions for biogas production or occurring during the summer in collection pipework) resulted in a decrease of about only 15 % of the adsorption capacity.

Regeneration of exhausted SG was carried out at 300 °C for 24 h for. The regeneration was only partial probably due to siloxane polymerization on SG, leading to about 90 % decrease of the SG adsorption capacity. This is in accordance with Montanari et al. [17] that observed an incomplete regeneration of SG exhausted with D3 after treatment at 200 °C. On the contrary Schweigkofler and Niessner [41] observed excellent desorption efficiency of L2 or D5 (greater than 95 % of SG) by thermal desorption at 250 °C with gas circulation that probably improved the desorption. According to Sorenau et al. [8] the interactions between siloxane molecules and silica gel are hydrogen bond type and thermal regeneration is easily achieved.

However Montanari et al. [17] observed polymerization of D3 to silicone during adsorption on SG in dynamic conditions which could explain the partial regeneration. A combination of both mechanisms can match all these results: mainly hydrogen bonds form at low siloxane uptake when SG load increases surface polymerization (stronger bonds) occurs and makes siloxanes difficult to desorb.

Montanari et al. [17] studied the adsorption of hexamethylcyclotrisiloxane (D3) on pure activated carbons, silica, and NaX zeolite and their regeneration using FT-IR spectroscopy [39, 53]. The experiments have been performed with a concentration of D3 far higher (250 times higher) than real one in landfill biogases that allow one-day experiments.

In Table 7.3 the properties of the materials are reported.

The results obtained confirm promising literature data on active carbons for removal of D3 from biogases [57, 72–76].

According to these data, silica and NaX zeolite are not only less efficient than ACs but show similar difficulties also in the regeneration step. Polymerization of D3 to silicone is proposed to occur on silica and NaX zeolite during the adsorption causing the adsorbent deactivation. D3 adsorbs on silica by hydrogen bonding on the surface hydroxyl groups and is only partially desorbed by heating up to 200 °C or by vacuum treatment. On NaX zeolite, purging at room temperature allows some D3 desorption that does not further occurs by increasing temperature.

Table 7.3 Adsorption and desorption capacities for HMCTS over solids [17]

Adsorbent	Supplier and type	Apparent density (g/mL)	BET surface area (m^2/g)	Effective adsorption capacity (gHMCTS/gADS)	Desorbed/adsorbed HMCTS (°C)
Silica gel	Grace	0.72	350	0.230	0 %
Faujasite NaX	Sylobead MS 544 Grace	0.69	500	0.276	16 % at 100
					23 % at 200
Pure activated carbon	NORIT RB4	0.41	>1000	0.580	4 % at 100
					8 % at 200

Polymerization of D3 is supposed to be the most likely cause of the only partial regenerability of all these solids after D3 adsorption.

Similar results are reported by Finocchio et al. [39] that studied the adsorption of D3 on different materials such as activated carbons (ACs), silica, and zeolite. The adsorption and regenerability have been investigated by infrared (IR) spectroscopy in the apparatus reported in Fig. 7.1. Pure ACs appeared efficient sorbents for D3, more effective than alkali-impregnated ACs and inorganic solids, such as zeolites and silica gel. The presence of transition metal in ACs enhances the adsorption capacity, although such metals may cause more difficulties in the handling and disposal of spent adsorbents.

The authors reported that D3 polymerizes in part upon adsorption into polydimethylsiloxane causing the partial regenerability. In Table 7.4 Finocchio et al. [39] summarize results concerning the adsorption of D3 on some ACs.

Gilson et al. [12] studied technique to simultaneously reduce both the hydrogen sulfide and siloxanes concentration to less than 1 ppm. Five different commercial activated carbons (AC) previously studied [77] and effective in H_2S removal have been tested at L2 at concentration of 100–200 ppm. Samples differ in specific surface area. Their performances are compared to understand which mechanism controls siloxane removal and which carbon characteristic plays a role in the adsorption process. Table 7.5 summarizes data of the tested ACs.

The adsorption was studied by varying concentration, grain size, and adsorbent bed height.

Two different zeolites and silica gel powder were also tested, but appeared to be inadequate as adsorbents with respect to L2.

The best adsorbent carbons were those with the larger surface area (AC1, AC3, AC7), while the ACs that break earlier are those with the lower specific area value (AC2 and AC5). The specific surface area that correlates with the

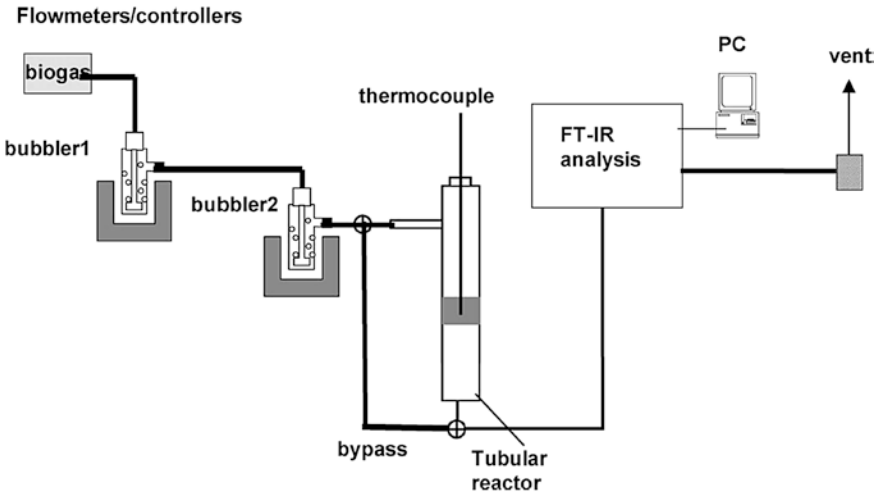

Fig. 7.1 Scheme of adsorption apparatus [17]

Table 7.4 Adsorption capacities for D3 over solids [39]

Adsorbent	Origin	Apparent density	Effective adsorption capacity (g_H/g_{CAT})
Silica gel	Grace	0.72	0.230
Faujasite NaX	Sylobead MS 544 Grace	0.69	0.276
AC	Picacarb		0.561
AC	NORIT RB4	0.41	0.580
AC impregnated with KI	NORIT ROZ	0.47	0.483
AC impregnated with Cu^{II} and Cr^{VI} salts	NORIT RGM1	0.49	0.878
AC impregnated with KOH < 15 %	NORIT RBAA1	0.53	0
AC impregnated with alkali	Carbonfilter Multisorb DS SH4		0.06
AC impregnated	Chemviron carbon Solcarb KS3		0.285
AC impregnated with KOH 8 %	Sicav Si 30 K		0.332
spent AC	NORIT RB4 spent end column		0.27
spent AC	NORIT RB4 spent half column		0.07

Table 7.5 Characterisitic of activated carbon [12]

Activated carbon	Impregnant	Specific area $m^2 g^{-1}$
AC1	Cu, Cr salt	978
AC2	KOH	691
AC5	KI	880
AC3	Virgin, basic	923
AC7	Virgin, acid	1100

adsorption capacity is the total internal area, without distinction between micro- and macroporous and not merely the macroporous one as reported by Oshita et al. [62]. The L2 molecules dimension, of some nanometers is anyway smaller than the micropore diameters so these can contribute to the active adsorption process.

The strict correlation of the adsorption capacity with the surface area points to an adsorption mechanism based on physical adsorption rather than chemical one.

The adsorption mechanism differs from that observed for H_2S on some AC that is based on chemical interactions [77].

The measured capacities vary from 10 mg of L2 adsorbed per gram (AC2) to 100 mg per gram (AC7) as reported for similar carbons [28, 64]. The adsorbed L2 amounts calculated from the breakthrough curves were in good agreement with results from TGA measurements.

The adsorption capacity was evaluated changing the input concentration of L2. As expected larger L2 concentration, that is, larger partial pressure, favors the kinetics and the filling of pores, otherwise not accessible.

The regeneration process by thermal desorption (up to 200 °C) degrades the adsorption capacity down to about 70 % of initial capacity probably because of the formation of nonvolatile compounds on the ACs surface. A thermal treatment at T > 200 °C was attempted in several studies [28, 64]. Successive studies [40] assessed a 5–25 % loss in adsorption capacity after regeneration regarding silica compounds and hydrogen sulfide. The impossibility to regenerate the spent carbon rises considerably its costs as purification system [39, 64], otherwise very low. Adsorbent beds have to be replaced regularly avoiding a continuous process.

References

1. Rasi S, Lehtinen J, Rintala J (2010) Determination of organic silicon compounds in biogas from wastewater treatments plants, landfills, and co-digestion plants. Renew Energy 35:2666–2673
2. Dewil R, Appels L, Baeyen SJ (2006) Energy use of biogas hampered by the presence of siloxanes. Energy Convers Manage 47:1711–1722
3. de Arespacochaga N, Valderrama C, Mesa C, Bouchy L, Cortina JL (2014) Biogas deep clean-up based on adsorption technologies for Solid Oxide Fuel Cell applications. Chem Eng J 255:593–603
4. Wheless E, Pierce J. http://www.scsengineers.com. Accessed 30 June 14
5. Faes A, Hessler-Wyser A, Presvytes D, Vayenas CG, Van Herle J (2009) Nickel-Zirconia anode degradation and triple phase boundary quantification from microstructural analysis. Fuel Cells 9:841–851
6. Ryckebosch E, Drouillon M, Vervaeren H (2011) Techniques for transformation of biogas to biomethane. Biomass Bioenergy 35:1633–1645
7. Sigot L, Ducom G, Benadda B, Laboure C (2014) Adsorption of octamethylcyclotetrasiloxane on silica gel for biogas purification. Fuel 135:205–209
8. Sorenau G, Beland M, Falletta P, Edmonson K, Svoboda L, Al-Jamal M et al (2011) Approaches concerning siloxanes removal from biogas—a review. Can Biosyst Eng 53:1–18
9. Appels L, Baeyens J, Dewil R (2008) Siloxane removal from biosolids by peroxidation. Energy Convers Manage 49:2859–2864
10. Gaj K, Pakuluk A (2015) Volatile methyl siloxanes as potential hazardous air pollutants. Pol J Environ Stud 24:937–943
11. Abatzoglou N, Boivin S (2009) A review of biogas purification processes. Biofuels Bioprod Bioref 3:42–71
12. Gislon P, Galli S, Monteleone G (2013) Siloxanes removal from biogas by high surface area adsorbents. Waste Manag 33:2687–2693
13. Mona A (2009) Reduction and monitoring of biogas trace compounds. VTT Res Notes 55:2496
14. Dewil R, Appels L, Baeyens J (2006) Energy use of biogas hampered by the presence of siloxanes. Energ Convers Manage 47:1711–1722
15. Ohannessian A, Desjardin V, Chatain V, Germain P (2008) Volatile organic silicon compounds: the most undesirable contaminants in biogases. Water Sci Technol 58:1775–1781
16. Ducom G, Laubie B, Ohannessian A, Chottier C, Germain P, Chatain V (2013) Hydrolysis of polydimethylsiloxane fluids in controlled aqueous solutions. Water Sci Technol 68:813–820

17. Montanari T, Finocchio E, Bozzano I, Garuti G, Giordano A, Pistarino C, Busca G (2010) Purification of landfill biogases from siloxanes by adsorption: a study of silica and 13X zeolite adsorbents on hexamethylcyclotrisiloxane separation. Chem Eng J 165:859–863
18. Verma S (2002). http://www.compost.org. Accessed 30 06 14
19. Wheless E, Gary D (2002) Siloxanes in landfill and digester gas. In: Proceedings of SWANA, 25th Annual Landfill Gas Symposium, Monterey, Calif. Solid Waste Association of North America (SWANA). Silver Springs, Md, pp 29–56, 25–28 March 2002
20. Papadias DD, Ahmed S, Kumar R http://www.ipd.anl.gov. Accessed 30 06 14
21. Arnold M, Kajolinna T (2010) Development of on-line measurement techniques for siloxanes and other trace compounds in biogas. Waste Manage 30:1011–1017
22. Appels L, Baeyens J, Degreve J, Dewil R (2008) Principles and potential of the anaerobic digestion of waste-activated sludge. Prog Energy Combust Sci 34:755–781
23. Dewil R, Appels L, Baeyens J (2006) https://lirias.kuleuven.be. Accessed 30 06 14
24. Vesterager, N, Matthiesen D (2004) http://cordis.europa.eu. Accessed 30 06 14
25. McBean EA (2008) Siloxanes in biogases from landfills and wastewater digesters. Can J Civ Eng 35:431–436
26. Hyutzinger O (ed) (1997) The handbook of environmental chemistry. Springer, Berlin
27. Watts RJ, Kong S, Haling CS, Gearhart L, Frye CL, Vigon BW (1995) Fate and effects of polydimethylsiloxanes on pilot and bench-top activated sludge reactors and anaerobic/ aerobic digesters. Water Res 29:2405–2411
28. Wheless E, Pierce J Siloxanes in landfill and digester gas update. http://www.scsengineers.com/Papers/Pierce_2004Siloxanes_Update_Paper.pdf
29. Glus PH, Liang KY, Li R, Pope R (1999) Recent advances in the removal of volatile methylsiloxanes from biogas at sewage treatment plants and landfills. In: Proceedings of the US Air and Waste Management Association Conference, St. Louis, Mo. Air and Waste Management Association, Pittsburgh, Pa, p 330
30. Arnold M, Kajolinna T (2010) Development of on-line measurement techniques for siloxanes and other trace compounds in biogas. Waste Manag 30:1011–1017
31. Ajhar M, Travesset M, Yüce S, Melin T (2010) Siloxane removal from landfill and digester gas—a technology overview. Bioresour Technol 101:2913–2923
32. Lipowitz J, Ziemelis M (1976) A model for combustion of poly (dimethylsiloxanes). J Fire Flammabl 7:482–503
33. Gaj K, Pakuluk A (2015) Volatile methyl siloxanes as potential hazardous air pollutants. Pol J Environ Stud 24:937–943
34. Tansel B, Surita SC (2014) Differences in volatile methyl siloxane (VMS) profiles in biogas from landfills and anaerobic digesters and energetics of VMS transformations. Waste Manage 34:2271–2277
35. Allen MR, Braithwaite A, Hills CC (1997) Landfill gas at seven U.K. waste disposal sites. Environ Sci Technol 31:1054
36. Surita SC, Tansel B (2014) Emergence and fate of cyclic volatile polydimethylsiloxanes (D4, D5) in municipal waste streams: release mechanisms, partitioning and persistence in air, water, soil and sediments. Sci Total Environ 468–469:46–52
37. Sevimoglu O, Tansel B (2013) Effect of persistent trace compounds in landfill gas on engine performance during energy recovery: a case study. Waste Manage 33:74–80
38. Haga K, Adachi S, Shiratori Y, Itoh K, Sasaki K (2008) Poisoning of SOFC anodes by various fuel impurities. Solid State Ionics 179:1427–1431
39. Finocchio E, Montanari T, Garuti G, Pistarino C, Federici F, Cugino M, Busca G (2009) Purification of biogases from siloxanes by adsorption: on the regenerability of activated carbon sorbents. Energy Fuels 23:4156–4159
40. Matsui T, Imamura S (2010) Removal of siloxane from digestion gas of sewage sludge. Bioresour Technol 101:S29–S32
41. Schweigkofler M, Niessner R (2001) Removal of siloxanes in biogases. J Hazard Mater 83:183–196

42. Madi H, Lanzini A, Diethelm S, Papurello D, Van Herle J, Lualdi M, Larsen JG, Santarelli M (2015) Solid oxide fuel cell anode degradation by the effect of siloxanes. J Power Sources 279:460–471
43. Kymalainen M, Lahde K, Arnold M, Kurola JM, Romantschuk M, Kautola H (2012) Biogasification of biowaste and sewage sludge—measurement of biogas quality. J Environ Manage 95:S122–S127
44. Van Herle J, Membrez Y, Bucheli O (2004) Biogas as a fuel source for SOFC cogenerators. J Power Sources 127:300–312
45. Sasaki K, Haga K, Yoshizumi T, Minematsu D, Yuki E, Liu R et al (2011) Chemical durability of Solid Oxide Fuel Cells: influence of impurities on long-term performance. J Power Sources 196:9130–9140
46. Gerdes K, Williams MC, Gemmen R, White B (2013) A global framework for examination of degradation in SOFC. ECS Trans 57:289–297
47. Sasaki K, Yoshizumi T, Haga K, Yoshitomi H, Hosoi T, Shiratori Y, Taniguchi S (2013) Chemical degradation of SOFCs: external impurity poisoning and internal diffusion-related phenomena. ECS Trans 57:315
48. Haga K, Shiratori Y, Ito K, Sasaki K (2008) Chlorine poisoning of SOFC Ni-Cermet anodes. J Electrochem Soc 155:B1233–B1239
49. Hauch A, Ebbesen SD, Jensen SH, Mogensen M (2008) Solid Oxide electrolysis cells: microstructure and degradation of the Ni/Yttria-stabilized zirconia electrode. J Electrochem Soc 155:B1184–B1193
50. Abatzoglou N, Boivin S (2009) A review of biogas purification processes. Biofuels Bioprod Biorefin 3:42–71
51. Ajhar M, Travesset M, Yüce S, Melin T (2010) Siloxane removal from landfill and digester gas. Technol Overview Bioresour Technol 101:2913–2923
52. Boulinguiez B, LeCloirec P (2010) Adsorption on activated carbons of five selected volatile organic compounds present in biogas: comparison of granular and fiber cloth materials. Energy Fuels 24:4756–4765
53. Finocchio E, Garuti G, Baldi M, Busca G (2008) Decomposition of hexamethylcyclotrisiloxane over solid oxides. Chemosphere 72:1659–1663
54. Urban W, Lohmann H, Salazar Gómez JI (2009) Catalytically upgraded landfillgas as a cost-effective alternative for fuel cells. J Power Sources 193:359–366
55. M. Hagmann, E. Hesse, P. Hentschel, T. Bauer (2001) Purification of biogas e removal of volatile silicones. In: Christensen TH, Cossu R, Stegmann R (eds) The eighth international waste management and landfill symposium, vol. II. Cagliari, Italy: Litotipografia Kalb, pp 641–644, 1–5 Oct 2001
56. Poat SC, Deshusses MA (2008) Biological removal of siloxanes from landfill and digster gases: opportunities and challenges. Environ Sci Technol 42:8510–8515
57. Giraudet S, Boulinguiez B, Le Cloirec P (2014) Adsorption and electrothermal desorption of volatile organic compounds and siloxanes onto an activated carbon fiber cloth for biogas purification. Energy Fuels 28:3924–3932
58. Ajhar M, Travesset M, Yüce S, Melin T (2010) Siloxane removal from landfill and digester gas–a technology overview. Biores Technol 101:2913–2923
59. Cabrera-Codony A, Montes-Moran MA, Sanchez-Polo M, Martin MJ, Gonzalez-Olmos R (2014) Biogas upgrading: optimal activated carbon properties for Siloxane removal. Environ Sci Technol 48:7187–7195
60. Ballantyne R, Ballantyne W, Knapke M, Neumann D, Rossin, J (2015) Process for removal of siloxanes and related compounds from biogas streams using porous adsorbent U.S. Pat Appl Publ, US 20150209717 A1 20150730
61. Izumi J, Wang HX (2009) Recovery and purification of methane from fermentation biogas provided with adsorbents PCT Int Appl, WO 2009101669 A1 20090820
62. Oshita K, Ishihara Y, Takaoka M, Takeda N, Matsumoto T, Morisawa S, Kitayama A (2010) Behaviour and adsorptive removal of siloxanes in sewage sludge biogas. Water Sci Technol 61:2003–2012

63. Sigot L, Ducom G, Germain P (2015) Adsorption of octamethylcyclotetrasiloxane (D4) on silica gel (SG): retention mechanism. Microporous Mesoporous Mater 213:118–124
64. Ricaurte D, Ortega A (2009) Siloxane treatment by adsorption into porous materials. Environ Technol 30:1073–1083
65. Ricaurte D, Ortega A (2009) Subrenat Elimination of siloxanes by adsorption process as a way of upgrading biogas Trans Ecol Environ (Energy and Sustainability II) 121:49–58
66. Sigot L, Ducom G, Benadda B, Laboure C (2015) Comparison of adsorbents for H_2S and D4 removal for biogas conversion in a solid oxide fuel cell. Environ Technol 1–10
67. Cheremisinoff P, Ellerbusch F (1978) Carbon adsorption handbook. Ann Arbor Science Publishers Inc., Ann Arbor, Mich
68. Liang K, Li R, Tudman S, Schneider R, Sheehan J, Anderson E (2001) Pilot testing case study: removal of volatile methylsiloxanes from anaerobic digestor gas-fired engines. In: Proceedings of the 2001 Annual AWMA Conference, Orlando, Fla., 24–28 June 2001. Air and Waste Management Association, Pittsburgh, Pa, p 960
69. Huppmann R, Lohoff HW, Schroder HF (1996) Cyclic siloxanes in the biological wastewater treatment process-determination, quantification and possibilities of elimination. Fresen J Anal Chem 354:66–71
70. Lee SH, Cho W, Song TY, Kim H, Lee WJ, Lee YC et al (2001) Removal process for octamethylcyclotetrasiloxane from biogas in sewage treatment plant. J Ind Eng Chem 7:276–280
71. Varaprath S, Stutts DH, Kozerski GE (2006) A primer on the analytical aspects of silicones at trace levels-challenges and artifacts–a review. Silicon Chem 3:79–102
72. Herrera D, Patton MA (2014) Siloxane removal from gases using lignite-enhanced activated carbons and adsorbent media used therefor. Int Appl, WO 2014099422 A1 20140626
73. Yu M, Gong H, Chen Z, Zhang M (2013) Adsorption characteristics of activated carbon for siloxanes. J Environ Chem. Eng. 1:1182–1187
74. Lee JY, Bae MS, Lee JG, Jung HJ, Kim YJ (2012) Method for manufacturing activated carbon adsorbent capable of simultaneously removing hydrogen sulfide and siloxane from biogases. From Repub Korean Kongkae Taeho Kongbo KR 2012018957 A 20120306
75. Piechota G, Hagmann M, Buczkowski R, Roman (2012) Removal and determination of trimethylsilanol from the landfill gas Biores. Bioresour Technol 103:16–20
76. Prasad A, Marchand K (2012) Integrated biogas cleaning system to remove water, siloxanes, sulfur, oxygen, chlorides and volatile organic compounds. PCT Int Appl WO 2012006729 A1 20120119
77. Monteleone G, De Francesco M, Galli S, Marchetti M, Naticchioni V (2011) Deep H_2S removal from biogas for molten carbonate fuel cell (MCFC) systems. Chem Eng J 173:407–414